The background is a surreal landscape painting. On the left, a dark, rocky cliff features a small industrial factory with several smokestacks emitting white smoke. A path of small, colorful pills leads from the factory down a steep slope towards a river. The river is composed of a stream of large, orange, pill-like capsules. In the foreground on the right, a large, detailed white flower with a bee on it is visible. The sky is filled with soft, hazy clouds in shades of yellow and grey.

The potential of tailor-made resistant starch type 3 as a health-beneficial ingredient for the gut

Cynthia E. Klostermann

Resistant starch type 3 as a health-beneficial ingredient for the gut

Cynthia E. Klostermann 2023

Propositions

1. Understanding degradation of resistant starch type 3 by gut microbiota, first requires a precise construction of the RS-3 substrate. (this thesis)
2. Resistant starch type 3 stimulates production of healthy butyrate by promoting bacteria not recognized as health-beneficial yet. (this thesis)
3. Learning to play a musical instrument is health-beneficial at all ages. (Jünemann et al., Front. Aging Neurosci., 2022, 14)
4. Microscopy is eye-candy that translates science to the public.
5. Agritourism helps in mutual understanding between farmers and citizens.
6. Persuading others is only justified when you understand the topic.

Propositions belonging to the thesis, entitled

The potential of tailor-made resistant starch type 3 as a health-beneficial ingredient for the gut

Cynthia E. Klostermann

Wageningen, 21 June 2023

The potential of tailor-made resistant starch type 3 as a health-beneficial ingredient for the gut

Cynthia E. Klostermann

Thesis committee

Promotors

Prof. Dr J.H. Bitter

Professor of Biobased Chemistry & Technology
Wageningen University & Research

Prof. Dr H.A. Schols

Personal chair at the Laboratory of Food Chemistry
Wageningen University & Research

Other members

Dr C. Belzer, Wageningen University & Research

Prof. Dr E.E. Blaak, Maastricht University

Prof. Dr L. Dijkhuizen, University of Groningen

Dr F.J. Warren, Quadram Institute, United Kingdom

This research was conducted under the auspices of the VLAG Graduate School
(Biobased, Biomolecular, Chemical, Food and Nutrition Sciences)

The potential of tailor-made resistant starch type 3 as a health-beneficial ingredient for the gut

Cynthia E. Klostermann

Thesis

Submitted in fulfilment of the requirements for the degree of doctor at
Wageningen University
by the authority of the Rector Magnificus,
Prof. Dr A.P.J. Mol,
in the presence of the
Thesis Committee appointed by the Academic Board
to be defended in public
on Wednesday 21 June 2023
at 11 a.m. in the Omnia Auditorium.

Cynthia E. Klostermann

The potential of tailor-made resistant starch type 3 as a health-beneficial ingredient for the gut,
268 pages.

PhD thesis, Wageningen University, Wageningen, the Netherlands (2023)
With references, with summary in English

ISBN: 978-94-6447-678-1

DOI: <https://doi.org/10.18174/629573>

Op een ochtend liepen de eekhoorn en de mier door het bos.
'Waar gaan we eigenlijk heen?' vroeg de eekhoorn.
'Naar de verte,' zei de mier.
'O,' zei de eekhoorn.
Het was een mooie dag en ze liepen het bos uit, de verte in.

Toon Tellegen, Misschien wisten zij alles

Abstract

Resistant starch is starch that escapes digestion in the small intestine and transits to the colon, where it is subjected to fermentation by gut microbiota that produce health-beneficial short-chain fatty acids. Usually, only part of the starch we consume is resistant to digestion. Here, we studied how to design resistant starch type 3 (RS-3), i.e. retrograded starch, in such a way that it is resistant to digestion in the small intestine, while still being fermentable by gut microbiota from various subjects.

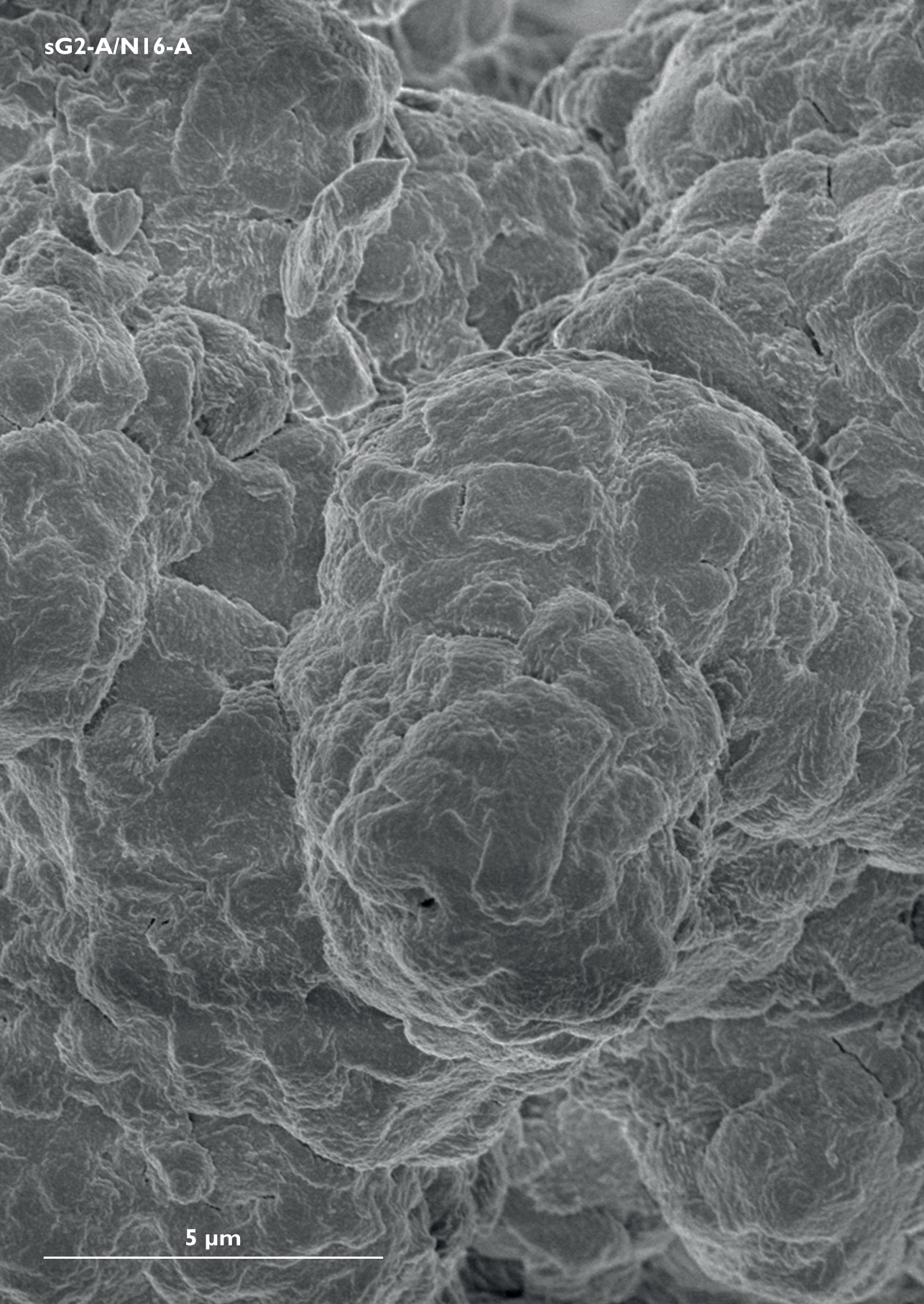
Twelve unique RS-3 preparations were produced from α -1,4 glucans, varying in chain length and molecular weight distribution, that were crystallized in A- or B-type crystals. These twelve RS-3 preparations were digested *in vitro* to mimic the small intestinal transit. This revealed that six RS-3 preparations were highly resistant to digestion (80-95 % RS, “intrinsic RS”). These six intrinsic RS-3 substrates were further studied for their fermentability *in vitro* using a pooled adult faecal inoculum. The six intrinsic RS-3 substrates were all slowly fermentable by such a mixed microbial population, although simultaneously promoting butyrate production. The other six RS-3 preparations, still containing digestible starch, were fermented much faster using the same faecal inoculum, while stimulating different microbial populations. *In vitro* fermentation of selected RS-3 preparations using pooled pre- or post-weaning piglet faecal inocula revealed that both communities were able to ferment RS-3 preparations containing digestible starch. In contrast, intrinsic RS-3 was clearly fermented by pooled post-weaning piglet faecal microbiota only. A selection of intrinsic RS-3 substrates was also inoculated with well-known RS-degrading species *Ruminococcus bromii* and *Bifidobacterium adolescentis* in mono-culture. The results showed that *R. bromii* was able to degrade all substrates properly and equally well, whereas *B. adolescentis* was only slightly able to ferment A-type intrinsic RS-3.

We now know how to design RS-3 substrates that are resistant to digestion in the small intestine, while still being fermentable by specific gut microbiota. These highly resistant RS-3 substrates are potential health-beneficial ingredients that might stimulate butyrate production in the distal colon.

Table of contents

| | | |
|------------------|--|-----|
| Chapter 1 | General introduction | 1 |
| Chapter 2 | Digestibility of resistant starch type 3 is affected by crystal type, molecular weight and molecular weight distribution | 33 |
| Chapter 3 | Type of intrinsic resistant starch type 3 determines <i>in vitro</i> fermentation by pooled adult faecal inoculum | 61 |
| Chapter 4 | Presence of digestible starch impacts <i>in vitro</i> fermentation of resistant starch | 105 |
| Chapter 5 | The prebiotic potential of RS-3 preparations for pre- and post-weaning piglets | 135 |
| Chapter 6 | Degradation of intrinsic resistant starch type 3 crystals by gut microbes <i>B. adolescentis</i> and <i>R. bromii</i> | 171 |
| Chapter 7 | General discussion | 219 |
| Summary | | 251 |
| Acknowledgement | | 257 |
| About the author | | 263 |

sG2-A/Ni6-A



5 μm

A scanning electron micrograph (SEM) showing a highly textured, granular surface. The surface is composed of numerous small, rounded, and irregularly shaped particles or grains that are closely packed together. The lighting creates strong highlights and shadows, emphasizing the three-dimensional nature and roughness of the material. The overall appearance is similar to a microscopic view of a mineral, metal, or polymer surface.

Chapter 1

General introduction

Project outline

Starch is an important source of energy within the human diet and mostly present in foods in a processed form. A small proportion of the dietary starch will survive digestion in the upper gastro-intestinal tract (GIT) and transit to the colon. This so-called resistant starch is then subject to fermentation by gut microbiota, that first initiate hydrolysis of the resistant starch into smaller fragments and subsequently metabolise these into health-beneficial short-chain fatty acids. The amount of digestible starch that arrives in the colon is unclear, since this depends largely on the starch form, food matrix and transit time and is therefore considered a kinetic parameter. Starch can also be intrinsically resistant to pancreatic digestion, allowing a larger proportion of resistant starch to transit to the colon. In this project, we aimed to understand how to prepare starch substrates in such a way that they resist digestion in the upper GIT and are subjected to fermentation in the colon. We specifically worked with resistant starch type 3 (RS-3), since the resistance to digestion in RS-3 can be influenced by processing parameters and such intrinsic RS-3 could be added to foods as a potential health-beneficial ingredient. Recent research has greatly put effort in understanding how to prepare RS-3 with high resistance to digestion, but knowledge on the fermentability of such highly resistant RS-3 ingredients is still lacking.

1. Native starch structure

Starch is a main storage polysaccharide in plants, consisting of two polymers, amylose and amylopectin^[1]. Amylose is a long linear α -1,4 linked glucose polymer (Figure 1.1-A1), with a minor amount of α -1,6 linked branch points, depending on the molecular weight. The molecular weight (Mw) of amylose is usually 10^5 - 10^6 Da, resulting in a degree of polymerization (DP) of 500-6000, depending on the botanical source^[2-4]. Amylopectin is a more branched polymer, with around 5 % α -1,6 linkages^[1] that connect short side-chains of α -1,4 linked glucose residues. The amylopectin molecule has usually a Mw of 10^6 - 10^7 Da^[5, 6] and consists of A-chains, B1-, B2-, B3- and C-chains, which are defined by the amount of α -1,6 linked branch points or carrying the reducing end (Figure 1.1-A2). Consequently, these chains all have a different chain length, with A-chains (DP 6-12)^[7] only having one α -1,6 linkage, which connects it to short B1-chains (DP 13-23)^[7, 8]. Long B-chains (B2 = 24-57, B3 > DP 50^[8]) are substituted by one or several other chains and connected to a C-chain (DP 10-130)^[9], which carries the reducing end.

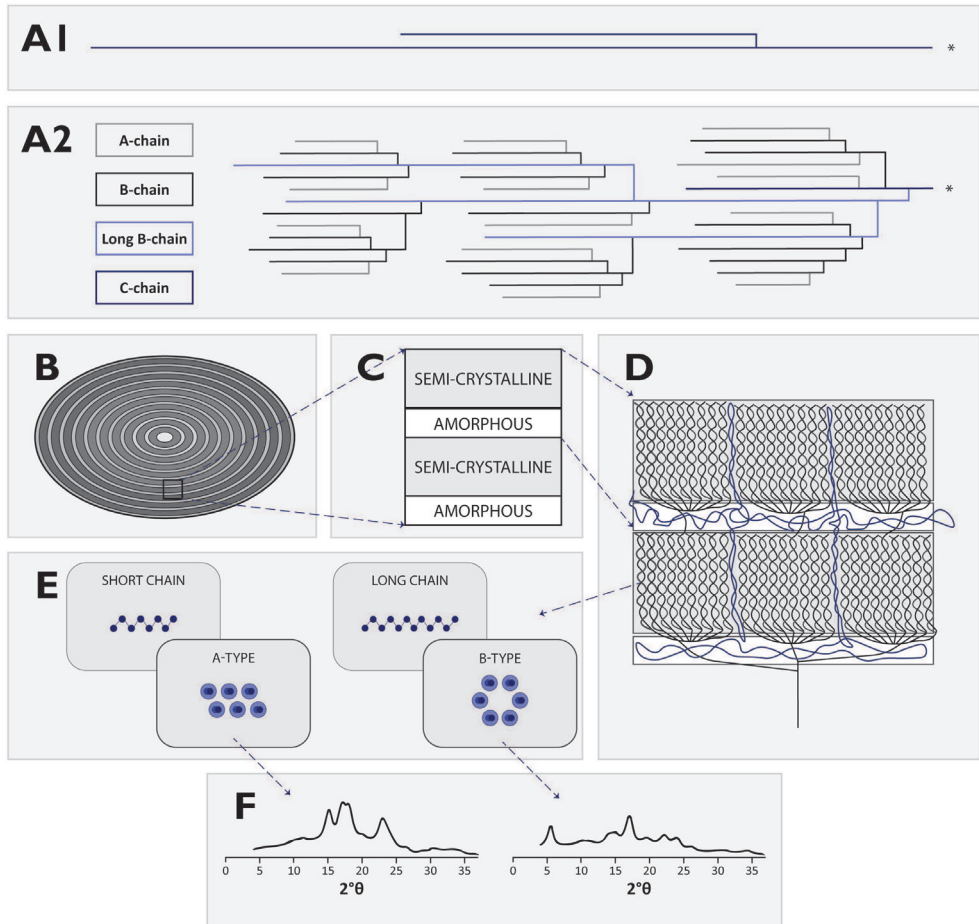


Figure 1.1. Overview of starch structure. A1: Amylose chain, A2: Amylopectin structure with A-, B- and C-chains, * shows the reducing end. B: Hypothetical granule with growth rings. C: Semi-crystalline and amorphous regions within growth rings. D: Amylopectin blocklet structure with amylose interspersed. E: Short amylopectin (side-)chains crystallize in an A-type polymorph, long amylopectin side-chains crystallize in a B-type polymorph. F: X-ray diffractogram of typical A-type (waxy maize) and B-type (potato) starch, adapted from Lopez-Rubio et al. (2008)^[10].

Within a plant, amylose and amylopectin are forming a supramolecular structure, with alternating semi-crystalline and more amorphous layers, called growth rings^[1] (Figure 1.1-B, C). The semi-crystalline layers primarily consist of the short (side-)chains of amylopectin that form double helices and cluster together, whereas the more amorphous layers within the growth rings contain the α -1,6 linked branch points (Figure 1.1-D). The double helices within the semi-crystalline part are left-handed and parallel stranded^[1] and packed in three different crystal types, depending on the botanical source. Short α -1,4 chains,

such as present in cereal starches, form A-type crystals, whereas longer chains, such as present in tuber starches form B-type crystals^[11] (Figure 1.1-E, F). Also a mixture of both A- and B-type polymorphs, the so-called C-type starches, can be found in e.g. legume starches^[1]. The amylose molecules are randomly interspersed between the semi-crystalline and amorphous regions of the amylopectin clusters (Figure 1.1-D)^[8]. Together, the supramolecular structure of amylose, amylopectin and minor components present, form a granule of varying morphologies, depending on the botanical source^[12].

Starch in plants is thus present within granules, of which the exact molecular details depend on the botanical source. Most native starches contain around 20 – 30 % amylose and 70 – 80 % amylopectin, but so-called waxy starches only contain amylopectin^[1, 13], whereas high-amylose starches contain up to 80 % amylose. Cooking granules, often performed to prepare foods, will gelatinize the starch, which causes irreversible disruption of the molecular order within the granules^[14] and solubilization of the amylopectin and amylose chains.

2. The starch journey through the upper gastrointestinal tract

2.1. Starch digestion *in vivo*

2.1.1. Mouth

Starch digestion starts in the mouth, where our food is masticated to decrease the particle size to 0.8 – 3 mm^[15], thereby increasing the surface area of the food particles. Simultaneously to mastication, the food particle is hydrated with saliva, until a food bolus can be formed. Saliva contains salivary α -amylase, an enzyme that usually hydrolyses up to 5 % of the α -1,4 linkages within starch present in the mouth^[16] to yield maltose, maltotriose and branched α -limit dextrins. Once the food bolus is formed, it will be swallowed and travel from the mouth via the esophagus to the stomach.

2.1.2. Stomach

In the stomach, the food bolus is mixed with gastric juices containing acid, pepsin, lipase and salts. The stomach itself does not produce starch-active enzymes, but depending on the pH (2-5), salivary α -amylase may still be active once the food bolus has arrived in the stomach^[17-19]. Although starch may be enzymatically hydrolysed in the stomach, it is generally accepted that such

hydrolysis is minor compared to starch hydrolysis in the small intestine. The amount of time that the digesta will stay in the stomach is usually between 4 – 20 h^[20] depending on gastric emptying, which allows the movement into the small intestine.

2.1.3. Small intestine

In the small intestine (pH around 6.0^[21]), multiple enzymes collaborate to digest starch to glucose. Pancreatic α -amylase hydrolyses the α -1,4 linkages within starch, releasing maltose, maltotriose and α -limit dextrins^[16]. These are further hydrolysed to glucose by brush-border enzyme complexes maltase-glucoamylase and sucrase-isomaltase. Together with pancreatic α -amylase, these enzymes are fully able to hydrolyse solubilized starch to glucose, which is taken up by glucose transporter proteins present in the epithelium^[22]. The transit time of digesta within the small intestine is around 4 h, both in a fasted or a fed state^[23]. Undigested nutrients reaching the ileum may trigger the ileal brake^[24], which releases the hormones GLP-1 and PYY. These hormones were shown to slow down the gastric emptying^[24], but might also slow down the flow of digesta into the large intestine^[22].

2.1.4. Factors impacting starch digestion

Not all starch present in foods is digested in the upper GIT. A fraction of starch may escape digestion and transit to the colon to be subject to fermentation. Starch digestion in the upper GIT may be hindered due to factors like the food matrix, the starch type and the use of inhibiting molecules, that allow a larger proportion of starch to transit to the colon. The food matrix of starch-rich foods such as bread and pasta consists next to starch of proteins and lipids, and digestibility of such food depends on its microstructure^[25, 26]. Furthermore, certain dietary fibres may affect the viscosity of the food and therefore slow down the digestion^[27, 28], resulting in a potential increased proportion of starch reaching the colon^[29-31]. Additionally, the use of acarbose^[32] or food polyphenols^[33] may inhibit pancreatic α -amylase activity, also increasing the proportion of digestible starch reaching the colon.

2.2. Starch digestion *in vitro*

Many models exist that mimic digestion *in vivo* by means of *in vitro* digestion. A widely accepted model is the INFOGEST model, that is focussing on digestion of whole food products^[34] and has been developed to better compare *in vitro* digestion data. According to the INFOGEST model, 15 % of the starch within various products such as bread, pasta and cookies would reach the colon^[35].

The Englyst model was specifically developed for starch digestion kinetics^[36] and recognizes three starch fractions, based on the time needed to digest the starch with an excess of pancreatic α -amylase and amyloglucosidase^[37]. Rapidly digestible starch (RDS) is the starch that is hydrolysed within 20 min of *in vitro* digestion in the Englyst model, whereas slowly digestible starch (SDS) is the starch that is hydrolysed within 20-120 min of *in vitro* digestion^[36]. The proportion of starch that is not digested *in vitro* within 120 min is considered resistant starch.

3. Resistant starch

The starch that arrives in the colon *in vivo* is considered resistant starch. Some starches are hard to be completely digested by the upper GIT enzymes, resulting in a transit of part of the starch to the colon. Different types of resistant starch are described, based on the nature of resistance^[38]. RS-1 refers to starch entrapped in a cell-wall matrix. Those cell-walls cannot be digested by host enzymes and therefore the entrapped starch will transit to the colon where bacterial enzymes first hydrolyse the cell-walls and consequently release the starch. RS-2 refers to native granules that resist digestion, from crops such as potato, high-amylose cereal or banana. RS-3 refers to retrograded starch, in which long amylopectin (side-)chains or amylose chains recrystallize after gelatinization. Usually, RS-3 is considered as present in cooked and cooled food products, but it can also be added as an ingredient to foods. RS-4 refers to chemically modified starches and RS-5 refers to the amylose-lipid complexes. Additionally, enzyme-resistant starch may also form during digestion, due to rearrangement of the amylose chains^[39, 40]. Most of these described resistant starches are not fully resistant to digestion directly, but contain a fraction of starch that is not hydrolysed within the transit time.

Resistant starch type 3 is of interest since, by processing, its resistance to digestion can be influenced. In foods, especially amylose molecules tend to retrograde quickly^[41], making linear α -1,4 glucans of interest to explore retrogradation into highly resistant RS-3 ingredients. The Mw and Mw distribution of linear α -1,4 glucans can be controlled by e.g. enzymatic modification, after which α -1,4 glucans are obtained with a defined chain length and Mw distribution that may form RS-3 substrates with high resistance to digestion.

3.1. An enzymatic toolbox for modifying starch molecular weight and molecular weight distribution

Starches can be modified enzymatically to change the molecular properties of the starch^[42]. Enzymatic modification of starches usually changes the chain length or the amount of branch points of the starch molecules (Figure 1.2).

3.1.1. The enzymatic toolbox

The amount of branch points within amylopectin can be modified by the use of so-called debranching enzymes isoamylase (EC 3.2.1.68^[43], Glycoside Hydrolase family (GH) 13^[44]) or pullulanase (EC 3.2.1.41^[43], GH13 and GH57^[44]), or by the use of branching enzymes (EC 2.4.1.18^[43], GH13 and GH57^[44]) that introduce new α -1,6 branch points (Figure 1.2). Debranching enzymes hydrolyse α -1,6 linked branch points within the amylopectin molecule, resulting in primarily linearly linked α -1,4 glucans after full hydrolysis. Contrary, branching enzymes are glucan transferases that act on linear α -1,4 linked chains and transfer these α -1,4 glucans to another chain via an α -1,6 linkage^[45-47], resulting in a much more branched molecule with up to 13 % branch points^[46, 48] and consequently much shorter side chains.

The Mw and/or Mw distribution of α -1,4 glucans within starch can be influenced by e.g. α -amylase (EC 3.2.1.1^[43], GH13, GH57, GH126^[44]) that hydrolyses α -1,4 linkages resulting in a decrease of the Mw, or by the use of transferases that e.g. elongate or disproportionate the starch molecules. Amylomaltase or 4- α -glucanotransferase (EC 2.4.1.25^[43], GH13, GH57, GH77^[44]) is a disproportionating enzyme that transfers a segment of an α -1,4 glucan to another α -1,4 glucan via an α -1,4 linkage^[49] (Figure 1.2). Incubation of e.g. potato starch with amylomaltase results in both shorter and longer amylopectin (side-)chains, compared to the initial amylopectin, at the expense of amylose^[50]. Elongation of starch molecules can also be achieved by enzymatic synthesis using, e.g. sucrose or glucose-1-phosphate (α -Glc-1-P) as donor molecules. Amylosucrase (EC 2.4.1.4^[43], GH13^[44]) elongates α -1,4 glucans at the non-reducing end, using sucrose as a donor and releasing fructose^[51, 52] (Figure 1.2). A lower sucrose concentration results in a higher average chain length at the end of synthesis by amylosucrase, but due to the random reaction mechanism of amylosucrase, a mixture of α -1,4 glucans is synthesized with a broad Mw distribution^[52]. In contrast, narrow dispersed α -1,4 glucans can be obtained by the use of α -glucan phosphorylase (EC 2.4.1.1^[43], GT35^[44]), also called potato glucan phosphorylase (PGP), that elongates a primer molecule \geq maltotetraose using α -Glc-1-P and producing inorganic phosphate^[53] (Figure 1.2). The average Mw at the end of the

enzymatic synthesis by PGP depends on the ratio between the primer molecule and α -Glc-1-P^[54]. Since PGP favours to elongate the shortest malto-oligomer present, the mixture of α -1,4 glucans at the end of synthesis will be more narrow disperse^[54], compared to e.g. debranched amyloamylase modified starch or α -1,4 glucans synthesized by amylosucrase.

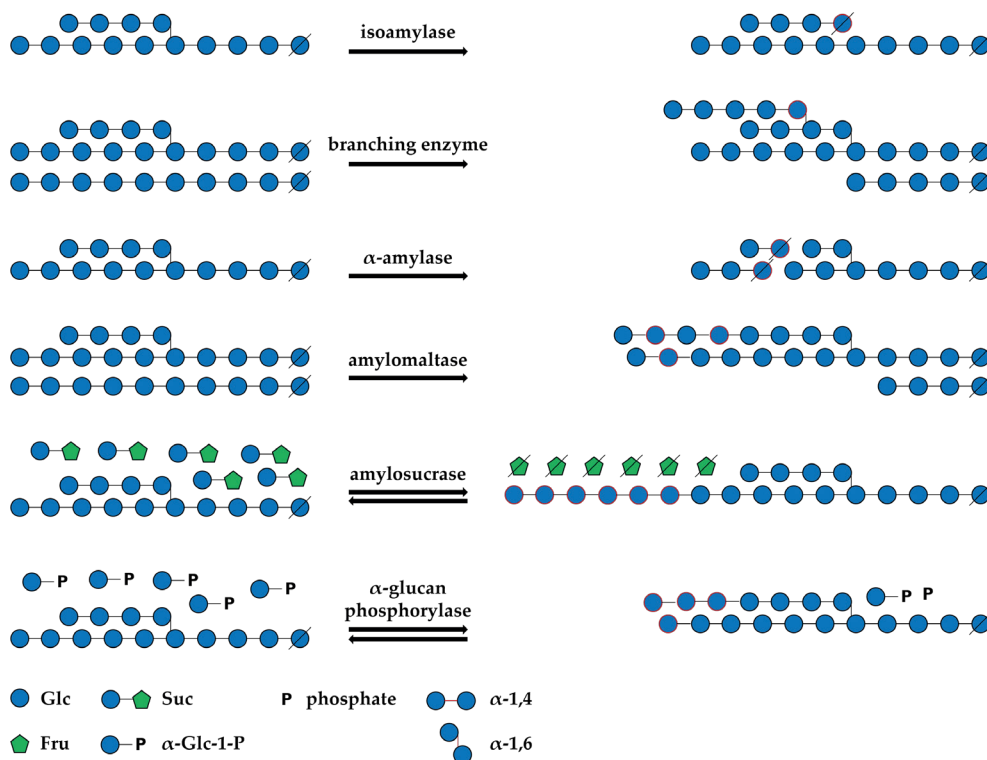


Figure 1.2. The enzymatic toolbox for enzymatic modification of starches. The diagonal line represents the reducing end. The glucose residue that is changed after enzymatic modification is indicated by a red outer line.

3.1.2. Using the enzymatic toolbox to obtain the desired Mw

Depending on the botanical source the average chain length after debranching differs; with e.g. debranched normal starches having a higher Mw than debranched waxy starches and e.g. debranched waxy wheat having a lower average size (DP 22) than debranched waxy potato (DP 32)^[11, 55]. Furthermore, debranching modified starches priorly treated with branching enzymes, results in short α -1,4 glucans^[56], whereas debranching modified starches priorly treated with amylomaltase or amylosucrase, results in extended α -1,4 glucans^[52, 57].

3.1.2. Using the enzymatic toolbox to obtain the desired Mw distribution

The Mw distribution of starch refers to the distribution of the α -1,4 glucans within a mixture and can be measured using high-performance size-exclusion chromatography^[58]. Mw distribution can be evaluated using the polydispersity index (PI), in which the mass-based Mw is divided over the number-based Mw. A high polydispersity index refers to a wide variety of α -1,4 glucans with different Mw within a mixture, whereas a low polydispersity index refers to a low variety of such α -1,4 glucans within a mixture, a so-called narrow disperse mixture. If the PI of a mixture equals 1, it has a monodisperse Mw distribution in which the mass-based Mw equals the number-based Mw.

Debranched normal starches usually have a trimodal Mw distribution^[59], consisting of the high Mw amylose part and the short amylopectin (side-)chains that differ in chain length (A, B and C-chains (Figure 1.1-A2)). The Mw distribution of debranched waxy starches is much lower and usually results in a bimodal Mw distribution^[59, 60]. Also, by the use of enzymatic modification, the Mw distribution of α -1,4 glucans can be influenced, with enzymatic synthesis by PGP resulting in a narrow disperse Mw distribution^[54] and enzymatic synthesis by amylomaltase^[57] or amylsucrase^[52] in a more polydisperse Mw distribution. A more narrow Mw distribution of α -1,4 linked glucans can also be achieved by fractionation of debranched amylopectins^[61, 62], although the PI of enzymatically synthesized α -1,4 glucans by PGP was found to be much lower^[54]. The Mw distribution of a mixture can thus be influenced by the choice of botanical source (waxy or native starches), enzymatic modification or by fractionation of the α -1,4 glucans after debranching.

By using this enzyme toolbox and starches of different botanical sources, α -1,4 glucans can be obtained with defined Mw and Mw distribution that could be used to prepare retrograded starches with high resistance to digestion.

3.2. Retrograded starch

As explained previously, native starch is present in an ordered structure inside granules. Cooking starch granules will irreversibly disrupt this ordered structure, resulting in solubilization of the starch molecules. Upon cooling, the starch molecules tend to reassociate and recrystallize in an ordered form, a process called retrogradation^[41]. Retrograded starch found in foods is often undesirable^[41], but the process of retrogradation can also be used at our benefit to make starch that resists digestion in the upper GIT.

3.2.1. Crystal type

During retrogradation, α -1,4 glucans tend to recrystallize in A- or B-type polymorphs (Figure 1.1-E)^[63], similar to the ones as found for native starches, as measured by X-ray diffraction (Figure 1.1-F)^[59, 64, 65]. Whether A- or B-type crystals are formed during recrystallization of starch depends on the chain length of the α -1,4 glucan, and the concentration and temperature during crystallization^[59, 66, 67]. Crystallization of long α -1,4 glucan chains at low temperatures usually results in a B-type polymorph, whereas crystallization of short α -1,4 glucans at high temperatures and high concentrations results in an A-type polymorph^[66, 68]. A minimum chain length of DP 10 is required to form a double helix^[67], but smaller oligosaccharides such as maltohexaose can co-crystallize^[1, 64]. At 50 °C debranched waxy maize starch (DP 24) crystallized in an A-type polymorph, whereas at 4 °C such α -glucans crystallized in a B-type polymorph^[60]. A-type crystals can also be formed using acetone precipitation from an aqueous solution^[69, 70]. Crystallization of narrow disperse α -1,4 glucans of DP 32 in acetone resulted in an A-type polymorph^[70], whereas in water α -1,4 glucans of DP 32 (polydisperse) crystallized in a B-type polymorph^[60].

After using the enzymatic toolbox and starches of different botanical sources to prepare α -1,4 glucans of defined chain length and Mw distribution, the α -1,4 glucans can thus be crystallized in A- or B-type retrograded starches. Together, α -1,4 glucan chain length, Mw distribution and crystal type are the three primary characteristics of retrograded starches, since their attributes can be steered (Figure 1.3).

3.3. Resistance to digestion of retrograded starches

Commercial retrograded starches used as RS-3 ingredients are C*Actistar™ and Novelose® 330. C*Actistar™ is prepared from partially debranched tapioca starch with > 50 % of the chains having DP 10-35^[71], retrograded in an A-type polymorph^[72] and containing approximately 55 % RS^[71]. Novelose® 330 is prepared from retrograded high-amylose maize starch (HAMS) and has a B-type polymorph, with approximately 40 % RS^[73]. Previously, it has been shown that addition of these RS-3 ingredients improved the RS content of food products, even after cooking^[74], since these ingredients are thermally stable. However, these commercial RS-3 ingredients still contain quite some digestible starch. In the past decade, many studies have been investigating how to increase the proportion of resistant starch in RS-3 ingredients, by e.g. the use of different botanical sources or processing parameters (Table 1.1).

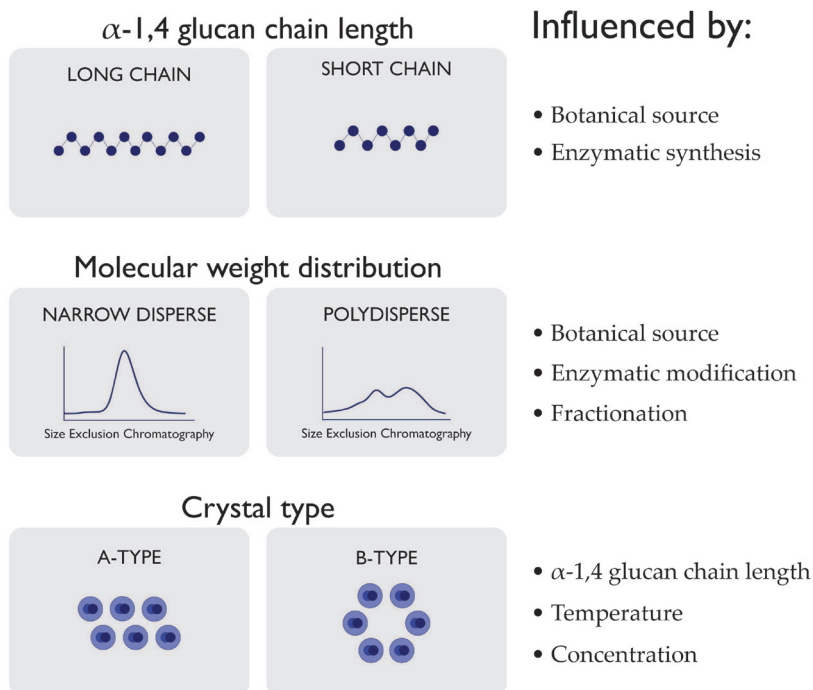


Figure 1.3. Primary characteristics of retrograded starches.

3.3.1. Effects of Mw, Mw distribution and crystal type on RS content

Retrograded starches prepared from partial pullulanase debranched waxy maize, high-amylose maize or waxy rice starch contained RS levels ≤ 29 %^[75-77]. *In vitro* digestion of crystallized fully isoamylase debranched waxy starches of different botanical sources showed that longer chain length α -1,4 glucans, obtained from debranched waxy potato starch, resulted in more resistance to digestion with up to 78 % RS^[55] (Table 1.1). Other studies reported branch-chain elongation of waxy maize, normal maize or amylo maize by amylosucrase, followed by crystallization and reported RS contents of up to 70 %^[78, 79]. Therefore, to obtain high proportions of RS within RS-3 preparations it seems necessary to either fully debranch starches to only obtain α -1,4 linked glucans or to elongate the branch chains to support the formation of double helices and subsequent crystallization.

Re-crystallized debranched normal and waxy rice starch differ in Mw distribution, but this was minorly affecting the resistance to digestion^[59] (Table 1.1), although it should be realized that such α -1,4 glucans also differ in average Mw. So far, no studies reported the resistance to digestion of RS-3 preparations made of α -1,4 glucans with a narrow disperse Mw distribution,

although previously it has been shown that such α -1,4 glucans crystallize perfectly^[69, 70]. The crystal type obtained after re-crystallization was shown to affect the RS content with A-type crystals being more resistant to digestion than B-type crystals of similar Mw^[60, 68] (Table 1.1).

3.1.2. Other processing factors impacting RS content

The resistant starch content of RS-3 preparations can also be affected by treatments after crystallization. Repeated temperature cycles such as boiling and storage at 4 °C for 48 h, or storage at 4 °C followed by storage at either -20 °C, 30 °C or 40 °C did not improve the RS content to more than 38 %^[80, 81]. Other treatments after crystallization such as annealing or heat-moisture treatment increased the RS content to 71 % for debranched cassava or debranched waxy rice starch^[59, 82] (Table 1.1). It is note-worthy that the drying method after crystallization hugely impacts the RS content found after crystallization of RS-3 preparations. Especially freeze-drying and spray-drying cause a lower RS content compared to air-drying^[83, 84].

As shown in Table 1.1, quite some research has been performed on improving the RS content within RS-3 preparations using various physico-chemical parameters. Some RS-3 preparations were shown to be very resistant to upper GIT digestion, with samples containing up to 85 % RS, which are likely to transit to the colon largely intact.

Table 1.1. Digestive properties of RS-3 preparations obtained from debranched starches having different origin, preparation methods and physicochemical properties.

| Effect studied | Botanical source | Crystallization (+ incubation) treatment | Drying treatment | RS ^a content | SDS ^b content | Method used | Crystal Type | Mw (kDa) | Tp ^c °C | Ref. |
|---------------------------------------|------------------|--|------------------|-------------------------|--------------------------|-------------------------|--------------|--------------|--------------------|------|
| Botanical sources | waxy wheat | | | 68 | 14 | | B-type | 4.6 | 100 | |
| | waxy maize | | dried at 40 °C | 68 | 14 | Englyst ^[86] | B-type | 4.7 | 100 | [55] |
| | waxy potato | | | 78 | 9 | | B-type | 5.8 | 116 | |
| | waxy rice | 25 °C, 3 days | dried at 25 °C | 27 | | AOAC | B-type | 7.0 | 84 | |
| | | 50 °C, 6 days | dried at 50 °C | 33 | not reported | method | A-type | 7.0 | 108 | [59] |
| | normal rice | 25 °C, 3 days | dried at 25 °C | 30 | | 2002.02 ^[85] | B-type | 8.4 | 88 | |
| | | 50 °C, 6 days | dried at 50 °C | 33 | | | A-type | 8.4 | 107 | |
| | waxy maize | 24 h 50 °C, 24 h 50 °C | dried at 40 °C | 85 | 10 | Englyst | A-type | 3.9 | 116 | [60] |
| | waxy potato | | | 72 | 15 | | B-type | 5.2 | 104 | |
| | | 50 °C, 24 h | | 85 | 12 | | A-type | 3.9 | 118 | |
| Crystallization temperature | waxy maize | 25 °C, 24 h | dried at 40 °C | 80 | 10 | Englyst | B-type | 3.9 | 92 | [68] |
| | | 4 °C, 24 h | | 78 | 12 | | B-type | 3.9 | 91 | |
| | | 25 °C, 3 days, followed by AT ^d | | 43 | | AOAC | B-type | 7.0 | 88 | |
| | | 50 °C, 6 days, followed by AT | | 68 | not reported | method | A-type | 7.0 | 111 | [59] |
| | waxy rice | 25 °C, 3 days, followed by HMT ^e | dried at 40 °C | 47 | | 2002.02 | A-type | 7.0 | 101 | |
| | | 50 °C, 6 days, followed by HMT | | 71 | | | A-type | 7.0 | 109 | |
| | | three cycles of 30 °C, 5 h and 80 °C for 5 h | | 37 | 45 | | B-type | | 109 | |
| | | three cycles of 30 °C, 5 h and 80 °C for 5 h, followed by AT | | 43 | 38 | | B-type | | 116 | |
| | | three cycles of 30 °C, 5 h and 80 °C for 5 h, followed by HMT | air-dried | 55 | 29 | AOAC 2002.02 | Cb-type | not reported | 116 | [82] |
| | cassava starch | three cycles of 30 °C, 5 h and 80 °C for 5 h, followed by AT --> HMT | | 46 | 25 | | Cb-type | | 118 | |
| Annealing / HMT after crystallization | | three cycles of 30 °C, 5 h and 80 °C for 5 h, followed by HMT --> AT | | 71 | 18 | | B-type | | 115 | |
| | | 4 °C, 7 days | freeze-dried | 10 | 39 | | no crystal | | 79 | |
| | waxy rice | 4 °C, 7 days | dried at 40 °C | 49 | 42 | Englyst | B-type | | 87 | [83] |
| | starch | 4 °C, 7 days | spray-dried | 18 | 52 | | B-type | | 83 | |
| | | | | | | | | | | |
| | | | | | | | | | | |
| | | | | | | | | | | |
| | | | | | | | | | | |
| | | | | | | | | | | |
| | | | | | | | | | | |
| | | | | | | | | | | |
| Effect of drying methods | waxy rice | | | | | | | | | |
| | starch | | | | | | | | | |

^aResistant starch content, ^bslowly digestible starch content, ^cTp: Peak temperature as measured with Differential Scanning Calorimetry, ^dAnnealing treatment, ^eHeat-moisture treatment

4. The starch journey continues through the lower gastro-intestinal tract

4.1. The gut microbiome and its activity

Once starch arrives in the colon, it is subject to fermentation by gut microbiota. The gut microbiome is a complex ecosystem where bacteria, archaea, viruses and eukaryotic microbes reside^[85], with around 10^{11} facultative anaerobe and obligate anaerobe bacteria per gram of faecal material^[86]. In adults, the bacterial phyla that are mostly represented within the gut microbiota are *Bacteroidetes* and *Firmicutes*, with low presence of *Proteobacteria*, *Actinobacteria*, *Fusobacteria* and *Verrucomicrobiota*^[87]. The microbiota composition is very host specific and resilient, and could be disturbed by dietary changes or antibiotics^[88]. It is generally accepted that although there is a wide variation in microbiota composition, the overall function of the microbiome is similar among individuals^[89]. The gut microbiome provides different functionalities for its host, such as fermentation of non-digestible food to metabolites that can be absorbed^[90], the synthesis of vitamins^[91], outcompeting pathogens^[92], strengthening of the intestinal barrier and stimulation and regulation of the immune system^[93, 94].

The fermentation of non-digestible food to metabolites such as short-chain fatty acids (SCFAs), consists of two steps: degradation to smaller sub-units, followed by fermentation. The non-digestible carbohydrates that are reaching the colon are degraded by carbohydrate-active enzymes (CAZymes) expressed by the gut microbiota^[95]. Some bacteria express many different CAZymes, such as members of the *Bacteroidetes* phylum, able to degrade a broad range of substrates, and are thus considered generalists, whereas other bacteria are real specialists, such as some members of the *Firmicutes* phylum^[96].

After degradation of the non-digestible carbohydrates, the mono-sugars or small oligomers are fermented by the gut microbiota to health-beneficial SCFAs such as acetate, propionate and butyrate^[97]. Some bacteria can directly degrade and ferment certain dietary fibres to e.g. acetate and lactate, whereas others rely on cross-feeding to produce propionate and butyrate from acetate, lactate or succinate^[98]. Formation of propionate from sugars is mostly through the succinate pathway^[98], frequently found in *Bacteroidetes* and the *Negativicutes* class of *Firmicutes*^[99]. Butyrate producing species are found in the *Firmicutes* families *Ruminococcaceae*, *Lachnospiraceae*, *Erysipelotrichaceae* and *Clostridiaceae*^[98]. Abundant butyrate-producing species found in the human gut are

Faecalibacterium prausnitzii, *Agathobacter rectalis* [*Eubacterium rectale*], or *Roseburia* species, that produce butyrate via the butyryl-CoA:acetate CoA-transferase pathway^[98]. Additionally, efficient cross-feeding between complex carbohydrate degrading species that produce lactate, and some lactate-utilizing *Firmicutes* species increases the production of butyrate^[100]. Butyrate is essential for health by providing energy to colonocytes^[101] and has been associated with many health benefits^[102, 103] such as modulation of immune and inflammatory responses, stimulation of intestinal barrier function and with the prevention of colorectal cancer^[104]. Fermentation of resistant starch has been associated with elevated butyrate levels^[105, 106] and therefore resistant starch is considered a health-beneficial dietary fibre.

4.2. The fermentability of resistant starch

Several studies have investigated the effect of including resistant starch in the human diet on faecal microbiota composition. These studies either included RS-2 such as raw potato starch granules^[107] or high-amylose maize starch^[106, 108-111], or commercial RS-3 ingredients^[112] like Novelose® 330^[113] and C*Actistar™^[114]. Other studies dealt with pigs or rats fed with resistant starches, such as RS-2 from potato starch^[115] or high-amylose starches^[116-118], or RS-3 from Novelose® 330^[119] or C*Actistar™^[120]. The faecal microbiota composition after a resistant starch intervention differs hugely between studies, but e.g. *Firmicutes*^[109] such as *Ruminococcus*^[109] *bromii*^[107, 108, 110, 112, 113], *Agathobacter rectalis* [*Eubacterium rectale*]^[107, 109, 110, 112], *Faecalibacterium prausnitzii*^[109, 110], *Roseburia*^[112] *faecis*^[109] and several *Clostridium* species^[113] were shown to increase in relative abundance. Furthermore, *Bacteroidetes* such as *Prevotellaceae*^[109], *Bacteroides thetaiotaomicron*^[110] and *Actinobacteria*^[107] such as bifidobacteria^[114] among which *B. adolescentis*^[107] or *Verrucomicrobiota* such as *Akkermansia*^[109] were increased in relative abundance after the intervention. Some studies also analysed the caecal (animal) and faecal SCFA contents and found increased butyrate levels in individuals, although highly variable^[106, 107].

Quantification of the starch throughout the gut was performed in some pig studies, in which it was shown that most of the resistant starch was fully degraded within the digestive tract^[116, 117, 120]. To the best of our knowledge, quantification of starch after *in vivo* studies in human was only performed once^[112]. Here, it was shown that 2 out of the 14 overweight men taking part in the study were unable to fully ferment RS-3 (> 60 % of RS remaining unfermented)^[112], thereby suggesting that resistant starch degrading bacteria might not always be present within the gut microbiome.

4.3. *In vitro* fermentation of resistant starch

In vitro studies can be performed to have a better understanding on the degradation of resistant starch type 3 (ingredients) and fermentation to SCFAs. Some *in vitro* studies investigated fermentability of commercial RS-3 ingredients Novelose® 330^[121] and C*ActistarTM^[121-125], whereas other studies were performed on non-commercial RS-3 rich ingredients^[126-130]. These studies were performed using faecal inocula from primarily adults^[121-126], but also faecal inocula from infants^[124-126] or pigs^[121, 130] were used. From Novelose® 330 (HAMS, B-type^[73]) and C*ActistarTM (partially debranched tapioca starch, A-type^[71]) the physico-chemical characteristics are known, whereas these were less clear for the RS-3 rich ingredients as prepared in other studies^[126-130]. Most of these studies analysed the SCFAs produced, representing the microbial activity. Only two studies investigated the effect of RS-3 on microbiota composition by the means of qPCR^[128] or 16S rRNA gene sequencing^[130]. This illustrates that although great efforts have been performed to improve the resistance to digestion of RS-3 ingredients (Table 1.1), their fermentation in general and their potential to act as a prebiotic i.e. “a substrate that is selectively utilized by host microorganisms conferring a health benefit”^[131] is still mainly unexplored.

5. Enzymatic starch hydrolysis throughout the gastro-intestinal tract

As elaborated, resistant starch is any starch that is not digested in the small intestine and transits to the colon to be subjected to fermentation. This is a rather broad definition that includes both starch (ingredients) that are highly resistant to digestion and “digestible” starches that transit to the colon due to transit time. The latter one could be considered kinetically resistant starch, since such starch is essentially fully digestible by pancreatic α -amylase and α -glucosidase *in vitro*^[132], but depending on other factors it might arrive in the colon *in vivo*. It is likely that hydrolysis of highly resistant starches requires different α -amylases, compared to starch that is kinetically resistant. Within the upper GIT, six host enzymes are recognized able to degrade starch, whereas in the colon, many more starch-active enzymes are present, as expressed by the various bacterial species. The most represented glycoside hydrolase (GH) family within the gut microbiome is family GH13, that harbours the most starch-active enzymes of all families^[95].

Full starch hydrolysis requires multiple enzymes, such as α -amylases, pullulanases and α -glucosidases. Some of the starch-active enzymes possess non-catalytic protein domains called carbohydrate binding modules (CBMs)^[133]. Such CBMs can bind to insoluble starch and therefore provide easier access to the catalytic domain of the starch-active enzyme to achieve hydrolysis. Other α -amylases do not possess such CBMs, but might have surface binding sites (SBSs), which are situated on the catalytic domain and assist in raw starch binding. Furthermore, α -amylases that contain both CBMs and SBSs also exist^[133].

The two main starch-degrading enzymes in the upper GIT are the endo-enzymes salivary α -amylase, primarily active on soluble starch, and pancreatic α -amylase, that is active on both soluble and insoluble starches^[134]. Pancreatic α -amylase also binds to retrograded starches, causing inhibition of the catalytic activity^[135]. Pancreatic α -amylase does not contain CBMs, but contains SBSs^[136-138], that, depending on the SBS, were shown to interact with glycogen, amylose, pullulan^[139] and raw starch^[138]. The brush-border enzymes maltase-glucoamylase and sucrase-isomaltase are exo-acting enzymes, but differ in their specificity^[16] with maltase, gluco-amylase and sucrase being active on α -1,4 linked chains, whereas isomaltase is mostly active on the α -1,6 linked branch point. The four brush-border enzymes are not only hydrolysing maltodextrins released by pancreatic α -amylase to glucose, but were also shown to hydrolyse cooked maize starch, whereas limited activity was found on native maize starch^[140].

Previously, it has been shown that certain bacteria increase in relative abundance when subjects consume a diet high in resistant starch. These bacteria are likely involved in either degradation of the resistant starch directly or they benefit from released soluble sugars or metabolites via cross-feeding^[141]. Soluble starch can be degraded by many different gut microbes, whereas the ability to degrade insoluble starch is more limited^[142, 143]. Known starch-degrading gut microbes include e.g. bifidobacteria^[144], *Ruminococcus bromii*^[143] and *Agathobacter rectalis* [*Eubacterium rectale*]^[145], but also *Bacteroides thetaiotaomicron* is described as a starch-degrader.

Bacteroidetes, such as *Bacteroides* and *Prevotella*, are Gram-negative bacteria that are known for their ability to degrade a broad variety of carbohydrates and are highly present within the adult gut microbiome. These bacteria possess gene clusters called polysaccharide utilization loci (PULs), that encode glycoside hydrolases, glycan-binding proteins and TonB-dependent transporters^[146]. *B. thetaiotaomicron* is a well-studied microbe that is able to hydrolyse and ferment

an enormous collection of different polysaccharides^[147], as illustrated by the presence of 283 glycoside hydrolases among 68 different GH families for e.g. *B. thetaiotaomicron* DSM2079 (Figure 1.4). Starch-utilization system (Sus)-like multiprotein complexes, present in *Bacteroidetes*, bind and partially degrade substrates prior to their transport in the periplasm, where final degradation occurs^[146]. *B. thetaiotaomicron* harbours some starch-active hydrolases in its genome and has been shown to hydrolyse soluble starch, whereas it was unable to degrade insoluble starch^[143].

Bifidobacteria, belonging to the *Actinobacteria* phylum, are known to hydrolyse human-milk oligosaccharides^[148] and galacto-oligosaccharides^[149] in the infant gut, but are also known for their quite broad substrate specificity. Some bifidobacteria, such as *B. breve*, *B. pseudolongum*, *B. infantis*, *B. dentium*, *B. pseudolongum* subsp. *globosum* and *B. thermophilum* can hydrolyse starch, amylopectin and pullulan, and secrete extracellular enzymes in the growth medium^[144]. *Bifidobacterium adolescentis* is present for 1-2 % within the adult gut microbiome^[150] and was shown to increase in relative abundance after consumption of a diet containing resistant starch^[107]. Many *B. adolescentis* strains encode GH13 enzymes and can grow on soluble starch or α -glucans like pullulan or small malto-oligosaccharides^[151], whereas only a few strains, such as *B. adolescentis* P2P3 and *B. adolescentis* L2-32 are able to degrade resistant starch^[143, 152]. Such *B. adolescentis* strains were shown to possess many GH13 enzymes in their genome (Figure 1.4) (17 out of 51 GHs^[44]), together with CBMS like CBM25, 26, 41, 48 and 74 that are associated with insoluble starch binding^[133].

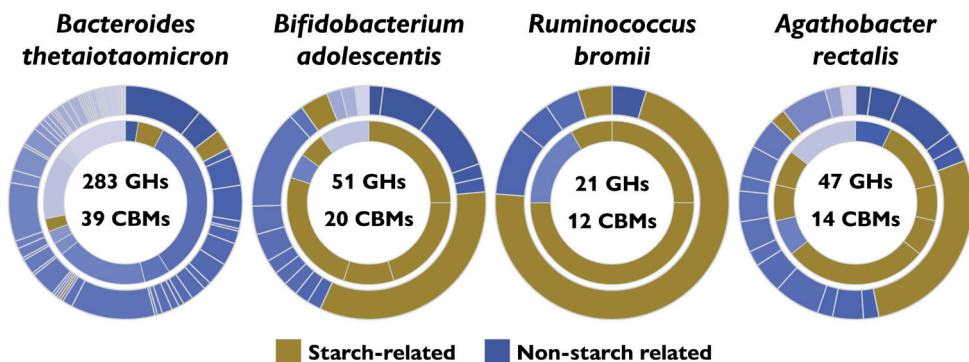


Figure 1.4. Glycoside hydrolases (GHs, outer ring) and carbohydrate binding modules (CBMs, inner ring), encoded in the genomes of *B. thetaiotaomicron* DSM2079, *B. adolescentis* P2P3, *R. bromii* L2-63, *A. rectalis* [*Eubacterium rectale*] DSM17629^[44]. GH-enzymes and CBMs being starch-related and being non-starch related are indicated.

Ruminococcus bromii, belonging to the *Firmicutes* phylum, is a well-known starch-degrading gut microbe^[143] and considered a real starch-degrading specialist as illustrated by encoding only 21 glycoside hydrolases of which 16 are starch-degrading enzymes (15 GH13 and 1 GH77) in strain L2-63 (Figure 1.4, CAZy database^[44]). *R. bromii* produces a multi-protein complex consisting of different amylases and starch-binding proteins (so-called amylosome)^[153] enabling it to fully hydrolyse insoluble starches to glucose and maltose^[143]. The exact starch-degrading machinery of *R. bromii* is not fully understood yet, but it is known that e.g. *R. bromii* L2-63 encodes 3 CBMs 26, 6 CBMs 48 and 1 CBM74 (CAZy database^[44]), associated with insoluble starch binding^[133, 154].

Agathobacter rectalis [*Eubacterium rectale*] and some *Roseburia* species, belonging to the *Firmicutes* phylum, are starch-degrading^[145, 155, 156] and butyrate producing^[157] gut microbes, abundantly present in the adult gut^[150]. *A. rectalis* possesses one extracellular α -amylase with five CBMs (CBM82, CBM26, CBM26, CBM41 and CBM83) encoded on the same protein^[158] that have been shown to bind to raw maize, but only minor to raw potato starch^[159]. *A. rectalis* can degrade and ferment soluble starch, but has limited capacity to degrade insoluble starches directly. *A. rectalis* benefits from insoluble starch degradation by *R. bromii* when incubated together^[143], which might result in enhanced butyrate production as observed when both *R. bromii* and *A. rectalis* increased in relative abundance in individuals consuming raw potato starch^[107].

6. Thesis outline

In almost all studies published before 2018, i.e., the starting period of this project, commercial ingredients like Novelose® 330 or C*Actistar™ were used in fermentation studies to investigate the prebiotic potential of RS-3. Although the effect of RS-3 physico-chemical properties on *in vitro* digestibility became more clear in the recent decade, and highly resistant RS-3 ingredients (> 85 % RS^[60]) were prepared, the prebiotic potential of such ingredients still requires investigation. Furthermore, previous research investigated the effect of Mw and/or crystal type, together with other thermal treatments for increasing the proportion of RS within RS-3 ingredients. The effect of Mw distribution of the α -1,4 glucans crystallized into RS-3 preparations on *in vitro* digestion and fermentation has not yet been discovered. In **Chapter 2**, we describe how α -1,4 glucan chain length, Mw distribution and crystal type of RS-3 preparations affect *in vitro* digestibility. For this purpose, we crystallized α -1,4 glucans of different chain length and Mw distribution, obtained by debranching waxy starches of different (modified) botanical sources or enzymatic synthesis, into RS-3 preparations with an A- or B-type polymorph. Some of these RS-3 preparations were highly resistant to digestion and were fermentable *in vitro* using pooled adult faecal inoculum as described in **Chapter 3**. Other RS-3 preparations as described in **Chapter 2**, contained a larger fraction of digestible starch and were subjected to fermentation to address the need for pre-digestion when studying the fermentability of RS-3 preparations *in vitro* (**Chapter 4**). To investigate if (highly resistant) RS-3 preparations were potential prebiotics for piglets, we also incubated selected substrates with pre- and post-weaning piglet faecal microbiota of which the results are described in **Chapter 5**. Since we found that highly resistant RS-3 preparations were difficult to degrade by most inocula (**Chapter 3-5**), we investigated the fermentability of these highly resistant RS-3 preparations using mono-cultures of well-known RS-degraders *B. adolescentis* and *R. bromii* (**Chapter 6**). Finally, in **Chapter 7**, the results obtained in this research are discussed and compared to recent literature. Furthermore, some additional findings are presented and future perspectives regarding the prebiotic potential of highly resistant RS-3 are discussed.

7. References

1. Perez S., Bertoft E. The molecular structures of starch components and their contribution to the architecture of starch granules: A comprehensive review. *Starch-Starke*. **2010**;62(8):389-420.
2. Torruco-Uco J.G., Chávez-Murillo C.E., Hernández-Centeno F., Salgado-Delgado R., Tirado-Gallegos J.M., Zamudio-Flores P.B. Use of High-Performance Size-Exclusion Chromatography for characterization of amylose Isolated from diverse botanical sources. *International Journal of Food Properties*. **2016**;19(6):1362-1369.
3. Bello-Pérez L.A., Rodríguez-Ambríz S.L., Agama-Acevedo E., Sanchez-Rivera M.M. Solubilization effects on molecular weights of amylose and amylopectins of normal maize and barley starches. *Cereal Chemistry*. **2009**;86(6):701-705.
4. Chung H.J., Liu Q. Impact of molecular structure of amylopectin and amylose on amylose chain association during cooling. *Carbohydrate Polymers*. **2009**;77(4):807-815.
5. Bello-Perez L.A., Paredes-Lopez O.R.P., Colonna P. Molecular characterization of some amylopectins. *Cereal Chemistry*. **1996**:12-17.
6. Tester R.F., Karkalas J., Qi X. Starch—composition, fine structure and architecture. *Journal of Cereal Science*. **2004**;39(2):151-165.
7. Hanashiro I., Abe J., Hizukuri S. A periodic distribution of the chain length of amylopectin as revealed by high-performance anion-exchange chromatography. *Carbohydrate Research*. **1996**;283:151-159.
8. Bertoft E., Piyachomkwan K., Chatakanonda P., Sriroth K. Internal unit chain composition in amylopectins. *Carbohydrate Polymers*. **2008**;74(3):527-543.
9. Hanashiro I., Tagawa M., Shibahara S., Iwata K., Takeda Y. Examination of molar-based distribution of A, B and C chains of amylopectin by fluorescent labeling with 2-aminopyridine. *Carbohydrate Research*. **2002**;337(13):1211-1215.
10. Lopez-Rubio A., Flanagan B.M., Gilbert E.P., Gidley M.J. A novel approach for calculating starch crystallinity and its correlation with double helix content: a combined XRD and NMR study. *Biopolymers*. **2008**;89(9):761-768.
11. Martens B.M.J., Gerrits W.J.J., Bruininx E., Schols H.A. Amylopectin structure and crystallinity explains variation in digestion kinetics of starches across botanic sources in an in vitro pig model. *Journal of Animal Science and Biotechnology*. **2018**;9:91.
12. Jane J.L., Kasemsuwan T., Leas S., Zobel H., Robyt J.F. Anthology of starch granule morphology by scanning electron microscopy. *Starch-Starke*. **1994**;46(4):121-162.
13. Wang K., Hasjim J., Wu A.C., Henry R.J., Gilbert R.G. Variation in amylose fine structure of starches from different botanical sources. *Journal of Agricultural and Food Chemistry*. **2014**;62(19):4443-4453.
14. Schirmer M., Jekle M., Becker T. Starch gelatinization and its complexity for analysis. *Starch-Starke*. **2015**;67(1-2):30-41.
15. Jalabert-Malbos M.-L., Mishellany-Dutour A., Woda A., Peyron M.-A. Particle size distribution in the food bolus after mastication of natural foods. *Food Quality and Preference*. **2007**;2007(5):803-812.
16. Lee B.H., Bello-Pérez L.A., Lin A.H.M., Kim C.Y., Hamaker B.R. Importance of location of digestion and colonic fermentation of starch related to its quality. *Cereal Chemistry*. **2013**;90(4):335-343.
17. Martens B.M.J., Bruininx E.M.A.M., Gerrits W.J., Schols H.A. The importance of amylase action in the porcine stomach to starch digestion kinetics. *Animal Feed Science and Technology*. **2020**;267:114546.
18. Freitas D., Le Feunteun S. Oro-gastro-intestinal digestion of starch in white bread, wheat-based and gluten-free pasta: Unveiling the contribution of human salivary alpha-amylase. *Food Chemistry*. **2019**;274:566-573.

19. Freitas D., Le Feunteun S., Panouille M., Souchon I. The important role of salivary α -amylase in the gastric digestion of wheat bread starch. *Food & Function*. **2018**;9:200-208.
20. Koziolok M., Schneider F., Grimm M., Modebeta C., Seekamp A., Roustom T., Siegmund W., Weitschies W. Intra gastric pH and pressure profiles after intake of the high-caloric, high-fat meal as used for food effect studies. *Journal of Controlled Release*. **2015**;220(Pt A):71-78.
21. Dressman J.B., Berardi R.R., Dermentzoglou L.C., Russell T.L., Schmaltz S.P., Barnett J.L., Jarvenpaa K.M. Upper gastrointestinal (GI) pH in young, healthy men and women. *Pharmaceutical Research*. **1990**;7(7):756-761.
22. Brownlee I.A., Gill S., Wilcox M.D., Pearson J.P., Chater P.I. Starch digestion in the upper gastrointestinal tract of humans. *Starch-Starke*. **2018**;70(9-10):1700111.
23. Schneider F., Grimm M., Koziolok M., Modess C., Dokter A., Roustom T., Siegmund W., Weitschies W. Resolving the physiological conditions in bioavailability and bioequivalence studies: Comparison of fasted and fed state. *European Journal of Pharmaceutics and Biopharmaceutics*. **2016**;108:214-219.
24. Maljaars P.W., Peters H.P., Mela D.J., Masclee A.A. Ileal brake: a sensible food target for appetite control. A review. *Physiology and Behavior*. **2008**;95(3):271-281.
25. Parada J., Aguilera J.M. Microstructure, mechanical properties, and starch digestibility of a cooked dough made with potato starch and wheat gluten. *LWT - Food Science and Technology*. **2011**;44(8):1739-1744.
26. Ye J., Hu X., Luo S., McClements D.J., Liang L., Liu C. Effect of endogenous proteins and lipids on starch digestibility in rice flour. *Food Research International*. **2018**;106:404-409.
27. Jenkins D.J., Wolever T.M., Leeds A.R., Gassull M.A., Haisman P., Dilawari J., Goff D.V., Metz G.L., Alberti K.G. Dietary fibres, fibre analogues, and glucose tolerance: importance of viscosity. *British Medical Journal*. **1978**;1(6124):1392-1394.
28. Koh L.W., Kasapis S., Lim K.M., Foo C.W. Structural enhancement leading to retardation of in vitro digestion of rice dough in the presence of alginate. *Food Hydrocolloids*. **2009**;23(6):1458-1464.
29. Luo K., Zhang G. Nutritional property of starch in a whole-grain-like structural form. *Journal of Cereal Science*. **2018**;79:113-117.
30. Bordoloi A., Singh J., Kaur L. In vitro digestibility of starch in cooked potatoes as affected by guar gum: Microstructural and rheological characteristics. *Food Chemistry*. **2012**;133(4):1206-1213.
31. Regand A., Chowdhury Z., Tosh S.M., Wolever T.M.S., Wood P. The molecular weight, solubility and viscosity of oat beta-glucan affect human glycemic response by modifying starch digestibility. *Food Chemistry*. **2011**;129(2):297-304.
32. Al Kazaz M., Desseaux V., Marchis-Mouren G., Prodanov E., Santimone M. The mechanism of porcine pancreatic α -amylase: Inhibition of maltopentaose hydrolysis by acarbose, maltose and maltotriose. *European Journal of Biochemistry*. **1998**;252(1):100-107.
33. Lochocka K., Bajerska J., Glapa A., Fidler-Witon E., Nowak J.K., Szczapa T., Grebowiec P., Lisowska A., Walkowiak J. Green tea extract decreases starch digestion and absorption from a test meal in humans: a randomized, placebo-controlled crossover study. *Scientific Reports*. **2015**;5:12015.
34. Minekus M., Alminger M., Alvito P., Ballance S., Bohn T., Bourlieu C., Carriere F., Boutrou R., Corredig M., Dupont D., Dufour C., Egger L., Golding M., Karakaya S., Kirkhus B., Le Feunteun S., Lesmes U., Macierzanka A., Mackie A., Marze S., McClements D.J., Menard O., Recio I., Santos C.N., Singh R.P., Vegarud G.E., Wickham M.S., Weitschies W., Brodtkorb A. A standardised static in vitro digestion method suitable for food - an international consensus. *Food & Function*. **2014**;5(6):1113-1124.
35. Bustos M.C., Vignola M.B., Pérez G.T., León A.E. In vitro digestion kinetics and bioaccessibility of starch in cereal food products. *Journal of Cereal Science*. **2017**;77:243-250.

36. Englyst H.N., Kingman S.M., Cummings J.H. Classification and measurement of nutritionally important starch fractions. *European Journal of Clinical Nutrition*. **1992**;46 Suppl 2:S33-50.
37. Dhital S., Warren F.J., Butterworth P.J., Ellis P.R., Gidley M.J. Mechanisms of starch digestion by alpha-amylase-structural basis for kinetic properties. *Critical Reviews in Food Science and Nutrition*. **2017**;57(5):875-892.
38. Birt D.F., Boylston T., Hendrich S., Jane J.L., Hollis J., Li L., McClelland J., Moore S., Phillips G.J., Rowling M., Schalinske K., Scott M.P., Whitley E.M. Resistant starch: promise for improving human health. *Advances in Nutrition*. **2013**;4(6):587-601.
39. Lopez-Rubio A., Flanagan B.M., Shrestha A.K., Gidley M.J., Gilbert E.P. Molecular rearrangement of starch during in vitro digestion: toward a better understanding of enzyme resistant starch formation in processed starches. *Biomacromolecules*. **2008**;9(7):1951-1958.
40. Teng A., Witt T., Wang K., Li M., Hasjim J. Molecular rearrangement of waxy and normal maize starch granules during in vitro digestion. *Carbohydrate Polymers*. **2016**;139:10-19.
41. Wang S., Copeland L., Niu Q., Wang S. Starch Retrogradation: A Comprehensive Review. *Comprehensive Reviews in Food Science and Food Safety*. **2015**;14(5):568-585.
42. Kaur B., Ariffin F., Bhat R., Karim A.A. Progress in starch modification in the last decade. *Food Hydrocolloids*. **2012**;26(2):398-404.
43. Chang A., Jeske L., Ulbrich S., Hofmann J., Koblit J., Schomburg I., Neumann-Schaal M., Jahn D., Schomburg D. BRENDA, the ELIXIR core data resource in 2021: new developments and updates. *Nucleic Acids Research*. **2021**;49(D1):D498-D508.
44. Drula E., Garron M.L., Dogan S., Lombard V., Henrissat B., Terrapon N. The carbohydrate-active enzyme database: functions and literature. *Nucleic Acids Research*. **2022**;50(D1):D571-D577.
45. Kim E.J., Ryu S.I., Bae H.A., Huong N.T., Lee S.B. Biochemical characterisation of a glycogen branching enzyme from *Streptococcus mutans*: Enzymatic modification of starch. *Food Chemistry*. **2008**;110(4):979-984.
46. Fan Q., Xie Z., Zhan J., Chen H., Tian Y. A glycogen branching enzyme from *Thermomonospora curvata*: Characterization and its action on maize starch. *Starch-Starke*. **2016**;68(3-4):355-364.
47. van der Maarel M., Leemhuis H. Starch modification with microbial alpha-glucanotransferase enzymes. *Carbohydrate Polymers*. **2013**;93(1):116-121.
48. Ciric J., Loos K. Synthesis of branched polysaccharides with tunable degree of branching. *Carbohydrate Polymers*. **2013**;93(1):31-37.
49. Kaper T., van der Maarel M.J., Euverink G.J., Dijkhuizen L. Exploring and exploiting starch-modifying amylomaltases from thermophiles. *Biochemical Society Transactions*. **2004**;32(Pt 2):279-282.
50. van der Maarel M., Capron I., Euverink G.W., Bos H., Kaper T., Binnema D.J., Steeneken P. A novel thermoreversible gelling product made by enzymatic modification of starch. *Starch-Starke*. **2005**;57(10):465-472.
51. Rolland-Sabate A., Collona P., Potocki-Veronese G., Monsan P., Planchot V. Elongation and insolubilisation of α -glucans by the action of *Neisseria polysaccharia* amylosucrase. *Journal of Cereal Science*. **2004**;40(1):17-30.
52. Potocki-Veronese G., Putaux J.L., Dupeyre D., Albenne C., Remaud-Simeon M., Monsan P., Buleon A. Amylose synthesized in vitro by amylosucrase: morphology, structure, and properties. *Biomacromolecules*. **2005**;6(2):1000-1011.
53. Kadokawa J. Precision polysaccharide synthesis catalyzed by enzymes. *Chemical Reviews*. **2011**;111(7):4308-4345.
54. Ohdan K., Fujii K., Yanase M., Takaha T., Kuriki T. Enzymatic synthesis of amylose. *Biocatalysis and Biotransformation*. **2006**;24(1-2):77-81.

55. Cai L.M., Shi Y.C. Structure and digestibility of crystalline short-chain amylose from debranched waxy wheat, waxy maize, and waxy potato starches. *Carbohydrate Polymers*. **2010**;79(4):1117-1123.
56. Van der Maarel M.J.E.C., Binnema D.J., Semeijn C., Buwalda P.L., inventors Novel slowly digestible storage carbohydrate patent EP1943908. **2007**.
57. Van der Maarel M.J.E.C., Capron I., Euverink G.J., Bos H.T., Kaper T., Binnema D.J., Steeneken P.A.M. A novel thermoreversible gelling product made by enzymatic modification of starch. *Starch-Starke*. **2005**;57(10):465-520.
58. Roger P., Axelos M.A.V., Colonna P. SEC-MALLS and SANS studies applied to solution behavior of linear alpha-glucans. *Macromolecules*. **2000**;33(7):2446-2455.
59. Kiatponglaip W., Tongta S., Rolland-Sabate A., Buleon A. Crystallization and chain reorganization of debranched rice starches in relation to resistant starch formation. *Carbohydrate Polymers*. **2015**;122:108-114.
60. Cai L.M., Shi Y.C. Preparation, structure, and digestibility of crystalline A- and B-type aggregates from debranched waxy starches. *Carbohydrate Polymers*. **2014**;105:341-350.
61. Chang R., Xiong L., Li M., Liu J., Wang Y., Chen H., Sun Q. Fractionation of debranched starch with different molecular weights via edible alcohol precipitation. *Food Hydrocolloids*. **2018**;83:430-437.
62. Zeng H., Chen P., Chen C., Huang C., Lin S., Zheng B., Zhang Y. Structural properties and prebiotic activities of fractionated lotus seed resistant starches. *Food Chemistry*. **2018**;251:33-40.
63. Popov D., Buléon A., Burghammer M., Chanzy H., Montesanti N., Puteaux J.-L., Potocki-Veronese G., Riekel C. Crystal structure of A-amylose: a revisit from synchrotron microdiffraction analysis of single crystals. *Macromolecules*. **2009**;42(4):1167-1174.
64. Gidley M.J., Bulpin P.V. Crystallization of maltooligosaccharides as models of the crystalline forms of starch - minimum chain-length requirement for the formation of double helices. *Carbohydrate Research*. **1987**;161(2):291-300.
65. Nishiyama Y., Putaux J.L., Montesanti N., Hazemann J.L., Rochas C. B→A Allomorphic transition in native starch and amylose spherocrystals monitored by in situ synchrotron X-ray diffraction. *Biomacromolecules*. **2010**;11(1):76-87.
66. Buleon A., Veronese G., Putaux J.L. Self-association and crystallization of amylose. *Australian Journal of Chemistry*. **2007**;60(10):706-718.
67. Pfannemuller B. Influence of chain-length of short monodisperse amyloses on the formation of A-type and B-type X-Ray-Diffraction patterns. *International Journal of Biological Macromolecules*. **1987**;9(2):105-108.
68. Cai L.M., Shi Y.C. Self-assembly of short linear chains to A- and B-type starch spherulites and their enzymatic digestibility. *Journal of Agricultural and Food Chemistry*. **2013**;61(45):10787-10797.
69. Kobayashi K., Kimura S., Naito P.K., Togawa E., Wada M. Thermal expansion behavior of A- and B-type amylose crystals in the low-temperature region. *Carbohydrate Polymers*. **2015**;131:399-406.
70. Montesanti N., Veronese G., Buleon A., Escalier P.C., Kitamura S., Putaux J.L. A-type crystals from dilute solutions of short amylose chains. *Biomacromolecules*. **2010**;11(11):3049-3058.
71. Kettlitz B.W., Coppin J.V.J.M., Roper H.W.W., Bornet F., inventors Highly fermentable resistant starch. U.S. patent No. 6,043,229. **2000**.
72. Fassler C., Arrigoni E., Venema K., Hafner V., Brouns F., Amado R. Digestibility of resistant starch containing preparations using two in vitro models. *European Journal of Nutrition*. **2006**;45(8):445-453.
73. Jacobasch G., Dongowski G., Schmiedl D., Muller-Schmehl K. Hydrothermal treatment of Novelose 330 results in high yield of resistant starch type 3 with beneficial prebiotic

- properties and decreased secondary bile acid formation in rats. *British Journal of Nutrition*. **2006**;95(6):1063-1074.
74. Aravind N., Sissons M., Fellows C.M., Blazek J., Gilbert E.P. Optimisation of resistant starch II and III levels in durum wheat pasta to reduce in vitro digestibility while maintaining processing and sensory characteristics. *Food Chemistry*. **2013**;136(2):1100-1109.
 75. Liu W., Hong Y., Gu Z., Cheng L., Li Z., Li C. In structure and in-vitro digestibility of waxy corn starch debranched by pullulanase. *Food Hydrocolloids*. **2017**;67:104-110.
 76. Zhang B., CHen L., Zhao Y., Li X. Structure and enzymatic resistivity of debranched high temperature-pressure treated high-amylose corn starch. *Journal of Cereal Science*. **2013**;57(3):348-355.
 77. Shi M.-M., Gao Q.-Y. Physicochemical properties, structure and in vitro digestion of resistant starch from waxy rice starch. *Carbohydrate Polymers*. **2011**;84(3):1151-1157.
 78. Ryu J.H., Lee B.H., Seo D.H., Baik M.Y., Park C.S., Wang R., Yoo S.H. Production and characterization of digestion-resistant starch by the reaction of *Neisseria polysaccharea* amylsucrase. *Starch-Starke*. **2010**;62(5):221-228.
 79. Zhang H., Zhou X., Wang T., He J., Yue M., Luo X.H., Wang L., Wang R., Chen Z.X. Enzymatically modified waxy corn starch with amylsucrase: The effect of branch chain elongation on structural and physicochemical properties. *Food Hydrocolloids*. **2017**;63:518-524.
 80. Zeng F., Ma F., Gao Q., Yu S., Kong F., Zhu S. Debranching and temperature-cycled crystallization of waxy rice starch and their digestibility. *Carbohydrate Polymers*. **2014**;113:91-96.
 81. Zeng F., Chen F.Q., Kong F.S., Gao Q.Y., Aadil R.M., Yu S.J. Structure and digestibility of debranched and repeatedly crystallized waxy rice starch. *Food Chemistry*. **2015**;187:348-353.
 82. Boonna S., Tongta S. Structural transformation of crystallized debranched cassava starch during dual hydrothermal treatment in relation to enzyme digestibility. *Carbohydrate Polymers*. **2018**;191:1-7.
 83. Zeng F., Zhu S.M., Chen F.Q., Gao Q.Y., Yu S.J. Effect of different drying methods on the structure and digestibility of short chain amylose crystals. *Food Hydrocolloids*. **2016**;52:721-731.
 84. Agama-Acevedo E., Pacheco-Vargas G., Bello-Pérez L.A., Alvarez-Ramirez J. Effect of drying method and hydrothermal treatment of pregelatinized Hylon VII starch on resistant starch content. *Food Hydrocolloids*. **2018**;77:817-824.
 85. Shreiner A.B., Kao J.Y., Young V.B. The gut microbiome in health and in disease. *Current Opinion in Gastroenterology*. **2015**;31(1):69-75.
 86. Cani P.D. Human gut microbiome: hopes, threats and promises. *Gut*. **2018**;67(9):1716-1725.
 87. Eckburg P.B., Bik E.M., Bernstein C.N., Purdom E., Dethlefsen L., Sargent M., Gill S.R., Nelson K.E., Relman D.A. Diversity of the human intestinal microbial flora. *Science*. **2005**;308(5728):1635-1638.
 88. Fassarella M., Blaak E.E., Penders J., Nauta A., Smidt H., Zoetendal E.G. Gut microbiome stability and resilience: elucidating the response to perturbations in order to modulate gut health. *Gut*. **2021**;70(3):595-605.
 89. Human Microbiome Project C. Structure, function and diversity of the healthy human microbiome. *Nature*. **2012**;486(7402):207-214.
 90. Tabernero M., Gómez de Cédron M. Microbial metabolites derived from colonic fermentation of non-digestible compounds. *Current Opinion in Food Science*. **2017**;13:91-96.
 91. LeBlanc J.G., Milani C., Savoy de Giori G., Sesma F., Van Sinderen D., Ventura M. Bacteria as vitamin suppliers to their host: a gut microbiota perspective. *Current Opinion in Biotechnology*. **2013**;24(2):160-168.
 92. Strecher B., Hardt W.-D. Mechanisms controlling pathogen colonization of the gut. *Current Opinion in Microbiology*. **2011**;14(1):82-91.

93. Heintz-Buschart A., Wilmes P. Human gut microbiome: function matters. *Trends in Microbiology*. **2018**;26(7):563-574.
94. Takiishi T., Fenero, C. I. M., & Câmara, N. O. S. Intestinal barrier and gut microbiota: Shaping our immune responses throughout life. *Tissue barriers*. **2017**;5(4):e1373208.
95. El Kaoutari A., Armougom F., Gordon J.I., Raoult D., Henrissat B. The abundance and variety of carbohydrate-active enzymes in the human gut microbiota. *Nature Reviews Microbiology*. **2013**;11(7):497-504.
96. Cockburn D.W., Koropatkin N.M. Polysaccharide degradation by the intestinal microbiota and its influence on human health and disease. *Journal of Molecular Biology*. **2016**;428(16):3230-3252.
97. Rios-Covian D., Ruas-Madiedo P., Margolles A., Gueimonde M., de Los Reyes-Gavilan C.G., Salazar N. Intestinal short chain fatty acids and their link with diet and human health. *Frontiers in Microbiology*. **2016**;7:185.
98. Louis P., Flint H.J. Formation of propionate and butyrate by the human colonic microbiota. *Environmental Microbiology*. **2017**;19(1):29-41.
99. Reichardt N., Duncan S.H., Young P., Belenguer A., McWilliam Leitch C., Scott K.P., Flint H.J., Louis P. Phylogenetic distribution of three pathways for propionate production within the human gut microbiota. *The ISME Journal*. **2014**;8(6):1323-1335.
100. Belenguer A., Duncan S.H., Calder A.G., Holtrop G., Louis P., Lobley G.E., Flint H.J. Two routes of metabolic cross-feeding between *Bifidobacterium adolescentis* and butyrate-producing anaerobes from the human gut. *Applied Environmental Microbiology*. **2006**;72(5):3593-3599.
101. Fu X., Liu Z., Zhu C., Mou H., Kong Q. Nondigestible carbohydrates, butyrate, and butyrate-producing bacteria. *Critical Reviews in Food Science & Nutrition*. **2019**;59(sup1):S130-S152.
102. McNabney S.M., Henagan T.M. Short chain fatty acids in the colon and peripheral tissues: a focus on butyrate, colon cancer, obesity and insulin resistance. *Nutrients*. **2017**;9(12).
103. Liu H., Wang J., He T., Becker S., Zhang G., Li D., Ma X. Butyrate: a double-edged sword for health? *Advances in Nutrition*. **2018**;9(1):21-29.
104. Chen J., Vitetta L. Inflammation-modulating effect of butyrate in the prevention of colon cancer by dietary fiber. *Clinical Colorectal Cancer*. **2018**;17(3):e541-e544.
105. Brouns F., Kettlitz B., Arrigoni E. Resistant starch and “the butyrate revolution”. *Trends in Food Science & Technology*. **2002**;13(8):251-261.
106. McOrist A.L., Miller R.B., Bird A.R., Keogh J.B., Noakes M., Topping D.L., Conlon M.A. Fecal butyrate levels vary widely among individuals but are usually increased by a diet high in resistant starch. *Journal of Nutrition*. **2011**;141(5):883-889.
107. Venkataraman A., Sieber J.R., Schmidt A.W., Waldron C., Theis K.R., Schmidt T.M. Variable responses of human microbiomes to dietary supplementation with resistant starch. *Microbiome*. **2016**;4(1):33.
108. Martínez I., Kim J., Duffy P.R., Schlegel V.L., Walter J. Resistant starches types 2 and 4 have differential effects on the composition of the fecal microbiota in human subjects. *PLoS One*. **2010**;5(11):e15046.
109. Maier T.V., Lucio M., Lee L.H., VerBerkmoes N.C., Brislawn C.J., Bernhardt J., Lamendella R., McDermott J.E., Bergeron N., Heinzmann S.S., Morton J.T., Gonzalez A., Ackermann G., Knight R., Riedel K., Krauss R.M., Schmitt-Kopplin P., Jansson J.K. Impact of dietary resistant starch on the human gut microbiome, metaproteome, and metabolome. *mBio*. **2017**;8(5).
110. Abell G.C., Cooke C.M., Bennett C.N., Conlon M.A., McOrist A.L. Phylotypes related to *Ruminococcus bromii* are abundant in the large bowel of humans and increase in response to a diet high in resistant starch. *FEMS Microbiology Ecology*. **2008**;66(3):505-515.
111. Ordiz M.I., May T.D., Mihindukulasuriya K., Martin J., Crowley J., Tarr P.I., Ryan K., Mortimer E., Gopalsamy G., Maleta K., Mitreva M., Young G., Manary M.J. The effect of

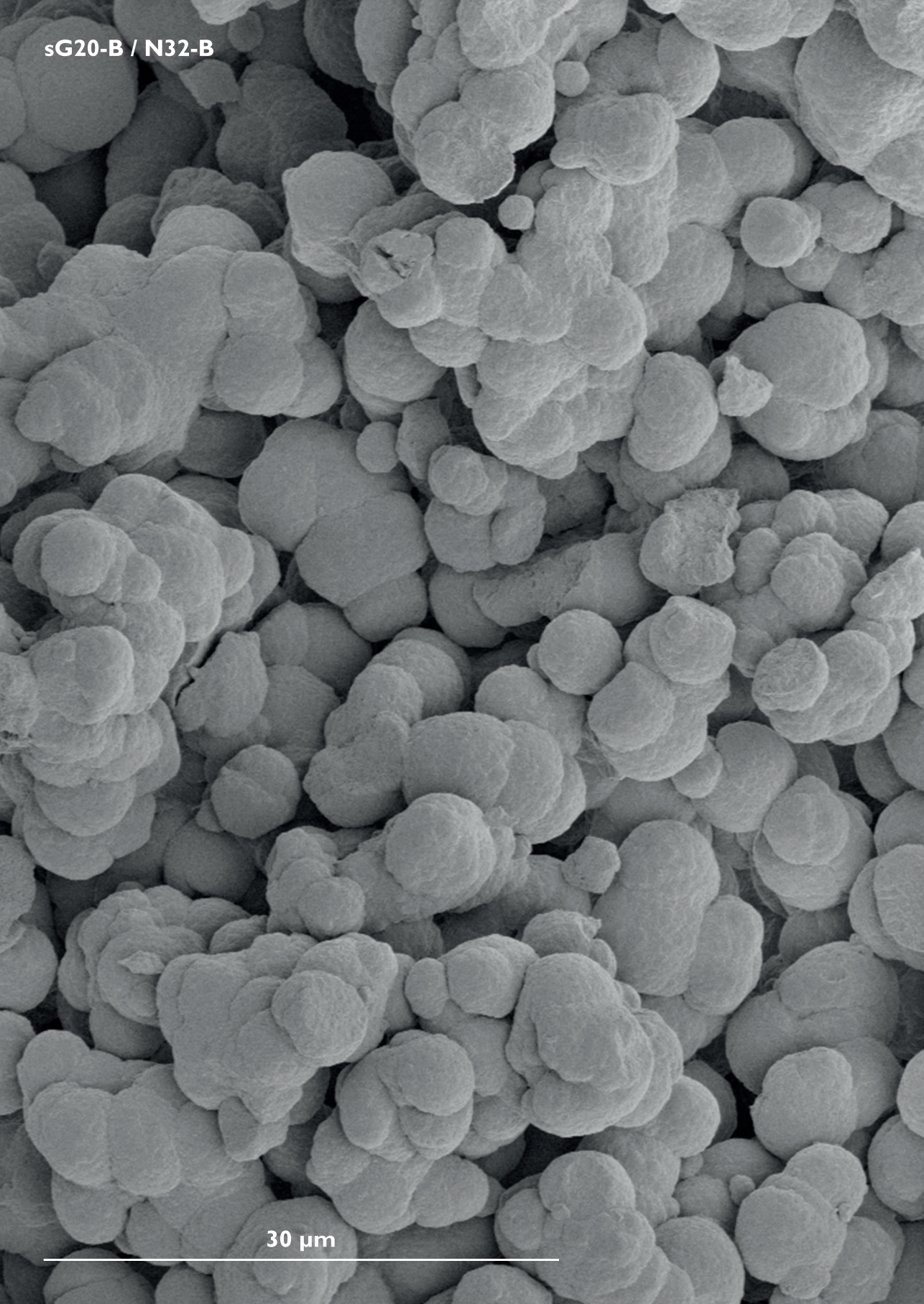
- dietary resistant starch type 2 on the microbiota and markers of gut inflammation in rural Malawi children. *Microbiome*. **2015**;3:37.
112. Walker A.W., Ince J., Duncan S.H., Webster L.M., Holtrop G., Ze X., Brown D., Stares M.D., Scott P., Bergerat A., Louis P., McIntosh F., Johnstone A.M., Lobley G.E., Parkhill J., Flint H.J. Dominant and diet-responsive groups of bacteria within the human colonic microbiota. *The ISME Journal*. **2011**;5(2):220-230.
 113. Salonen A., Lahti L., Salojärvi J., Holtrop G., Korpela K., Duncan S.H., Date P., Farquharson F., Johnstone A.M., Lobley G.E., Louis P., Flint H.J., de Vos W.M. Impact of diet and individual variation on intestinal microbiota composition and fermentation products in obese men. *The ISME Journal*. **2014**;8(11):2218-2230.
 114. Bouhnik Y., Raskine L., Simoneau G., Vicaud E., Neut C., Flourie B., Brouns F., Bornet F.R. The capacity of nondigestible carbohydrates to stimulate fecal bifidobacteria in healthy humans: a double-blind, randomized, placebo-controlled, parallel-group, dose-response relation study. *The American Journal of Clinical Nutrition*. **2004**;80(6):1658-1664.
 115. Sun Y., Su Y., Zhu W. Microbiome-metabolome responses in the cecum and colon of pig to a high resistant starch diet. *Frontiers in Microbiology*. **2016**;7:779.
 116. Foubse J.M., Ganzle M.G., Regmi P.R., van Kempen T.A., Zijlstra R.T. High amylose starch with low in vitro digestibility stimulates hindgut fermentation and has a bifidogenic effect in weaned pigs. *Journal of Nutrition*. **2015**;145(11):2464-2470.
 117. Regmi P.R., Metzler-Zebeli B.U., Ganzle M.G., van Kempen T.A., Zijlstra R.T. Starch with high amylose content and low in vitro digestibility increases intestinal nutrient flow and microbial fermentation and selectively promotes bifidobacteria in pigs. *Journal of Nutrition*. **2011**;141(7):1273-1280.
 118. Tachon S., Zhou J., Keenan M., Martin R., Marco M.L. The intestinal microbiota in aged mice is modulated by dietary resistant starch and correlated with improvements in host responses. *FEMS Microbiology Ecology*. **2013**;83(2):299-309.
 119. Umu O.C., Frank J.A., Fangel J.U., Oostindjer M., da Silva C.S., Bolhuis E.J., Bosch G., Willats W.G., Pope P.B., Diep D.B. Resistant starch diet induces change in the swine microbiome and a predominance of beneficial bacterial populations. *Microbiome*. **2015**;3:16.
 120. Haenen D., Zhang J., Souza da Silva C., Bosch G., van der Meer I.M., van Arkel J., van den Borne J.J., Perez Gutierrez O., Smidt H., Kemp B., Muller M., Hooiveld G.J. A diet high in resistant starch modulates microbiota composition, SCFA concentrations, and gene expression in pig intestine. *Journal of Nutrition*. **2013**;143(3):274-283.
 121. Jonathan M.C., Borne J.J., van Wiechen P., da Silva C.S., Schols H.A., Gruppen H. In vitro fermentation of 12 dietary fibres by faecal inoculum from pigs and humans. *Food Chemistry*. **2012**;133(3):889-897.
 122. Fassler C., Arrigoni E., Venema K., Brouns F., Amado R. In vitro fermentability of differently digested resistant starch preparations. *Molecular Nutrition & Food Research*. **2006**;50(12):1220-1228.
 123. Fassler C., Gill C.I., Arrigoni E., Rowland I., Amado R. Fermentation of resistant starches: influence of in vitro models on colon carcinogenesis. *Nutrition and Cancer*. **2007**;58(1):85-92.
 124. Scheiwiller J., Arrigoni E., Brouns F., Amado R. Human faecal microbiota develops the ability to degrade type 3 resistant starch during weaning. *Journal of Pediatric Gastroenterology and Nutrition*. **2006**;43(5):584-591.
 125. Brouns F., Arrigoni E., Langkilde A.M., Verkooijen I., Fassler C., Andersson H., Kettlitz B., van Nieuwenhoven M., Philipsson H., Amado R. Physiological and metabolic properties of a digestion-resistant maltodextrin, classified as type 3 retrograded resistant starch. *Journal of Agricultural & Food Chemistry*. **2007**;55(4):1574-1581.
 126. Zhao X.H., Lin Y. Resistant starch prepared from high-amylose maize starch with citric acid hydrolysis and its simulated fermentation in vitro. *European Food Research and Technology*. **2009**;228(6):1015-1021.

127. Zhu C.-L., Zhao X.-H. In vitro fermentation of a retrograded maize starch by healthy adult fecal extract and impacts of exogenous microorganisms on three acids production. *Starch-Stärke*. **2013**;65(3-4):330-337.
128. Zhou Z., Zhang Y., Zheng P., Chen X., Yang Y. Starch structure modulates metabolic activity and gut microbiota profile. *Anaerobe*. **2013**;24:71-78.
129. Goñi I., García-Alonso A., Martín-Carrón N., Saura-Calixto F. In vitro fermentation of different types of α -amylase resistant corn starches. *European Food Research and Technology*. **2000**;211:316-321.
130. Warren F.J., Fukuma N.M., Mikkelsen D., Flanagan B.M., Williams B.A., Lisle A.T., P O.C., Morrison M., Gidley M.J. Food starch structure impacts gut microbiome composition. *mSphere*. **2018**;3(3).
131. Gibson G.R., Hutkins R., Sanders M.E., Prescott S.L., Reimer R.A., Salminen S.J., Scott K., Stanton C., Swanson K.S., Cani P.D., Verbeke K., Reid G. Expert consensus document: The International Scientific Association for Probiotics and Prebiotics (ISAPP) consensus statement on the definition and scope of prebiotics. *Nature Reviews Gastroenterology & Hepatology*. **2017**;14(8):491-502.
132. Warren F.J., Zhang B., Waltzer G., Gidley M.J., Dhital S. The interplay of alpha-amylase and amyloglucosidase activities on the digestion of starch in in vitro enzymic systems. *Carbohydrate Polymers*. **2015**;117:192-200.
133. Janecek S., Marecek F., MacGregor E.A., Svensson B. Starch-binding domains as CBM families-history, occurrence, structure, function and evolution. *Biotechnology Advances*. **2019**;37(8):107451.
134. Hall F.F., Ratliff C.R., Hayakawa T., Culp T.W., Hightower N.C. Substrate differentiation of human pancreatic and salivary alpha-amylases. *The American Journal of Digestive Diseases*. **1970**;15(11):1031-1038.
135. Patel H., Royall P.G., Gaisford S., Williams G.R., Edwards C.H., Warren F.J., Flanagan B.M., Ellis P.R., Butterworth P.J. Structural and enzyme kinetic studies of retrograded starch: Inhibition of alpha-amylase and consequences for intestinal digestion of starch. *Carbohydrate Polymers*. **2017**;164:154-161.
136. Qian M., Haser R., Payan F. Carbohydrate binding sites in a pancreatic alpha-amylase-substrate complex, derived from X-ray structure analysis at 2.1 Å resolution. *Protein Science*. **1995**;4(4):747-755.
137. Payan F., Qian M. Crystal structure of the pig pancreatic alpha-amylase complexed with malto-oligosaccharides. *Journal of Protein Chemistry*. **2003**;22(3):275-284.
138. Zhang X., Caner S., Kwan E., Li C., Brayer G.D., Withers S.G. Evaluation of the significance of starch surface binding sites on human pancreatic alpha-amylase. *Biochemistry*. **2016**;55(43):6000-6009.
139. Cockburn D., Wilkens C., Dilokpimol A., Nakai H., Lewinska A., Abou Hachem M., Svensson B. Using carbohydrate interaction assays to reveal novel binding sites in carbohydrate active enzymes. *PLoS One*. **2016**;11(8):e0160112.
140. Lin A.H., Nichols B.L., Quezada-Calvillo R., Avery S.E., Sim L., Rose D.R., Naim H.Y., Hamaker B.R. Unexpected high digestion rate of cooked starch by the Ct-maltase-glucoamylase small intestine mucosal alpha-glucosidase subunit. *PLoS One*. **2012**;7(5):e35473.
141. Flint H.J., Duncan S.H., Scott K.P., Louis P. Interactions and competition within the microbial community of the human colon: links between diet and health. *Environmental Microbiology*. **2007**;9(5):1101-1111.
142. Wang X., Conway P.L., Brown I.L., Evans A.J. In vitro utilization of amylopectin and high-amylose maize (Amylomaize) starch granules by human colonic bacteria. *Applied Environmental Microbiology*. **1999**;65(11):4848-4854.

143. Ze X., Duncan S.H., Louis P., Flint H.J. Ruminococcus bromii is a keystone species for the degradation of resistant starch in the human colon. *The ISME Journal*. **2012**;6(8):1535-1543.
144. Ryan S.M., Fitzgerald G.F., van Sinderen D. Screening for and identification of starch-, amylopectin-, and pullulan-degrading activities in bifidobacterial strains. *Applied Environmental Microbiology*. **2006**;72(8):5289-5296.
145. Purwani E.Y., Purwadaria T., Suhartono M.T. Fermentation RS3 derived from sago and rice starch with *Clostridium butyricum* BCC B2571 or *Eubacterium rectale* DSM 17629. *Anaerobe*. **2012**;18(1):55-61.
146. Martens E.C., Koropatkin N.M., Smith T.J., Gordon J.I. Complex glycan catabolism by the human gut microbiota: the Bacteroidetes Sus-like paradigm. *Journal of Biological Chemistry*. **2009**;284(37):24673-24677.
147. Martens E.C., Lowe E.C., Chiang H., Pudlo N.A., Wu M., McNulty N.P., Abbott D.W., Henrissat B., Gilbert H.J., Bolam D.N., Gordon J.I. Recognition and degradation of plant cell wall polysaccharides by two human gut symbionts. *PLoS Biology*. **2011**;9(12):e1001221.
148. Asakuma S., Hatakeyama E., Urashima T., Yoshida E., Katayama T., Yamamoto K., Kumagai H., Ashida H., Hirose J., Kitaoka M. Physiology of consumption of human milk oligosaccharides by infant gut-associated bifidobacteria. *Journal of Biological Chemistry*. **2011**;286(40):34583-34592.
149. Watson D., O'Connell Motherway M., Schoterman M.H., van Neerven R.J., Nauta A., van Sinderen D. Selective carbohydrate utilization by lactobacilli and bifidobacteria. *Journal of Applied Microbiology*. **2013**;114(4):1132-1146.
150. Agans R., Rigsbee L., Kenche H., Michail S., Khamis H.J., Paliy O. Distal gut microbiota of adolescent children is different from that of adults. *FEMS Microbiology Ecology*. **2011**;77(2):404-412.
151. Duranti S., Milani C., Lugli G.A., Mancabelli L., Turrone F., Ferrario C., Mangifesta M., Viappiani A., Sanchez B., Margolles A., van Sinderen D., Ventura M. Evaluation of genetic diversity among strains of the human gut commensal *Bifidobacterium adolescentis*. *Scientific Reports*. **2016**;6:23971.
152. Jung D.H., Kim G.Y., Kim I.Y., Seo D.H., Nam Y.D., Kang H., Song Y., Park C.S. *Bifidobacterium adolescentis* P2P3, a human gut bacterium having strong non-gelatinized resistant starch-degrading activity. *Journal of Microbiology and Biotechnology*. **2019**;29(12):1904-1915.
153. Mukhopadhyay I., Morais S., Laverde-Gomez J., Sheridan P.O., Walker A.W., Kelly W., Klieve A.V., Ouwerkerk D., Duncan S.H., Louis P., Koropatkin N., Cockburn D., Kibler R., Cooper P.J., Sandoval C., Crost E., Juge N., Bayer E.A., Flint H.J. Sporulation capability and amylose conservation among diverse human colonic and rumen isolates of the keystone starch-degrader *Ruminococcus bromii*. *Environmental Microbiology*. **2018**;20(1):324-336.
154. Valk V., Lammerts van Bueren A., van der Kaaij R.M., Dijkhuizen L. Carbohydrate-binding module 74 is a novel starch-binding domain associated with large and multidomain alpha-amylase enzymes. *FEBS Journal*. **2016**;283(12):2354-2368.
155. Duncan S.H., Aminov R.I., Scott K.P., Louis P., Stanton T.B., Flint H.J. Proposal of *Roseburia faecis* sp. nov., *Roseburia hominis* sp. nov. and *Roseburia inulinivorans* sp. nov., based on isolates from human faeces. *International Journal of Systematic and Evolutionary Microbiology*. **2006**;56(Pt 10):2437-2441.
156. Scott K.P., Martin J.C., Chassard C., Clerget M., Potrykus J., Campbell G., Mayer C.D., Young P., Rucklidge G., Ramsay A.G., Flint H.J. Substrate-driven gene expression in *Roseburia inulinivorans*: importance of inducible enzymes in the utilization of inulin and starch. *Proceedings of the National Academy of Sciences (Proceedings of the National Academy of Sciences of the United States of America)*. **2011**;108 Suppl 1(Suppl 1):4672-4679.
157. Louis P., Flint H.J. Diversity, metabolism and microbial ecology of butyrate-producing bacteria from the human large intestine. *FEMS Microbiology Letters*. **2009**;294(1):1-8.

158. Cockburn D.W., Orlovsky N.I., Foley M.H., Kwiatkowski K.J., Bahr C.M., Maynard M., Demeler B., Koropatkin N.M. Molecular details of a starch utilization pathway in the human gut symbiont *Eubacterium rectale*. *Molecular Microbiology*. **2015**;95(2):209-230.
159. Cockburn D.W., Suh C., Medina K.P., Duvall R.M., Wawrzak Z., Henrissat B., Koropatkin N.M. Novel carbohydrate binding modules in the surface anchored alpha-amylase of *Eubacterium rectale* provide a molecular rationale for the range of starches used by this organism in the human gut. *Molecular Microbiology*. **2018**;107(2):249-264.

sG20-B / N32-B



30 μm

The background of the entire page is a scanning electron micrograph (SEM) showing a dense collection of resistant starch type 3 granules. These granules are generally spherical or sub-spherical in shape, with some showing a more irregular, textured surface. They vary in size, with many appearing to be between 1 and 5 micrometers in diameter. The granules are closely packed together, creating a complex, three-dimensional texture. The lighting in the SEM image highlights the surface features of the granules, giving them a three-dimensional appearance.

Chapter 2

Digestibility of resistant starch type 3 is affected by crystal type, molecular weight and molecular weight distribution

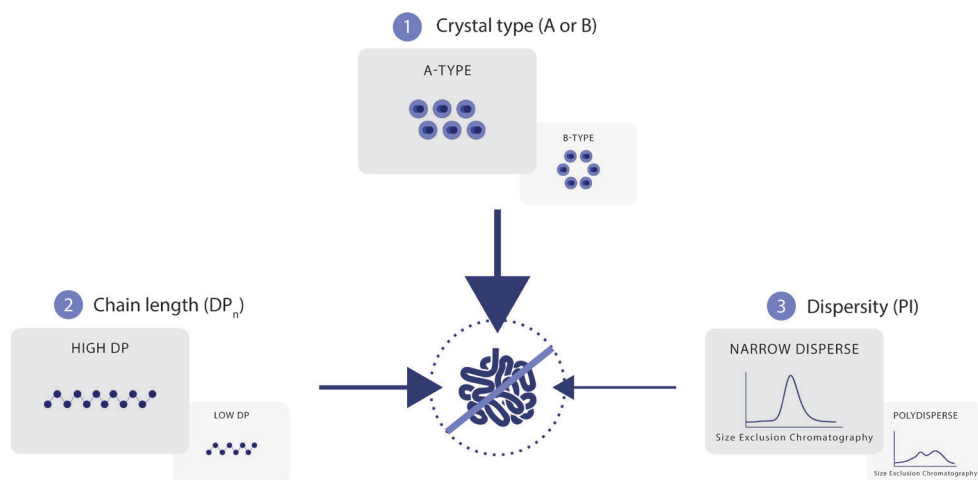
Cynthia E. Klostermann, Piet L. Buwalda †, Hans

Leemhuis, Paul de Vos, Henk A. Schols, Johannes H. Bitter

Carbohydrate Polymers, 2021, 265

Abstract

Resistant starch type 3 (RS-3) holds great potential as a prebiotic by supporting gut microbiota following intestinal digestion. However the factors influencing the digestibility of RS-3 are largely unknown. This research aims to reveal how crystal type and molecular weight (distribution) of RS-3 influence its resistance. Narrow and polydisperse α -glucans of degree of polymerization (DP_n) 14 – 76, either obtained by enzymatic synthesis or debranching amylopectins from different sources, were crystallized in 12 different A- or B-type crystals and *in vitro* digested. Crystal type had the largest influence on resistance to digestion (A >>> B), followed by molecular weight (Mw) (high DP_n >> low DP_n) and Mw distribution (narrow disperse > polydisperse). B-type crystals escaping digestion changed in Mw and Mw distribution compared to that in the original B-type crystals, whereas A-type crystals were unchanged. This indicates that pancreatic α -amylase binds and acts differently to A- or B-type RS-3 crystals.



1. Introduction

Resistant starch (RS) is starch that resists digestion in the small intestine by human digestive enzymes and therefore ends up in the colon. In the colon RS will be fermented and may even act as a prebiotic by positively influencing beneficial gut microbiota^[1-3]. Recently, it was shown that RS also may directly interact with the immune system to activate several immune responses^[4, 5]. Five different types of RS exist: physically inaccessible starch (RS-1), native starch granules (RS-2), retrograded starch (RS-3), chemically modified starch (RS-4) and amylose-lipid complexes (RS-5)^[2, 6]. RS-3 is of interest as food ingredient since it is thermally stable^[7] and can easily be added to foods as dietary fibre. RS-3 preparations can be made by debranching amylopectins to short chain α -glucans followed by controlled crystallization^[8]. However, to be able to act as dietary fibre, RS-3 preparations should be resistant to enzymatic digestion in the small intestine. Recently, it was suggested that RS-3 may be resistant to digestion due to slow enzyme binding of pancreatic α -amylase to the RS-3 crystals in combination with slow catalytic hydrolysis^[9]. However, it is not yet clear which physicochemical characteristics of RS-3 cause the resistance to digestion. Differences in digestibility of RS-3 preparations might be caused by characteristics like crystal type and molecular weight (distribution) of the crystallized α -glucans.

Resistant starch type 3 (RS-3) preparations or so-called short chain α -glucan crystals can be produced by gelatinizing starch at elevated temperatures followed by slow cooling, which results in recrystallization of the starch. The crystals formed by recrystallization can be recognized as A-type or B-type, as measured by X-ray diffraction^[10-12]. Whether A- or B-type crystals are formed depends on the chain length of the α -glucan, the concentration during crystallization and temperature of crystallization^[10, 13-15]. In addition, RS-3 preparations differing in crystal type can be formed using different solvents like acetone, ethanol or polyethylene glycol^[16-18]. *In vitro*, native A-type starches are easier to digest compared to native B-type starches^[19]. In contrast, research on digestibility of retrograded short chain α -glucans has shown that retrograded A-type crystals are more resistant to digestion than retrograded B-type crystals^[8, 20].

In addition to crystal type, average molecular weight also affects resistance to digestion of RS-3 preparations. Most research on RS-3 is performed by crystallization of debranched amylopectins resulting in a wide range of short chain linear α -1,4 linked glucans^[8, 10]. By choosing waxy starches of different

botanical sources, variations in average chain length (DPn) can be achieved after debranching^[21]. For example, debranched waxy maize starch has a DPn of 24, waxy wheat of DPn 22 and waxy potato of DPn 32^[21]. In addition, starches can be modified by branching enzymes or by amylomalases, due to which amylopectins are produced that have very short chains or elongated chains, respectively^[22]. After digestion of RS-3 preparations made of debranched amylopectins of different botanical sources, it was found that a higher DPn resulted in more resistance to digestion^[21].

However, it is largely unknown how molecular weight distribution influences the resistance to digestion of RS-3 preparations. Such a broad range of α -1,4 glucans can be obtained by debranching amylopectins, as shown for waxy wheat amylopectin resulting in chain lengths of DPn 6 – 66 with an average of DPn 22^[21]. When such a polydisperse mixture is crystallized and subjected to digestion, it is not yet clear how the presence of different chain lengths influences the crystal formation and resistance to digestion. Previously, the effect of polydispersity on digestion was studied by debranching waxy and native rice starch. Debranching waxy rice starch results in α -glucan chains with a DPn varying from 6 – 90, whereas debranching native rice starch also includes the linear amylose part, which has a DPn up to 1000^[10]. It was shown that crystals produced from relatively narrow disperse debranched waxy rice starch are 10 % more resistant to digestion than crystals produced from polydisperse debranched native rice starch^[23]. Another study focussed on the fractionation of debranched waxy rice starch (polydispersity index (PI) 2.2)^[24]. This fractionation caused narrowing of the molecular weight distribution to a PI of 1.5 at most. After crystallization and digestion, it was shown that these crystals made of relatively narrow disperse α -glucans were 10 – 20 % more resistant to digestion compared to the unfractionated polydisperse crystals^[24]. However, the polydispersity index of before mentioned debranched and fractionated starches is still relatively high, making it hard to draw conclusions on the influence of polydispersity on crystal formation and subsequent digestibility.

In contrast to polydisperse α -1,4 glucans obtained by debranching amylopectins, narrow disperse amyloses can be enzymatically synthesized by potato glucan phosphorylase from glucose-1-phosphate (G-1-P)^[17, 25-27]. Potato glucan phosphorylase uses glucose-1-phosphate as a substrate and transfers the glucose residue to a primer molecule, being maltotetraose or an α -1,4 linked oligomer of DP > 4^[28]. The ratio between the glucose-1-phosphate and primer molecule determines the DPn at the end of the enzymatic synthesis. By choosing the right ratio, narrow disperse equivalents of debranched amylopectins can be

synthesized that have a similar average molecular weight (M_w) but a lower polydispersity index. However, glucose-1-phosphate as substrate is quite expensive. As an alternative, the combination of sucrose and sucrose phosphorylase can be used to produce glucose-1-phosphate^[29, 30]. Using sucrose as substrate also has shown to improve the yield of synthesis, compared to using glucose-1-phosphate directly^[28].

The present study focusses on the effect of crystal type, M_w and M_w distribution on the resistance to digestion of RS-3 preparations. Different resistant starches were produced by debranching amylopectins (polydisperse) or through synthesis with the help of potato glucan phosphorylase and sucrose phosphorylase (narrow disperse). The ratio of G-1-P and sucrose was chosen to obtain α -1,4 linked glucans with a similar average number molecular weight (M_{w_n}) as the debranched amylopectins, but with a lower polydispersity index. The linear α -glucans were crystallized at different concentrations and temperatures to obtain A- and B-type crystals. These RS-3 preparations were digested to study the effect of crystal type, average M_w and M_w distribution on the resistance to digestion.

2. Materials and methods

2.1. Materials

Waxy potato starch (Eliane100), amylomaltase modified potato starch (Etenia 457) and highly branched starch of potato ($M_w \pm 100$ kDa, 8 % branch points) were provided by AVEBE (Veendam, The Netherlands). Waxy rice starch (Remyline XS) was purchased from Beneo (Mannheim, Germany). Isoamylase (EC 3.2.1.68) and maltotetraose were obtained from Megazyme (Bray, Wicklow, Ireland). Sucrose, glucose, maltose, maltotriose, pancreatin, amyloglucosidase, Lennox B (LB) medium, kanamycin sulphate, isopropyl β -D-1-thiogalactopyranoside, glucose-1-phosphate potassium salt and imidazole of high purity were obtained from Sigma-Aldrich (St. Louis, MO, USA). Bugbuster (Novagen) and benzonase nuclease were purchased from Merck (Darmstadt, Germany). MilliQ (MQ) water was used unless stated otherwise (Arium mini essential UV Ultrapure water filter, Sartorius, Göttingen, Germany).

2.2. Production of potato glucan phosphorylase and sucrose phosphorylase

The potato glucan phosphorylase (PGP) (EC 2.4.1.1) and the *Bifidobacterium adolescentis* sucrose phosphorylase (SP) (EC 2.4.1.7)^[31] were produced in

Escherichia coli BL21 DE3 carrying the pET28a expression vector. The genes encoding PGP and SP were codon optimized for expression in *E. coli*, synthesized and cloned in pET28a by GenScript (Leiden, the Netherlands). The *E. coli* cells containing the PGP plasmid were grown for 16 h at 37 °C in LB medium that contained 25 µg/mL kanamycin while shaking at 200 rpm. The culture was transferred to 500 mL LB broth that contained 25 µg/mL kanamycin and kept for 2-3 h at 37 °C, shaking at 200 rpm until OD₆₀₀=0.5-0.7. The culture was cooled down on ice and 0.1 mM isopropyl β-D-1-thiogalactopyranoside was added, after which the culture was incubated for 24 h at 18 °C, 200 rpm. *E. coli* cells containing the SP plasmid were grown similarly until the inducer was added. To the SP culture of OD₆₀₀=0.5-0.7 0.4 mM isopropyl β-D-1-thiogalactopyranoside was added and incubation was continued for 4 h at 30 °C, 200 rpm. Cells were centrifuged for 10 min at 16,000 x g, 4 °C. The cell pellets were resuspended in Bugbuster, causing lysis of the *E. coli* cells, and supplemented with benzonase nuclease, according to the company protocol. The lysed cells were centrifuged for 10 min at 16,000 x g, 4 °C. The supernatant was decanted and stored for 30 min at 60 °C. This suspension was centrifuged and the supernatant was filtered over an 0.2 µm filter to obtain a sterile cell-free enzyme extract. The enzymes were purified using a His-Tag purification column, according to the company protocol (GE Healthcare Life Sciences, Amersham, United Kingdom). Sample and washing buffer contained 20 mM imidazole and elution of pure enzymes was performed with 800 mM imidazole. The final PGP or SP concentration was determined by the Bradford protein assay^[32].

2.3. Production of polydisperse α-1,4 linked glucans

Highly branched potato starch (HBPS), waxy potato starch (WPS), amylomaltase modified potato starch (AMPS) and waxy rice starch (WRS) were suspended in a 20 mM sodium acetate buffer of pH 5 and autoclaved. The solutions were cooled to 40 °C and isoamylase was added (8 U/g). The amylopectins were debranched for 48 h at 40 °C, 100 rpm and freeze-dried to produce debranched HBPS (dHBPS), WPS (dWPS), AMPS (dAMPS) and WRS (dWRS).

2.4. Enzymatic synthesis of narrow disperse α-1,4 linked glucans

For studying reaction dynamics of PGP and SP, sucrose and dHBPS were mixed at 105 mM in a molar ratio of 20/1 in a 30 mM sodium phosphate buffer of pH 7.0. His-tag purified PGP and SP were added (25 µg/mL) and the mixtures were incubated at 50 °C, 100 rpm in a shaking incubator. After 0, 0.5, 1 and 4 h a 50 µL sample was taken for chemical analysis (section 2.7) and heated for 15 min at 100 °C to inactivate the enzymes. For further incubations sucrose and dHBPS

were mixed at 105 mM in a molar ratio of 2/1, 5/1, 20/1 and 65/1 in a 30 mM sodium phosphate buffer of pH 7.0. His-tag purified PGP and SP were added (6.25 µg/mL) and samples were incubated for 24 h at 50 °C, 100 rpm in a shaking incubator. After 24 h of incubation, the remaining samples were freeze-dried and washed with cold MQ and 80 % ethanol to remove salts, enzymes and small sugars and freeze-dried again to yield purified sG2 (2/1), sG5 (5/1), sG20 (20/1) and sG65 (65/1).

2.5. Crystallization of poly- and narrow disperse α -1,4 linked glucans

Poly- and narrow disperse α -glucans of similar DP_n were suspended in MQ in different concentrations: dHBPS: 40 % w/w; sG2, dWRS and sG5: 30 % w/w; dWPS and sG20: 10 % w/w; dAMPS and sG65: 5 % w/w. The suspensions were autoclaved and stored at 80 °C prior to crystallization. Half of the dHBPS, sG2, dWRS and sG5 samples were stored for 24 h at 50 °C to produce A-type crystals, according to Cai & Shi (2014). The other half of dHBPS, sG2, dWRS and sG5 were immediately cooled on ice and stored for 24 h at 4 °C to produce B-type crystals, similar to the method proposed by Cai & Shi (2014). In addition, dWPS, sG20, dAMPS and sG65 were also immediately cooled on ice and stored for 24 h at 4 °C, to produce B-type crystals. After 24 h storage, the samples were centrifuged for 10 min at 7000 × g, 4 °C and washed with cold MQ and 80 % ethanol. The supernatants were decanted and pellets containing crystallized α -1,4 linked glucans were dried for 48 h at 40 °C. Crystallization yield was calculated as (total mass after crystallization) / (mass at start) * 100 %.

2.6. Digestion of RS-3 preparations

Digestion was performed according to Martens et al. with minor modifications^[19]. RS-3 preparations were suspended in 100 mM sodium acetate buffer pH 5.9 at 20 mg/mL. Pancreatin solution was prepared according to Martens et al. (2018), without addition of invertase. Samples were incubated for 0, 20, 60, 120 and 240 min and enzymes were inactivated by heat treatment for 15 min at 100 °C. After 360 min of incubation, the samples were centrifuged for 10 min at 19,000 × g, 4 °C and the enzymes in the supernatant were inactivated by heat treatment for 15 min at 100 °C. The remaining pellet was washed twice with MQ and oven-dried at 40 °C overnight. Free glucose content in the heat-treated samples was measured with the GOPOD assay from Megazyme. To study the effect of pancreatic α -amylase on the Mw distribution of dWRS-A and dWRS-B crystals, a similar method was used as described before, with some minor modifications. Pancreatin solution was prepared according to Martens et al. (2018), without addition of invertase and amyloglucosidase. Samples were

incubated for 0, 20, 60 and 360 min and immediately centrifuged for 10 min at 19,000 x g, 4 °C. The pellets were washed twice with MQ and oven-dried at 40 °C overnight. The supernatants were inactivated and analysed as described before.

2.7. Molecular weight distribution of RS-3 preparations, before and after digestion

RS-3 preparations of DP_n < 25 were suspended in MQ at 2.5 mg/mL and dissolved by boiling. RS-3 preparations of DP_n > 32 were solubilised in 1 M NaOH at 60 mg/mL sample. The samples were diluted to 2.5 mg/mL and neutralized by addition of 1 M HCl. Samples were centrifuged at 19,000 x g for 10 min and the supernatant was analysed with a Dionex Ultimate 3000 system (Sunnyvale, USA). Ten µL sample was injected on a column set that consisted of three in series connected TSKgel SuperAW columns (SuperAW4000 6.0 x 150 mm, 6 µm; SuperAW3000 6.0 x 150 mm, 4 µm; SuperAW2500 6.0 x 150 mm, 4 µm) (Tosoh Bioscience, Tokyo, Japan) with a TSKgel guard column (SuperAW-L 4.6 x 35 mm, 7 µm). Elution was performed with 0.6 mL/min and 0.2 M NaNO₃, at 55 °C. Detection was performed with a Shodex RI-101 detector (Showa Denko, K.K., Kawasaki, Japan). Calibration of the column was performed with pullulan standards (Supelco, Bellefonte, USA).

From the HPSEC-RI results, DP_n, DP_m and PI were calculated using pullulan calibration. Intensities were normalized and base-line corrected, after which Mn was calculated using formula 1. Mm was calculated using formula 2 and PI was calculated by dividing Mm over Mn. The retention time frame of each peak was taken into account to calculate Mn and Mm.

$$1. \quad Mn = \sum Mw_p * I_n$$

$$2. \quad Mm = \frac{\sum Mw_p^2 * I_n}{Mn}$$

In which Mn is the number based average Mw, whereas Mm is the mass based average Mw, Mw_p is the Mw based on pullulan calibration and I_n is the normalised and base-line corrected intensity at retention time x.

Samples were diluted to 0.25 mg/mL and centrifuged at 19,000 x g for 10 min. The supernatant was analysed using an ICS 3500 HPAEC system from Dionex, in combination with a CarboPac PA-1 (2 x 250 mm) column, with a CarboPac PA-1 guard column (Dionex). The detector used was an electrochemical Pulsed Amperometric detector from Dionex. Ten µL of supernatant was injected on the column and eluted by a gradient consisting of eluent A (0.1 M NaOH solution)

and eluent B (1 M NaOAc in 0.1 M NaOH). The gradient used was 2.5 – 40 % B (0-50 min), 40-100 % B (50-65 min), 100 % B (65-70 min), 2.5 % B (70-85 min). Elution was performed with 0.3 mL/min at 25 °C. A calibration curve of 5-10 µg/mL of malto-oligosaccharides (DP 1 – DP 7) was run for quantification. Data analysis was performed with Chromeleon™ 7.2.6 software from Thermo Fisher Scientific (Waltham, Massachusetts, USA).

2.8. Crystal type determination by X-ray Diffraction

Wide angle X-ray scattering (WAXS) powder diffractograms of the RS-3 preparations were measured on a Bruker Discover D8 diffractometer (Bruker corporation, Billerica, Massachusetts, USA) using Cu radiation (1.54 Å) in the reflection geometry in the angular range of 5-35 2°θ with a step size of 0.051 °2θ and 1 s per step in a rotating stage of 10 °/min. Detection was performed with Lynxeye XE-T (Bruker corporation). XRD diffractograms were background corrected and normalized.

2.9. Scanning Electron Microscopy of RS-3 preparations

Crystal morphology was determined with Scanning Electron Microscopy (SEM) (Magellan 400, FEI, Eindhoven, The Netherlands) at the Wageningen Electron Microscopy Center (WEMC). The RS-3 preparations were attached to sample holders containing carbon adhesive tabs (EMS, Washington, USA) and coated with 12 nm tungsten (EM SCD 500, Leica, Vienna, Austria). The crystals were analysed with a field emission SEM at 2 kV and magnification of 10,000 times.

3. Results & Discussion

3.1. Production of narrow disperse α-glucans

Narrow disperse α-glucans were enzymatically synthesized by potato glucan phosphorylase (PGP) and sucrose phosphorylase (SP) using debranched highly branched potato starch (dHBPS) as primer molecule and sucrose as a substrate. The synthesis was followed over time and analysed by HPAEC-PAD (Figure 2.1). At t = 0 min, the chromatogram shows several peaks which can be identified as malto-oligomers of dHBPS and G-1-P formed after enzymatic hydrolysis of sucrose by SP (Figure 2.1). The figure inset shows peaks that can be identified as sucrose, fructose and glucose. Over time (t=30, t=60, t=240 min), the sucrose was hydrolysed and fructose formed, showing activity of SP. The PAD signal of G-1-P increased and decreased over time, whereas the malto-oligomers of dHBPS were elongated up to at least DPn 40 over time,

indicating PGP activity. Due to this shift in malto-oligomers towards higher DP's over time, it can be stated that PGP favoured to elongate the smallest malto-oligomer present ($DP > 4$). Although literature states that based on the polydispersity index, enzymatically synthesized α -glucans are narrow disperse [17, 28], this result shows that still a rather broad mixture of α -glucans was formed after enzymatic synthesis.

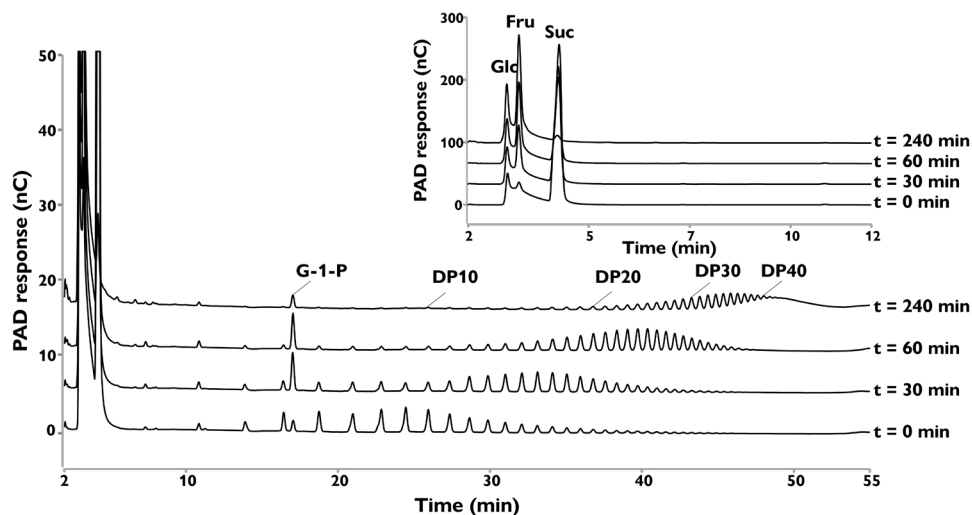


Figure 2.1. HPAEC elution pattern of the one-pot incubation of sucrose and debranched HBPS (ratio 20/1) with potato glucan phosphorylase and sucrose phosphorylase during 240 min of incubation. Abbreviations used: Glc = glucose, Fru = fructose, Suc = sucrose, G-1-P = glucose-1-phosphate, DP = degree of polymerization. The inset shows the first 12 min of the chromatogram; a decrease of sucrose and an increase of fructose over time can be observed.

Sucrose and dHBPS were incubated at a ratio of 2/1, 5/1, 20/1 and 65/1 with PGP and SP to synthesize α -glucans of DPn 14 (sG2), 18 (sG5), 32 (sG20) and 78 (sG65). The synthesis yields after 24 h of incubation were between 65 – 85 %. The average Mw and polydispersity index (PI) of the synthesized and purified α -glucans were analysed and calculated after size exclusion chromatography (Table 2.1, Supplementary figure 2.1).

Table 2.1. Average chain length (DPn) and polydispersity index (PI) of synthesized α -glucans before and after purification after 24 h of one-pot incubation of sucrose and debranched HBPS in different molar ratios with potato glucan phosphorylase and sucrose phosphorylase.

| Sample name | Sucrose/dHBPS | DPn _{t=24 h} | PI _{t=24 h} | DPn _{purified} | PI _{purified} |
|-------------|---------------|-----------------------|----------------------|-------------------------|------------------------|
| sG2 | 2/1 | 13.9 ± 0.1 | 1.40 ± 0.01 | 16.3 ± 0.2 | 1.32 ± 0.01 |
| sG5 | 5/1 | 15.9 ± 0.1 | 1.33 ± 0.01 | 18.2 ± 0.3 | 1.25 ± 0.01 |
| sG20 | 20/1 | 29.1 ± 0.3 | 1.20 ± 0.00 | 30.7 ± 0.3 | 1.12 ± 0.01 |
| sG65 | 65/1 | 74.7 ± 0.3 | 1.06 ± 0.01 | 72.0 ± 0.3 | 1.08 ± 0.02 |

The results show that the Mw of the final α -glucan after enzymatic synthesis increased with the sucrose/dHBPS ratio (Table 2.1). The higher the sucrose/dHBPS molar ratio, the more G-1-P was available for the reaction and thus the higher Mw α -glucans were formed, as stated in literature previously^[28]. The DPn at the end of the synthesis can be predicted by the choice of primer and the ratio between substrate and primer^[33]. The primer used in the present experiment was dHBPS which has a DPn of 12. The DPn at the end of synthesis can be calculated by:

$$\text{DPn} = [\text{sucrose}]/[\text{dHBPS}] + 12$$

As the table shows, this equation matched quite well with the results obtained. It should be noted that dHBPS has a PI of 1.51 and thus is not a monodisperse α -glucan by itself (Figure 2.1, t=0).

After synthesis, the α -glucans were purified to remove left-over sucrose, G-1-P, salts, SP and PGP. The HPSEC profiles clearly show that some small malto-oligomers were washed away during purification of sG2 and sG5 (Supplementary figure 2.2). Therefore, this purification step resulted in a lower PI, with a slightly higher DPn in case of low Mw α -glucans (sG2, sG5) and a similar DPn in case of higher Mw α -glucans (sG20, sG65).

In addition, the results show that the higher the Mw of the formed α -glucan, the lower the PI found (Table 2.1; e.g. DPn 13.9, PI 1.40 vs DPn 74.7, PI 1.06). The PI of the synthesized α -glucans is quite high, especially compared to literature that showed PI < 1.07^[28] or PI < 1.17^[27]. However, both studies focused on synthesis of high Mw amyloses of DP >> 75, due to which lower PI values were obtained. In addition, both studies used the monodisperse primers maltotetraose^[28] and maltohexaose^[27] whereas the present study used a polydisperse debranched amylopectin as primer molecule. A previous study using glycogen phosphorylase for enzymatic synthesis was able to synthesize α -glucans of

DPn 21 with a polydispersity index of 1.1, using maltopentaose as a primer molecule^[17].

Although our purified narrow disperse α -glucans of DPn 16 and 18 were still not fully monodisperse, it was decided that they were different enough from their polydisperse equivalents and thus useful to study the effect of Mw distribution on resistance to digestion in RS-3.

3.2. Crystallization of narrow- and polydisperse α -glucans

In order to produce RS-3 preparations differing in Mw, PI and crystal type, the purified narrow disperse α -glucans were autoclaved and crystallized at 4 °C or 50 °C, according to Cai & Shi (2014), aiming at B-type and A-type crystals, respectively. Different types of debranched amylopectin were used as polydisperse equivalents of narrow disperse synthesized sG2, sG5, sG20 and sG65, namely: debranched highly branched potato starch (dHBPS), debranched waxy rice starch (dWRS), debranched potato starch (dWPS) and debranched amylomaltase modified potato starch (dAMPS), respectively. Crystallization was done similarly to the narrow disperse α -glucans. The α -glucans of DPn \geq 32 were only stored at 4 °C, since previous research showed that these always crystallize in a B-type polymorph, irrespectively of crystallization temperature^[8]. The crystal type of the α -glucans was determined and their Mw distribution was analysed after solubilization in NaOH (Table 2.2). The crystallization yield was calculated based on the recovery of crystallized molecules (Table 2.2).

Table 2.2. Crystal type, Mw and Mw distribution and crystallization yield of purified narrow and polydisperse RS-3 preparations.

| α -glucan | Crystal type | DPn _{crystal} | PI _{crystal} | Crystallization yield (%) |
|------------------|--------------|------------------------|-----------------------|---------------------------|
| sG2-A | A | 15.6 \pm 0.3 | 1.23 \pm 0.01 | 35 \pm 1 |
| sG2-B | B | 15.2 \pm 0.1 | 1.25 \pm 0.00 | 86 \pm 0 |
| dHBPS-A | A | 14.3 \pm 0.1 | 1.33 \pm 0.01 | 21 \pm 1 |
| dHBPS-B | B | 14.0 \pm 0.1 | 1.35 \pm 0.00 | 45 \pm 3 |
| sG5-A | A | 18.0 \pm 0.2 | 1.21 \pm 0.01 | 60 \pm 2 |
| sG5-B | B | 18.0 \pm 0.0 | 1.21 \pm 0.00 | 89 \pm 2 |
| dWRS-A | A | 21.4 \pm 1.9 | 1.59 \pm 0.01 | 63 \pm 2 |
| dWRS-B | B | 21.9 \pm 0.5 | 1.50 \pm 0.01 | 79 \pm 1 |
| sG20-B | B | 31.6 \pm 0.3 | 1.14 \pm 0.00 | 87 \pm 8 |
| dWPS-B | B | 39.9 \pm 0.7 | 2.11 \pm 0.02 | 78 \pm 10 |
| sG65-B | B | 75.6 \pm 0.9 | 1.07 \pm 0.00 | 97 \pm 3 |
| dAMPS-B | B | 53.0 \pm 2.3 | 1.67 \pm 0.03 | 86 \pm 4 |

The results from X-ray diffraction show that crystallization at 4 and 50 °C indeed resulted in the desired crystal polymorphs (Table 2.2). Although differences in relative intensity of the peaks were observed between the diffractograms of the crystallized α -glucans, still clear A- and B-type polymorphism could be recognized (Figure 2.2). Previously, in-depth studies were performed on identification of A- and B-type peak positions of crystallized amylose^[12, 17]. The XRD patterns of our crystallized α -glucans match the peak positions of Nishiyama (2010), although differences in relative intensities were observed.

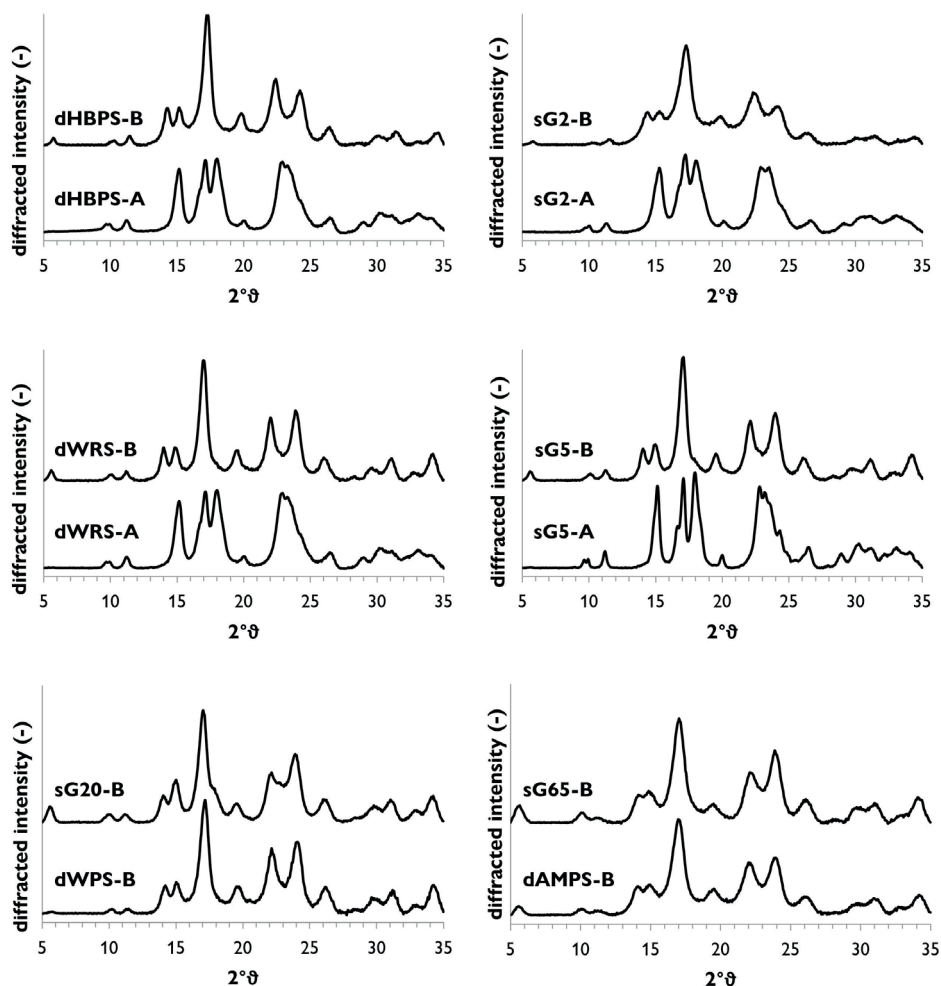


Figure 2.2. XRD profiles of narrow and polydisperse RS-3 preparations.

Debranching of amylopectins of selected sources followed by crystallization resulted in crystals having similar Mw and crystal type compared to their synthesized equivalents, but differing in polydispersity index. Despite large differences in PI and Mw distribution (Supplementary figure 2.3), sG20-B and dWPS-B had a comparable Mw and crystal type. The polydisperse equivalent of sG65-B (dAMPS) was found to have a much lower average Mw compared to sG65-B (Table 2.2). Therefore, these samples cannot be used to study the effect of PI on resistance to digestion.

Crystallization yield was found to be highly dependent on DPn and crystallization temperature; at 50 °C much lower yields were obtained compared to crystallization at 4 °C for α -glucans of the same Mw (Table 2.2, A- vs B-type crystals). In addition, the lower the DPn, the lower crystallization yields were found, although lower Mw α -glucans were crystallized at higher concentrations (Table 2.2).

3.3. Morphology of narrow- and polydisperse RS-3 preparations

The RS-3 preparations were analysed on their morphology by scanning electron microscopy (Figure 2.3). The images clearly show differences between A- and B-type RS-3 crystals. The A-type RS-3 crystals seem to consist of very tiny substructures that had been aggregated. The narrow disperse B-type RS-3 crystals are regularly formed spherical particles, except for sample sG65-B. sG65-B crystals seem to consist of smaller particles, compared to the other narrow disperse B-type crystals. The polydisperse B-type crystals show very different appearances: dHBPS-B looks like sG2-B, which can be explained by a similar Mw and a relatively similar PI (Table 2.2). However, dWRS-B, dWPS-B and dAMPS-B, which differ in Mw but all have a $PI \geq 1.50$ do not show a regular structure and seem to be more amorphous, although a clear crystal type was confirmed by XRD (Figure 2.3).

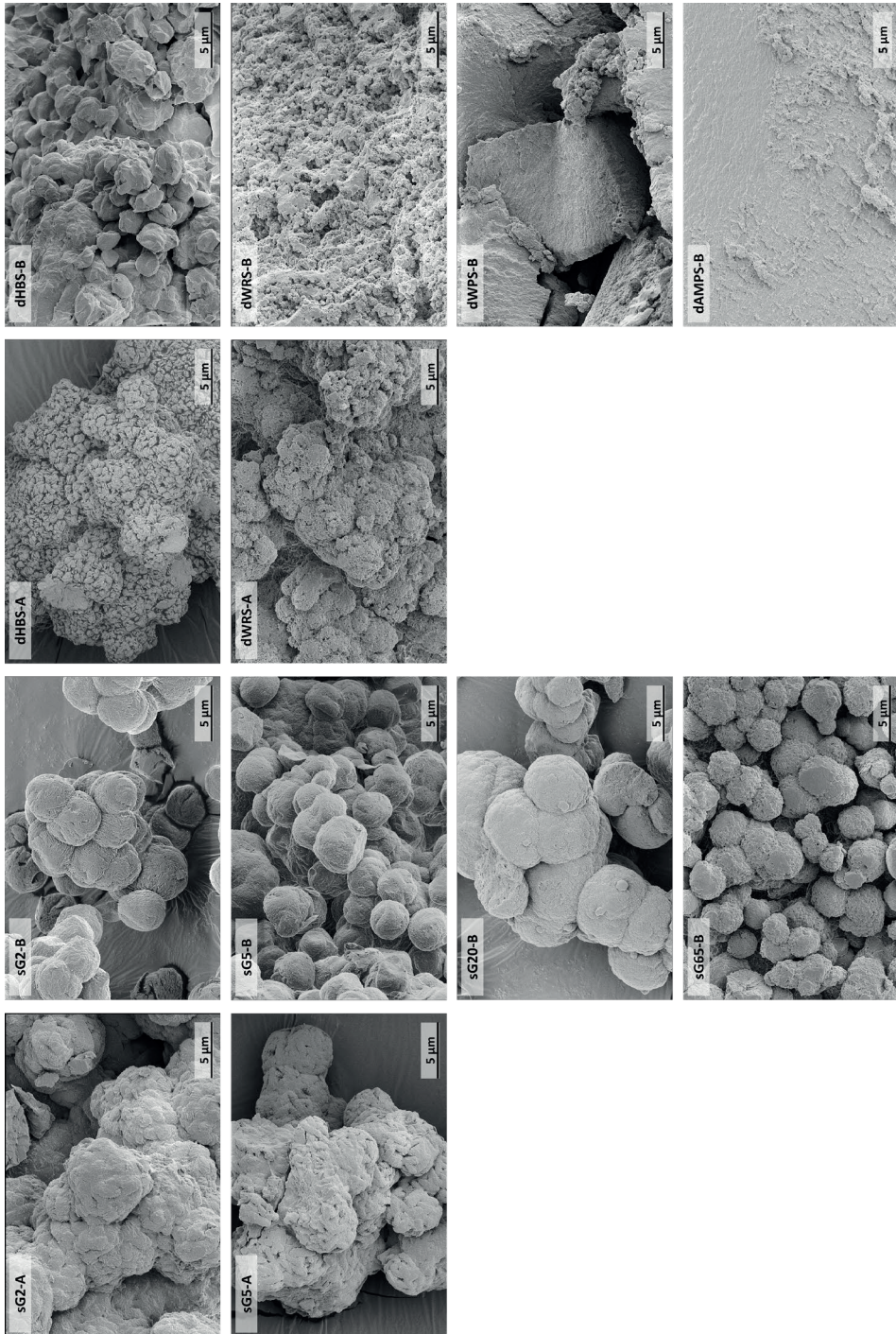


Figure 2.3. Scanning electron microscopic images of RS-3 preparations differing in Mw, Mw distribution and crystal type. Sample codes are explained in **Table 2.2**.

Previously, studies were performed on crystallization of debranched amylopectins^[8, 20]. The SEM images of the debranched waxy maize starch spherulites showed similar morphology as our narrow disperse B-type crystals (Figure 2.3). In addition, Kiatpongarp et al. (2016) studied crystallization of debranched native and waxy rice starches^[23]. These α -glucans all crystallized in a B-type polymorph, but showed very different appearances. Their native rice starch crystals showed a rough surface morphology, similar to our sG65 crystals^[23]. Also, Zeng et al. (2016) studied morphology of crystallized α -glucans produced by different drying methods^[34]. Their air-dried debranched waxy rice starch crystals greatly resembled our air-dried dWRS crystals. In addition, narrow disperse α -glucans were previously crystallized to A- and B-type crystals^[17]. The B-type crystals that had similar Mw values compared to the crystals in the current study had the same morphology as we observed. However, the previously produced A-type crystals showed a much more structured morphology, which can be explained by precipitation with acetone^[17] instead of self-assembly as in the present study. It should be noted that our study focused on the retrogradation of α -glucans from aqueous environment, mimicking resistant starch formation during cooking in a simplified way.

To summarize, 12 different RS-3 preparations were produced that differed in crystal type (A/B), Mw (DPn \pm 15, 20, 32 and 75) and PI (\leq 1.25 or \geq 1.35). These RS-3 preparations were used to study the effect of crystal type, Mw and Mw distribution on resistance to digestion.

3.4. Digestibility of narrow and polydisperse RS-3 preparations

In order to investigate the effect of crystal type, Mw and Mw distribution on the resistance to digestion, the twelve narrow and polydisperse RS-3 preparations were digested according to Englyst et al. and Martens et al.^[19, 35] (Figure 2.4).

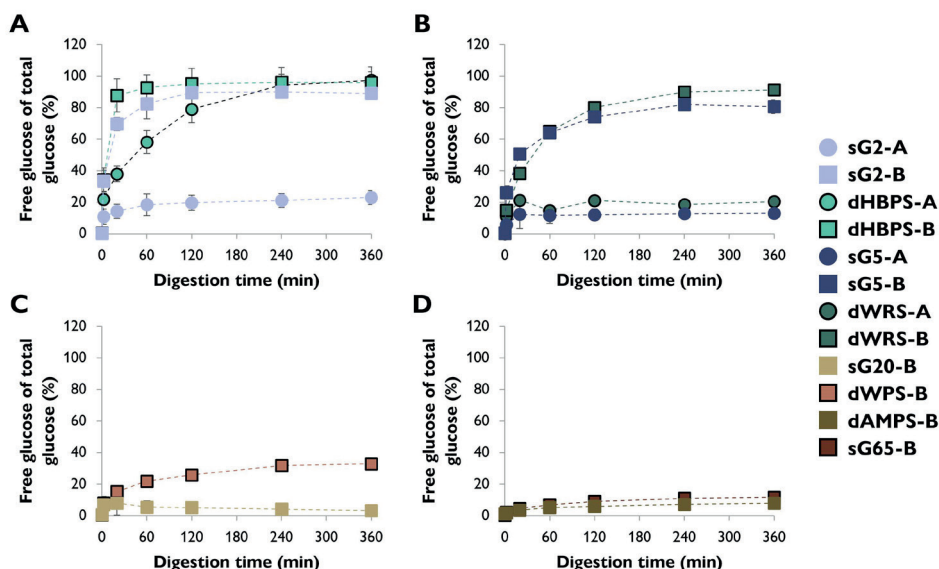


Figure 2.4. *In vitro* digestion profiles of narrow and polydisperse RS-3 preparations. A (DPn ± 15): dHBPS, sG2; B (DPn ± 20): dWRS, sG5; C (DPn ± 32): dWPS, sG20; D (DPn ≥ 50): dAMPS, sG65. Digestibility curves of dHBPS are from 5 individually produced samples, all others are from triplicate produced samples, all digested in duplicate.

3.4.1. RS-3 A-type crystals are more resistant to digestion than B-type crystals

Firstly, the results show that both dHBPS-A and dHBPS-B were digested completely within 360 min and thus these RS-3 preparations cannot be considered as RS-3, although being retrograded, insoluble and showing a clear crystal type (Figure 2.4-A, Figure 2.2). However, the results do show that dHBPS-A (DPn 14) was slower digested than dHBPS-B (DPn 14), indicating that B-type crystals were easier digested than A-type crystals. Moreover, the narrow disperse A-type crystals (sG2-A, DPn 15) were digested for 20 % during the first 60 min of digestion, whereas the narrow disperse B-type crystals (sG2-B, DPn 15) were digested for 80 % (Figure 2.4-A). Slower digestion of A-type crystals compared to B-type crystals was also observed for poly- and narrow disperse A- and B-type RS-3 preparations of DPn 18-22 (Figure 4-B). Therefore, it can be stated that A-type crystals were more resistant to digestion than B-type crystals, comparing A- and B-type digestibility within one chain length. This aligns with previous research showing that retrograded A-type crystals of similar chain length were more resistant to digestion than B-type crystals^[8].

3.4.2. RS-3 preparations of longer chain length α -glucans are more resistant to digestion than that of shorter chain length, irrespectively of crystal type

The results also show that A-type crystals made of longer chain length α -glucans were more resistant to digestion than A-type crystals made of shorter chain length α -glucans (dHBPS-A vs dWRS-A, sG2-A vs sG5-A, Figure 2.4-A-B, Table 2.3). In addition, polydisperse B-type crystals made of longer chain length α -glucans were also more resistant to digestion than polydisperse B-type crystals made of shorter chain length α -glucans (dHBPS-B, dWRS-B, dWPS-B, dAMPS-B (Figure 2.4-A-D), Table 2.3). Moreover, narrow disperse B-type crystals of longer DPn were also more resistant to digestion, although a minor difference in final digestibility was observed between sG20-B and sG65-B (sG2-B, sG5-B, sG20-B, sG65-B) (Figure 2.4, Table 2.3). Therefore, it can be stated that RS-3 preparations made of longer chain length α -glucans were more resistant to digestion, compared to RS-3 preparations made of shorter chain length α -glucans, irrespectively of crystal type.

3.4.3. RS-3 preparations of narrow disperse α -glucans are slightly more resistant to digestion than that of polydisperse α -glucans

Lastly, the results show that RS-3 preparations made of narrow disperse α -glucans were more resistant to digestion than RS-3 preparations made of polydisperse α -glucans, although no major differences were found for most samples (Figure 2.4-A (dHBPS-B vs sG2-B), B, Table 2.3). A-type crystals with a low PI and low Mw were found to be more resistant than their polydisperse equivalent (dHBPS-A vs sG2-A or dWRS-A vs sG5-A, Table 2.3). Interestingly, sG2-A was much more resistant to digestion than its polydisperse counterpart dHBPS-A (23 vs 100 % digestible, respectively). This, although their Mw and PI only differed slightly from each other (Table 2.2). We hypothesize that a lower limit of DPn 15 is needed to remain connected to the A-type crystal during enzymatic digestion. Because of this, the dHBPS-A crystal was 100 % digestible, whereas the sG2-A crystal was only digestible for 23 % after 360 min. B-type crystals with a low PI and DPn 32 (sG20-B) were much more resistant to digestion than their polydisperse equivalents (dWPS-B), with a difference in PI of 0.97 (Figure 2.4-C, Table 2.2). The morphology of these crystals was very different, which might explain this difference (Figure 2.3). It can be stated that narrow disperse crystals were slightly more resistant to digestion than polydisperse crystals.

3.5. Digestion affects Mw (distribution) of especially B-type RS-3 crystals that remain after digestion

The RS-3 crystals that resist digestion in the small intestine will arrive in the colon where they might be degraded and fermented by specific gut microbiota. To examine whether these remaining RS-3 crystals had physically been changed due to the attack of pancreatic α -amylase, the Mw and PI of the remaining crystals that escaped digestion was analysed (Table 2.3).

Table 2.3. Molecular weight and polydispersity (changes) of RS-3 crystals remaining after 360 min of *in vitro* digestion, together with total digestibility (%).

| Sample name | Digestibility (%) | DP _n _{crystal} | PI _{crystal} | Δ DP _n _{crystal} (%) | Δ PI _{crystal} (%) |
|-------------|-------------------|------------------------------------|-----------------------|---|------------------------------------|
| sG2-A | 23 \pm 4 | 15.2 \pm 0.5 | 1.25 \pm 0.01 | -2.7 | 1.5 |
| sG2-B | 89 \pm 2 | n.a. | n.a. | n.a. | n.a. |
| dHBPS-A | 100 % | n.a. | n.a. | n.a. | n.a. |
| dHBPS-B | 100 % | n.a. | n.a. | n.a. | n.a. |
| sG5-A | 13 \pm 3 | 17.0 \pm 0.8 | 1.22 \pm 0.01 | -5.9 | 1.5 |
| sG5-B | 81 \pm 4 | 12.7 \pm 2.6 | 1.22 \pm 0.33 | -41.9 | 1.1 |
| dWRS-A | 20 \pm 0 | 24.8 \pm 0.3 | 1.53 \pm 0.01 | 13.7 | -4.1 |
| dWRS-B | 91 \pm 3 | 18.5 \pm 1.2 | 1.43 \pm 0.06 | -18.5 | -4.5 |
| sG20-B | 3 \pm 1 | 30.9 \pm 0.5 | 1.09 \pm 0.00 | -2.5 | -3.7 |
| dWPS-B | 33 \pm 4 | 41.8 \pm 1.5 | 2.01 \pm 0.02 | 4.4 | -4.7 |
| sG65-B | 8 \pm 1 | 68.5 \pm 1.2 | 1.10 \pm 0.01 | -10.1 | 2.6 |
| dAMPS-B | 12 \pm 2 | 50.0 \pm 0.8 | 1.69 \pm 0.02 | -6.2 | 1.4 |

The results show that for most remaining RS-3, digestion only had a minor effect on the Mw and PI compared to the undigested crystalline α -glucans (sG2-A, sG5-A, dWRS-A, sG20-B, dWPS-B) (Table 2.2, 2.3). This indicates that in most digestions, pancreatic α -amylase hydrolysed some crystals completely, whereas others were completely untouched. However, for some other samples a change in Mw and PI can be observed (sG5-B, dWRS-B, sG65-B). sG5-B crystals decreased in Mw, whereas their PI remained similar after digestion. This indicates that for sG5-B, all crystals were hydrolysed to a certain extent, without a preference for either longer or shorter α -glucans within the crystal. Furthermore, dWRS-B crystals decreased in both Mw and in PI, which indicates that all crystals were hydrolysed to a certain extent and interestingly, pancreatic α -amylase caused narrowing of the PI. In contrast, sG65-B crystals also decreased in average Mw but increased slightly in PI. This indicates that pancreatic α -amylase hydrolysed some α -glucans within the sG65-B crystals to a certain extent. Probably, the hydrolysed α -glucan remained connected to the

insoluble sG65-B crystal, thereby limiting further hydrolysis and therefore increasing the PI.

To understand how the digestion of dWRS A- and B-type crystals occurred, the digestion was monitored in time and remaining crystals that escaped digestion were analysed on Mw distribution (Figure 2.5).

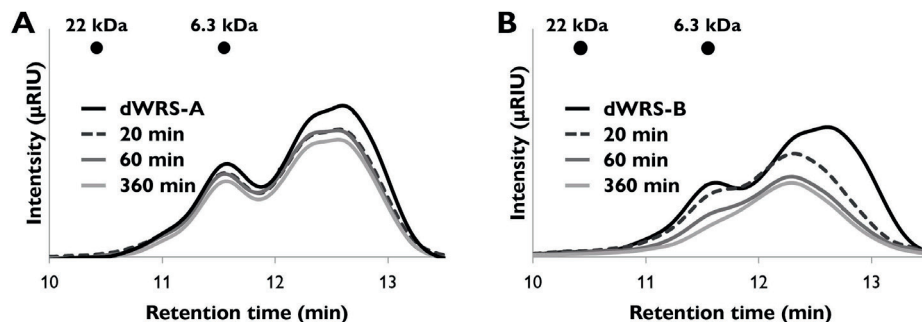


Figure 2.5. HPSEC profile of A: remaining dWRS-A and B: remaining dWRS-B crystals after 0, 20, 60 and 360 min of digestion.

The results show that A-type crystals did not change in Mw over time. Therefore, we state that the crystals were digested in a crystal-by-crystal manner: some crystals were hydrolysed completely, whereas others were untouched. However, dWRS-B type crystals changed in Mw due to digestion: the crystals consisted of a bimodal distribution at $t = 0$, which changed slowly over time to a normal distribution after 6 h of digestion (Figure 2.5).

Although activity of pancreatic α -amylase was studied extensively from a biochemistry point of view in the past, not much research is performed on the activity of pancreatic α -amylase on insoluble substrates and even less literature can be found on activity of pancreatic α -amylase on RS-3. Previously, it was revealed that human pancreatic α -amylase has two starch surface binding sites: one that binds to soluble starch molecules and another that binds to insoluble starch granules^[36]. Whether this starch surface binding site is also able to bind insoluble RS-3, is still unknown.

Our research and that of others has shown that retrograded A-type crystals were more resistant to digestion than retrograded B-type crystals^[8]. As proposed by Dhital et al. (2017), digestion of retrograded starches is probably limited due to a combination of slow enzyme binding to the surface of the substrate and slow catalysis in the active site^[9]. Retrograded A-type crystals have a much denser structure, containing less water molecules than B-type crystals^[13]. Due to this

dense structure, it might be that A-type crystals are not recognized by the surface binding sites of the enzyme. In addition, due to this dense structure, it seems likely that A-type crystals get much harder into solution compared to B-type crystals, therefore limiting enzymatic hydrolysis. Our results also show that digestion of A-type crystals reached a certain plateau value after 120 min (Figure 2.4). Since we have observed that this plateau value is reached after 120 min of digestion and no change in Mw was found due to digestion, we propose that although the crystals were bound to the surface binding site, the retrograded A-type crystals are resistant to digestion due to limited catalytic activity by the enzyme; the catalytic centre of pancreatic α -amylase was unable to hydrolyse further, probably due to the dense structure of A-type crystals.

In case of B-type crystals that have a high PI, we propose that the limited digestion is related to the slow binding to the surface binding site of the enzyme rather than the catalytic activity of the enzyme, since we did not reach plateau values at 120 or even after 360 min of digestion (Figure 2.4). Narrow disperse B-type crystals were shown to be more resistant to digestion compared to polydisperse B-type crystals (Figure 2.4, Table 2.3). Because of the low PI it seems likely that crystallization of narrow disperse α -glucans resulted in more perfect crystals, compared to polydisperse α -glucans (Figure 2.3). Consequently, narrow disperse α -glucans within the crystal are less likely to go into solution and are less hydrolysed, compared to crystals made of polydisperse α -glucans. Narrow disperse B-type crystals of DPn ≥ 32 were shown to be very resistant to digestion (Figure 2.4). Whereas sG65-B (DPn 75) did not reach a plateau value after 360 min of digestion, sG20-B (DPn 32) did. Therefore, based on our results we cannot conclude whether resistance to digestion of narrow disperse B-type crystals is more related to limited binding to the surface binding site of the enzyme or to limited catalytic activity in the active site of the enzyme. Furthermore, our results have shown that RS-3 preparations produced from low Mw α -glucans (DPn ≤ 14) cannot be considered RS, since they were fully digested within 120 min, although insoluble. Unfortunately, we were not able to confirm our hypotheses on differences in digestibility mechanism by pancreatic α -amylase by SEM on these digested samples without major sample pre-treatment that might influence the outcome. However, previous research by others has not shown major differences in morphology of the α -glucan crystals due to enzymatic digestion^[37].

Our research is the first that used enzymatic synthesis from sucrose for the production of RS-3 with defined and narrow distributed chain length. Twelve unique RS-3 preparations were produced of which half were enzymatically

synthesized and narrow disperse. The other six RS-3 preparations were produced by debranching amylopectins of different botanical sources to obtain polydisperse equivalents of similar average Mw compared to the narrow disperse α -glucans. From these twelve samples, four A-type crystals and eight B-type crystals were produced. Because of this relatively large number of unique samples, we were able to study the effect of crystal type, Mw and Mw distribution on digestibility. Our rather unique approach allowed us to study for the first time the structural properties of the RS-3 crystals that escaped enzymatic hydrolysis by pancreatic α -amylase. Rather than only analysing the released glucose after *in vitro* digestion, we also analysed the remaining RS-3 crystals on Mw distribution. This makes it possible to not only predict the amount of RS-3 that enters the colon, but also to understand the substrate for beneficial gut microbes in the colon. Our results suggest that pre-digestion experiments of B-type crystals are of importance before studying the degradation and utilisation of B-type RS-3 by gut microbiota, whereas pre-digestion is hardly of any value when exploring fermentability of A-type crystals.

4. Conclusions

Our study is the first to investigate the role of crystal type, Mw and Mw distribution on the resistance to digestion of RS-3 preparations on both released glucose after *in vitro* digestion and on the crystals that escaped digestion. It has been found that A-type crystals are much more resistant to digestion than B-type crystals, potentially caused by a reduced catalytic activity of pancreatic α -amylase towards A-type crystals. A-type crystals are digested in a crystal-by-crystal manner and therefore the Mw and Mw distribution of the remaining A-type crystals does not change. Resistance to digestion of B-type crystals is potentially caused by limited binding to the surface binding site of pancreatic α -amylase. In contrast to remaining A-type crystals, remaining B-type crystals change in Mw and/or PI which might be due to surface-hydrolysis by pancreatic α -amylase. Narrow disperse RS-3 preparations are slightly more resistant to digestion than polydisperse ones and crystals made of higher DPn α -glucans are more resistant than that of lower DPn α -glucans, irrespectively of crystal type. In addition, RS-3 preparations of DPn ≤ 14 cannot be considered RS, since they are 100 % digestible by pancreatic α -amylase, although insoluble. This study can help to design RS-3 preparations with a preferred degree of digestibility.

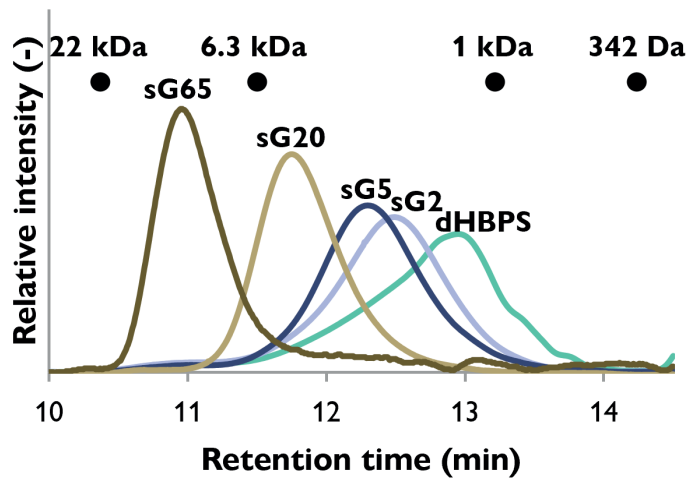
5. References

1. Zaman S.A., Sarbini S.R. The potential of resistant starch as a prebiotic. *Critical Reviews in Biotechnology*. **2016**;36(3):578-584.
2. Fuentes-Zaragoza E., Sanchez-Zapata E., Sendra E., Sayas E., Navarro C., Fernandez-Lopez J., Perez-Alvarez J.A. Resistant starch as prebiotic: A review. *Starch-Starke*. **2011**;63(7):406-415.
3. Haenen D., Zhang J., Souza da Silva C., Bosch G., van der Meer I.M., van Arkel J., van den Borne J.J., Perez Gutierrez O., Smidt H., Kemp B., Muller M., Hooiveld G.J. A diet high in resistant starch modulates microbiota composition, SCFA concentrations, and gene expression in pig intestine. *Journal of Nutrition*. **2013**;143(3):274-283.
4. Bermudez-Brito M., Rosch C., Schols H.A., Faas M.M., de Vos P. Resistant starches differentially stimulate Toll-like receptors and attenuate proinflammatory cytokines in dendritic cells by modulation of intestinal epithelial cells. *Molecular Nutrition & Food Research*. **2015**;59(9):1814-1826.
5. Lépine A.F.P., de Hilster R.H.J., Leemhuis H., Oudhuis L., Buwalda P.L., de Vos P. Higher chain length distribution in debranched type-3 resistant starches (RS3) increases TLR signaling and supports dendritic cell cytokine production. *Molecular Nutrition & Food Research*. **2018**;63(2):1801007.
6. Birt D.F., Boylston T., Hendrich S., Jane J.L., Hollis J., Li L., McClelland J., Moore S., Phillips G.J., Rowling M., Schalinske K., Scott M.P., Whitley E.M. Resistant starch: promise for improving human health. *Advances in Nutrition*. **2013**;4(6):587-601.
7. Haralampu S.G. Resistant starch - a review of the physical properties and biological impact of RS3. *Carbohydrate Polymers*. **2000**;41(3):285-292.
8. Cai L.M., Shi Y.C. Preparation, structure, and digestibility of crystalline A- and B-type aggregates from debranched waxy starches. *Carbohydrate Polymers*. **2014**;105:341-350.
9. Dhital S., Warren F.J., Butterworth P.J., Ellis P.R., Gidley M.J. Mechanisms of starch digestion by alpha-amylase-structural basis for kinetic properties. *Critical Reviews in Food Science and Nutrition*. **2017**;57(5):875-892.
10. Kiatpongarp W., Tongta S., Rolland-Sabate A., Buleon A. Crystallization and chain reorganization of debranched rice starches in relation to resistant starch formation. *Carbohydrate Polymers*. **2015**;122:108-114.
11. Gidley M.J., Bulpin P.V. Crystallization of maltooligosaccharides as models of the crystalline forms of starch - minimum chain-length requirement for the formation of double helices. *Carbohydrate Research*. **1987**;161(2):291-300.
12. Nishiyama Y., Putaux J.L., Montesanti N., Hazemann J.L., Rochas C. B->A Allomorphic transition in native starch and amylose spherocrystals monitored by in situ synchrotron X-ray diffraction. *Biomacromolecules*. **2010**;11(1):76-87.
13. Buleon A., Veronese G., Putaux J.L. Self-association and crystallization of amylose. *Australian Journal of Chemistry*. **2007**;60(10):706-718.
14. Creek J.A., Ziegler G.R., Runt J. Amylose crystallization from concentrated aqueous solution. *Biomacromolecules*. **2006**;7(3):761-770.
15. Pfanemuller B. Influence of chain-length of short monodisperse amyloses on the formation of A-type and B-type X-Ray-Diffraction patterns. *International Journal of Biological Macromolecules*. **1987**;9(2):105-108.
16. Huang Z., Zeng Z., Gao Y., Liu C., Wu J., Hu X. Crystallization of short-chain amylose: effect of precipitant. *Starch-Starke*. **2019**;71(9-10):1900007.
17. Kobayashi K., Kimura S., Naito P.K., Togawa E., Wada M. Thermal expansion behavior of A- and B-type amylose crystals in the low-temperature region. *Carbohydrate Polymers*. **2015**;131:399-406.

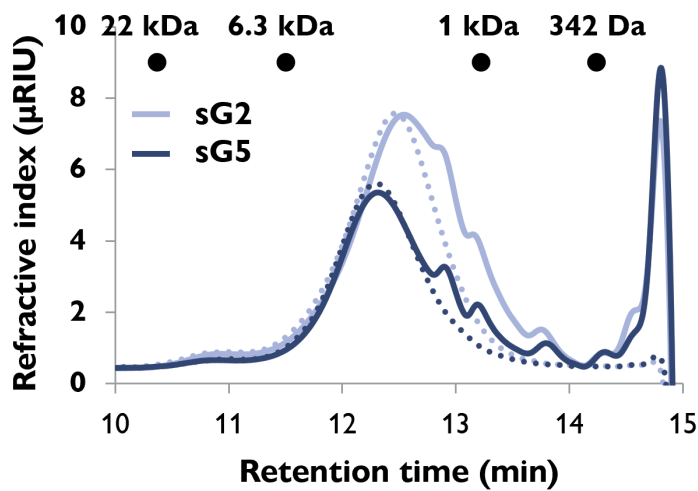
18. Montesanti N., Veronese G., Buleon A., Escalier P.C., Kitamura S., Putaux J.L. A-type crystals from dilute solutions of short amylose chains. *Biomacromolecules*. **2010**;11(11):3049-3058.
19. Martens B.M.J., Gerrits W.J.J., Bruininx E., Schols H.A. Amylopectin structure and crystallinity explains variation in digestion kinetics of starches across botanic sources in an in vitro pig model. *Journal of Animal Science and Biotechnology*. **2018**;9:91.
20. Cai L.M., Shi Y.C. Self-assembly of short linear chains to A- and B-type starch spherulites and their enzymatic digestibility. *Journal of Agricultural and Food Chemistry*. **2013**;61(45):10787-10797.
21. Cai L.M., Shi Y.C. Structure and digestibility of crystalline short-chain amylose from debranched waxy wheat, waxy maize, and waxy potato starches. *Carbohydrate Polymers*. **2010**;79(4):1117-1123.
22. van der Maarel M., Leemhuis H. Starch modification with microbial alpha-glucanotransferase enzymes. *Carbohydrate Polymers*. **2013**;93(1):116-121.
23. Kiatpongarp W., Rugmai S., Rolland-Sabate A., Buleon A., Tongta S. Spherulitic self-assembly of debranched starch from aqueous solution and its effect on enzyme digestibility. *Food Hydrocolloids*. **2016**;55:235-243.
24. Hu X., Huang Z., Zeng Z., Deng C., Luo S., Liu C. Improving resistance of crystallized starch by narrowing molecular weight distribution. *Food Hydrocolloids*. **2020**;103:105641.
25. Yanase M., Takaha T., Kuriki T. alpha-Glucan phosphorylase and its use in carbohydrate engineering. *Journal of the Science of Food and Agriculture*. **2006**;86(11):1631-1635.
26. Chang R., Xiong L., Li M., Liu J., Wang Y., Chen H., Sun Q. Fractionation of debranched starch with different molecular weights via edible alcohol precipitation. *Food Hydrocolloids*. **2018**;83:430-437.
27. Roger P., Axelos M.A.V., Colonna P. SEC-MALLS and SANS studies applied to solution behavior of linear alpha-glucans. *Macromolecules*. **2000**;33(7):2446-2455.
28. Ohdan K., Fujii K., Yanase M., Takaha T., Kuriki T. Enzymatic synthesis of amylose. *Biocatalysis and Biotransformation*. **2006**;24(1-2):77-81.
29. Luley-Goedl C., Nidetzky B. Carbohydrate synthesis by disaccharide phosphorylases: reactions, catalytic mechanisms and application in the glycosciences. *Biotechnology Journal*. **2010**;5(12):1324-1338.
30. Qi P., You C., Zhang Y.-H.P. One-pot enzymatic conversion of sucrose to synthetic amylose by using enzyme cascades. *ACS Catalysis*. **2014**;4(5):1311-1317.
31. van den Broek L.A., van Boxtel E.L., Kievit R.P., Verhoef R., Beldman G., Voragen A.G. Physico-chemical and transglucosylation properties of recombinant sucrose phosphorylase from *Bifidobacterium adolescentis* DSM20083. *Applied Microbiology and Biotechnology*. **2004**;65(2):219-227.
32. Bradford M.M. A rapid and sensitive method for the quantitation of microgram quantities of protein utilizing the principle of protein-dye binding. *Analytical Biochemistry*. **1976**;72:248-254.
33. van der Vlist J., Reixach M.P., van der Maarel M., Dijkhuizen L., Schouten A.J., Loos K. Synthesis of branched polyglucans by the tandem action of potato phosphorylase and *Deinococcus geothermalis* glycogen branching enzyme. *Macromolecular Rapid Communications*. **2008**;29(15):1293-1297.
34. Zeng F., Zhu S.M., Chen F.Q., Gao Q.Y., Yu S.J. Effect of different drying methods on the structure and digestibility of short chain amylose crystals. *Food Hydrocolloids*. **2016**;52:721-731.
35. Englyst H.N., Kingman S.M., Cummings J.H. Classification and measurement of nutritionally important starch fractions. *European Journal of Clinical Nutrition*. **1992**;46 Suppl 2:S33-50.

36. Zhang X., Caner S., Kwan E., Li C., Brayer G.D., Withers S.G. Evaluation of the significance of starch surface binding sites on human pancreatic alpha-amylase. *Biochemistry*. **2016**;55(43):6000-6009.
37. Ziegler G.R. Enzyme-resistant starch spherulites. *Starch-Starke*. **2020**;72(7-8):1900217.

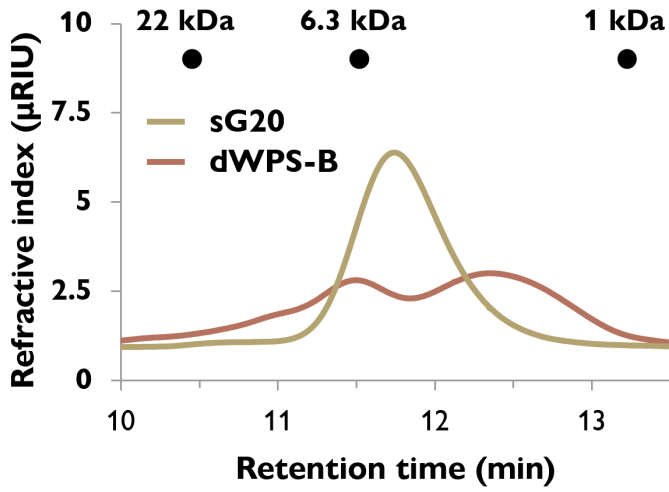
6. Supplementary information



Supplementary figure 2.1. HPSEC elution profiles of purified enzymatically synthesized α -glucans sG65, sG20, sG5 and sG2 together with acceptor dHBPS.

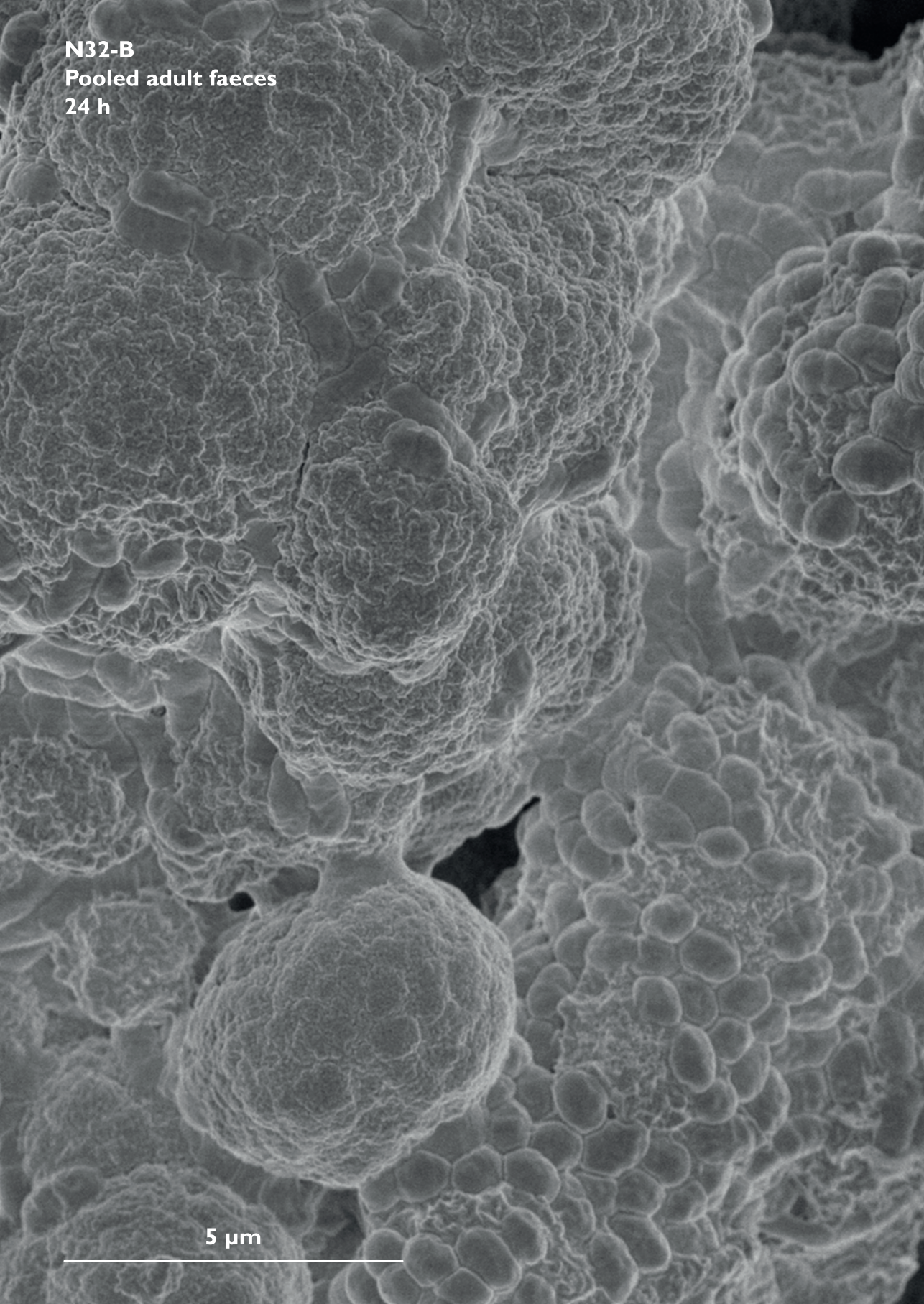


Supplementary figure 2.2. HPSEC elution profiles of synthesized narrow disperse α -glucans sG2 and sG5 before (solid) and after (dotted) purification.



Supplementary figure 2.3. HPSEC elution profiles of polydisperse dWPS-B and narrow disperse sG20-B crystals.

N32-B
Pooled adult faeces
24 h



5 µm

A scanning electron micrograph (SEM) showing several starch granules. The granules have a highly textured, reticulated surface with numerous small, rounded protrusions and deep, irregular grooves. The granules are clustered together, with some appearing more rounded and others more elongated. The overall appearance is that of a complex, porous network of organic material.

Chapter 3

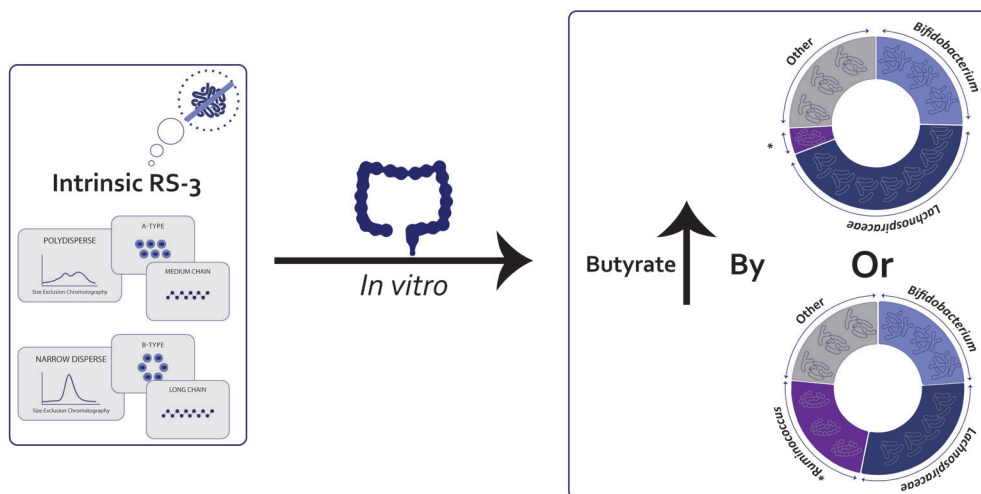
Type of intrinsic resistant starch type 3
determines *in vitro* fermentation by pooled
adult faecal inoculum

Cynthia E. Klostermann, Martha F. Endika,
Evert ten Cate, Piet L. Buwalda †, Paul de Vos,
Johannes H. Bitter, Erwin G. Zoetendal, Henk. A. Schols

Accepted for publication in *Carbohydrate Polymers*

Abstract

Resistant starch (RS) results in relatively high health-beneficial butyrate levels upon fermentation by gut microbiota. We studied how physico-chemical characteristics of RS-3 influenced butyrate production during fermentation. Six highly resistant RS-3 substrates (intrinsic RS-3, 80-95 % RS) differing in chain length (DPn 16 - 76), Mw distribution (PI) and crystal type (A/B) were fermented *in vitro* by pooled adult faecal inoculum. All intrinsic RS-3 substrates were fermented to relatively high butyrate levels (acetate / butyrate ≤ 2.5), but especially fermentation of A-type RS-3 prepared from polydisperse α -1,4 glucans resulted in the highest relative butyrate amount produced (acetate / butyrate: 1). Analysis of the microbiota composition after fermentation revealed that intrinsic RS-3 stimulated primarily *Lachnospiraceae*, *Bifidobacterium* and *Ruminococcus*, but the relative abundances of these taxa differed slightly depending on the RS-3 physico-chemical characteristics. Especially intrinsic RS-3 of narrow disperse Mw distribution stimulated relatively more *Ruminococcus*. Selected RS fractions (polydisperse Mw distribution) obtained after pre-digestion were fermented to acetate and butyrate (ratio ≤ 1.8) and stimulated *Lachnospiraceae* and *Bifidobacterium*. This study indicates that especially Mw distribution of RS-3 influences butyrate production and microbiota composition during RS-3 fermentation.



1. Introduction

Butyrate is a short-chain fatty acid (SCFA) that is among others essential for health by providing energy to colonocytes^[1]. In addition, butyrate has been associated with modulation of immune and inflammatory responses, stimulation of intestinal barrier function and with prevention of colorectal cancer^[2-6]. To increase butyrate production in the colon and promote a healthy colonic environment, resistant starch (RS) could be a promising fibre to be included in the diet. RS is defined as starch that escapes digestion and arrives in the colon, where it will be fermented by colonic bacteria to SCFAs like acetate, propionate and butyrate. Compared to other dietary fibres, RS is known to be fermented to high amounts of butyrate by gut microbiota^[7, 8]. Five different types of RS exist, of which type 1 and 2 are native starch forms that can be found in plants, type 3 is retrograded starch, produced after gelatinization and cooling of starch, type 4 is chemically modified starch and type 5 comprises the amylose-lipid complexes^[9]. The fermentability of these 5 types of RS by gut microbiota differs immensely, both between RS types as within an RS type^[10-14]. Among the different types of RS, resistant starch type 3 is of interest for its thermal stability and applicability as food ingredient^[15].

Fermentation of resistant starch has been associated with increased levels of *Bifidobacterium*, *Ruminococcus* and genera often associated with butyrate production such as *Eubacterium*, *Faecalibacterium* and *Roseburia*^[16]. It has been shown that *Bifidobacterium adolescentis* and *Ruminococcus bromii* are the species that are mostly responsible for primary degradation of RS, since they express many α -amylases and carbohydrate binding modules (CBMs) that are associated with degradation of insoluble starches^[17, 18]. Both *R. bromii* and *B. adolescentis* do not produce butyrate themselves^[19, 20], but cross-feed with butyrate producing bacteria like *Agathobacter rectalis* (previously known as *Eubacterium rectale*), *Faecalibacterium prausnitzii* and *Roseburia faecis*^[21], that use acetate, alone or in combination with lactate, as energy sources resulting in the production of butyrate. This cross-feeding results in an efficient degradation of RS^[18] and a relatively high production of butyrate^[22].

Resistant starch type 3 (RS-3) can be produced by gelatinizing starch followed by retrogradation and is commercially produced from high-amylose starch^[23] or long-chain maltodextrin obtained after partial enzymatic debranching of tapioca starch^[24]. RS-3 can also be produced by controlled crystallization of debranched amylopectins at specific temperatures to result in either A- or B-type crystals^[25, 26]. However, debranching amylopectins results in α -glucans with a

quite broad Mw distribution (polydispersity index (PI) > 1.3)^[26]. A controlled chain length of α -1,4 glucans can be achieved by the use of synthesizing enzymes^[26, 27], resulting in α -1,4 glucans with a more narrow Mw distribution (PI < 1.3). Recently, twelve unique RS-3 preparations differing in Mw, Mw distribution and crystal type were produced, obtained by crystallization of either debranched amylopectins or enzymatically synthesized α -1,4 glucans^[26]. Pancreatic digestion of these twelve RS-3 preparations revealed that especially long chain B-type crystals (DPn 32 – 75) and short-chain A-type crystals (DPn 15 – 22) are resistant to digestion by pancreatic α -amylase, with 80 – 95 % of the starch expected to reach the colon^[26]. Since these specific RS-3 preparations do only contain a minor fraction of digestible starch, they are considered as “intrinsic RS” and are quite different from commercial RS-3 ingredients like Novelose® 330 and C*Actistar, that contain up to 50 % RS^[10], and thereby should better be referred to as “RS-rich”.

Not many studies focussed on the fermentability of RS-3 *in vitro* and *in vivo*. Only few studies used commercial RS-rich RS-3 ingredients^[10, 28], used RS-3 preparations from debranched starches produced in a laboratorial setting^[11, 29-31], or produced RS-3 rich starches from raw potatoes^[13]. All these studies thus used RS-3 preparations made of α -glucans with a polydisperse Mw distribution. These studies mentioned the production of SCFAs and changes in microbiota composition during *in vitro* fermentation, but did not include a quantitative analysis on the starch consumption by the gut microbiota. An *in vitro* fermentation study incorporating RS-3 structures with a defined crystal type, Mw and especially Mw distribution is still lacking, but needed to understand which chemical features are responsible for distinct SCFA production by the gut microbiota.

We investigated how RS-3 is fermented by gut microbiota of healthy adults and which RS-3 physico-chemical characteristics influence butyrate production in the colon. To study the butyrogenic potential of novel and well-characterized RS-3 preparations^[26], six intrinsic RS-3 substrates and two RS-fractions obtained after pre-digestion of selected RS-3 preparations were fermented *in vitro* by an inoculum consisting of a pool of four adult faecal samples. A new sampling method for insoluble fibres was developed to enable to quantification of the remaining soluble and insoluble starch during fermentation. Starch degradation, SCFA production and microbiota composition were determined during *in vitro* fermentation. Additionally, the change in morphology of RS-3 particles due to fermentation was analysed over time using scanning electron microscopy.

2. Materials and methods

2.1. Materials

Medium components used for the *in vitro* fermentation and dialysate solution containing 25 g/L $\text{K}_2\text{HPO}_4 \cdot 3\text{H}_2\text{O}$, 45 g/L NaCl, 0.05 g/L $\text{FeSO}_4 \cdot 7\text{H}_2\text{O}$ and 0.5 g/L ox-bile were obtained from Tritium Microbiologie (Eindhoven, The Netherlands). L-cysteine-hydrochloride, 2-(N-morpholino)ethanesulfonic acid, soluble potato starch and porcine pancreatin were obtained from Sigma-Aldrich (St. Louis, Missouri, USA).

2.1.1. RS-3 preparations

RS-3 preparations were prepared by crystallizing α -1,4 glucans obtained by either debranched (enzymatically modified) amylopectins or enzymatic synthesis as described in Chapter 2^[26]. The (enzymatically modified) amylopectins included waxy potato starch (WPS, Eliane100) and amylomaltase-modified potato starch (AMPS, Etenia457) provided by AVEBE (Veendam, The Netherlands) and waxy rice starch (WRS, Remyline XS) obtained from Beneo (Mannheim, Germany). The specific physico-chemical characteristics and *in vitro* digestibility of the obtained RS-3 preparations have been described in Chapter 2^[26] and are presented in Table 3.1 in the Results section.

2.1.2. Faecal slurry

Faecal material of four healthy adults was collected, after signing a written informed consent. Subjects were between 27 and 35 years old, had a BMI between 19 – 22 kg/m², were non-smokers, did not have any health complaints, and did not use antibiotics for over 6 months prior to collection. Faecal samples were stored immediately in a sterile 50 mL container with filter screw cap (Greiner Bio-One CELLSTAR™ tube, Kremsmünster, Austria). The container was placed inside a pouch with a BD GasPak EZ anaerobe gas generating system with indicator (BD Diagnostics, Sparks, Maryland, USA) and stored at 4 °C for a maximum of 24 h until processing. Pooled adult faecal slurry was prepared in an anaerobic chamber (gas composition: 4 % H_2 , 15 % CO_2 , 81 % N_2 , Bactron 300, Sheldon Manufacturing, Cornelius, Oregon, USA) by mixing equal aliquots of fresh faeces with a pre-reduced dialysate-glycerol solution to 25 % w/v as previously described^[32]. The pre-reduced dialysate-glycerol solution contained ten times diluted dialysate solution, 10 % glycerol, 0.5 mg/L resazurin, 0.4 g/L L-cysteine-hydrochloride, supplemented with 0.45 g/L $\text{CaCl}_2 \cdot 2\text{H}_2\text{O}$ and 0.5 g/L

MgSO₄·7H₂O. The final faecal slurry was snap-frozen using liquid nitrogen and stored at -80 °C prior to use.

2.2. *In vitro* batch fermentation of RS-3 preparations

2.2.1. Culture medium

The culture medium was based on Simulated Ileal Efflux Medium (SIEM) as described previously^[33] with minor modifications and is referred to as mSIEM. The carbohydrate component, pre-mixed from Tritium Microbiologie, was ten times lowered when compared to Minekus et al. (1999) and consisted of pectin, xylan, arabinogalactan, amylopectin (all at 0.048 g/L) and soluble starch (0.4 g/L). The protein component consisted of bactopectone and casein (both at 3 g/L). Additionally, the medium contained 0.05 g/L ox-bile, 2.5 g/L K₂HPO₄·3H₂O, 4.5 g/L NaCl, 0.45 g/L CaCl₂·2H₂O, 0.005 g/L FeSO₄·7H₂O and 0.01 g/L haemin, 0.5 g/L MgSO₄, and 0.4 g/L L-cysteine-hydrochloride. A vitamin mix was added with a final concentration of 1 µg/L menadione, 2 µg/L D-biotin, 0.5 µg/L vitamin B12, 10 µg/L D-pantothenate, 5 µg/L nicotinamide adenine dinucleotide, 5 µg/L aminobenzoic acid, 4 µg/L thiamine HCl. The medium was buffered at pH 5.8 using 0.1 M MES buffer. The medium was stored overnight in the anaerobic chamber with an opened lid to remove head-space oxygen.

Culture medium containing soluble potato starch (mSIEM + SPS) was prepared by dissolving 40 mg/mL SPS in sterile milliQ (MQ) water in a boiling water bath for 10 min. After cooling, the solubilized SPS was mixed with concentrated mSIEM to obtain a final concentration of 11.11 mg/mL SPS in mSIEM. The final mSIEM + SPS medium was stored overnight in the anaerobic chamber with an opened lid to remove head-space oxygen.

2.2.2. Pre-digestion of RS-3 preparations

Pre-digestion was performed based on methods as previously described by Martens and colleagues^[34], with 2 mg pancreatin per mg starch. In short, porcine pancreatin solution was prepared by mixing 12 gram pancreatin (8 × USP specifications (P7545), Sigma-Aldrich; enzyme was sufficient to theoretically degrade digestible starch in less than 1 minute) in 80 mL MQ head-over-tail for 10 min, followed by centrifugation at 4 °C, 10,000 × g for 10 min. The supernatant was collected and an aliquot of 48.8 mL of the supernatant was diluted with 11.2 mL MQ to obtain pancreatin solution. Pancreatin solution (20 %), 0.5 M sodium acetate buffer pH 5.9 (20 %) and MQ were added to RS-3 preparations P40-B, P21-A and P22-B to obtain a suspension of

approximately 20 mg/mL in 100 mM sodium acetate buffer pH 5.9^[26]. The suspension was incubated at 37 °C for 6 h in a shaking incubator at 100 rpm. Afterwards, the suspension was centrifuged at 4 °C, 7000 x g for 10 min, and the supernatant was decanted. The remaining pellet was washed 4 times with MQ water, after which the pellet was dried at 40 °C for 48 h. The remaining material was homogenized with a mortar to obtain pre-digested (pd) RS-3 starches P40-B-pd, P21-A-pd and P22-B-pd. Within P40-B-pd and P21-A-pd ± 23 and ± 18 % of the total starch was digested, respectively, which was close to the digestible starch fraction reported previously^[26]. Within P22-B-pd ± 47 % of the total starch was digested, which was lower compared to digestible starch fraction reported previously^[26], indicating that P22-B-pd might still contain a fraction of digestible starch.

2.2.3. *In vitro* batch fermentation

RS-3 preparations (± 20 mg dry weight), either directly or after pre-digestion (section 2.2.2.), were weighed in duplicate in sterile 5 mL serum bottles for each individual sampling time. The weighed RS-3 preparations were stored overnight in the anaerobic chamber.

In the anaerobic chamber, inoculum was prepared by diluting pooled adult faecal slurry to 10 mg/mL faeces in mSIEM. An aliquot of 1.8 mL mSIEM was added to the serum bottles containing RS-3 preparations and subsequently 0.2 mL inoculum was added. Serum bottles containing mSIEM + SPS were also incubated with inoculum to obtain 10 mg/mL SPS with 1 mg/mL faeces. In addition, substrate blanks (without inoculum) and medium blanks (including mSIEM carbohydrates, without additional substrate) were included. All serum bottles were capped with butyl rubber stoppers. In a first fermentation experiment, intrinsic RS-3 substrates (N16-A, N18-A, P21-A, N32-B and N76-B) were incubated at 37 °C, 100 rpm for 0, 24 and 48 h (section 3.2.). In a second fermentation experiment, pre-digested RS-3 preparations (P22-B-pd and P40-B-pd) and controls (N32-B and P21-A-pd) were incubated at 37 °C, 100 rpm for 0, 8, 24, 36 and 48 h (section 3.3.).

To accurately quantify the degradation of insoluble (resistant) starches, a dedicated sampling method was developed. At each time point, the serum bottles were decapped and the insoluble RS-3 preparations were re-suspended. Immediately, 1.8 mL was transferred to sterile weighed Safe-Lock Eppendorf tubes (Eppendorf, Hamburg, Germany). These were subsequently centrifuged at 4 °C, 20,000 x g for 10 min and the supernatant was separated from the pellet. The supernatant was heated to 100 °C in a Safe-Lock Eppendorf tube at 800 rpm

for 10 min in an Eppendorf shaker (Eppendorf) and subsequently stored at -20 °C for chemical analysis. In the case of N32-B, P21-A-pd, P22-B-pd and P40-B-pd, an aliquot of 25 µL of the contents of the serum bottle containing some remaining RS-3 particles was used for Scanning Electron Microscopy analyses (section 2.6.). The remaining contents in the serum bottles were washed with 0.75 mL sterile MQ twice and added to the Eppendorf tube containing the pellet, mixed and centrifuged once more (4 °C, 20,000 × g, 10 min). The second supernatant was decanted and the Safe-Lock Eppendorf tubes containing the pellet were snap-frozen with liquid nitrogen, stored at -80 °C and freeze-dried. The times indicated in all figures are the inactivation times, except for t_0 ; total sampling time took around 2 – 3 h.

2.3. Total starch quantification of fermented RS-3 preparations

Starch was quantified in the fermentation supernatants and pellets using the Megazyme Total Starch Kit (AA/AMG) (Megazyme, Wicklow, Ireland). For analysis of glucose + soluble starch in the supernatant, company protocol f was used, adjusted for smaller sample sizes. In short, the supernatant was defrosted and 50 µL was taken in duplicate. To each sample 50 µL 200 mM sodium acetate buffer pH 4.5 was added and incubated with 2 µL α -amylase (2,500 U/mL on Ceralpha reagent at pH 5.0 and 40 °C, according to the company protocol) and 2 µL amyloglucosidase (3,300 U/mL on soluble starch at pH 4.5 and 40 °C, according to the company protocol) at 50 °C for 30 min. The samples were further diluted with 100 mM sodium acetate buffer pH 5 to reach a final concentration of < 0.8 mg/mL glucose.

To determine the total starch content in the initial RS-3 preparations, pre-digested RS-es and freeze-dried pellets after fermentation, approximately 500 µg sample was weighed in glass vials in duplicate using a microbalance (Mettler Toledo XP6 Microbalance, Columbus, Ohio, USA).

For pre-digested substrates and RS-3 preparations having a chain length > DPn 30, company protocol b was used, adjusted for smaller sample sizes. In short, 6 µL cold 80 % EtOH was added to 500 µg material and mixed. Next, 60 µL cold 1.7 M NaOH was added and mixed for 10 seconds. The mixture was stored on ice for 15 min while mixing multiple times. Subsequently, 240 µL 600 mM sodium acetate buffer pH 3.8 was added and mixed. Freeze-dried RS-3 preparations having a chain length < DPn 25 were hot-water soluble. Therefore, to the weighed samples obtained from these RS-3 preparations, 300 µL 100 mM sodium acetate buffer pH 4.5 was added and heated in a boiling water bath for 10 min to dissolve the starch. After dissolving the starch by either

1.7 M NaOH or by boiling, 250 μ L was transferred to a new tube and 2 μ L α -amylase (2,500 U/mL) and 2 μ L amyloglucosidase (3,300 U/mL) were added. The samples were incubated at 50 °C for 30 min in an Eppendorf shaker (800 rpm) and 100 mM sodium acetate buffer pH 5 was added to obtain a final concentration of < 0.8 mg/mL glucose.

Free glucose content was analysed with the GOPOD assay kit (Megazyme) using microtiter plates. Briefly, 15 μ L diluted sample was added to a 96-well-plate in triplicate and 225 μ L GOPOD reagents was added. A calibration curve of 0.1 – 0.8 mg/mL glucose was included in the analysis for quantification. The 96-well plates were incubated at 40 °C for 20 min and analysed with a Tecan Spectrophotometer at 520 nm (Tecan Infinite F500, Männedorf, Switzerland).

2.4. Molecular weight distribution of RS-3 remaining after fermentation

Freeze-dried pellets were solubilized in 1 M NaOH at 60 mg/mL sample. The samples were diluted to 2.5 mg/mL, to avoid re-precipitation of the linear α -1,4 glucans and neutralized by addition of 1 M HCl. The molecular weight distribution was analysed using HPSEC-RI according to Klostermann et al. (2021) (Chapter 2^[26]).

2.5. Short-chain fatty acids and other organic acids produced by fermentation

SCFAs, lactic and succinic acid were analysed as previously described^[35]. Samples were diluted 5 times with MQ and centrifuged at 19,000 x g for 10 min. The supernatant (10 μ L injection volume) was analysed using an Ultimate 3000 HPLC system (Dionex, Sunnyvale, California, USA) in combination with an Aminex HPX-87H column (Bio-Rad laboratories Inc, Hercules, California, USA). Acids were detected by a refractive index detector (RI-101, Shodex, Yokohama, Japan) and a UV detector set at 210 nm (Dionex Ultimate 3000 RS variable wavelength detector). Elution was performed at 0.5 mL/min and 50 °C using 50 mM sulphuric acid as eluent. Acetic, propionic, butyric, lactic and succinic acid standard curves were used for quantification (0.05 – 2 mg/mL). Data analysis was performed with Chromeleon™ 7.2.6 software from Thermo Fisher Scientific (Waltham, Massachusetts, USA).

2.6. Scanning Electron Microscopy of fermented RS-3 preparations

Fermented substrates N32-B, P21-A-pd, P22-B-pd and P40-B-pd were dried on 13 mm filters with 10 μ m pores (Merck Isopore™ membrane filter (Merck, Burlington, Massachusetts, USA)), in a flow cabinet, attached to sample holders containing carbon adhesive tabs (EMS, Washington, USA) and sputter coated

with 12 nm tungsten (EM SCD 500, Leica, Vienna, Austria). The samples were analysed using scanning electron microscopy (SEM) (Magellan 400, FEI, Eindhoven, The Netherlands) at the Wageningen Electron Microscopy Center. SEM images were recorded at an acceleration voltage of 2 kV and 13 pA and magnification of 5,000 (Everhart-Thornley detector), 10,000 and 25,000 (Through Lens Detector) times.

2.7. Microbiota composition analysis

DNA was extracted from approximately 1 – 10 mg of freeze-dried pellet followed by repeated bead-beating steps in Stool Transport and Recovery (STAR) buffer as previously described^[36]. Afterwards, the DNA was purified using the Maxwell 16 Tissue LEV Total RNA Purification Kit Cartridge (XAS1220) (Promega, Madison, Wisconsin, USA). The purified DNA was diluted to 20 ng/μL using nuclease-free water.

Duplicate PCRs were performed using barcoded primers to amplify the V4 region of the 16S ribosomal RNA (rRNA) gene. The unique barcoded primer pair 515F^[37] – 806R^[38] was used. Each PCR reaction contained 10 μL of 5x Phusion Green HF buffer (Thermo Fisher Scientific), 1 μL of 10 mM dNTPs (Promega), 0.5 μL of Phusion Hot start II DNA polymerase (2U/μL) (Thermo Fisher Scientific), 1 μL of barcoded primers (10 μM) and 20 ng purified DNA. The reaction mixture was filled up with nuclease-free water to 50 μL (Qiagen, Hilden, Germany). The PCR program included an initial denaturation step for 30 s at 98 °C, followed by 25 cycles of 98 °C for 10 s, of 50 °C for 10 s and of 70 °C for 10 s, with a final extension of 70 °C for 7 min. For samples that had a DNA concentration < 20 ng/μL more DNA was added during PCR amplification or 30 PCR cycles were performed. The obtained PCR products were visualized on agarose gels, pooled and purified using CleanPCR (CleanNA, Waddinxveen, The Netherlands). The purified PCR products were quantified using QubitTM dsDNA BR assay kit (Invitrogen by Thermo Fisher Scientific) and a DeNovix DS-11 Fluorometer (DeNovix Inc., Wilmington, Delaware, USA). Two mock communities of known composition and one no-template control were included in each library. The PCR products were pooled in equimolar amounts and concentrated to 40 μL using CleanPCR. Libraries were sent for Illumina HiSeq2500 (2 x 150 bp) sequencing (Novogene, Cambridge, UK).

2.8. Data analysis

Raw sequence data of the 16S rRNA gene amplicons was processed using the NG-Tax 2.0 pipeline and default settings^[39]. Taxonomy of each amplicon

sequence variant (ASV) was assigned based on the SILVA database version 138.1^[40, 41]. Data was analysed using R version 4.1.0, using the R packages phyloseq version 1.38.0^[42], microbiome version 1.17.42^[43] and microViz version 0.10.1^[44]. Relative abundance of microbial taxa was calculated based on the 16S rRNA gene sequence read counts. Taxa with unidentified genus were renamed to the lowest classified taxonomic rank and sorted based on taxon abundance, e.g. the ASV of *Lachnospiraceae* Family 01 is the most abundant ASV of unidentified genus of *Lachnospiraceae*. The relative abundances of ASVs were visualized in a heatmap using the microViz package^[44]. Principle component analysis (PCA) and principle coordinate analysis (PcoA) were used to visualize the microbiota variation between substrates after centered-log-ratio (CLR) transformation or Generalized UniFrac and Unweighted UniFrac distances, respectively. PERMANOVA analyses were performed to determine if physico-chemical characteristics of RS-3 significantly influenced the microbiota composition using the adonis function of the vegan package version 2.6.2^[45], and statistically different parameters were visualized by redundancy analyses using crystal type, Mw distribution (dispersity) and chain length as constraint variables. Statistical analyses on starch degradation and SCFA formation were not performed due to the too low number of biological replicates. The standard deviation obtained from biological duplicates is shown in the figures.

3. Results

3.1. Characteristics of RS-3 preparations

RS-3 preparations with known crystal type (A vs B), chain length (DP16 – 76) and Mw distribution (PI 1.07 – 2.11) consisted of six RS-3 substrates which were highly resistant (≥ 80 %) to pancreatic digestion (defined as “intrinsic RS-3”) and two other RS-3 preparations with lower resistance (20 – 70 %, defined as “RS-rich”), and were prepared previously, as described in Chapter 2^[26]. The most relevant physico-chemical characteristics of the eight RS-3 preparations are shown in Table 3.1. The sample name has been recoded compared to Klostermann et al., 2021, with N: narrow disperse, P: polydisperse, **number**: DPn, **A**: A-type crystal, **B**: B-type crystal.

The intrinsic RS-3 preparations comprised of three substrates with an A-type crystal pattern (N16-A, N18-A, P21-A) and three with a B-type crystal pattern (N32-B, P53-B and N76-B). The intrinsic RS-3 preparations with an A-type crystal had a lower average Mw, compared to intrinsic RS-3 preparations with a B-type

crystal (Table 3.1). The RS-rich RS-3 preparations comprised of two substrates with a B-type crystal, prepared from α -1,4 glucans of polydisperse Mw. These RS-3 preparations were partially pre-digested prior to fermentation to obtain an RS-rich fraction.

Table 3.1. Physico-chemical and digestibility characteristics of RS-3 preparations used in this study as described in Klostermann et al. (2021)^[26].

| Sample name | Reported in [26] | Crystal type | DP _n _{crystal} | PI _{crystal} | <i>In vitro</i> digestibility (120 min (%)) | RS category |
|-------------|------------------|--------------|------------------------------------|-----------------------|---|-------------|
| N16-A | sG2-A | A | 16 | 1.23 | 20 | Intrinsic |
| N18-A | sG5-A | A | 18 | 1.21 | 12 | Intrinsic |
| P21-A | dWRS-A | A | 21 | 1.59 | 21 | Intrinsic |
| P22-B | dWRS-B | B | 22 | 1.50 | 80 | RS-rich |
| N32-B | sG20-B | B | 32 | 1.14 | 5 | Intrinsic |
| P40-B | dWPS-B | B | 40 | 2.11 | 26 | RS-rich |
| P53-B | dAMPS-B | B | 53 | 1.67 | 9 | Intrinsic |
| N76-B | sG65-B | B | 76 | 1.07 | 6 | Intrinsic |

DP_n (number-based degree of polymerization) and PI (polydispersity index) were determined using HPSEC-RI, crystal type was determined using XRD and *in vitro* digestion was performed using pancreatin and amyloglucosidase^[26]. RS-rich refers to 20 – 70 % RS and intrinsic RS refers to ≥ 80 % RS.

3.2. Fermentation of intrinsic RS-3 preparations by adult gut microbiota

The six intrinsic RS-3 preparations were fermented *in vitro* during 48 h using an inoculum of a pool of four healthy adult faecal samples. After fermentation, the starch degradation and SCFA formation were quantified and the changes in microbiota composition were evaluated.

3.2.1. Intrinsic RS-3 substrates are degradable by adult gut microbiota

After incubation, the remaining insoluble and soluble starch fractions were quantified at given time points (Supplementary table 3.1; Supplementary table 3.2 for recoveries in substrate blanks). Up to 10 % of the intrinsic RS-3 preparations solubilized during incubation of intrinsic RS-3 preparations without inoculum. However, in the fermented intrinsic RS-3 substrates hardly any soluble starch was found, which indicates that fermentation of soluble starch was favoured over insoluble starch (Supplementary table 3.1).

Quantifying the remaining starch at different time points showed that all A-type intrinsic RS-3 substrates were fermented quite similarly (Figure 3.1-A).

N18-A was fermented slightly slower compared to N16-A and P21-A during the first 24 h, but its fermentation rate increased during the last 24 h of incubation. After 48 h, 65 % of all A-type intrinsic RS-3 preparations were degraded.

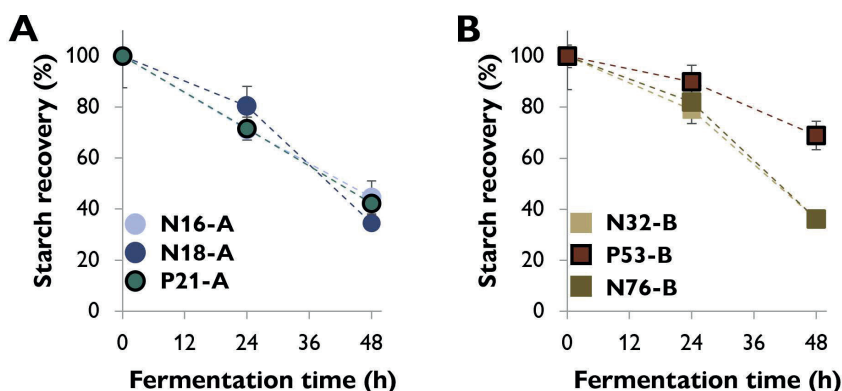


Figure 3.1. Starch recovery after *in vitro* batch fermentation of intrinsic RS-3 with pooled adult faecal inoculum for 0, 24 and 48 h. Figure A and B represent A-type and B-type intrinsic RS-3, respectively. All starch recovery values were normalized for starch recovery found at t0. Non-normalized starch recoveries can be found in Supplementary table 3.1. The average of biological duplicates is shown.

B-type intrinsic RS-3 preparations were fermented differently (Figure 3.1-B). N32-B and N76-B (narrow disperse Mw distribution) were fermented at a very similar rate; after 24 h of fermentation the fermentation rate increased until around 65 % of the initial starch was fermented, similar to A-type intrinsic RS-3. The fermentation rate of P53-B (polydisperse Mw distribution) also increased after 24 h of fermentation, but after 48 h only 30 % of P53-B was fermented and thus final fermentability was lower compared to narrow disperse B-type intrinsic RS-3.

It should be noted that compared to intrinsic RS-3, digestible starch was already almost completely fermented within 24 h (Supplementary table 3.1), indicating the slow fermentability of intrinsic RS-3.

3.2.2. Intrinsic RS-3 preparations stimulate colonic butyrate production

To study the butyrogenic potential of intrinsic RS-3 substrates, SCFAs, lactic and succinic acid were quantified during the *in vitro* fermentation. In contrast to digestible starch which showed high lactate production, intrinsic RS-3 substrates were mainly fermented to acetate and butyrate with only traces of propionate and lactate (< 0.4 and < 0.1 $\mu\text{mol}/\text{mg}$ substrate, respectively) after 24 and 48 h of

fermentation (Figure 3.2), whereas no succinate was detected. As expected, very low concentrations of SCFAs were observed in the medium blanks (Supplementary figure 3.1).

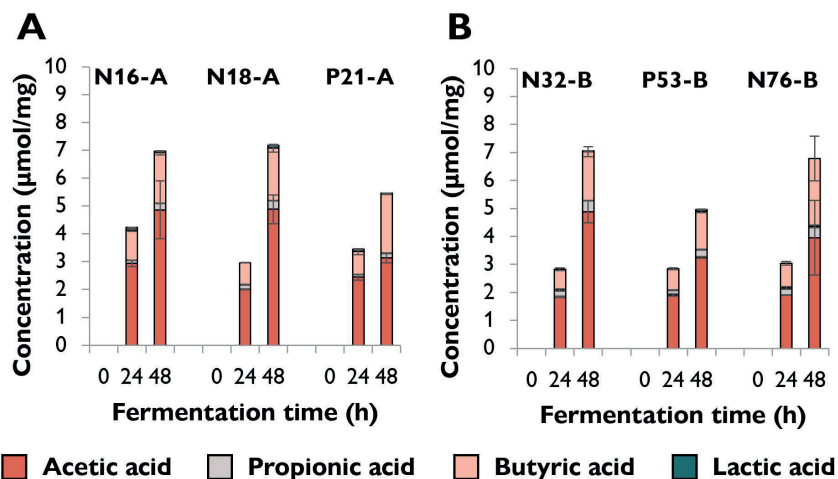


Figure 3.2. SCFA and lactic acid formation ($\mu\text{mol/mg}$ substrate) during 48 h fermentation of intrinsic RS-3 by pooled adult faecal inoculum. Figure A and B represent A-type and B-type intrinsic RS-3, respectively. Results for the medium blank and positive control SPS are shown in Supplementary figure 3.1. The average of biological duplicates is shown.

N16-A was fermented to acetate and butyrate in a ratio of ± 2.7 , illustrating a relatively high proportion of butyrate, at both 24 and 48 h of fermentation and a total amount of $7.0 \mu\text{mol/mg}$ substrate after 48 h of fermentation (Figure 3.2-A). The acetate-butyrate ratio of N18-A was ± 2.5 at 24 and 48 h of fermentation with a total SCFA content of $7.2 \mu\text{mol/mg}$ substrate (48 h). In contrast, fermentation of P21-A resulted in a decrease in the acetate-butyrate ratio from 3.0 to 1.5 after 24 and 48 h of incubation, respectively, with a total SCFA content of $5.5 \mu\text{mol/mg}$ substrate after 48 h of fermentation. P21-A (polydisperse Mw distribution) was thus fermented differently, compared to N16-A and N18-A (narrow disperse Mw distribution), although a rather similar amount of starch was utilized (Figure 3.1-A).

Intrinsic RS-3 substrates with a B-type crystal pattern (N32-B, P53-B and N76-B) were mostly fermented to acetate and butyrate in an acetate-butyrate ratio of approximately 2.5 after 24 and 48 h, with a total SCFA content of 7.1, 5.0 and $6.8 \mu\text{mol/mg}$ substrate, respectively (Figure 3.2-B). After 48 h, N76-B was fermented to acetate and butyrate in a ratio of 2.6 in one of the two duplicates, whereas a ratio of 1 was found in the other biological duplicate. The degradation

of N76-B was similar for both biological duplicates (Figure 3.1-B), which together indicates that the cross-feeding between the microbes was different in the two biological duplicates. P53-B was fermented to lower amounts of SCFAs (5.0 $\mu\text{mol}/\text{mg}$ substrate at 48 h) compared to the other B-type intrinsic RS-3 substrates, which was in line with the higher starch recovery after fermentation (Figure 3.1-B).

Overall, the intrinsic RS-3 substrates with a narrow disperse Mw distribution (N16-A, N18-A, N32-B and N76-B) were fermented to similar amounts of SCFAs ($\pm 7 \mu\text{mol}/\text{mg}$ substrate at 48 h) and a similar acetate-butyrate ratio (± 2.5). In contrast, intrinsic RS-3 substrates with a polydisperse Mw distribution (P21-A and P53-B) were fermented to lower amounts of SCFAs ($\pm 5 - 5.5 \mu\text{mol}/\text{mg}$ substrate).

3.2.3. Intrinsic RS-3 preparations stimulate gut microbiota differently, depending on the physico-chemical characteristics

To study if intrinsic RS-3 preparations differing in crystal type, Mw and Mw distribution stimulated different microbial populations during fermentation, the microbiota composition over time was determined. Beta-diversity was determined after centered-log-ratio (CLR) transformation of relative abundances of ASVs (Supplementary figure 3.2) and CLR-PCA showed that the microbiota in t0 samples clearly separated from fermented intrinsic RS-3 and medium blanks, indicating that fermentation selectively stimulated microbial populations compared to the initial inoculum. Independent of the intrinsic RS-3 physico-chemical characteristics, the same nine family level taxa covered > 95 % of the relative abundance during all incubations (Supplementary figure 3.3).

To have a more in-depth look on microbiota composition, we looked at ASVs explaining ≥ 2 % of the total relative abundance within an individual sample (medium blank or intrinsic RS-3) and together explaining ≥ 80 % of the total relative abundance at 24 or 48 h of fermentation (Figure 3.3). Using the NCBI database we identified the ASVs further and found different species groups within obtained ASVs for e.g. *Bifidobacterium* and *Bacteroides* (Supplementary table 3.3). Within ASV *Bifidobacterium* 01, we found a 100 % match with among others *B. adolescentis*, a primary degrader of RS in the gut^[18]. ASV *Ruminococcus* 01 had a 100 % match with key-stone RS degrader *R. bromii*^[18] and recently discovered *Ruminococcoides bili* found in human bile^[46], for which RS degrading capability was proven as well.

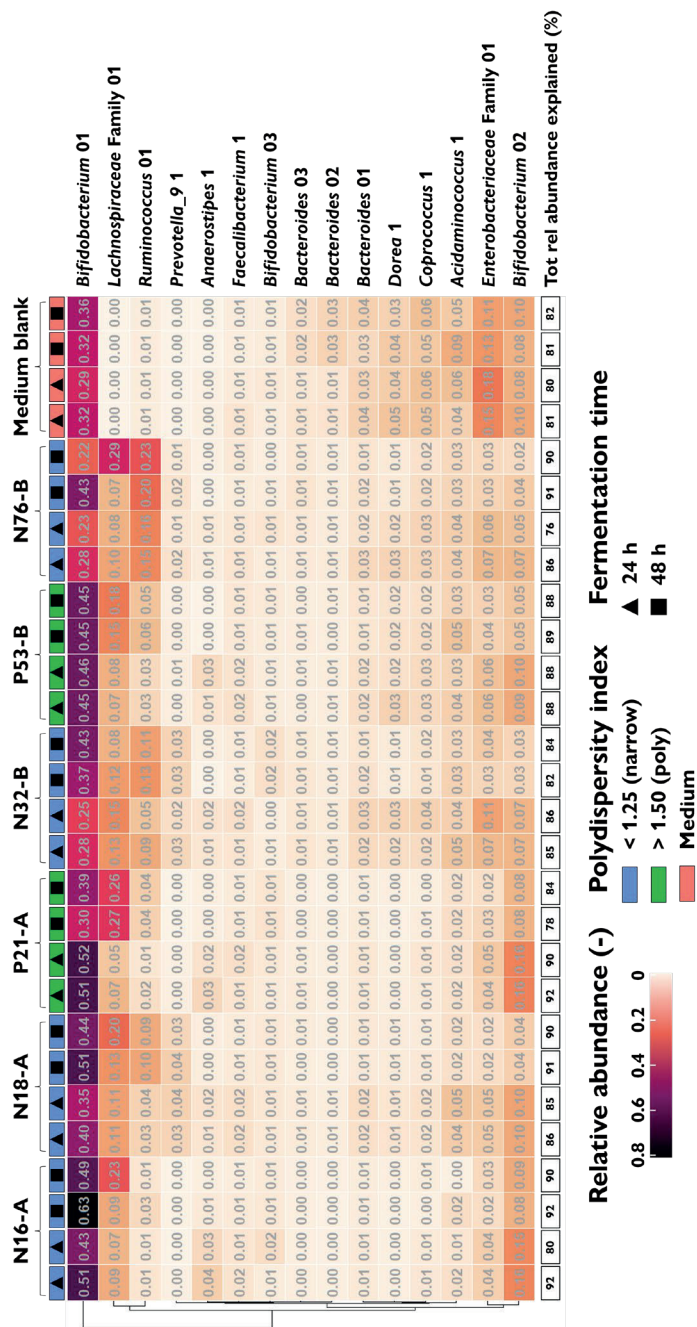


Figure 3.3. Heatmap showing ASVs contributing $\geq 2\%$ to the total relative abundance within a sample, after 24 and 48 h of fermentation of intrinsic RS-3 and medium blank using pooled adult faecal inoculum. The total relative abundance explained (%) is also provided. The taxa are sorted by hierarchical clustering of Euclidean distances.

In the heatmap, it is shown that around 80 – 90 % of the total relative abundance was explained by the same 15 ASVs for all samples, with *Bifidobacterium* 01, *Bifidobacterium* 02, *Lachnospiraceae* Family 01, and *Ruminococcus* 01 as the most dominant taxa (Figure 3.3). *Bifidobacterium* 01 as well as *Bifidobacterium* 02 were present in all fermented intrinsic RS-3 substrates and medium blanks. Whereas *Bifidobacterium* 01 accounted for more than 20 % after 24 h of fermentation and increased in relative abundance to at least 30 % after 48 h of fermentation, the relative abundances of *Bifidobacterium* 02 were drastically lower. *Lachnospiraceae* Family 01 was present in all fermented intrinsic RS-3 substrates and varied between 5 – 15 % after 24 h of fermentation and increased to 9 – 29 % after 48 h of fermentation. This taxon was not present after fermentation in the medium blank without RS-3 and therefore is likely to be involved in the fermentation of intrinsic RS-3. It is noteworthy that the relative abundance of *Lachnospiraceae* Family 01 differed between biological duplicates of 48 h fermented N76-B (7 and 29 %) (Figure 3.3), which could explain the differences found in SCFA ratio of this substrate (Figure 3.2). *Ruminococcus* 01 was present for only 1 – 3 % in the fermented medium and most intrinsic RS-3 substrates, but specifically increased in relative abundance after fermentation of 1 A-type and two B-type intrinsic RS-3 substrates (N18-A, N32-B and N76-B), where it contributed for 10 – 20 % to the relative abundance (Figure 3.3). For intrinsic RS-3 preparations N18-A and N32-B we also found 3 – 4 % *Prevotella*_9 1, which was absent in the medium blank and RS-3 substrates N16-A, P21-A and P53-B, indicating a minor role during fermentation of certain RS-3 substrates. Since *Lachnospiraceae* Family 01 and *Ruminococcus* 01 were dominant in the RS-3 incubations with neglectable growth in the medium blanks and showed co-occurring patterns across the incubations, we speculate that they are the primary fermenters of the RS-3 substrates.

3.3. Fermentation of pre-digested RS-3 preparations

In vitro fermentation of intrinsic RS-3 showed that small differences in physico-chemical characteristics impacted the rate of starch degradation, SCFA production and microbiota composition. Most RS-3 preparations described in literature contain a digestible fraction and are thus not considered RS-3 directly. To study if the RS-fractions of RS-3 preparations that are rich in digestible starch showed similar microbial succession and activity compared to intrinsic RS-3 during *in vitro* fermentation, selected RS-3 preparations (P22-B and P40-B) were pre-digested and subsequently fermented *in vitro* and compared to fermentation of intrinsic RS-3 N32-B and pre-digested intrinsic RS-3 P21-A, using the same conditions as used in section 3.2. The starch degradation, SCFA and lactic acid

formation (Figure 3.4) and changes in microbiota composition (Figure 3.5) during *in vitro* fermentation were evaluated.

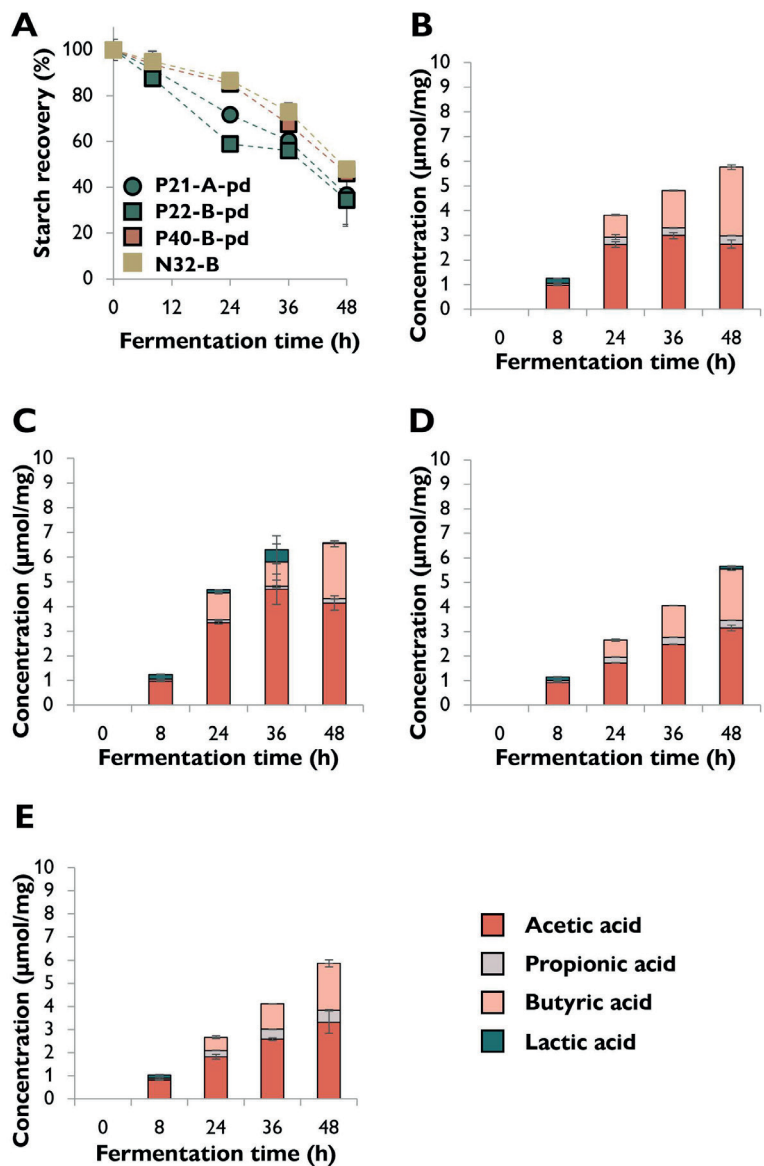


Figure 3.4. A: Starch recovery during *in vitro* fermentation of pre-digested RS-3 preparations and N32-B using pooled adult faecal inoculum, normalized for starch recovery at t0. Non-normalized starch recoveries can be found in Supplementary table 3.4 and Supplementary table 3.5. Figure B-E: SCFA and lactic acid formation (μmol/mg substrate) during 48 h of *in vitro* fermentation of P21-A-pd, P22-B-pd, P40-B-pd and N32-B, respectively. The average of biological duplicates is shown.

All pre-digested RS-fractions were degraded for approximately 50 – 60 % within 48 h of fermentation, similarly to intrinsic RS-3 N32-B (Figure 3.4-A). The fermentation rate of P21-A-pd and P22-B-pd was initially slightly faster than that of P40-B-pd and N32-B. The fermentation rate of P40-B-pd increased after 24 h of fermentation, similarly to N32-B. The microbial degradation of P21-A-pd, P22-B-pd and P40-B-pd did not influence the Mw distribution of the remaining substrate (Supplementary figure 3.4).

SCFA analysis showed that all substrates were fermented to mostly acetate and butyrate during 48 h of fermentation (Figure 3.4-B-E), irrespectively of starch degradation. During the first 8 h of incubation mostly acetate was formed, with minor amounts of lactate ($<0.2 \mu\text{mol/mg}$ substrate), whereas butyrate was formed only from 24 h of fermentation onwards. The acetate-butyrate ratio after 48 h of fermentation was 1, 1.8, 1.5 and 1.6 for P21-A-pd, P22-B-pd, P40-B-pd and N32-B, respectively.

Fermented pre-digested RS-3 preparations showed the same nine family level taxa, covering > 95 % of the relative abundance during all incubations (Supplementary figure 3.5), similar to results obtained for intrinsic RS-3 (Supplementary figure 3.3), but showing higher relative abundance of *Lachnospiraceae* across incubations.

The same 18 ASVs, contributing ≥ 2 % to the total relative abundance and together accounting for around 80 – 90 % of the total relative abundance, were found for all samples (Figure 3.5) of which 13 ASVs were also found for fermentation of intrinsic RS-3 (Figure 3.3). *Bifidobacterium* 01, *Bifidobacterium* 02, *Lachnospiraceae* Family 01, *Ruminococcus* 01 and *Enterobacteriaceae* Family 01 were the most dominant taxa present (Figure 3.5). Relative abundance of *Bifidobacterium* 01 decreased between 24 and 48 h of fermentation for pre-digested RS-3 preparations, whereas relative abundance of *Lachnospiraceae* Family 01 increased from 2 – 12 % at 24 h to 13 – 44 % after 48 h. Relative abundance of *Ruminococcus* 01 increased in all fermented RS-3 substrates between 24 and 48 h, but was especially dominant in N32-B. Pre-digested RS-3 preparations P22-B-pd and P40-B-pd were thus fermented by slightly different microbial populations compared to intrinsic RS-3 N32-B. Especially for P21-A-pd, high relative abundance of *Lachnospiraceae* Family 01 was found, with an enormous increase between 24 and 48 h, similar to fermentation of P21-A without a pre-digestion treatment (Figure 3.3). P21-A was fermented to the highest amount of butyrate among all fermentations, both when pre-digested or when used as such (Figure 3.2-A, Figure 3.4-B).

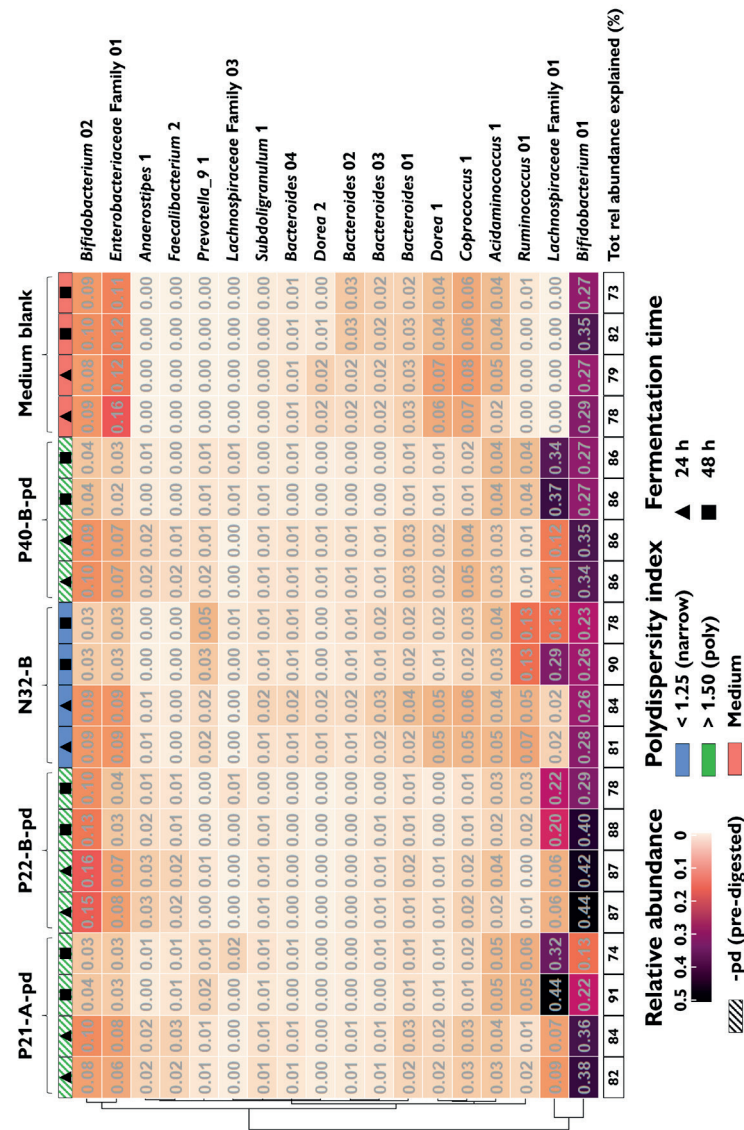


Figure 3.5. Heatmap showing ASVs contributing ≥ 2 % to the total relative abundance within a sample after 24 and 48 h of fermentation of P21-A-pd, P22-B-pd, P40-pd, N32-B and medium blank using pooled adult faecal inoculum. The total relative abundance explained (%) is also provided. The taxa are sorted by hierarchical clustering of Euclidean distances.

3.4. Pre-digested RS-3 fractions behave like intrinsic RS-3

To compare the RS-fractions of RS-rich RS-3 preparations with the intrinsic RS-3 substrates on microbiota composition during fermentation, β -diversities were determined after 24 and 48 h of fermentation (Supplementary figure 3.6)

using CLR-transformation, Unweighted UniFrac and Generalized UniFrac distances. PERMANOVA analyses of Aitchison distances demonstrated that at 24 h of fermentation, crystal type explained 14.1 % ($P = 0.0038$) and Mw distribution explained 9.7 % of the variation ($P = 0.0319$) (Supplementary table 3.6). These parameters also approached significance using Unweighted UniFrac distances ($P \sim 0.05$), but using Generalized UniFrac only crystal type was significant, indicating that crystal type and Mw distribution affected the presence of certain taxa, whereas crystal type alone was significantly affecting the abundance of certain taxa. No taxa contributing ≥ 2 % of the total relative abundance (Figure 3.3, Figure 3.5) were observed that were absent in RS-3 preparations differing in either Mw distribution or crystal type. This indicates that the variation explained by crystal type and Mw distribution using unweighted UniFrac distances was due to presence or absence of taxa contributing ≤ 2 % of the total relative abundance within a sample.

At 48 h of fermentation, Mw distribution (dispersity) explained 12.3 % ($P = 0.0084$) and chain length explained 14.7 % of the variation ($P = 0.0035$) using Aitchison distances. These parameters were also significant using Unweighted UniFrac ($P \leq 0.01$) and Generalized UniFrac ($P < 0.05$) distances. To visualize the most significant parameters, redundancy analysis was performed on CLR-transformed microbial compositions at ASV level using crystal type and dispersity (24 h of fermentation) or dispersity and chain length (48 h of fermentation) as constraint variables (Figure 3.6).

Although Mw distribution (dispersity) was not significantly affecting the abundance of certain taxa, the results show that at 24 h of fermentation, *Ruminococcus* 01 was associated with RS-3 preparations with a more narrow disperse Mw distribution (Figure 3.6-A). This is in line with results presented in Figure 3.3 and Figure 3.5, where especially RS-3 preparations with a narrow Mw distribution overall showed a higher relative abundance of *Ruminococcus* 01. *Ruminococcus* 01 negatively correlated with *Faecalibacterium* 2 (Figure 3.6-A), in line with results shown in Figure 3.5. Furthermore, *Dorea* 1 was associated with RS-3 preparations with a B-type crystal, in line with results shown in Figure 3.3 and Figure 3.5, although this taxon was not among the most dominantly present taxa. At 48 h of fermentation, no clear associations between RS-3 physico-chemical parameters and taxa contributing ≥ 2 % to the total relative abundance were found (Figure 3.6-B). In both plots, P22-B-pd seems to behave more like an A-type crystal, although it was confirmed that pre-digestion did not alter the crystal type (data not shown).

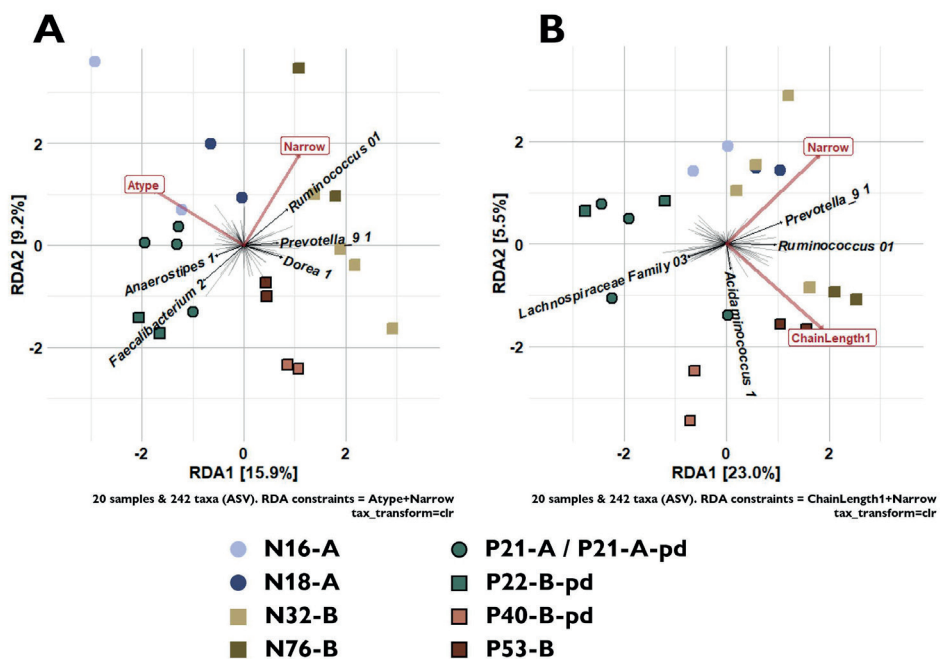


Figure 3.6. RDA plots on CLR-transformed relative abundances of ASVs using physico-chemical parameters as constraint variables with A: Crystal type and dispersity at 24 h incubation and B: Chain length and dispersity at 48 h of incubation. Taxa are shown that contribute $\geq 2\%$ to the total relative abundance within a sample and contribute for $> 60\%$ relative to the largest taxa loadings within the RDA plot.

3.5. Visual degradation of RS-3 by adult gut microbiota

Since we observed different microbial populations associated with the different RS-3 physico-chemical characteristics and *Ruminococcus* 01 and *Lachnospiraceae* Family 01 as likely candidates for primary fermenters, we conducted SEM on N32-B, P21-A-pd, P22-B-pd and P40-B-pd to evaluate whether microbial populations attached to the RS-3 preparations and whether these populations differed among the RS-3 preparations.

The initial N32-B substrate consisted of quite regularly shaped spheres of around 5-7 μm (Figure 3.7-A). Figure 3.7-B and -C clearly show that over time the shape of the substrate changed and became less smooth. In addition, the surface of the substrate was dominantly attached by a coccus-shaped bacterium (Figure 3.7-B, C), with an occasional presence of a rod-shaped bacterium (Supplementary figure 3.7). Altogether, these results indicate that the N32-B substrate was degraded from the surface by coccus-shaped bacteria.

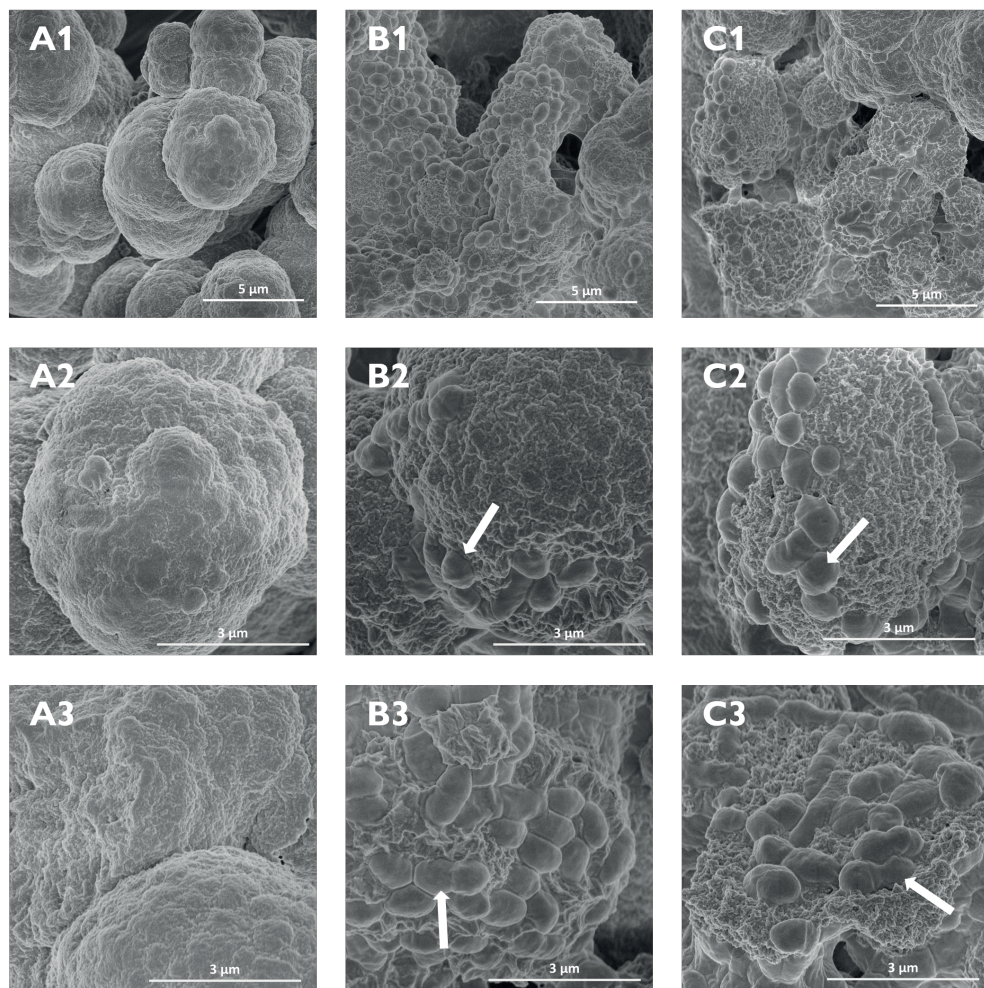


Figure 3.7. SEM images of intrinsic RS-3 N32-B during fermentation. Figure A, B and C represent N32-B blank and after 24 and 48 h of fermentation, respectively. Images 1 are 10,000 times magnified and images 2 and 3 are 25,000 times magnified. Arrows point towards the bacteria.

The SEM images of P21-A-pd and P22-B-pd show that these substrates consisted of tiny spheres that were connected to each other (Figure 3.8-A1, B1). In contrast, P40-B-pd consisted of large chunks, without a clear microstructure (Figure 3.8-C1). All pre-digested RS-3 preparations (polydisperse Mw distribution), had a very different structure than the regularly shaped and dense structure of N32-B (narrow disperse Mw distribution) (Figure 3.7-A). The results show that after 24 h of fermentation rod-shaped bacteria attached to the pre-digested RS-3 substrates (Figure 3.8-2), but also many non-degraded RS-3 particles were found. For P21-A-pd and P22-B-pd, still some untouched

substrate was recognized after 48 h of fermentation, whereas for P40-B-pd, most chunks were covered by bacteria (Supplementary figure 3.8). The rod-shaped bacteria seem to make holes within the substrates and hydrolyse/solubilise the RS-3 substrates from inside, irrespectively of crystal type or chain length.

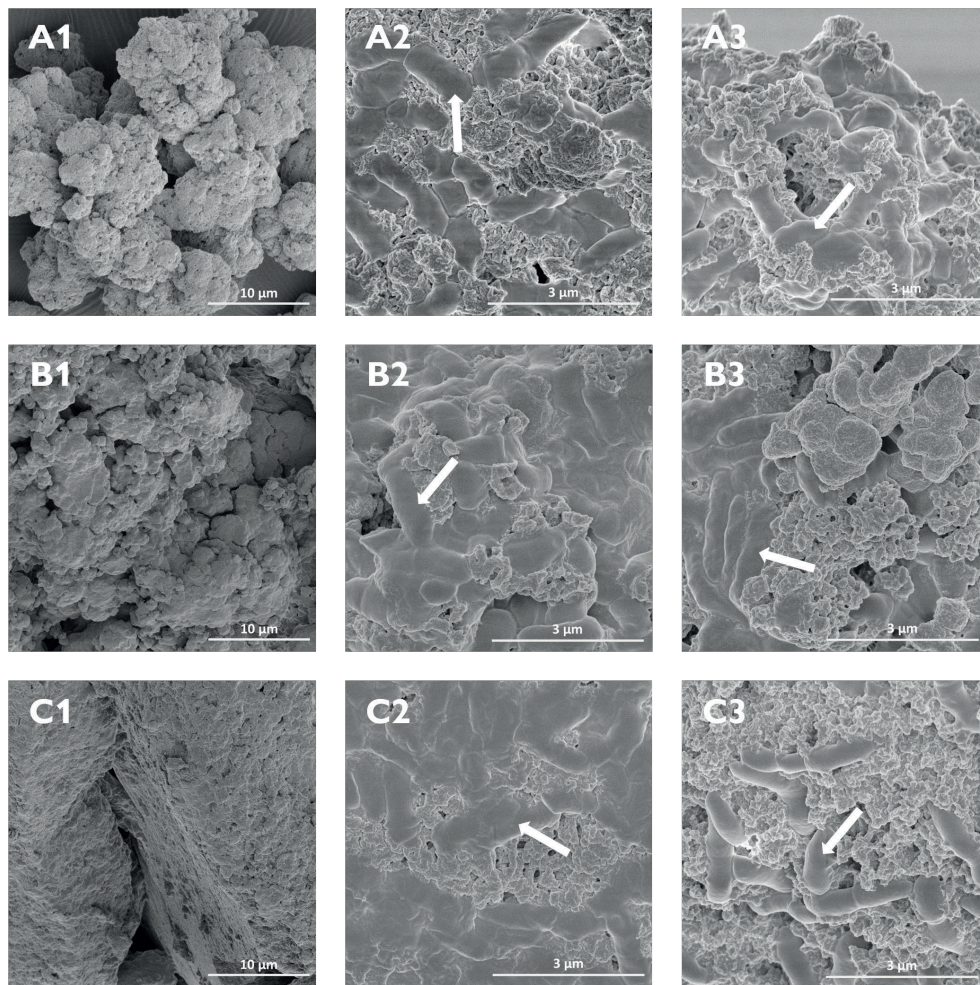


Figure 3.8. SEM images of pre-digested RS-3 substrates (1), after 24 h of fermentation (2) and after 48 h of fermentation (3). A, B and C: P21-A-pd, P22-B-pd and P40-B-pd, respectively. Arrows point towards the bacteria.

Combining the SEM images after fermentation of N32-B and pre-digested RS-es (Figure 3.7, Figure 3.8), it becomes obvious that the degradation of these substrates by gut microbiota is different. Whereas rod-shaped bacteria were mostly attached to the RS-3 preparations with a polydisperse Mw distribution (Figure 3.8), cocci were mostly attaching RS-3 preparations with a narrow

disperse Mw distribution (Figure 3.7). Combined with our earlier observations on microbiota composition, we speculate that the coccus-shaped bacterium belongs to the *Ruminococcus* 01 taxon and the rod-shaped bacterium to *Lachnospiraceae* Family 01.

4. Discussion

Our results show that intrinsic RS-3 and pre-digested RS-rich RS-3 preparations were fermented slowly by gut microbiota (Figure 3.1, Figure 3.4-A). After 24 h of fermentation, no solubilized starch was detected, indicating that hydrolysis of starch was more limiting than the conversion to SCFAs. Fermentation of intrinsic and pre-digested RS-3 stimulated the growth of bacteria belonging to the genera *Bifidobacterium*, *Lachnospiraceae* and *Ruminococcus*. Previously, it has already been shown that fermentation of RS-3 preparations increased the relative abundance of *Bifidobacterium* and *Lachnospiraceae* members^[13]. Fermentation of A- and B-type RS-3 preparations made of debranched waxy maize starch showed an increase in relative abundance of *Lachnospiraceae* members and *Prevotella*, but no distinct differences in microbial populations among fermented A- or B-type RS-3 preparations^[29].

We found two different ASVs for *Bifidobacterium*, namely *Bifidobacterium* 01 and *Bifidobacterium* 02 (Figure 3.3, Figure 3.5). *Bifidobacterium* 01 was present for around 15 % in the initial inoculum and increased in all samples after fermentation to 20 – 60 % of the total relative abundance, whereas the relative abundance of *Bifidobacterium* 02 decreased between 24 – 48 h of fermentation of RS-3 substrates. The V4 region of *Bifidobacterium* 01 was 100 % identical to *B. adolescentis*, *B. faecale* and *B. dentium*, whereas the V4 region of *Bifidobacterium* 02 was 100 % identical to *B. pseudocatenulatum*, *B. longum* subsp. *longum*, *B. longum* subsp. *infantis*, *B. longum*, *B. breve* and *B. miconisargentati* (Supplementary table 3.3). Although all bifidobacteria mentioned encode genes for starch-degrading enzymes (Glycosyl Hydrolase family 13 (GH13); CAZY database^[47]) and some have been shown to actively ferment starch^[48, 49], only *B. adolescentis* is described as a primary degrader of RS^[50]. *B. pseudocatenulatum* (covered by *Bifidobacterium* 02) has similar CBMs, including a raw starch-binding CBM74^[51], and GH13 enzymes in its genome compared to *B. adolescentis* (CAZY^[47]) and was shown to grow on cooked commercial RS-3 (Novelose® 330, ± 50 % RS^[10])^[52]. Nevertheless, real RS-degrading capacities of this species have not yet been shown^[53].

Whereas *Bifidobacterium* 01 increased in relative abundance in all fermented RS-3 substrates and the medium blank, *Ruminococcus* 01 only increased in some specific samples up to 20 % of the total relative abundance (Figure 3.3, Figure 3.5). The V4 region of *Ruminococcus* 01 was 100 % identical with *Ruminococcus bromii* and *Ruminococcoides bili*, according to NCBI Blast. From *R. bromii* it is known to be an RS degrading specialist^[18], while also *R. bili*, isolated from human bile, was shown to be able to degrade a range of starches^[46].

The degradation rate during fermentation of N18-A, N32-B, N76-B (narrow disperse Mw distribution) increased after 24 h and especially during the last 24 h of incubation an increase in relative abundance of up to 20 % *Ruminococcus* 01 was found. Therefore, we speculate that *Ruminococcus* 01 was, at least partly, responsible for the degradation of N18-A, N32-B and N76-B. This hypothesis is strengthened by the recognition of mostly coccus-shaped bacteria after fermentation of intrinsic RS-3 N32-B, as shown by SEM images (Figure 3.7). The degradation rate during fermentation of P40-B-pd and P53-B also increased during the last 24 h, but here we did not find such a pronounced increase in relative abundance of *Ruminococcus* 01. The degradation rate of N16-A, P21-A, P21-A-pd and P22-B-pd was very stable over time, stimulating mostly *Bifidobacterium* 01 and *Lachnospiraceae* Family 01. Although *Bifidobacterium* 01 matches with primary degrader *B. adolescentis*, it also increased in relative abundance in the medium blank, limiting us to speculate on primary degradation of these RS-3 preparations by *Bifidobacterium* 01. Since *Lachnospiraceae* specifically increased in relative abundance upon fermentation of RS-3, we speculate that N16-A, P21-A, P21-A-pd, P22-B-pd, P40-B-pd and P53-B (mostly polydisperse Mw distribution) were degraded by this bacterium, of which some members, such as *A. rectalis*, are recognized as secondary degraders of RS^[17, 54]. This hypothesis is strengthened by the presence of mostly rod-shaped bacteria after fermentation of P21-A-pd, P22-B-pd and P40-B-pd as visualized by SEM images (Figure 3.8).

Our results showed that intrinsic RS-3 and pre-digested RS-rich RS-3 preparations were fermented to acetate and butyrate. Fermentation of RS-3 stimulated *Bifidobacterium* 01, *Ruminococcus* 01 and *Lachnospiraceae* Family 01. *Bifidobacterium* ferments its substrate to acetate and lactate^[20], whereas *Lachnospiraceae* is known to harbour many butyrate producing genera^[55, 56], of which some use lactate and acetate for their butyrate production^[57]. For all intrinsic RS-3 substrates, we found an increase in ASV *Lachnospiraceae* Family 01, but also *Faecalibacterium*, *Coprococcus* and *Anaerostipes*, present in lower relative abundance, might have contributed to the butyrate production via cross-feeding.

The negative correlation found between *Ruminococcus* 01 and *Faecalibacterium* 02 (Figure 3.6-A) can be explained by *R. bromii* degrading starch to malto-oligomers, maltose and accumulating glucose^[58], whereas *F. prausnitzii* prefers to ferment acetate over glucose for the production of butyrate^[59]. In contrast, enhanced butyrate production from starch was demonstrated by cross-feeding between *B. adolescentis* and *F. prausnitzii* previously^[60]. Especially butyrate production after fermentation of P21-A (polydisperse Mw distribution) was high, compared to intrinsic RS-3 with a narrow disperse Mw distribution. The acetate-butyrate ratio of fermented P21-A was also higher, compared to acetate-butyrate ratios found for RS-3 with an A-type crystal made from debranched waxy maize starch^[29, 30]. Our study showed that small differences in physico-chemical characteristics of RS-3 influenced microbiota composition, and consequently butyrate production during fermentation. Also Gu et al. (2020) showed that RS-3 characteristics such as crystal type and chain length influenced the production of SCFAs and microbiota composition^[11]. Interestingly, our study showed that especially Mw distribution of the α -1,4 glucan chains is an important factor influencing microbiota composition and butyrate production.

5. Conclusions

Our study is the first to investigate the role of crystal type, Mw and Mw distribution on the *in vitro* fermentability of RS-3 preparations by adult faecal microbiota. We showed that by tuning RS-3 physico-chemical characteristics, the microbiota composition and butyrate production during fermentation can be influenced. Intrinsic RS-3 substrates are slowly fermentable fibres that are stimulating *Lachnospiraceae*, *Ruminococcus* and *Bifidobacterium*. Especially the Mw distribution of α -1,4 glucans within RS-3 substrates is influencing the *Lachnospiraceae* / *Ruminococcus* ratio after fermentation. Our results suggest that a more dense and homogeneous RS-3 structure, such as present in intrinsic RS-3 with a narrow disperse Mw distribution, requires RS-degrading specialists such as *Ruminococcus* for degradation, irrespectively of crystal type. In contrast, a less homogeneous microstructure, such as present in RS-3 preparations with a polydisperse Mw distribution could potentially be degraded by *Lachnospiraceae*. Especially A-type intrinsic RS-3 with a polydisperse Mw distribution yielded relatively high levels of butyrate (acetate / butyrate ratio: 1). Due to the slow fermentation, intrinsic RS-3 will potentially arrive in the distal colon and have a beneficial effect for the host by promoting saccharolytic fermentation and butyrate production.

6. References

1. Fu X., Liu Z., Zhu C., Mou H., Kong Q. Nondigestible carbohydrates, butyrate, and butyrate-producing bacteria. *Critical Reviews in Food Science & Nutrition*. **2019**;59(sup1):S130-S152.
2. Chen J., Vitetta L. Inflammation-modulating effect of butyrate in the prevention of colon cancer by dietary fiber. *Clinical Colorectal Cancer*. **2018**;17(3):e541-e544.
3. Cushing K., Alvarado D.M., Ciorba M.A. Butyrate and mucosal inflammation: new scientific evidence supports clinical observation. *Clinical and Translational Gastroenterology*. **2015**;6:e108.
4. Markiewicz L.H., Ogrodowczyk A.M., Wiczowski W., Wroblewska B. Phytate and butyrate differently influence the proliferation, apoptosis and survival pathways in human cancer and healthy colonocytes. *Nutrients*. **2021**;13(6).
5. McNabney S.M., Henagan T.M. Short chain fatty acids in the colon and peripheral tissues: a focus on butyrate, colon cancer, obesity and insulin resistance. *Nutrients*. **2017**;9(12).
6. Ryu S.H., Kaiko G.E., Stappenbeck T.S. Cellular differentiation: Potential insight into butyrate paradox? *Molecular & Cellular Oncology*. **2018**;5(3):e1212685.
7. Jonathan M.C., Borne J.J., van Wiechen P., da Silva C.S., Schols H.A., Gruppen H. In vitro fermentation of 12 dietary fibres by faecal inoculum from pigs and humans. *Food Chemistry*. **2012**;133(3):889-897.
8. Wang M., Wichienchot S., He X., Fu X., Huang Q., Zhang B. In vitro colonic fermentation of dietary fibers: Fermentation rate, short-chain fatty acid production and changes in microbiota. *Trends in Food Science & Technology*. **2019**;88:1-9.
9. Birt D.F., Boylston T., Hendrich S., Jane J.L., Hollis J., Li L., McClelland J., Moore S., Phillips G.J., Rowling M., Schalinske K., Scott M.P., Whitley E.M. Resistant starch: promise for improving human health. *Advances in Nutrition*. **2013**;4(6):587-601.
10. Giuberti G., Gallo A. In vitro evaluation of fermentation characteristics of type 3 resistant starch. *Heliyon*. **2020**;6(1):e03145.
11. Gu F., Li C., Hamaker B.R., Gilbert R.G., Zhang X. Fecal microbiota responses to rice RS3 are specific to amylose molecular structure. *Carbohydrate Polymers*. **2020**;243:116475.
12. Li L., Jiang H.X., Kim H.J., Yum M.Y., Campbell M.R., Jane J.L., White P.J., Hendrich S. Increased butyrate production during long-term fermentation of in vitro-digested high amylose cornstarch residues with human feces. *Journal of Food Science*. **2015**;80(9):M1997-M2004.
13. Teichmann J., Cockburn D.W. In vitro fermentation reveals changes in butyrate production dependent on resistant starch source and microbiome composition. *Frontiers in Microbiology*. **2021**;12:640253.
14. Zhou Z., Cao X., Zhou J.Y.H. Effect of resistant starch structure on short-chain fatty acids production by human gut microbiota fermentation in vitro. *Starch-Starke*. **2013**;65(5-6):509-516.
15. Haralampu S.G. Resistant starch - a review of the physical properties and biological impact of RS3. *Carbohydrate Polymers*. **2000**;41(3):285-292.
16. Baxter N.T., Schmidt A.W., Venkataraman A., Kim K.S., Waldron C., Schmidt T.M. Dynamics of human gut microbiota and short-chain fatty acids in response to dietary interventions with three fermentable fibers. *mBio*. **2019**;10(1).
17. Cerqueira F.M., Photenhauer A.L., Pollet R.M., Brown H.A., Koropatkin N.M. Starch digestion by gut bacteria: crowdsourcing for carbs. *Trends in Microbiology*. **2020**;28(2):95-108.
18. Ze X., Duncan S.H., Louis P., Flint H.J. Ruminococcus bromii is a keystone species for the degradation of resistant starch in the human colon. *The ISME Journal*. **2012**;6(8):1535-1543.
19. Laverde Gomez J.A., Mukhopadhyaya I., Duncan S.H., Louis P., Shaw S., Collie-Duguid E., Crost E., Juge N., Flint H.J. Formate cross-feeding and cooperative metabolic interactions

- revealed by transcriptomics in co-cultures of acetogenic and amylolytic human colonic bacteria. *Environmental Microbiology*. **2019**;21(1):259-271.
20. Pokusaeva K., Fitzgerald G.F., van Sinderen D. Carbohydrate metabolism in Bifidobacteria. *Genes & Nutrition*. **2011**;6(3):285-306.
21. Maier T.V., Lucio M., Lee L.H., VerBerkmoes N.C., Brislaw N.C., Bernhardt J., Lamendella R., McDermott J.E., Bergeron N., Heinzmann S.S., Morton J.T., Gonzalez A., Ackermann G., Knight R., Riedel K., Krauss R.M., Schmitt-Kopplin P., Jansson J.K. Impact of dietary resistant starch on the human gut microbiome, metaproteome, and metabolome. *mBio*. **2017**;8(5).
22. Pryde S.E., Duncan S.H., Hold G.L., Stewart C.S., Flint H.J. The microbiology of butyrate formation in the human colon. *FEMS Microbiology Letters*. **2002**;217(2):133-139.
23. Jacobasch G., Dongowski G., Schmiedl D., Muller-Schmehl K. Hydrothermal treatment of Novelose 330 results in high yield of resistant starch type 3 with beneficial prebiotic properties and decreased secondary bile acid formation in rats. *British Journal of Nutrition*. **2006**;95(6):1063-1074.
24. Scheiwiller J., Arrigoni E., Brouns F., Amado R. Human faecal microbiota develops the ability to degrade type 3 resistant starch during weaning. *Journal of Pediatric Gastroenterology and Nutrition*. **2006**;43(5):584-591.
25. Cai L.M., Shi Y.C. Preparation, structure, and digestibility of crystalline A- and B-type aggregates from debranched waxy starches. *Carbohydrate Polymers*. **2014**;105:341-350.
26. Klostermann C.E., Buwalda P.L., Leemhuis H., de Vos P., Schols H.A., Bitter J.H. Digestibility of resistant starch type 3 is affected by crystal type, molecular weight and molecular weight distribution. *Carbohydrate Polymers*. **2021**;265:118069.
27. Kobayashi K., Kimura S., Naito P.K., Togawa E., Wada M. Thermal expansion behavior of A- and B-type amylose crystals in the low-temperature region. *Carbohydrate Polymers*. **2015**;131:399-406.
28. Plongbunjong V., Graidist P., Bach Knudsen K.E., Wichienchot S. Starch-based carbohydrates display the bifidogenic and butyrogenic properties in pH-controlled faecal fermentation. *International Journal of Food Science & Technology*. **2017**;52(12):2647 - 2653.
29. Liu J., Liu F., Arıoğlu-Tuncel S., Xie Z., Fu X., Huang Q., Zhang B. In vitro fecal fermentation outcomes and microbiota shifts of resistant starch spherulites. *International Journal of Food Science & Technology*. **2022**;57(5).
30. Chang R., Jin Z., Lu H., Qiu L., Sun C., Tian Y. Type III resistant starch prepared from debranched starch: structural changes under simulated saliva, gastric, and intestinal conditions and the impact on short-chain fatty acid production. *Journal of Agricultural and Food Chemistry*. **2021**;69(8):2595-2602.
31. Zhang C., Qiu M., Wang T., Luo L., Xu W., Wu J., Zhao F., Liu K., Zhang Y., Wang X. Preparation, structure characterization, and specific gut microbiota properties related to anti-hyperlipidemic action of type 3 resistant starch from *Canna edulis*. *Food Chemistry*. **2021**;351:129340.
32. Aguirre M., Eck A., Koenen M.E., Savelkoul P.H., Budding A.E., Venema K. Evaluation of an optimal preparation of human standardized fecal inocula for in vitro fermentation studies. *Journal of Microbiological Methods*. **2015**;117:78-84.
33. Minekus M., Smeets-Peters M., Bernalier A., Marol-Bonnin S., Havenaar R., Marteau P., Alric M., Fonty G., Huis in't Veld J.H. A computer-controlled system to simulate conditions of the large intestine with peristaltic mixing, water absorption and absorption of fermentation products. *Applied Microbiology & Biotechnology*. **1999**;53(1):108-114.
34. Martens B.M.J., Gerrits W.J.J., Bruininx E., Schols H.A. Amylopectin structure and crystallinity explains variation in digestion kinetics of starches across botanic sources in an in vitro pig model. *Journal of Animal Science and Biotechnology*. **2018**;9:91.

35. Kong C., Akkerman R., Klostermann C.E., Beukema M., Oerlemans M.M., Schols H.A., De Vos P. Distinct fermentation of human milk oligosaccharides 3-FL and LNT2 and GOS/inulin by infant gut microbiota and impact on adhesion of *Lactobacillus plantarum* WCFS1 to gut epithelial cells. *Food & Function*. **2021**;12(24):12513-12525.
36. Salonen A., Nikkila J., Jalanka-Tuovinen J., Immonen O., Rajilic-Stojanovic M., Kekkonen R.A., Palva A., de Vos W.M. Comparative analysis of fecal DNA extraction methods with phylogenetic microarray: effective recovery of bacterial and archaeal DNA using mechanical cell lysis. *Journal of Microbiological Methods*. **2010**;81(2):127-134.
37. Parada A.E., Needham D.M., Fuhrman J.A. Every base matters: assessing small subunit rRNA primers for marine microbiomes with mock communities, time series and global field samples. *Environmental Microbiology*. **2016**;18(5):1403-1414.
38. Apprill A., McNally S., Parsons R., Weber L. Minor revision to V4 region SSU rRNA 806R gene primer greatly increases detection of SAR11 bacterioplankton. *Aquatic Microbial Ecology*. **2015**;75(2):129-137.
39. Poncheewin W., Hermes G.D.A., van Dam J.C.J., Koehorst J.J., Smidt H., Schaap P.J. NG-Tax 2.0: A semantic framework for high-throughput amplicon analysis. *Frontiers in Genetics*. **2020**;10:1366.
40. Quast C., Pruesse E., Yilmaz P., Gerken J., Schweer T., Yarza P., Peplies J., Glockner F.O. The SILVA ribosomal RNA gene database project: improved data processing and web-based tools. *Nucleic Acids Research*. **2013**;41(Database issue):D590-596.
41. Yilmaz P., Parfrey L.W., Yarza P., Gerken J., Pruesse E., Quast C., Schweer T., Peplies J., Ludwig W., Glockner F.O. The SILVA and "All-species Living Tree Project (LTP)" taxonomic frameworks. *Nucleic Acids Research*. **2014**;42(Database issue):D643-648.
42. McMurdie P.J., Holmes S. phyloseq: an R package for reproducible interactive analysis and graphics of microbiome census data. *PLoS One*. **2013**;8(4):e61217.
43. Lahti R., Shetty S. Microbiome r package: Tools for microbiome analysis in R. 2012-2019 [Available from: <https://github.com/microbiome/microbiome>].
44. Barnett D.J.M., Arts I.C.W., Penders J. microViz: an R package for microbiome data visualization and statistics. *Journal of Open Source Software*. **2021**;6(63):3201.
45. Oksanen J., Simpson G.L., Kindt R., Legendre P., Minchin P.R., O'Hara R.B., Solymos P., Henry M., Stevens H., Szoecs E., Wagner H., Barbour M., Bedward M., Bolker B., Borcard D., Carvalho G., Chirico M., De Caceres M., Durand S., Antoniazzi Evangelista H.B., FitzJohn R., Friendly M., Furneaux B., Hannigan G., Hill M.O., Lahti L., McGlinn D., Ouellette M.-H., Ribeiro Cunha R., Smith T., Stier A., Ter Braak C.J.F., Weedon J. Package 'vegan'. **2022**.
46. Molinero N., Conti E., Sánchez B., Walker A.W., Margolles A., Duncan S.H., Delgado S. *Ruminococcoides bili* gen. nov., sp. nov., a bile-resistant bacterium from human bile with autolytic behavior. *International Journal of Systematic and Evolutionary Microbiology*. **2021**;71(8):004960.
47. Drula E., Garron M.L., Dogan S., Lombard V., Henrissat B., Terrapon N. The carbohydrate-active enzyme database: functions and literature. *Nucleic Acids Research*. **2022**;50(D1):D571-D577.
48. Ryan S.M., Fitzgerald G.F., van Sinderen D. Screening for and identification of starch-, amylopectin-, and pullulan-degrading activities in bifidobacterial strains. *Applied Environmental Microbiology*. **2006**;72(8):5289-5296.
49. Belenguer A., Duncan S.H., Calder A.G., Holtrop G., Louis P., Lobley G.E., Flint H.J. Two routes of metabolic cross-feeding between *Bifidobacterium adolescentis* and butyrate-producing anaerobes from the human gut. *Applied Environmental Microbiology*. **2006**;72(5):3593-3599.
50. Dobranowski P.A., Stintzi A. Resistant starch, microbiome, and precision modulation. *Gut Microbes*. **2021**;13(1):1926842.

51. Valk V., Lammerts van Bueren A., van der Kaaij R.M., Dijkhuizen L. Carbohydrate-binding module 74 is a novel starch-binding domain associated with large and multidomain alpha-amylase enzymes. *FEBS Journal*. **2016**;283(12):2354-2368.
52. Baruzzi F., de Candia S., Quintieri L., Caputo L., De Leo F. Development of a synbiotic beverage enriched with bifidobacteria strains and fortified with whey proteins. *Frontiers in Microbiology*. **2017**;8:640.
53. Jung D.H., Kim G.Y., Kim I.Y., Seo D.H., Nam Y.D., Kang H., Song Y., Park C.S. Bifidobacterium adolescentis P2P3, a human gut bacterium having strong non-gelatinized resistant starch-degrading activity. *Journal of Microbiology and Biotechnology*. **2019**;29(12):1904-1915.
54. Cockburn D.W., Cerqueira F.M., Bahr C., Koropatkin N.M. The structures of the GH13_36 amylases from Eubacterium rectale and Ruminococcus bromii reveal subsite architectures that favor maltose production. *Amylase*. **2020**;4(1):24-44.
55. Vacca M., Celano G., Calabrese F.M., Portincasa P., Gobbetti M., De Angelis M. The Controversial Role of Human Gut Lachnospiraceae. *Microorganisms*. **2020**;8(4).
56. Meehan C.J., Beiko R.G. A phylogenomic view of ecological specialization in the Lachnospiraceae, a family of digestive tract-associated bacteria. *Genome Biology and Evolution*. **2014**;6(3):703-713.
57. Duncan S.H., Louis P., Flint H.J. Lactate-utilizing bacteria, isolated from human feces, that produce butyrate as a major fermentation product. *Applied Environmental Microbiology*. **2004**;70(10):5810-5817.
58. Crost E.H., Le Gall G., Laverde-Gomez J.A., Mukhopadhyaya I., Flint H.J., Juge N. Mechanistic insights into the cross-feeding of Ruminococcus gnavus and Ruminococcus bromii on host and dietary carbohydrates. *Frontiers in Microbiology*. **2018**;9:2558.
59. Duncan S.H., Holtrop G., Lobley G.E., Calder A.G., Stewart C.J., Flint H.J. Contribution of acetate to butyrate formation by human faecal bacteria. *British Journal of Nutrition*. **2007**;91(6).
60. Rios-Covian D., Gueimonde M., Duncan S.H., Flint H.J., de los Reyes-Gavilan C.G. Enhanced butyrate formation by cross-feeding between Faecalibacterium prausnitzii and Bifidobacterium adolescentis. *FEMS Microbiology Letters*. **2015**;362(21).

7. Supplementary information

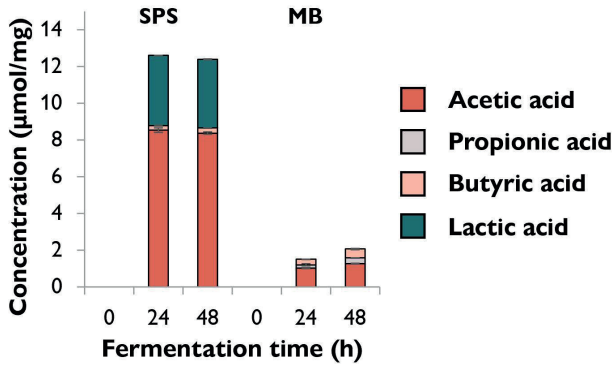
Supplementary table 3.1. Starch recovery in soluble and insoluble fractions of duplicate fermentations of different RS-3 preparations and digestible starch (SPS) with pooled adult faecal inoculum during 48 h of incubation.

| Sample name | Time 0 h | | Time 24 h | | Time 48 h | |
|-------------|-------------|---------------|-------------|---------------|-------------|---------------|
| | Soluble (%) | Insoluble (%) | Soluble (%) | Insoluble (%) | Soluble (%) | Insoluble (%) |
| N16-A | 3.7 ± 0.6 | 99.4 ± 0.7 | 0.3 ± 0.0 | 73.3 ± 0.4 | 0.3 ± 0.0 | 45.9 ± 6.7 |
| N18-A | 2.9 ± 0.2 | 87.7 ± 11.1 | 0.3 ± 0.0 | 72.5 ± 7.1 | 0.2 ± 0.0 | 30.9 ± 1.5 |
| P21-A | 4.0 ± 0.0 | 74.7 ± 1.3 | 0.0 ± 0.0 | 56.3 ± 3.5 | 0.0 ± 0.0 | 33.2 ± 3.5 |
| N32-B | 1.6 ± 0.1 | 92.9 ± 1.9 | 0.2 ± 0.0 | 74.4 ± 1.6 | 0.3 ± 0.1 | 33.9 ± 2.2 |
| N76-B | 1.2 ± 0.1 | 99.8 ± 4.5 | 0.1 ± 0.0 | 82.7 ± 8.4 | 0.4 ± 0.5 | 36.0 ± 0.2 |
| P53-B | 3.2 ± 0.5 | 93.1 ± 12.2 | 0.1 ± 0.0 | 86.5 ± 6.4 | 0.1 ± 0.0 | 66.3 ± 5.4 |
| SPS | 83.3 ± 0.9 | n.a. | 0.6 ± 0.0 | n.a. | 0.3 ± 0.0 | n.a. |

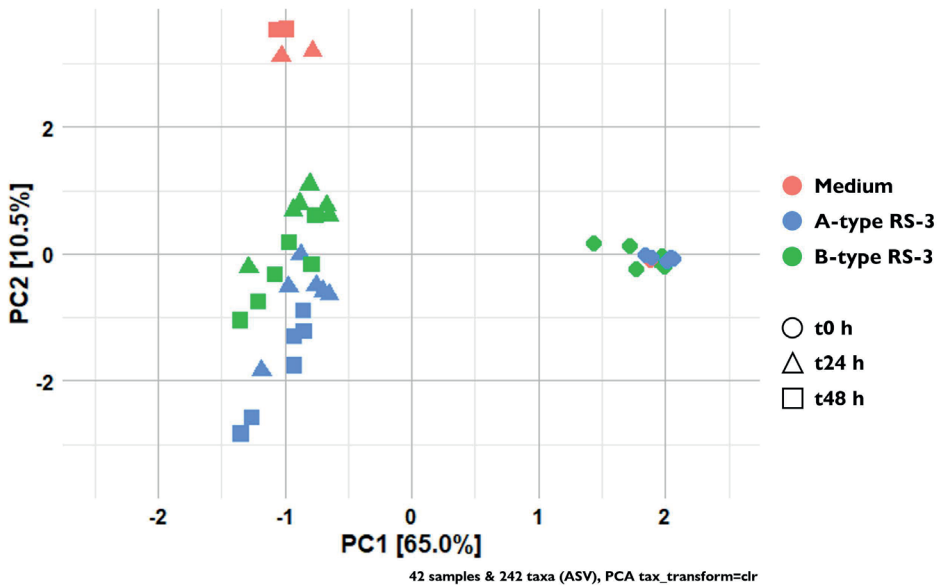
Supplementary table 3.2. Starch recovery in soluble and insoluble fractions of duplicate incubations of RS-3 preparations and digestible starch (SPS) during 48 h without presence of faecal inoculum.

| Sample name | Time 0 h | | Time 24 h | | Time 48 h | |
|-------------|-------------|---------------|-------------|---------------|-------------|---------------|
| | Soluble (%) | Insoluble (%) | Soluble (%) | Insoluble (%) | Soluble (%) | Insoluble (%) |
| N16-A | 2.6 ± 0.4 | 97.0 ± 6.1 | 9.9 ± 0.0 | 89.1 ± 4.3 | 10.8 ± 1.3 | 86.8 ± 1.8 |
| N18-A | 1.9 ± 0.0 | 90.8 ± 5.4 | 6.5 ± 0.7 | 83.4 ± 9.1 | 6.7 ± 0.2 | 88.4 ± 2.7 |
| P21-A | 3.1 ± 0.0 | 88.6 ± 3.1 | 8.3 ± 0.2 | 82.9 ± 4.7 | 9.8 ± 0.2 | 81.7 ± 1.6 |
| N32-B | 1.5 ± 1.4 | 91.0 ± 0.8 | 1.5 ± 1.2 | 88.9 ± 1.2 | 2.3 ± 0.1 | 88.9 ± 4.0 |
| N76-B | 0.2 ± 0.0 | 94.7 ± 1.6 | 0.9 ± 0.3 | 101.3 ± 1.0 | 0.5 ± 0.1 | 98.9 ± 3.0 |
| P53-B | 2.1 ± 0.5 | 98.9* | 4.6 ± 0.1 | 90.1 ± 0.9 | 5.6 ± 0.2 | 94.0 ± 3.5 |
| SPS | 100.6 ± 12 | n.a. | 99.1 ± 0.9 | n.a. | 100.0 ± 1.3 | n.a. |

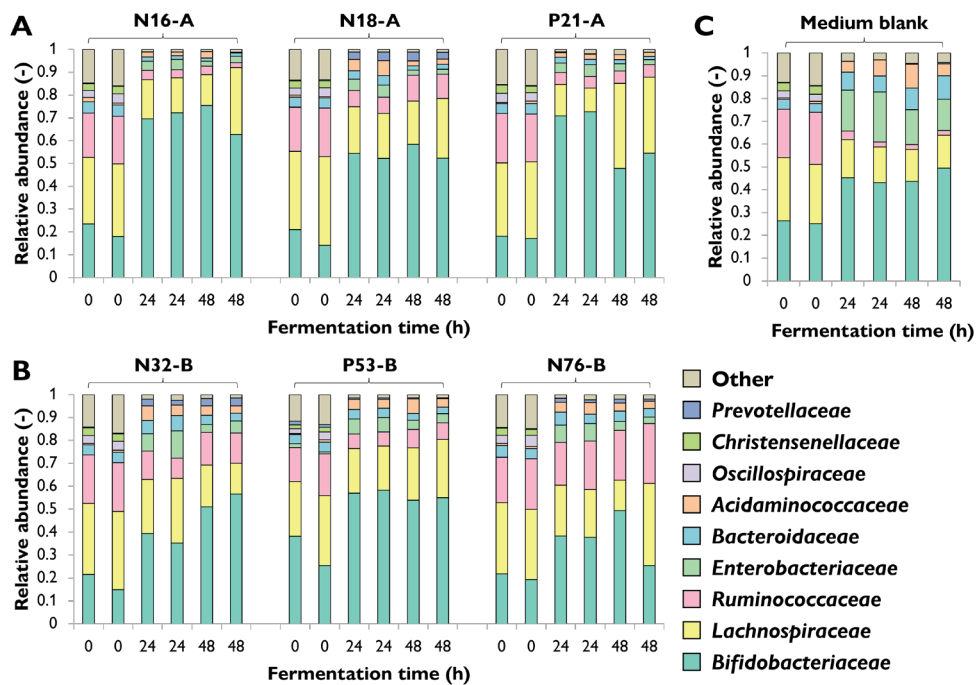
*Only 1 of two biological duplicates



Supplementary figure 3.1. SCFA and lactic acid formation ($\mu\text{mol/mg}$ substrate) during 48 h of *in vitro* fermentation using pooled adult faecal inoculum. SPS and MB refer to soluble potato starch and medium blank, respectively. The average of biological duplicates is shown.



Supplementary figure 3.2. Ordination plot of CLR-transformed relative abundances of ASVs from fermented RS-3 substrates over time. PERMANOVA indicated that incubation time explained 48.8 % of the variation ($P = 1\text{e-}04$) and crystal type explained 5.3 % of the variation ($P = 0.063$).



Supplementary figure 3.3. Microbiota composition in relative abundance after *in vitro* fermentation of intrinsic RS-3 and medium blank over time at family level. Figure A, B and C refer to fermented substrates of intrinsic A-type RS-3, intrinsic B-type RS-3 and the medium blank, respectively. Results of both biological duplicates are indicated.

Supplementary table 3.3. Identified ASVs with corresponding species according to NCBI Blast. Only 100 % matches to 16S rRNA gene sequences of described species in the NCBI database are given. Species in bold are described as primary RS degraders^[18, 46].

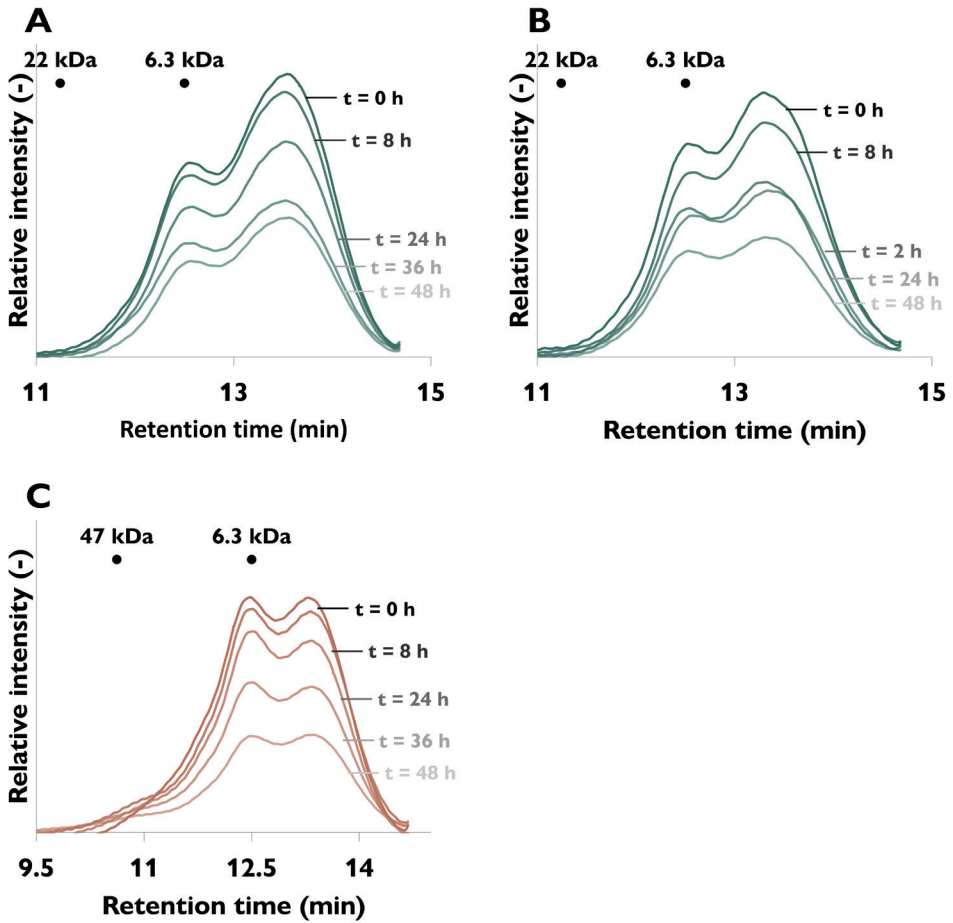
| Unique ASV | A | 16s rRNA part identified |
|--|---|--|
| | B | 100 % match NCBI for species only |
| <i>Bifidobacterium</i> 01 | A | F: TACGTAGGGTGCAAGCGTTATCCGGAATTATTGGGCGTAAAGGGCTCGTAGGCGGTTCTGCGCTCCGGT B: CCTGTTTCGCTCCCAACGCTTTCGCTCTCAGCGTCAGTGACGGCCAGAGACCTGCCTTCGCCATTGGTG |
| | B | <i>B. dentium</i> , <i>B. faecale</i> , <i>B. adolescentis</i> , |
| <i>Bifidobacterium</i> 02 | A | F: TACGTAGGGTGCAAGCGTTATCCGGAATTATTGGGCGTAAAGGGCTCGTAGGCGGTTCTGCGCTCCGGT B: CCTGTTTCGCTCCCAACGCTTTCGCTCTCAGCGTCAGTGACGGCCAGAGACCTGCCTTCGCCATTGGTG |
| | B | <i>B. pseudocatenulatum</i> , <i>B. longum</i> subsp. <i>longum</i> , <i>B. longum</i> subsp. <i>infantis</i> , <i>B. longum</i> , <i>B. breve</i> , <i>B. miconisargentati</i> |
| <i>Bifidobacterium</i> 03 | A | F: TACGTAGGGTGCAAGCGTTATCCGGAATTATTGGGCGTAAAGGGCTCGTAGGCGGTTCTGCGCTCCGGT B: CCTGTTTCGCTCCCAACGCTTTCGCTCTCAGCGTCAGTGACGGCCAGAGACCTGCCTTCGCCAGTGGTG |
| | B | No 100 % matches on species level |
| <i>Ruminococcus</i> 01 | A | F: TACGTAGGGAGCAAGCGTTGTCGGATTACTGGGTGTAAAGGGTCGCTAGGCGGCTTGCAGTCAGAT B: CCTGTTTGCTACCCACGCTTTCGCTCTCAGCGTCAGTTAAAGCCAGCAGGCGCCCTTCGCCACTGGTG |
| | B | <i>R. bromii</i> , <i>Ruminococcoides</i> <i>bili</i> |
| <i>Lachnospiraceae</i> Family 01 | A | F: TACGTATGGTGCAAGCGTTATCCGGAATTACTGGGTGTAAAGGGAGCGCAGGCGGTTGCGGCAAGTCTGAT B: CCTGTTTGCTCCCAACGCTTTCGAGCCTCAGCGTCAGTTATCGTCCAGTAAGCCGCTTCGCCACTGGTG |
| | B | No 100 % matches on species level |
| <i>Acidaminococcus</i> 1 | A | F: TACGTAGGTGGCAAGCGTTGTCGGGAATTATTGGGCGTAAAGAGCATGAGGCGGCTTTTAAGTCTGAC B: CCGGTTTGCTACCCCTGGCTTCGCATCTCAGCGTCAGACACAGTCCAGAAAGGCGCTTCGCCACTGGTG |
| | B | <i>A. intestini</i> |
| <i>Enterobacteriaceae</i> Family 01 | A | F: TACGGAAGGTCCGGCGTTATCCGGAATTACTGGGCGTAAAGCGCAGCAGGCGGTTGTTAAGTCAGAT B: CCTGTTTGCTCCCAACGCTTTCGACCTCAGCGTCAGTCTTCGTCAGGGGGCGGCTTCGCCACCGGTA |
| | B | No 100 % matches on species level |
| <i>Prevotella</i> _9 1 | A | F: TACGGAAGGTCCGGCGTTATCCGGAATTATTGGGTTTAAAGGGAGCGTAGGCGGAGATTAAAGCGTGT B: CCTGTTGATACCCGACCTTCGAGCTTCAGCGTCAGTTGCGCTCCAGTGAGCTGCCTTCGAATCGGAG |
| | B | <i>P. copri</i> |
| <i>Coprococcus</i> 1 | A | F: TACGTATGGTGCAAGCGTTATCCGGAATTACTGGGTGTAAAGGGAGCGTAGACGGCTGTGTAAGTCTGAA B: CCTGTTTGCTCCCAACGCTTTCGAGCCTCAACGTCAGTCACTGCAGTAAGCCGCTTCGCCAATCGGAG |
| | B | No 100 % matches on species level |
| <i>Bacteroides</i> 01 | A | F: TACGAGGATCCGAGCGTTATCCGGAATTATTGGGTTTAAAGGGAGCGTAGATGGATGTTAAGTCAGTT B: CCTGTTTGATACCCACACTTTCGAGCCTCAATGTCAGTTGACGTTAGCAGGCTGCCTTCGCAATCGGAG |
| | B | <i>B. vulgatus</i> , <i>B. dorei</i> , <i>Phocaeicola</i> <i>dorei</i> , <i>Phocaeicola</i> <i>vulgatus</i> |
| <i>Dorea</i> 1 | A | F: TACGTAGGGGCAAGCGTTATCCGGAATTACTGGGTGTAAAGGGAGCGTAGACGGCAGGCAAGCCAGAT B: CCTGTTTGCTCCCAACGCTTTCGAGCCTCAACGTCAGTCACTGCAGCAAGCCGCTTCGCCACTGGTG |
| | B | <i>D. longicatena</i> , |
| <i>Faecalibacterium</i> 1 | A | F: AACGTAGGTCAAGCGTTGTCGGGAATTACTGGGTGTAAAGGGAGCGTAGGCGGGAAGCAAGTTGGAA B: CCTGTTTGCTACCCACACTTTCGAGCCTCAGCGTCAGTTGGTCCCAAGTAGGCGGCTTCGCCACTGGTG |
| | B | <i>F. prausnitzii</i> , <i>F. duncaniae</i> |
| <i>Anaerostipes</i> 1 | A | F: TACGTAGGGGCAAGCGTTATCCGGAATTACTGGGTGTAAAGGGTCGCTAGGTGGTATGGCAAGTCAGAA B: CCTGTTTGCTCCCAACGCTTTCGCTCAGTGTCACTTCAGTCCAGTAAGCCGCTTCGCCACTGATG |
| | B | <i>A. hadrus</i> , <i>A. faecalis</i> |
| <i>Bacteroides</i> 03 | A | F: TACGAGGATCCGAGCGTTATCCGGAATTATTGGGTTTAAAGGGAGCGTAGGTGGACAGTTAAGTCAGTT B: CCTGTTTGATACCCACACTTTCGAGCATCAGTGTCACTTCAGTCCAGTACGCTGCCTTCGCAATCGGAG |
| | B | <i>B. bouchesdurhonensis</i> , <i>B. zhangwenhongii</i> , <i>B. thetaiotaomicron</i> |
| <i>Bacteroides</i> 02 | A | F: TACGAGGATCCGAGCGTTATCCGGAATTATTGGGTTTAAAGGGAGCGTAGGCGGACGCTTAAGTCAGTT B: CCTGTTTGATACCCACACTTTCGAGCATCAGGTACAGTCCAGCAGGCTGCCTTCGCAATCGGAG |
| | B | <i>B. uniformis</i> |

Supplementary table 3.4. Starch recovery (%) in soluble and insoluble fractions of duplicate fermentations of pre-digested RS-es with pooled adult faecal inoculum during 48 h of incubation.

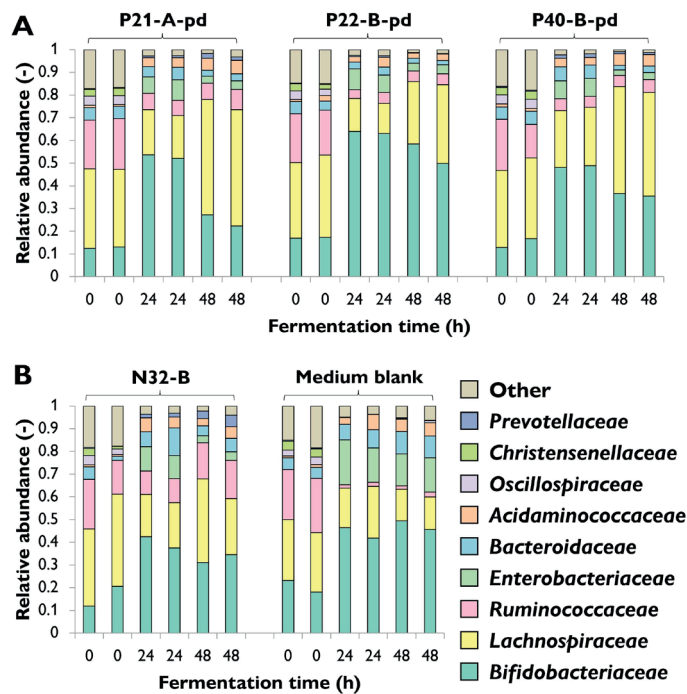
| | | P21-A-pd | P22-B-pd | P40-B-pd | N32-B |
|------------------|----------------------|-----------------|-----------------|-----------------|--------------|
| Time 0 h | Soluble (%) | 4.2 ± 0.2 | 8.0 ± 0.2 | 3.5 ± 0.4 | 2.4 ± 0.1 |
| | Insoluble (%) | 90.4 ± 0.9 | 90.1 ± 1.7 | 92.7 ± 4.8 | 90.0 ± 0.5 |
| Time 8 h | Soluble (%) | 1.2 ± 0.6 | 7.4 ± 0.1 | 0.2 ± 0.0 | 0.2 ± 0.1 |
| | Insoluble (%) | 85.4 ± 0.7 | 78.5 ± 2.2 | 89.9 ± 5.7 | 87.7 ± 4.0 |
| Time 24 h | Soluble (%) | 0.3 ± 0.0 | 0.0 ± 0.1 | 0.1 ± 0.0 | 0.5 ± 0.1 |
| | Insoluble (%) | 67.5 ± 2.2 | 57.8 ± 0.2 | 81.9 ± 2.1 | 79.7 ± 2.7 |
| Time 36 h | Soluble (%) | 0.3 ± 0.0 | 0.4 ± 0.6 | 0.1 ± 0.0 | 0.4 ± 0.0 |
| | Insoluble (%) | 56.8 ± 6.4 | 54.6 ± 2.5 | 64.9 ± 1.8 | 67.1 ± 3.5 |
| Time 48 h | Soluble (%) | 0.3 ± 0.0 | 0.0 ± 0.1 | 0.1 ± 0.0 | 0.3 ± 0.0 |
| | Insoluble (%) | 34.3 ± 12.8 | 33.8 ± 10.4 | 44.1 ± 1.1 | 43.9 ± 1.3 |

Supplementary table 3.5. Starch recovery (%) in soluble and insoluble fractions of duplicate incubations of pre-digested RS-es during 48 h of incubation.

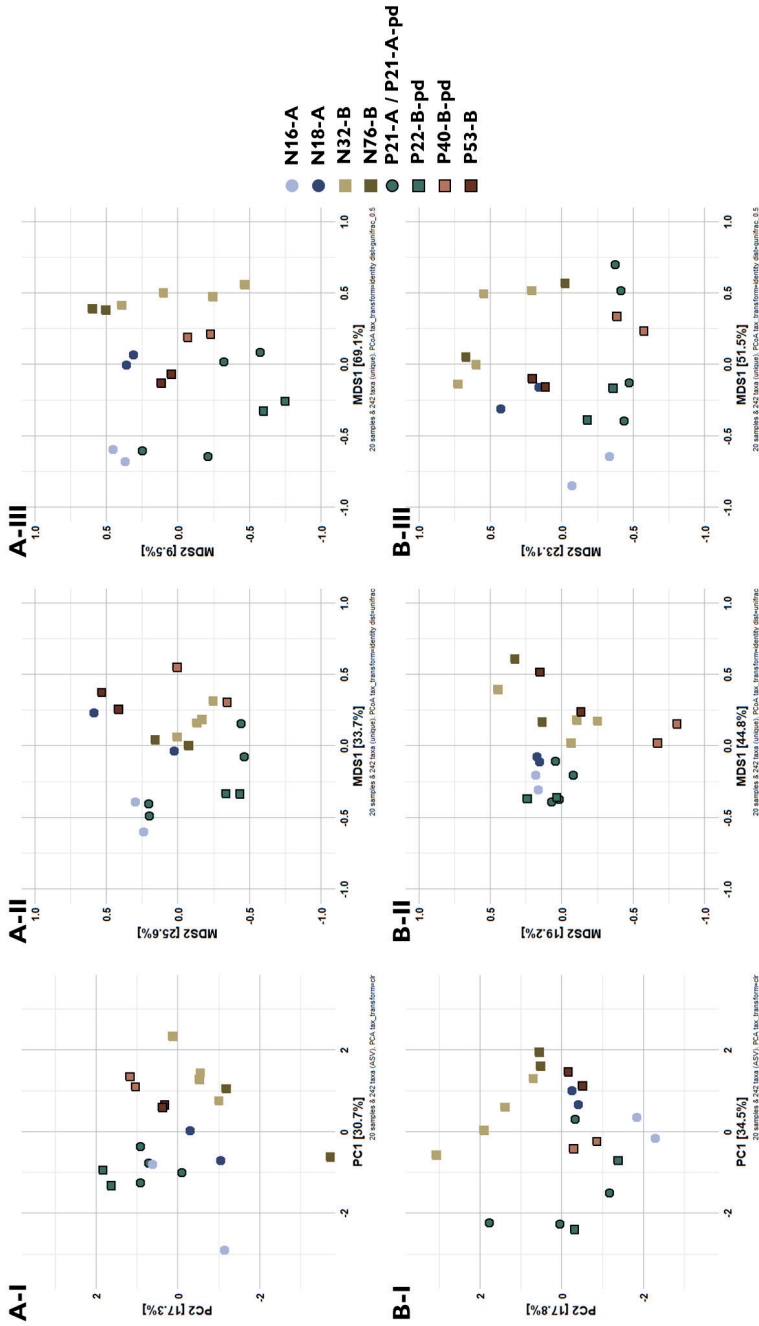
| | | SB | SB | SB | SB |
|------------------|----------------------|-----------------|-----------------|-----------------|--------------|
| | | P21-A-pd | P22-B-pd | P40-B-pd | N32-B |
| Time 0 h | Soluble (%) | 4.3 ± 0.6 | 7.6 ± 0.3 | 2.6 ± 0.1 | 1.5 ± 0.1 |
| | Insoluble (%) | 93.6 ± 2.5 | 87.6 ± 0.0 | 94.1 ± 3.6 | 92.8 ± 1.6 |
| Time 8 h | Soluble (%) | 7.6 ± 0.9 | 12.8 ± 0.9 | 5.0 ± 0.5 | 2.7 ± 0.1 |
| | Insoluble (%) | 95.3 ± 12.8 | 87.6 ± 3.1 | 85.4 ± 3.1 | 91.6 ± 0.1 |
| Time 24 h | Soluble (%) | 12.0 ± 0.5 | 14.6 ± 0.1 | 7.6 ± 0.1 | 3.3 ± 0.1 |
| | Insoluble (%) | 88.1 ± 3.2 | 85.4 ± 0.7 | 90.4 ± 0.4 | 92.1 ± 1.5 |
| Time 36 h | Soluble (%) | 10.3 ± 1.0 | 14.6 ± 0.1 | 7.2 ± 0.5 | 3.7 ± 0.8 |
| | Insoluble (%) | 88.5 ± 0.8 | 86.0 ± 2.5 | 91.6 ± 5.1 | 91.8 ± 0.1 |
| Time 48 h | Soluble (%) | 13.1 ± 1.1 | 16.0 ± 0.0 | 7.8 ± 0.6 | 3.6 ± 0.2 |
| | Insoluble (%) | 84.6 ± 3.2 | 87.5 ± 0.2 | 93.5 ± 3.0 | 91.6 ± 0.5 |



Supplementary figure 3.4. Molecular weight distribution of residual RS-3 during *in vitro* fermentation by pooled adult faecal inoculum, corrected for the amount of starch remaining. From dark to light intensity represents t0, t8, t24, t36 and t48 h. Figure A, B and C represent P21-A-pd, P22-B-pd and P40-B-pd, respectively.



Supplementary figure 3.5. Microbiota composition in relative abundance after *in vitro* fermentation of pre-digested RS-3, N32-B and medium blank over fermentation time at family level. Figure A refers to fermented substrates P21-A-pd, P22-B-pd P40-B-pd, and Figure B refers to fermented N32-B and medium blank, respectively. Results of both biological duplicates are indicated.



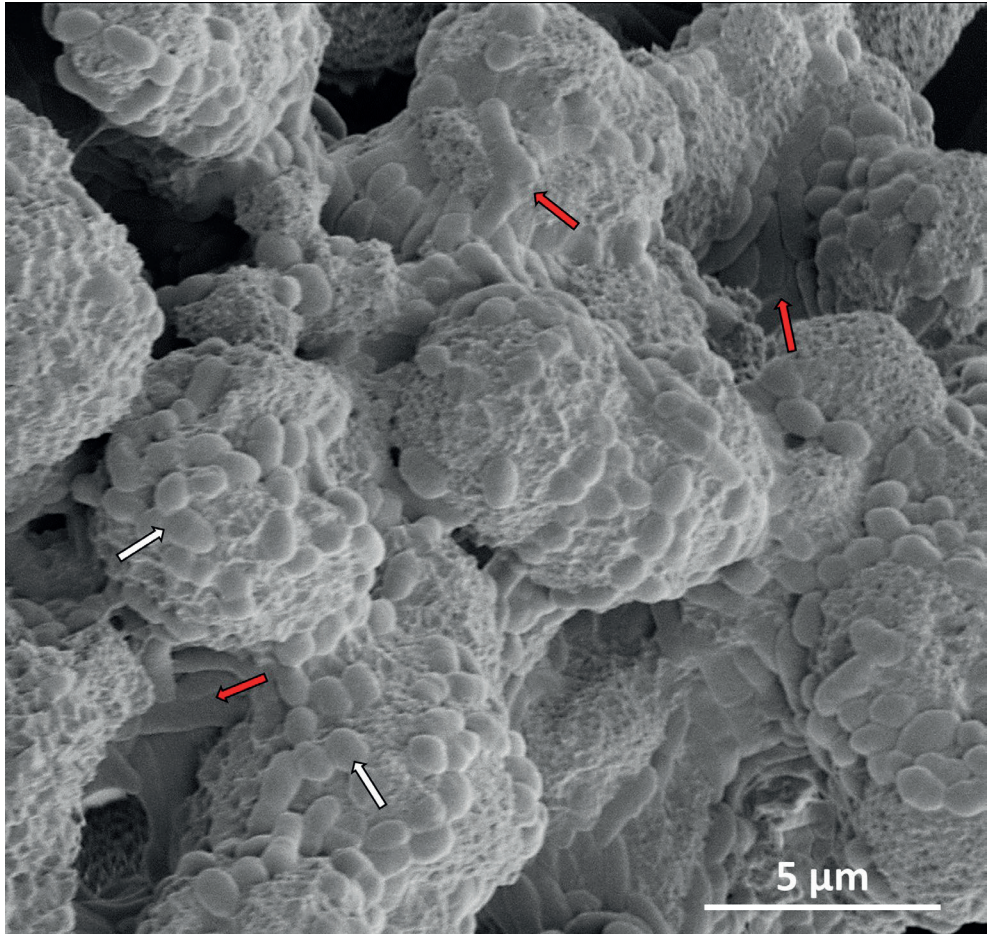
Supplementary figure 3.6. Beta-diversities of intrinsic and pre-digested RS-3 at A: 24 h, and B: 48 h of fermentation. I, II and III give PCA after CLR, PCoA of Unweighted and Generalized UniFrac distances, respectively.

Supplementary table 3.6. Results of PERMANOVA analyses of Dispersity (Mw distribution), Crystal type and Chain length using Aitchison distances, Generalized UniFrac and Unweighted UniFrac distances on fermented RS-3 substrates.

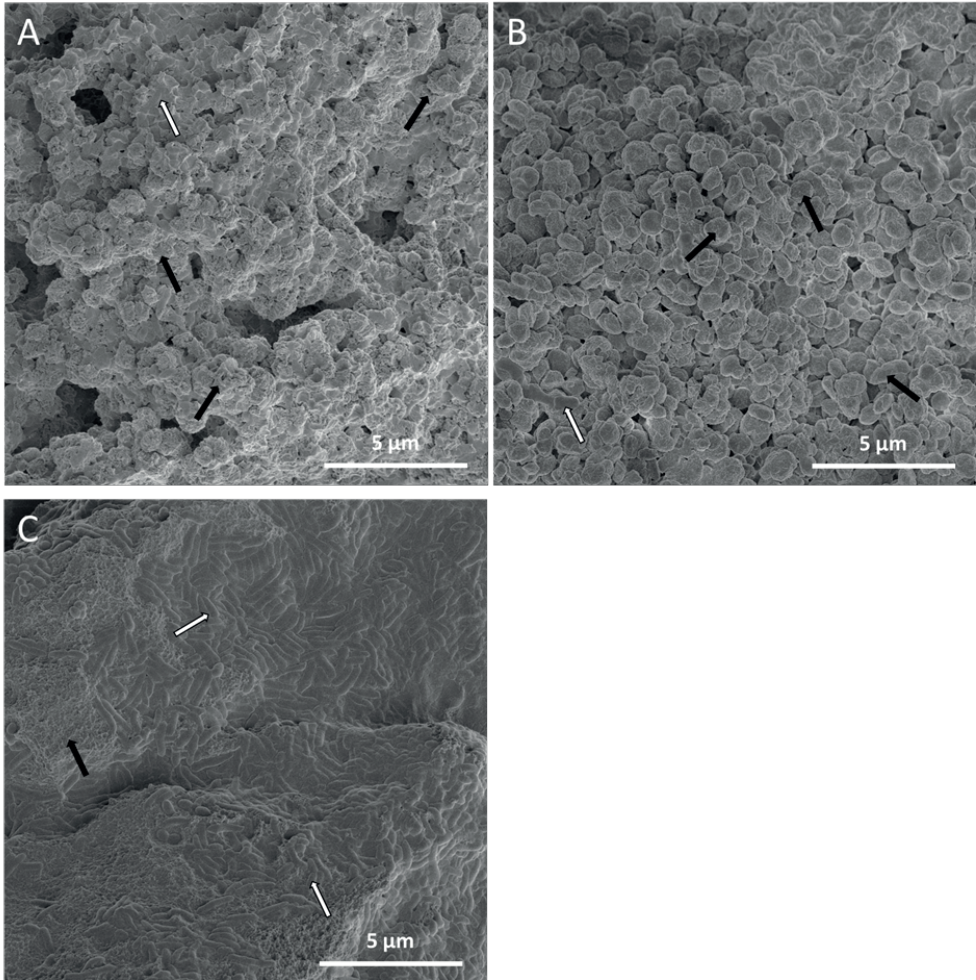
| | Factor | 24 h fermentation | | 48 h fermentation | |
|---------------------|-------------|-------------------|--------|-------------------|--------|
| | | R2 | Pr(>F) | R2 | Pr(>F) |
| Aitchison | Dispersity | 0.09713 | 0.0539 | 0.12856 | 0.0137 |
| | Residual | 0.90287 | | 0.87144 | |
| | Total | 1.00000 | | 1.00000 | |
| | CrystalType | 0.14117 | 0.0057 | 0.08528 | 0.1043 |
| | Residual | 0.85883 | | 0.91472 | |
| | Total | 1.00000 | | 1.00000 | |
| | ChainLength | 0.11534 | 0.021 | 0.15327 | 0.0051 |
| | Residual | 0.88466 | | 0.84673 | |
| | Total | 1.00000 | | 1.00000 | |
| | Dispersity | 0.09725 | 0.0319 | 0.13319 | 0.0083 |
| | CrystalType | 0.14129 | 0.0038 | 0.08991 | 0.0630 |
| | Residual | 0.76158 | | 0.78153 | |
| | Total | 1.00000 | | 1.00000 | |
| | CrystalType | 0.11012 | 0.0147 | 0.05296 | 0.3066 |
| | ChainLength | 0.08428 | 0.0616 | 0.12095 | 0.0161 |
| | Residual | 0.77455 | | 0.79377 | |
| | Total | 1.00000 | | 1.00000 | |
| | Dispersity | 0.09350 | 0.0453 | 0.12251 | 0.0084 |
| | ChainLength | 0.11171 | 0.0183 | 0.14722 | 0.0035 |
| | Residual | 0.79116 | | 0.72422 | |
| | Total | 1.00000 | | 1.00000 | |
| Generalized UniFrac | Dispersity | 0.0806 | 0.1887 | 0.14416 | 0.0343 |
| | Residual | 0.9194 | | 0.85584 | |
| | Total | 1.00000 | | 1.00000 | |
| | CrystalType | 0.27084 | 0.006 | 0.10676 | 0.0876 |
| | Residual | 0.72916 | | 0.89324 | |
| | Total | 1.00000 | | 1.00000 | |
| | ChainLength | 0.20357 | 0.0169 | 0.07598 | 0.0587 |
| | Residual | 0.79643 | | 0.54169 | |
| | Total | 1.00000 | | 0.61767 | |
| | Dispersity | 0.09178 | 0.0941 | 0.14762 | 0.0238 |
| | CrystalType | 0.28202 | 0.0039 | 0.11023 | 0.0595 |
| | Residual | 0.63738 | | 0.74561 | |
| | Total | 1.00000 | | 1.00000 | |
| | CrystalType | 0.12940 | 0.0489 | 0.03864 | 0.4907 |
| | ChainLength | 0.06212 | 0.1949 | 0.05488 | 0.3331 |
| | Residual | 0.66703 | | 0.83836 | |
| | Total | 1.00000 | | 1.00000 | |
| | Dispersity | 0.07182 | 0.1734 | 0.14271 | 0.0253 |
| | ChainLength | 0.19479 | 0.0176 | 0.12156 | 0.0432 |
| | Residual | 0.72461 | | 0.73428 | |
| | Total | 1.00000 | | 1.00000 | |

Supplementary table 3.6, continued

| | | | | | |
|-------------------------------|-------------|---------|--------|---------|--------|
| Unweighted UniFrac | Dispersity | 0.11389 | 0.0586 | 0.13923 | 0.0323 |
| | Residual | 0.88611 | | 0.86077 | |
| | Total | 1.00000 | | 1.00000 | |
| | ChainLength | 0.09291 | 0.1169 | 0.28461 | 5e-04 |
| | Residual | 0.90709 | | 0.71539 | |
| | Total | 1.00000 | | 1.00000 | |
| | CrystalType | 0.11777 | 0.0511 | 0.20653 | 0.0047 |
| | Residual | 0.88223 | | 0.79347 | |
| | Total | 1.00000 | | 1.00000 | |
| | Dispersity | 0.10884 | 0.0537 | 0.14258 | 0.0135 |
| | CrystalType | 0.11272 | 0.0463 | 0.20988 | 0.0024 |
| | Residual | 0.77339 | | 0.65089 | |
| | Total | 1.00000 | | 1.00000 | |
| | CrystalType | 0.09809 | 0.0874 | 0.05092 | 0.2620 |
| | ChainLength | 0.07322 | 0.1847 | 0.12901 | 0.0189 |
| | Residual | 0.80900 | | 0.66446 | |
| | Total | 1.00000 | | 1.00000 | |
| | Dispersity | 0.11461 | 0.0476 | 0.13459 | 0.0113 |
| | ChainLength | 0.09363 | 0.0906 | 0.27997 | 0.0003 |
| | Residual | 0.79248 | | 0.58080 | |
| | Total | 1.00000 | | 1.00000 | |

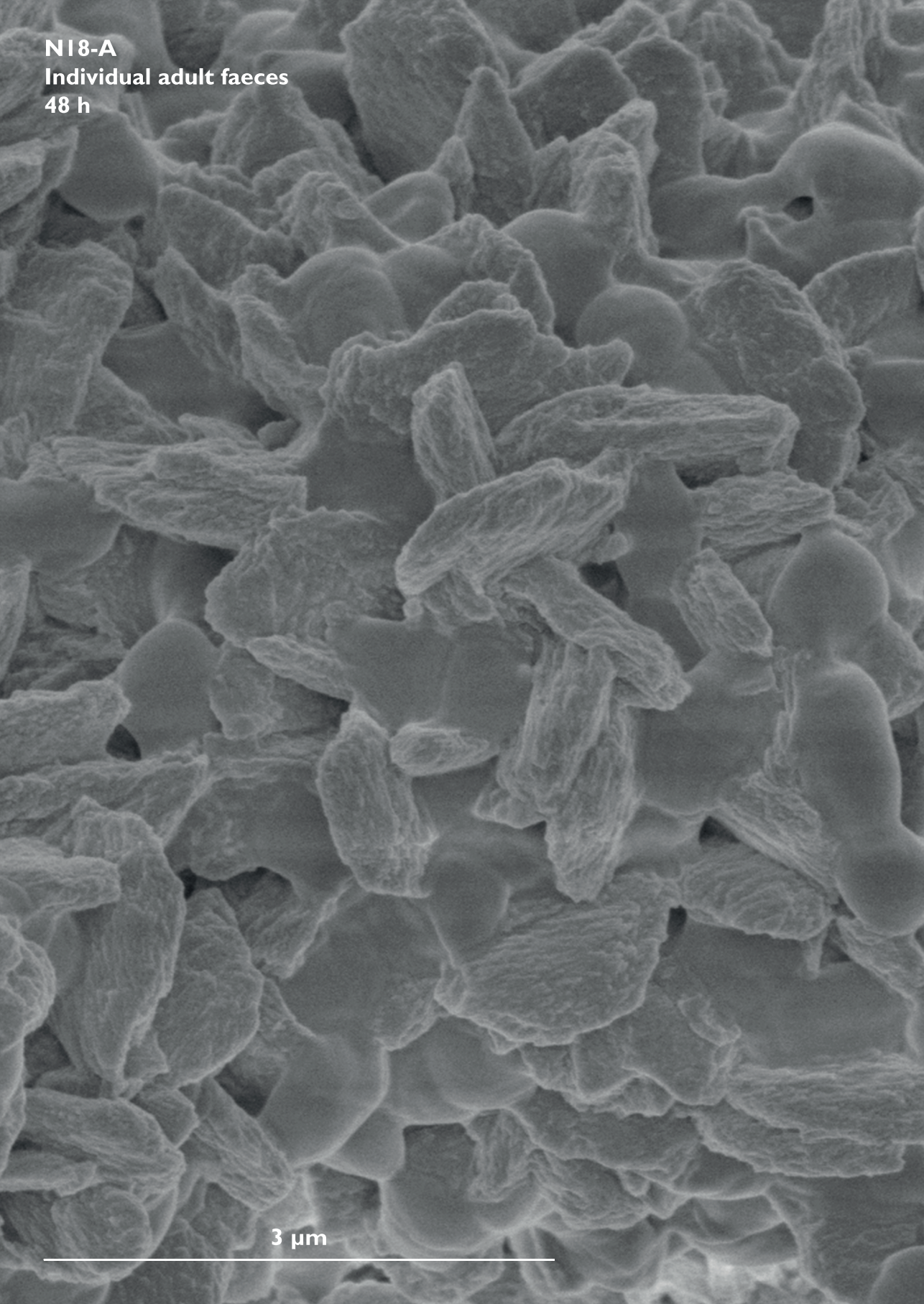


Supplementary figure 3.7. SEM image of RS-3 N32-B after 48 h of *in vitro* fermentation by pooled adult faecal inoculum. White arrows point towards coccus-shaped bacteria, whereas red arrows point towards rod-shaped bacteria.



Supplementary figure 3.8. SEM images of P21-A-pd (A), P22-B-pd (B) and P40-B-pd (C) after 48 h of fermentation with pooled adult faecal inoculum, showing untouched RS-3 particles (black arrows) and bacteria (white arrows).

N18-A
Individual adult faeces
48 h



3 μm

A scanning electron micrograph (SEM) showing a dense collection of starch granules. The granules vary in size and shape, with some appearing as smooth spheres and others as more elongated, angular structures. The surface of the granules shows fine, concentric growth lines, giving them a textured appearance. The background is a soft, out-of-focus grey.

Chapter 4

Presence of digestible starch impacts *in vitro*
fermentation of resistant starch

Cynthia E. Klostermann, Martha F. Endika, Piet L. Buwalda †,

Paul de Vos, Erwin G. Zoetendal, Johannes H. Bitter, Henk A. Schols

Submitted

Abstract

Starch is an important energy source for humans. When starch escapes digestion in the small intestine, it will transit to the colon and will be fermented by gut microbes. Many gut microbes express α -amylases that can degrade soluble starch, but only a few are able to degrade intrinsic resistant starch (RS), that is insoluble and highly resistant to digestion ($\geq 80\%$ RS). We studied the *in vitro* fermentability of eight retrograded starches (RS-3 preparations) differing in rapidly digestible starch content ($\geq 70\%$, $35\text{--}50\%$, $\leq 15\%$) by an inoculum consisting of a pool of four healthy adult faecal samples and found that fermentability depends on the digestible starch fraction present. Digestible starch was readily fermented and generated acetate and lactate, whereas resistant starch was fermented much slower and generated acetate and butyrate. Primarily *Bifidobacterium* increased in relative abundance after fermentation of digestible starch, whereas fermentation of resistant starch also increased relative abundance of *Ruminococcus* and *Lachnospiraceae*. Even the presence of a relatively small fraction of total digestible starch ($\pm 25\%$) within RS-3 preparations influenced the fermentation rate and microbiota composition in such a way that the resistant starch fraction was hardly fermented. By quantification of short-chain fatty acids, we observed that six individual faecal inocula obtained from infants and adults were able to ferment digestible starch, whereas only one adult faecal inoculum was clearly able to ferment intrinsic RS-3. This suggests that, in contrast to digestible starch, intrinsic RS-3 is only fermentable when specific microbes are present. In conclusion, our data illustrates that awareness is required for the presence of digestible starch during *in vitro* fermentation of resistant starch, since such digestible fraction could influence and overrule the outcomes of the prebiotic potential of resistant starches.

1. Introduction

Starch is an important energy source for humans. The major proportion of the starch we consume consists of digestible starch, that is partially digested by salivary α -amylase in the mouth and, depending on the pH, in the stomach and is further digested by pancreatic α -amylase in the small intestine to malto-oligomers^[1]. These malto-oligomers are hydrolysed by brush-border enzymes maltase-glucoamylase and sucrase-isomaltase to glucose^[1] and further metabolised to energy. If starch escapes digestion in the upper gastro-intestinal tract (GIT), it will transit to the colon where it will be fermented by gut microbiota to yield health-beneficial short-chain fatty acids (SCFAs)^[2]. The amount of starch arriving in the colon depends largely on the digestion kinetics^[3] and is influenced by, among others, the type of starch, surrounding food matrices, transit time and age of the subject^[1, 4-6].

A widely accepted model to study *in vitro* starch digestion in the upper GIT describes different fractions of digestible starch: rapidly digestible starch (RDS), which is digested within 20 min of a standardized incubation, and slowly digestible starch (SDS), which is digested between 20-120 min of incubation^[7]. The starch that is remaining after 120 min of digestion is considered resistant starch (RS)^[7]. Nevertheless, this “RS” might be degradable using higher enzyme concentrations^[8] or longer incubation times^[3] and is therefore considered kinetically resistant starch. Such starches are different from intrinsic resistant starches, since these are not digestible by upper GIT enzymes.

Some starches are more resistant to upper GIT digestion than others due to their granular structure (type 2 RS) or conformation (type 3 RS (retrograded starches)) or due to a surrounding cell-wall matrix (type 1 RS) which is protecting the granular starches from pancreatic digestion^[4]. Also type 4 and type 5 RS are described, which resist digestion due to chemical modification or due to complexing with lipids, respectively^[4]. Although these five types of RS are defined and considered as “resistant starch”, most of them are partially digestible and only contain a fraction of RS^[9-12]. Previously, we made resistant starch type 3 (RS-3) preparations differing in molecular weight, molecular weight distribution and crystal type and found that the proportion of RDS, SDS and RS depended on these characteristics (Chapter 2^[13]).

To our knowledge, only few studies have been targeting the *in vivo* starch digestion in human directly^[9, 14]. This is probably due to the use of invasive techniques that are needed to quantify released malto-oligomers and glucose in the small intestine. Starch digestion *in vivo* is mostly predicted indirectly by

addressing the glycaemic response and comparing this to *in vitro* digestion assays^[15-17]. Since there is a lack of *in vivo* studies in human, it is still hard to predict how much of the digestible fraction of kinetically resistant starch will arrive in the colon. It has been speculated that a more rapid transit-time or starch-rich meals may result in the presence of digestible starch in the colon^[18]. A previous study supplementing subjects with 20 or 40 g/day digestible starch did not find changes in faecal microbiota composition after the intervention^[19]. This indicates that either all digestible starch had been absorbed in the small intestine or that the presence of digestible starch in the colon did not result in specific changes in microbiota composition. Animal studies that quantified remaining starch throughout the GIT showed that digestible starch had fully disappeared at the end of the small intestine, either by digestion or ileal fermentation^[20, 21].

Although most of the starch will be digested in the small intestine, still many studies discussing the fermentability of RS do not report the digestible fraction neither remove this fraction prior to *in vitro* fermentation^[12, 22-27]. Additionally, media used for *in vitro* fermentation, such as simulated ileal efflux medium (SIEM), routinely contain digestible starch^[28]. The presence of a large fraction of digestible starch in the colon of healthy adults is only likely when acarbose is used to block pancreatic digestion^[29] or originating from RS-1, in which otherwise digestible granules, such as present in wheat, rice or maize kernels, are protected by a cell-wall matrix and therefore not digested in the small intestine^[11]. Once the gut microbes open the cell-wall matrix, this starch is released and subject to fast fermentation. Although the impact of a digestible fraction on *in vitro* fermentation is not always clear, it should be realized that many different gut microbes are able to ferment soluble -digestible- starch due to the presence of starch-degrading glycoside hydrolase family 13 (GH13) enzymes in their genome^[30] (CAZy database^[31]). In contrast, only a few microbes are reported to be able to degrade and ferment RS type 2 and 3 directly, such as *Ruminococcus bromii* and *Bifidobacterium adolescentis*^[32, 33]. These microbes express, next to specific α -amylases, also specific carbohydrate binding modules (CBMs), such as CBM74, that are able to bind to insoluble starch particles^[34] and therefore accelerate hydrolysis.

The presence of a digestible fraction during *in vitro* fermentation is thus likely to affect the prediction of the prebiotic potential of RS, making pre-digestion to remove digestible starch necessary. Although *in vitro* digestion assays are developed to determine the amount of RS within a source and not necessarily as a pre-treatment prior to *in vitro* fermentation, many researchers used this pre-

digestion treatment for studying the prebiotic potential of RS^[35-42]. Pre-digestion assays prior to *in vitro* fermentation have their weaknesses, such as inactivation of digestive enzymes without heat treatment, and drying of the obtained pre-digested fractions. The impact of the presence of a digestible starch fraction during *in vitro* fermentation of partially resistant starches by gut microbiota is not studied in detail yet.

In the present study we determined the impact of digestible starch fractions within RS-3 preparations on *in vitro* fermentation. Eight RS-3 preparations differing in rapidly digestible starch (RDS) content (grouped in categories ≥ 70 % RDS, 35-50 % RDS and ≤ 15 % RDS) were inoculated with a pool of four healthy adult faecal samples and subsequently, the starch degradation, SCFA production and changes in microbiota composition were determined at different incubation times. To investigate a possible generic impact of gut microbiota on the fermentability of digestible versus resistant starch, we also incubated one fully digestible starch (from the category ≥ 70 % RDS) and two intrinsic RS-3 substrates (from the category ≤ 15 % RDS) with faecal inocula of two adults and two weaning infants at six and nine-ten months old and quantified the SCFAs produced.

2. Materials and methods

2.1. Materials

L-cysteine hydrochloride, 2-(N-morpholino)ethanesulfonic acid and soluble potato starch (SPS) were obtained from Sigma-Aldrich (St. Louis, Missouri, USA).

2.1.1. RS-3 preparations

RS-3 preparations were prepared by crystallizing α -1,4 glucans obtained by either debranched (enzymatically modified) amylopectins or by enzymatic synthesis (Chapter 2^[13]). The (enzymatically modified) amylopectins included waxy potato starch (Eliane100) and highly branched starch of potato ($M_w \pm 100$ kDa, 8 % branch points) provided by AVEBE (Veendam, The Netherlands) and waxy rice starch (Remyline XS) obtained from Beneo (Mannheim, Germany). The physico-chemical characteristics of the RS-3 preparations and the *in vitro* digestibility were described in Chapter 2^[13] and are summarized in Table 4.1 in the results section.

2.1.2. Faecal slurry

Faecal material of four healthy adults was collected, after signing a written informed consent. Subjects were between 27 and 35 years old, had a BMI between 19 – 22 kg/m², were non-smokers, did not have any health complaints, and did not use antibiotics for over 6 months prior to collection. Pooled adult faecal slurry was prepared as previously described (Chapter 3), snap-frozen in liquid nitrogen and stored at -80 °C prior to use. Faecal samples of infants were collected within the Baby Carbs Study as briefly reported by Endika and co-authors^[43]. Faecal slurries of two individual adults, two weaning infants at 6 months old and the same two infants at 9-10 months old were prepared as previously described (Chapter 3), snap-frozen in liquid nitrogen and stored at -80 °C prior to use.

2.2. *In vitro* batch fermentation of RS-3 preparations

The culture medium was based on Simulated Ileal Efflux Medium (SIEM) as described by Minekus et al. (1999) with minor modifications as reported in Chapter 3. Especially the carbohydrate component within modified SIEM (mSIEM) was lowered to 0.592 g/L. Culture medium containing 11.11 mg/mL soluble potato starch (mSIEM + SPS) was prepared as described previously (Chapter 3).

The *in vitro* batch fermentations were performed as described previously (Chapter 3). In short, ± 20 mg (dry weight) RS-3 preparations were weighed in duplicate in sterile 5 mL serum bottles for each individual sampling time. The weighed RS-3 preparations were stored overnight in an anaerobic chamber (gas composition: 4 % H₂, 15 % CO₂, 81 % N₂; Bactron 300, Sheldon Manufacturing, Cornelius, Oregon, USA).

In the anaerobic chamber, inoculum was prepared by diluting pooled adult faecal slurry to 10 mg/mL faeces in mSIEM. An aliquot of 1.8 mL mSIEM was added to the serum bottles containing RS-3 preparations and 0.2 mL inoculum was added to reach final substrate concentrations of ± 10 mg/mL. Similarly, an aliquot of 1.8 mL mSIEM + SPS was added to empty serum bottles and 0.2 mL inoculum was added. In addition, substrate blanks (without inoculum) and medium blanks (without additional substrate) were included. The serum bottles were capped with butyl rubber stoppers and incubated at 37 °C, 100 rpm for 0, 24 and 48 h.

At each time point, the serum bottles were decapped and the contents were transferred to Safe-Lock Eppendorf tubes (Eppendorf, Hamburg, Germany). The

tubes were centrifuged, the pellet and supernatant were separated and further processed as described previously (Chapter 3). The pH was measured using non-bleeding pH indicator strips 4.0-7.0 (Merck, Darmstadt, Germany). The supernatant was heated in a Safe-Lock Eppendorf tube to 100 °C, 800 rpm for 10 min in an Eppendorf shaker (Eppendorf) and stored at -20 °C until analysis. The pellet was snap-frozen with liquid nitrogen, stored at -80 °C and freeze-dried.

In a second, independent fermentation experiment, we investigated the fermentability of SPS and two intrinsic RS-3 substrates (N18-A and N76-B) using individual faecal inocula obtained from adults and infants (Supplementary information 4.1).

2.3. Total starch quantification of fermented RS-3 preparations

Starch was quantified in the supernatant and in the freeze-dried pellets obtained after fermentation using the Megazyme Total Starch Kit (AA/AMG) (Megazyme, Wicklow, Ireland), according to the company protocol and adjusted for smaller sample sizes as described in Chapter 3.

2.4. Short-chain fatty acids and other organic acids produced by fermentation

Short-chain fatty acids, lactic and succinic acid were analysed using HPLC-RI/UV as previously described (Chapter 3).

2.5. Microbiota composition & data analysis

Microbiota composition was determined as described previously (Chapter 3) in all biological duplicates, except for SPS t0 since only 1 freeze-dried pellet contained enough DNA to perform 16s ribosomal RNA (rRNA) gene sequencing. In short, the V4 region of the 16S rRNA gene of purified DNA was amplified in duplicate using barcoded primers. The PCR products were purified, pooled and sent for Illumina Hiseq2500 (2 x 150 bp) sequencing (Novogene, Cambridge, UK). Raw sequence data of the 16S rRNA gene amplicons was processed using the NG-Tax 2.0 pipeline with default settings^[44]. Taxonomy of each amplicon sequence variant (ASV) was assigned based on the SILVA database version 138.1^[45, 46]. Data was analysed using R version 4.1.0 and the R packages phyloseq version 1.38.0^[47], microbiome version 1.17.42^[48] and microViz version 0.10.1^[49] as previously described (Chapter 3). Principle component analysis (PCA) and principle coordinate analysis (PCoA) were used to visualize the microbiota variation between substrates after centered-log-ratio (CLR) transformation or Generalized UniFrac distances (i.e. taking phylogenetic relatedness and relative abundance of taxa into account, with an extra parameter α controlling the weight

of abundant lineages^[50]) and Unweighted UniFrac distances (i.e. taking phylogenetic relatedness between taxa, but no relative abundance of taxa into account), respectively. PERMANOVA analyses were performed to determine if the % RDS, % SDS and % RS (as a continuous variable) present within RS-3 preparations significantly influenced the microbiota composition.

3. Results

3.1. RS-3 preparations

We investigated the impact of the presence of a digestible starch fraction of nine different starches on *in vitro* fermentation characteristics, such as starch degradation, short-chain fatty acid (SCFA) formation and microbiota composition. Eight starches studied were so-called RS-3 preparations while soluble potato starch (SPS) was taken as a positive control. The RS-3 preparations were prepared from α -1,4 glucans of different average Mw, obtained either by debranching amylopectins of different sources or by enzymatic synthesis. The obtained α -1,4 glucans were crystallized in A- or B-type polymorphs. To determine the fractions of rapidly and slowly digestible starch (total digestible starch) and resistant starch, the samples were *in vitro* digested using porcine pancreatin and amyloglucosidase (Chapter 2^[13]). The overall characteristics of the eight RS-3 preparations are shown in Table 4.1. The sample codes are named after the RS-3 physico-chemical characteristics with **N**: narrow disperse, **P**: polydisperse, **number**: DPn, **A**: A-type crystal, **B**: B-type crystal.

The RS-3 preparations obtained from debranched amylopectins had a more polydisperse Mw distribution ($PI \geq 1.3$), whereas those obtained from enzymatically synthesized α -1,4 glucans had a more narrow disperse Mw distribution ($PI \leq 1.25$). After *in vitro* digestion, the RS-3 preparations and SPS were grouped in categories based on their RDS content. These groups consisted of samples having ≥ 70 % RDS (SPS, P14-B, N15-B), 35-50 % RDS (P14-A, N18-B, P22-B) and samples having ≤ 15 % RDS (P40-B, N18-A and N76-B). Especially N18-A and N76-B contained a very low amount of total digestible starch (RDS + SDS) and were therefore considered intrinsic RS-3. Some RS-3 preparations with similar Mw and Mw distribution but differing in crystal type fell into different categories based on their digestion properties (P14-A vs P14-B, N18-A vs N18-B) (Chapter 2^[13]). Together, these eight RS-3 preparations and SPS represent a broad collection of starches differing in contents of RDS, SDS and RS, which allows us

to study the effect of a digestible fraction on *in vitro* fermentation of RS-3 preparations.

Table 4.1. Characteristics of RS-3 preparations used in this study, as described in Klostermann et al. (2021)^[13].

| Name | Reported as ^[13] | DPn | PI | Crystal type | RDS (%) | SDS (%) | RS (%) | RDS cat. |
|-------|--------------------------------|------|------|-----------------|-------------|------------|------------|-------------|
| P14-A | dHBPS-A | 14.3 | 1.33 | A | 40.1 ± 5.4 | 44.7 ± 8.9 | 15.2 ± 3.6 | 35-50 % |
| P14-B | dHBPS-B | 14.0 | 1.35 | B | 92.1 ± 12.0 | 7.6 ± 1.8 | 0.2 ± 10.3 | ≥ 70 % |
| N15-B | sG2-B | 15.2 | 1.25 | B | 69.6 ± 4.2 | 19.9 ± 2.0 | 10.5 ± 2.2 | ≥ 70 % |
| P22-B | dWRS-B | 21.9 | 1.50 | B | 38.2 ± 2.2 | 41.9 ± 0.7 | 19.9 ± 2.4 | 35-50 % |
| N18-A | sG5-A | 18.0 | 1.21 | A | 12.4 ± 9.1 | -0.3 ± 6.1 | 88.0 ± 3.8 | ≤ 15 % |
| N18-B | sG5-B | 18.0 | 1.21 | B | 50.7 ± 0.4 | 23.4 ± 3.0 | 25.9 ± 3.3 | 35-50 % |
| P40-B | dWPS-B | 39.9 | 2.11 | B | 15.3 ± 1.7 | 10.5 ± 1.9 | 74.2 ± 2.0 | ≤ 15 % |
| N76-B | sG65-B | 75.6 | 1.07 | B | 3.2 ± 0.9 | 2.6 ± 0.2 | 94.2 ± 0.8 | ≤ 15 % |

DPn (number-based degree of polymerization) and PI (polydispersity index) were determined using HPSEC-RI analysis, crystal type was determined using XRD and rapidly digestible starch (RDS), slowly digestible starch (SDS) and resistant starch (RS) were determined after digestion using porcine pancreatin and amyloglucosidase^[13]. RDS cat. = RDS category, used for grouping substrates. The sample names have been recoded compared to Klostermann et al., 2021^[13].

3.2. Starch having a digestible fraction is fermented differently compared to intrinsic resistant starch

The RS-3 preparations and SPS were fermented *in vitro* during 48 h using an inoculum of a pool of four healthy adult faecal samples. The starch was quantified based on the presence of soluble starch in the supernatant and insoluble starch in the obtained pellet after incubation with (Supplementary table 4.1) and without faecal inoculum (Supplementary table 4.2). This revealed that some RS-3 preparations solubilized during 24 h of incubation (Supplementary table 4.2) and that these soluble fractions were not detected in the presence of the faecal inoculum (Supplementary table 4.1), indicating that the soluble fraction was fermented prior to the insoluble fraction. Especially P14-B solubilized for ± 70 % after 24 h of incubation, but also other RS-3 preparations like N15-B and P14-A solubilized for ± 30 % after 24 h of incubation (Supplementary table 4.2), which is likely caused by the short α -1,4 glucan chain length of these RS-3 preparations. Previously, it has been shown that especially short α -1,4 glucans present within recrystallized starch tend to solubilize when heated; and when present in B-type crystallites these short α -1,4 glucans tend to solubilize faster than when present in A-type crystallites^[51], clearly confirming our observations. It should be noted that insoluble starch was hard to quantify accurately since sampling of insoluble starch had some limitations (i.e. the

pellets obtained after centrifugation were very instable), especially for samples at t0 and samples without inoculum. When fermentation proceeded, the biomass together with the insoluble starch particles made quantification easier and more reliable. To achieve a useful comparison among fermentation rates of RS-3 preparations by gut microbiota, we normalized the obtained starch recovery during fermentation for total starch content at t0.

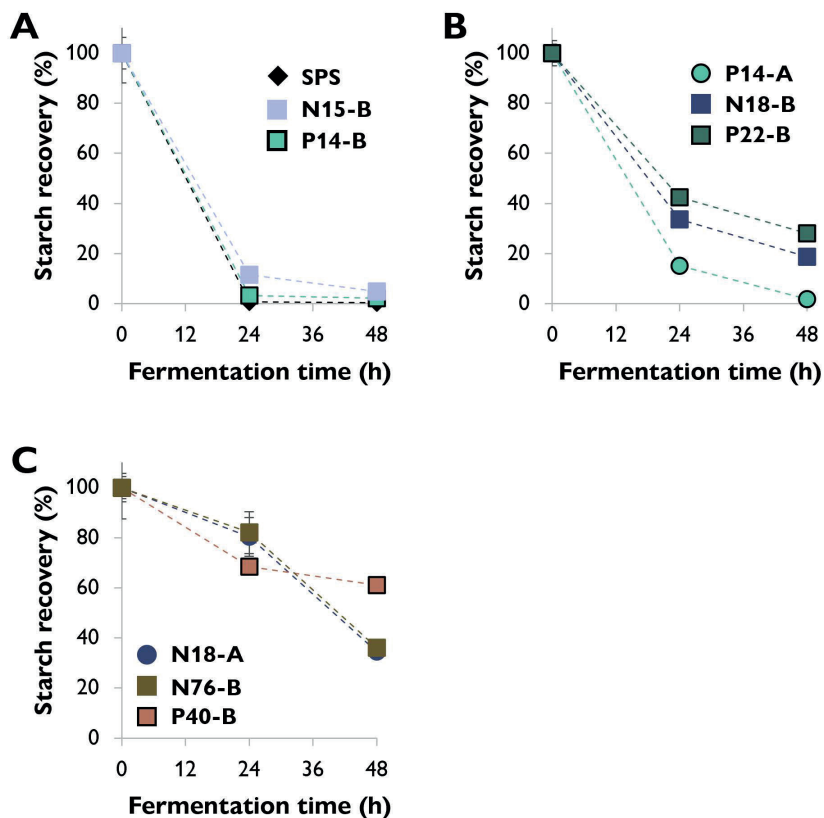


Figure 4.1. Starch recovery (soluble + insoluble starch) during 48 h of fermentation of RS-3 preparations by pooled adult faecal inoculum, normalized for the total starch content at t0. Figure A, B and C represent RS-3 preparations containing $\geq 70\%$ RDS, 35-50 % RDS or $\leq 15\%$ RDS, respectively. The average of biological duplicates is shown. Standard deviations might be smaller than the marker used.

Complete starch degradation of samples containing $\geq 70\%$ RDS (SPS, N15-B, P14-B) occurred during the first 24 h of incubation (Figure 4.1-A). As stated before, RS-3 preparations N15-B and P14-B partly solubilized during incubation without inoculum (Supplementary table 4.2). However, the amount of starch

degraded during the first 24 h of fermentation of P14-B and N15-B was higher than the solubilized part only (Figure 4.1-A). Samples containing 35-50 % RDS (P14-A, N18-B, P22-B) were degraded for 60-80 % during the first 24 h of incubation (Figure 4.1-B). The starch degradation in these samples continued up to 48 h of incubation, but degradation rate slowed down for N18-B and P22-B. P14-A was degraded to a larger extent than N18-B and P22-B, probably due to the presence of a larger total amount of digestible starch within P14-A, compared to N18-B and P22-B (Table 4.1). RS-3 preparations having ≤ 15 % RDS (N18-A, N76-B, P40-B) behaved differently during 48 h of incubation (Figure 4.1-C). Intrinsic RS-3 with a narrow disperse Mw distribution (N18-A and N76-B) were degraded at a similar rate with ± 40 % starch remaining after 48 h, whereas P40-B (polydisperse Mw distribution) showed a different degradation pattern with ± 60 % starch remaining after 48 h.

SCFAs and lactic acid were quantified after fermentation (Figure 4.2); no succinic acid was detected in the fermentation supernatants. Fermentation of the medium blank resulted in low levels of SCFAs (total content of ± 2 $\mu\text{mol/mg}$) and no lactic acid was detected (Supplementary figure 4.1).

The results show that RS-3 preparations containing ≥ 70 % RDS were rapidly fermented to ± 8 -9 $\mu\text{mol/mg}$ acetate and ± 4 -4.5 $\mu\text{mol/mg}$ lactate during 48 h of fermentation by this inoculum (Figure 4.2-A). Only minor amounts of butyrate (≤ 0.4 $\mu\text{mol/mg}$ substrate) and no propionate were formed during fermentation of these substrates. RS-3 preparations containing 35-50 % RDS were also predominantly fermented to acetate and lactate, with ≤ 0.7 $\mu\text{mol/mg}$ butyrate and ≤ 0.2 $\mu\text{mol/mg}$ propionate after 48 h of fermentation (Figure 4.2-B). An increase in acid production was observed between 24 and 48 h of fermentation for all substrates, in line with the decrease in starch recovery (Figure 4.1-B). After 48 h, P14-A reached a similar total amount of acids (± 14.6 $\mu\text{mol/mg}$) compared to samples having ≥ 70 % RDS, likely since it was also fully degraded after 48 h of incubation (Figure 4.1-B). Fermentation of N18-B and P22-B resulted in lower amounts of total acids produced (12.7 $\mu\text{mol/mg}$ and 10.1 $\mu\text{mol/mg}$, respectively), in line with the lower starch degradation (Figure 4.1-B). The production of SCFAs and lactate during fermentation of RS-3 preparations ≥ 35 % RDS resulted in a drop in pH to 4 - 4.5 after 24 h.

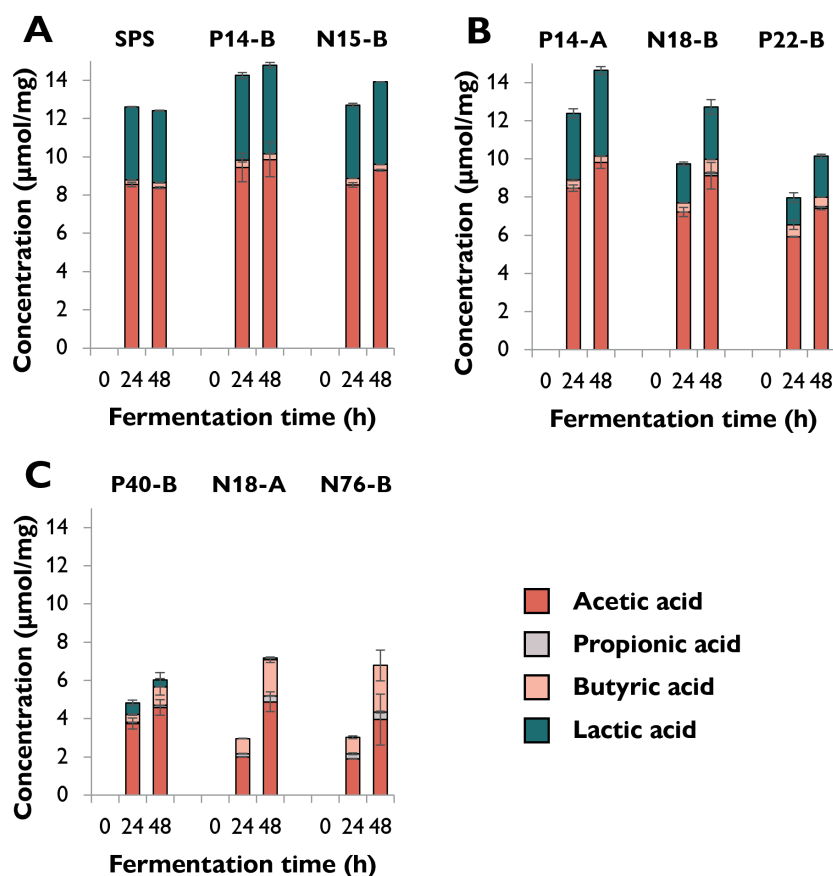


Figure 4.2. Short-chain fatty acid and lactic acid formation ($\mu\text{mol/mg}$ substrate) during 48 h of fermentation of RS-3 preparations by pooled adult faecal inoculum. Figure A, B and C represent RS-3 preparations containing ≥ 70 % RDS, 35-50 % RDS or ≤ 15 % RDS, respectively. The average of biological duplicates is shown.

Fermentation of RS-3 preparations containing ≤ 15 % RDS (P40-B and intrinsic RS-3 (N18-A and N76-B)) resulted in different amounts of SCFAs and lactate produced after 24 and 48 h of incubation (Figure 4.2-C). Intrinsic RS-3 substrates (N18-A and N76-B) were predominantly fermented to acetate and butyrate (± 2.0 and ± 0.8 $\mu\text{mol/mg}$, respectively) after 24 h of incubation, whereas fermentation of P40-B generated more acetate (± 3.8 $\mu\text{mol/mg}$) and also some lactate (0.6 $\mu\text{mol/mg}$). The amount of additional acid produced after 48 h of fermentation was low for P40-B (± 1.2 $\mu\text{mol/mg}$), in line with the decreased starch degradation rate (Figure 4.1-C). In contrast, the amount of additional acid produced was much higher for N18-A and N76-B (4.2 and 3.7 $\mu\text{mol/mg}$, respectively), in line with the increased starch degradation rate between 24 and 48 h of incubation

(Figure 4.1-C). The production of SCFAs and lactate during fermentation resulted in a lower pH for P40-B ($\text{pH} \pm 4.7$), compared to intrinsic RS-3 N18-A and N76-B ($\text{pH} \pm 5.3$) at 24 h.

3.3. Partially digestible starch stimulates different microbial populations compared to intrinsic RS-3

The changes in microbiota composition during fermentation of RS-3 preparations differing in RDS content were determined using 16S rRNA gene sequencing and visualized using β -diversity analysis after centered-log-ratio (CLR) transformation of relative abundances of ASVs (Figure 4.3).

The PCA plot shows that t0 samples clearly differed from the samples taken after 24 and 48 h of incubation (Figure 4.3-A), indicating that *in vitro* fermentation selectively stimulated microbial populations compared to the initial inoculum. After 24 and 48 h of fermentation, RS-3 preparations with ≥ 70 % RDS and 35 - 50 % RDS fully overlapped and clustered together (Figure 4.3-B, C), in agreement with the similar SCFA profiles observed. Intrinsic RS-3 substrates N18-A and N76-B clearly separated from RS-3 preparations having a high fraction of digestible starch, in line with the different SCFA profiles. The microbiota in fermented P40-B, with ≤ 15 % RDS and ± 25 % total digestible starch, was closer to RS-3 preparations ≥ 35 % RDS and separated clearly from intrinsic RS-3 (N18-A and N76-B). In terms of starch degradation and SCFA production, P40-B also differed from N18-A and N76-B (Figure 4.1-C, Figure 4.2-C), but also did not resemble fermentation of RS-3 preparations ≥ 35 % RDS. PERMANOVA analyses confirmed a significant effect of % RDS and % RS on microbiota composition after 48 h of fermentation using Aitchison (% RDS: $P = 2e-04$, % RS: $P = 0.0018$), Unweighted UniFrac (% RDS: $P = 1e-04$, % RS: $P = 0.0059$) and Generalized UniFrac (% RDS: $P = 7e-04$, % RS: $P = 2e-04$) distances (Supplementary table 4.4), indicating that both these factors contributed significantly to the overall microbiota composition, the presence of certain taxa and the abundance of those taxa.

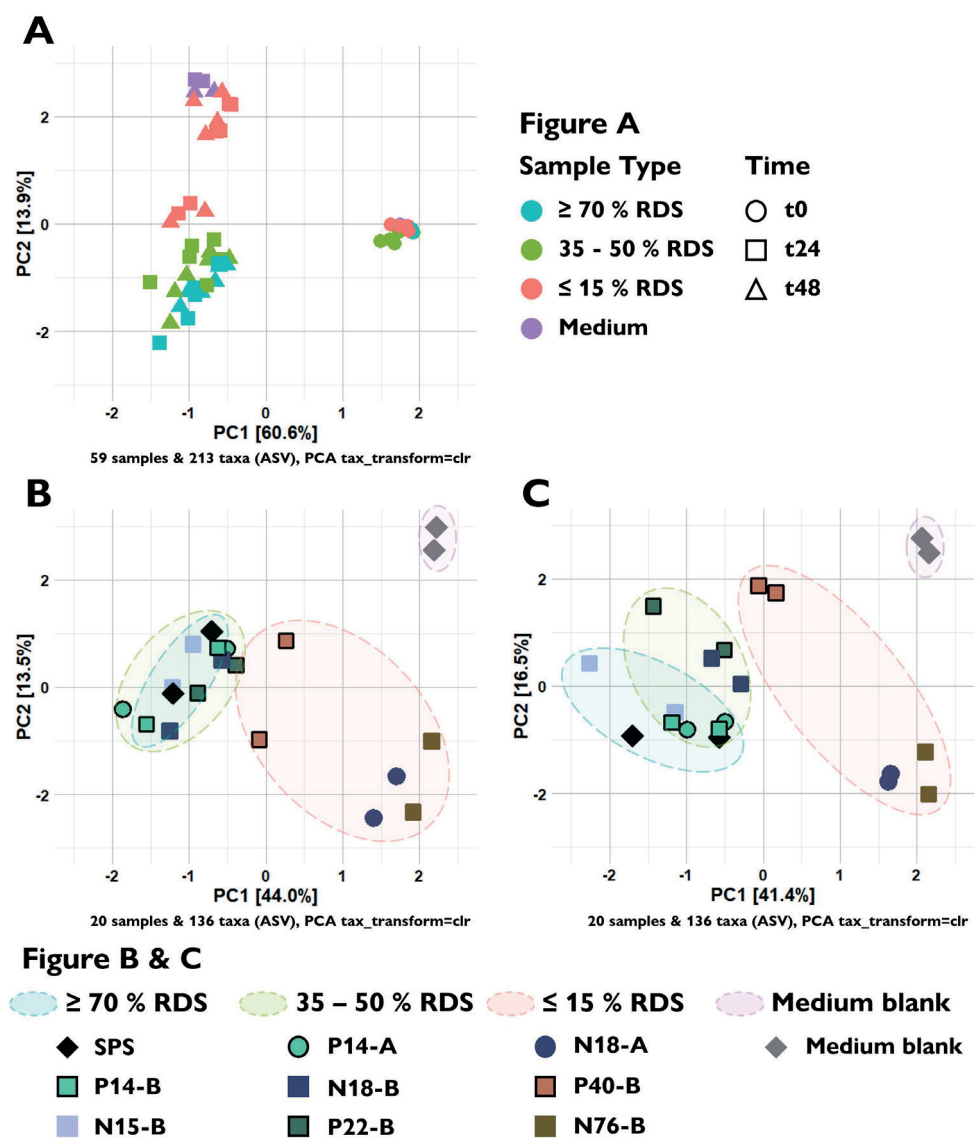


Figure 4.3. A: Ordination plot of CLR-transformed relative abundances of ASVs from fermented RS-3 preparations by pooled adult faecal inoculum over time. Figure B and C refer to CLR-transformed relative abundances of ASVs at t24 and t48, respectively.

The microbiota compositions in relative abundance during fermentation of RS-3 preparations differing in % RDS were determined at family level and indicated that the microbiota composition at t0 obviously was quite similar for all fermentations, with around 15 % *Bifidobacteriaceae*, 40 % *Lachnospiraceae*, 15 % *Ruminococcaceae*, 5 % *Bacteroidaceae* and 3 % *Oscillospiraceae* (Figure 4.4).

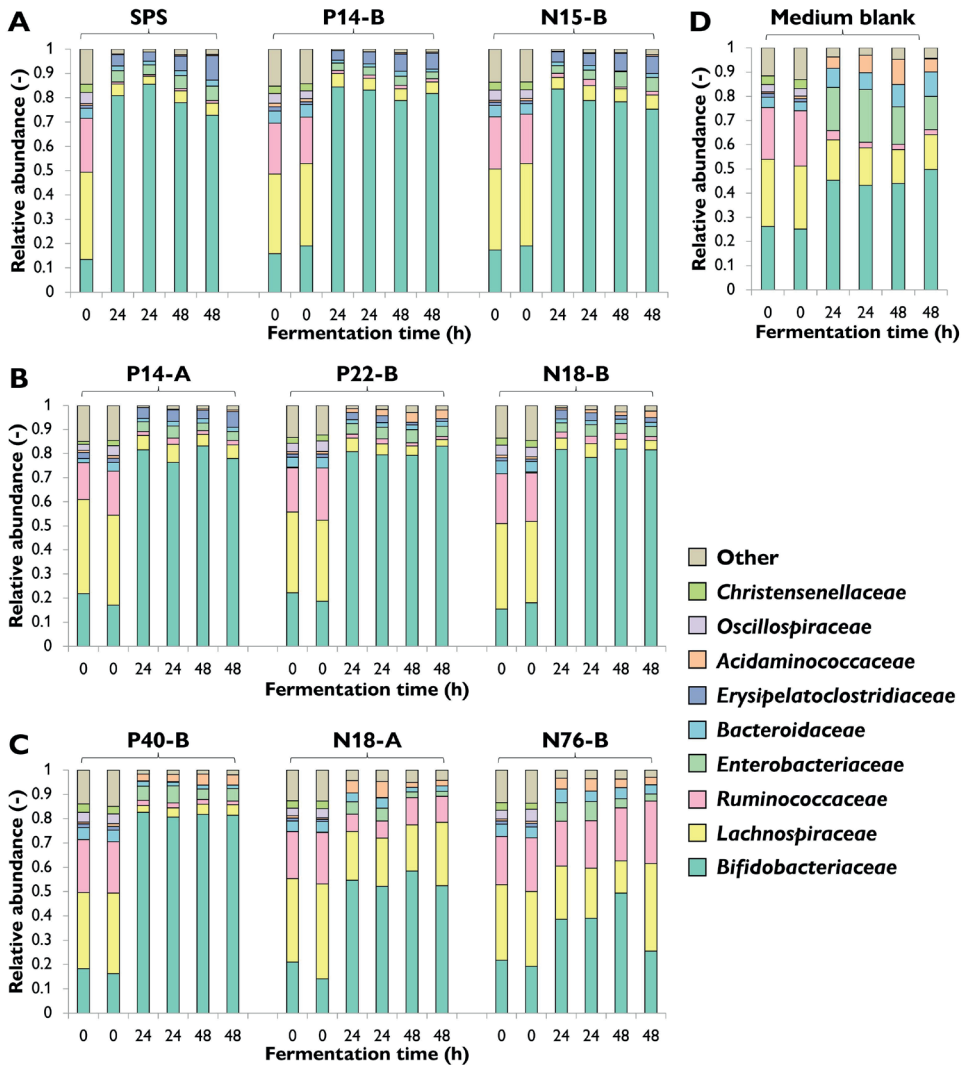


Figure 4.4. Microbiota composition in relative abundance at family level during 48 h of duplicate fermentations of RS-3 preparations by pooled adult faecal inoculum. Figure A, B, C and D represent ≥ 70 % RDS, 35-50 % RDS, ≤ 15 % RDS and medium blank, respectively. Results of both biological duplicates are indicated.

After 24 - 48 h of fermentation of RS-3 preparations containing ≥ 35 % RDS and P40-B, the relative abundance of *Bifidobacteriaceae* increased to ± 80 % (Figure 4.4-A-C). Fermentation of intrinsic RS-3 N18-A and N76-B (≤ 15 % RDS) resulted in more diverse communities with an increase in relative abundance of *Bifidobacteriaceae* to 40-50 %, ± 20 % *Lachnospiraceae* and 5 % (N18-A) or 20 %

(N76-B) *Ruminococcaceae* (Figure 4.4-C). Fermentation of intrinsic RS-3 substrates N18-A and N76-B ($\leq 15\%$ RDS) compared to P40-B ($\leq 15\%$ RDS) and RS-3 preparations $\geq 35\%$ RDS resulted thus clearly in different microbial populations, in line with the results shown in the PCA plots (Figure 4.3). Fermentation of the medium blank, containing a minor amount of mSIEM carbohydrates and no additional carbohydrate source, resulted in an increase in relative abundance of *Bifidobacteriaceae* to 50 %, and showed presence of *Lachnospiraceae*, *Enterobacteriaceae*, *Bacteroidaceae* and *Acidaminococcaceae*.

To further investigate the effect of % RDS on microbiota composition after 48 h of fermentation, we looked at ASVs explaining $\geq 2\%$ of the total relative abundance within an individual sample and together explaining $\geq 70\%$ of the total relative abundance (Figure 4.5). The results show that the increase in relative abundance of *Bifidobacteriaceae* as shown in Figure 4.4 for all samples, can be explained by the presence of primarily two ASVs (Figure 4.5), both showing a co-occurrence pattern across fermentations. *Bifidobacterium* 01 was present in all fermented samples, varying from 19 % for SPS to 57 % for P40-B. *Bifidobacterium* 02 was especially present in fermented samples containing $\geq 35\%$ RDS; the higher the amount of RDS, the higher the relative abundance of *Bifidobacterium* 02 observed. In contrast, fermented intrinsic RS-3 substrates (N18-A and N76-B) did show low ($\leq 4\%$) relative abundance of *Bifidobacterium* 02. Figure 4.5 shows that both *Lachnospiraceae* and *Ruminococcaceae* as present in N18-A and N76-B were each primarily explained by one ASV: *Lachnospiraceae* Family 1 and *Ruminococcus* 2, respectively. Both taxa were hardly present in the fermented medium blank, indicating that these taxa were likely involved in the fermentation of intrinsic RS-3. It is noteworthy that the microbiota composition obtained after fermentation of P40-B, an RS-3 preparation with $\pm 15\%$ RDS and $\pm 10\%$ SDS (Table 4.1), showed no increase in relative abundance of *Lachnospiraceae* Family 1 and *Ruminococcus* 2.

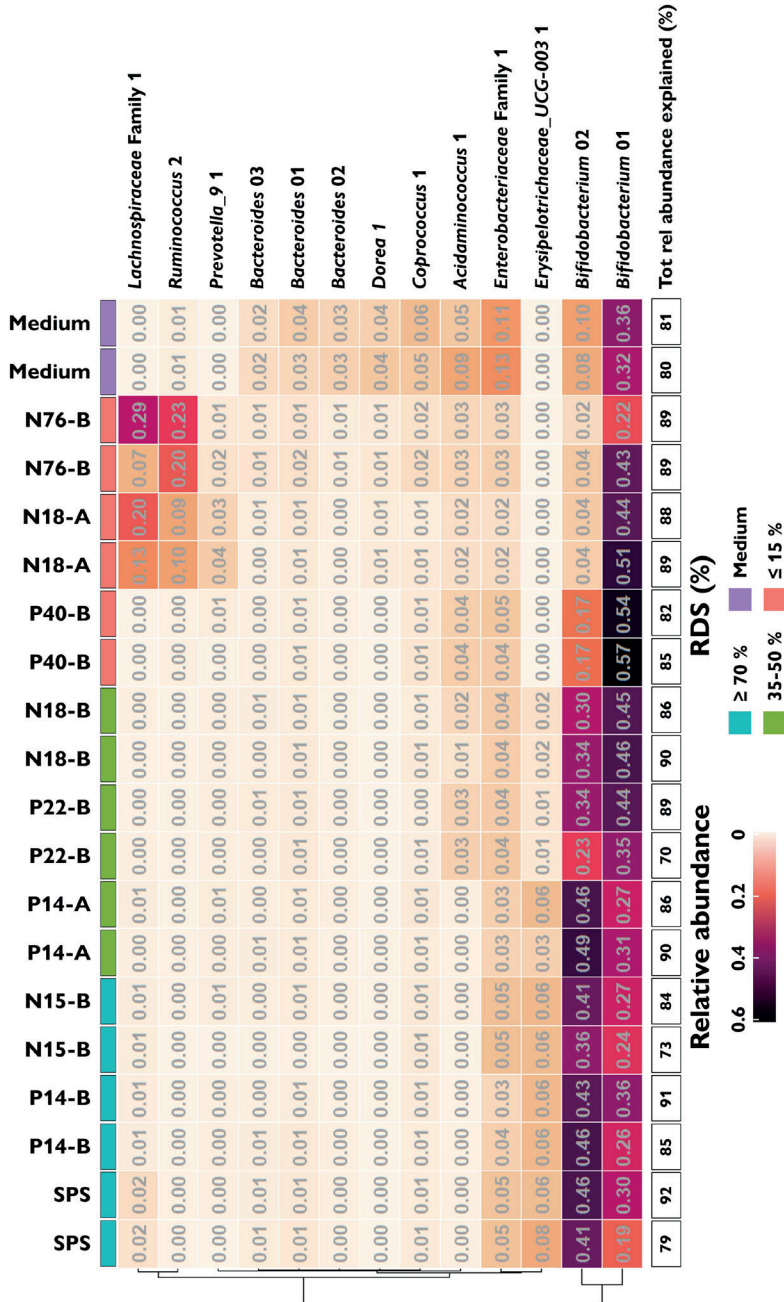


Figure 4.5. Heatmap showing the relative abundance of taxa at ASV level $\geq 2\%$ in at least one individual sample after 48 h of fermentation of RS-3 preparations differing in % RDS and medium blank using pooled adult faecal inoculum. The total relative abundance explained (%) is also provided. The taxa are sorted by hierarchical clustering of Euclidean distances.

3.4. Soluble starch and intrinsic RS-3 differ in fermentability by various microbial populations

In vitro fermentation of RS-3 preparations differing in % RDS by pooled adult faecal inoculum showed differences in starch degradation, SCFA formation and microbiota composition, depending on the amount of digestible starch present. To further investigate whether the fermentability of digestible starch versus intrinsic RS-3 is universal or sample-specific, we incubated digestible starch (SPS) and intrinsic RS-3 (N18-A and N76-B) with individual faecal inocula obtained from 2 adults, 2 weaning 6-month-old infants and from the same 2 infants at 9-10 months old and quantified the SCFAs, lactic and succinic acid produced after 48 h of fermentation (Supplementary table 4.5). Here, it is clearly shown by an increase in SCFAs, lactic and succinic acid compared to the medium blank that digestible starch was fermented by all faecal inocula, whereas intrinsic RS-3 was obviously fermented by the faecal inoculum of only one adult.

4. Discussion

We examined the impact of the presence of a digestible starch fraction during *in vitro* fermentation of RS-3 preparations by pooled adult faecal inoculum. Our results show that the presence of such fraction within RS-3 preparations influenced the fermentation rate, production of SCFAs and microbiota composition. *In vitro* fermentation of RS-3 preparations containing ≥ 25 % total digestible starch within RS-3 preparations resulted in a different SCFA profile and microbiota composition compared to intrinsic RS-3 (≤ 20 % digestible starch). By analysis of the SCFAs produced after fermentation, it was shown that digestible starch was obviously fermentable by an inoculum prepared of a pool of four adult faecal samples and by 6 individual faecal inocula tested. In contrast, as determined by additional SCFAs production compared to the medium blank, intrinsic RS-3 was only fermentable by the pooled faecal inoculum and the inoculum of 1 individual adult faecal sample, suggesting that intrinsic RS-3 requires different microbes to be effectively degraded than digestible starch. Walker et al. (2011) studied the response of a diet high in RS-3 on the faecal microbiota composition of overweight men and showed by quantifying remaining starch in the faeces that some subjects were unable to ferment RS-3, likely since they had low presence of *Ruminococcus*^[52]. In a follow-up study, the ability to degrade RS was restored when faecal inoculum of one of the subjects was supplemented with *R. bromii*^[32], clearly demonstrating the need for specialized microbes to achieve degradation of RS.

Our results indicate that even a small proportion of digestible starch, such as present within P40-B, an RS-3 preparation obtained from debranched waxy potato starch crystallized in a B-type polymorph, could steer *in vitro* fermentation. The presence of the digestible fraction within P40-B caused an initial fast fermentation and increased relative abundance of *Bifidobacterium*, after which fermentation of the resistant fraction was not possible anymore. However, in our previous study, we showed that pre-digested P40-B and pre-digested P22-B (i.e. with an enriched RS fraction) behaved quite similarly to intrinsic RS-3 in terms of fermentation rate, SCFA production and microbiota composition (Chapter 3^[53]). Previously, something similar was shown for the fermentability of isomalto/malto-polysaccharides (IMMPs)^[54], a soluble starch-based dietary fibre, that consist of a long chain of linearly linked α -1,6 glucose residues, connected to a short α -1,4 linked glucose chain^[55, 56]. *In vitro* fermentation of these IMMPs, with and without the presence of the α -1,4 linked fraction showed that the microbiota favoured to ferment the α -1,4 linked fraction (i.e. the digestible fraction) over the α -1,6 linked fraction, while once the α -1,4 linked fraction was depleted, the microbiota could not ferment the α -1,6 linked fraction anymore^[54]. In contrast, when the α -1,4 linked fraction was removed prior to fermentation, the microbiota was able to fully ferment the α -1,6 linked fraction within 24 h^[54]. Also these findings indicate that presence of a small proportion of digestible starch could steer fermentation *in vitro* and thus overrule the true fermentability of the dietary fibre studied. Although we and others^[40, 54] found differences in fermentability of starches depending on the presence of a digestible fraction, such differences were not always found. Warren et al. (2018) studied *in vitro* fermentability of RS-3 preparations from maize and potato starch using pig faecal inoculum and found a similar microbiota composition after fermentation with and without α -amylase pre-treatment^[57]. Nevertheless, the pre-treated RS-3 preparations still contained a digestible fraction, whereas different resistant starches (non RS-3) containing low digestible starch stimulated different microbial populations^[57].

As previously reported, a small proportion of digestible starch may arrive in the colon^[18] and be fermented quickly by several different gut microbes, thereby not affecting faecal microbiota composition^[19]. The resistant fraction will be further fermented by highly specialized gut microbes, that need to be present within the gut microbiome to achieve degradation^[52]. When studying fermentability of resistant starches *in vitro*, fast fermentation of the digestible fraction may cause a drop in pH resulting in lactate accumulation and limiting further cross-feeding^[58], as observed during *in vitro* fermentation of RS-3 preparations having ≥ 35 % RDS (Figure 4.2). This is in agreement with Belenguer et al. (2007)

who showed limited propionate and butyrate production at pH 5.2, while lactate was accumulating^[58]. Fermentation of RS-3 preparations having $\geq 35\%$ RDS resulted in a relative abundance of $\pm 80\%$ *Bifidobacteriaceae* (Figure 4.4, 4.5), which are known to ferment their substrates to acetate and lactate^[59] and of which some species are known starch degraders^[60]. Microbes differ in their pH tolerance with e.g. *Bifidobacterium* being more acidic-pH tolerant than *Ruminococcus bromii*^[61]. Probably due to the acidification observed, specialized microbes able to degrade resistant starch could not grow anymore causing the slowing down of the fermentation rate as observed in Figure 4.1. This clearly illustrates that it is essential to be aware of the presence of a digestible fraction when studying fermentability of resistant starches *in vitro*. Preferably, the digestible fraction should be removed to study the prebiotic potential of resistant starches, especially when a non-pH controlled system is used.

In our study, we quantified the amount of solubilized starch during incubation of RS-3 preparations without inoculum and found especially an increased solubilization for RS-3 preparations containing high amounts of digestible starch (Supplementary table 4.2). Due to their solubility and *in vitro* digestibility, such substrates are not likely to reach the colon *in vivo*. Although useful, quantification of remaining starch during *in vitro* fermentation is often not mentioned in literature. Bui et al. (2020) quantified the total amount of remaining starch during *in vitro* fermentation^[26], but did not separate the insoluble and potentially present soluble fractions. Some starches, such as Novelose® 330, a commercial RS-3 ingredient prepared from high amylose maize starch, have low solubility at room temperature^[62]. Low solubility of substrates might make separation in soluble and insoluble fractions unnecessary, assuming that insoluble starch degradation into soluble oligomers by gut microbes is slower than the uptake and further conversion to SCFAs. RS-3 prepared from debranched starches or low Mw α -1,4 glucans may partially solubilize during incubation^[51], which makes quantification of soluble and insoluble fractions during *in vitro* fermentation necessary.

5. Conclusions

This study investigated the impact of the presence of a digestible starch fraction during *in vitro* fermentation of RS-3 preparations. The results showed that the presence of such digestible fraction, even when only present in a relatively small amount, may steer *in vitro* fermentation and overrule the true fermentability of the resistant starch fraction as would arrive in the colon *in vivo*. In order to evaluate the prebiotic potential of resistant starch, quantification of the remaining soluble and insoluble starch fractions after *in vitro* fermentation is beneficial to draw valid conclusions. Starch should be considered a generic carbohydrate for gut microbiota, fermentable by many different gut microbial populations, whereas this is not the case for intrinsic RS-3. Our study shows that awareness of the presence of a digestible starch fraction during *in vitro* fermentation of resistant starches is essential to evaluate its prebiotic potential. Depending on the research question, the digestible starch fraction within RS (preparations) should be removed, especially when a non-pH controlled system is used.

6. References

1. Brownlee I.A., Gill S., Wilcox M.D., Pearson J.P., Chater P.I. Starch digestion in the upper gastrointestinal tract of humans. *Starch-Starke*. **2018**;70(9-10):1700111.
2. Rios-Covian D., Ruas-Madiedo P., Margolles A., Gueimonde M., de Los Reyes-Gavilan C.G., Salazar N. Intestinal short chain fatty acids and their link with diet and human health. *Frontiers in Microbiology*. **2016**;7:185.
3. Dhital S., Warren F.J., Butterworth P.J., Ellis P.R., Gidley M.J. Mechanisms of starch digestion by alpha-amylase-structural basis for kinetic properties. *Critical Reviews in Food Science and Nutrition*. **2017**;57(5):875-892.
4. Birt D.F., Boylston T., Hendrich S., Jane J.L., Hollis J., Li L., McClelland J., Moore S., Phillips G.J., Rowling M., Schalinske K., Scott M.P., Whitley E.M. Resistant starch: promise for improving human health. *Advances in Nutrition*. **2013**;4(6):587-601.
5. Miao M., Hamaker B.R. Food matrix effects for modulating starch bioavailability. *Annual Review of Food Science and Technology*. **2021**;12:169-191.
6. Rodriguez M.D., Leon A.E., Bustos M.C. Starch digestion in infants: an update of available in vitro methods-a mini review. *Plant Foods for Human Nutrition*. **2022**;77(3):345-352.
7. Englyst H.N., Kingman S.M., Cummings J.H. Classification and measurement of nutritionally important starch fractions. *European Journal of Clinical Nutrition*. **1992**;46 Suppl 2:S33-50.
8. Warren F.J., Zhang B., Waltzer G., Gidley M.J., Dhital S. The interplay of alpha-amylase and amyloglucosidase activities on the digestion of starch in in vitro enzymic systems. *Carbohydrate Polymers*. **2015**;117:192-200.
9. Petropoulou K., Salt L.J., Edwards C.H., Warren F.J., Garcia-Perez I., Chambers E.S., Alshaalan R., Khatib M., Perez-Moral N., Cross K.L., Kellingray L., Stanley R., Koev T., Khimyak Y.Z., Narbad A., Penney N., Serrano-Contreras J.I., Charalambides M.N., Miguens Blanco J., Castro Seoane R., McDonald J.A.K., Marchesi J.R., Holmes E., Godslund I.F., Morrison D.J., Preston T., Domoney C., Wilde P.J., Frost G.S. A natural mutation in *Pisum sativum* L. (pea) alters starch assembly and improves glucose homeostasis in humans. *Nature Food*. **2020**;1:693 - 704.
10. Giuberti G., Gallo A., Moschini M., Masoero F. In vitro production of short-chain fatty acids from resistant starch by pig faecal inoculum. *Animal*. **2013**;7(9):1446-1453.
11. Martens B.M.J., Gerrits W.J.J., Bruininx E., Schols H.A. Amylopectin structure and crystallinity explains variation in digestion kinetics of starches across botanic sources in an in vitro pig model. *Journal of Animal Science and Biotechnology*. **2018**;9:91.
12. Liang D., Li N., Dai X., Zhang H., Hu H. Effects of different types of potato resistant starches on intestinal microbiota and short-chain fatty acids under in vitro fermentation. *International Journal of Food Science & Technology*. **2021**;56:2432-2442.
13. Klostermann C.E., Buwalda P.L., Leemhuis H., de Vos P., Schols H.A., Bitter J.H. Digestibility of resistant starch type 3 is affected by crystal type, molecular weight and molecular weight distribution. *Carbohydrate Polymers*. **2021**;265:118069.
14. Edwards C.H., Grundy M.M., Grassby T., Vasilopoulou D., Frost G.S., Butterworth P.J., Berry S.E., Sanderson J., Ellis P.R. Manipulation of starch bioaccessibility in wheat endosperm to regulate starch digestion, postprandial glycemia, insulinemia, and gut hormone responses: a randomized controlled trial in healthy ileostomy participants. *The American Journal of Clinical Nutrition*. **2015**;102(4):791-800.
15. Ferrer-Mairal A., Penalva-Lapuente C., Iglesia I., Urtasun L., De Miguel-Etayo P., Remon S., Cortes E., Moreno L.A. In vitro and in vivo assessment of the glycemic index of bakery products: influence of the reformulation of ingredients. *European Journal of Nutrition*. **2012**;51(8):947-954.

16. Ren X., Chen J., Molla M.M., Wang C., Diao X., Shen Q. In vitro starch digestibility and in vivo glycemic response of foxtail millet and its products. *Food & Function*. **2016**;7(1):372-379.
17. Wolter A., Hager A.-S., Zannini E., Arendt E.K. In vitro starch digestibility and predicted glycaemic indexes of buckwheat, oat, quinoa, sorghum, teff and commercial gluten-free bread. *Journal of Cereal Science*. **2013**;58(3):431-436.
18. Flint H.J., Scott K.P., Duncan S.H., Louis P., Forano E. Microbial degradation of complex carbohydrates in the gut. *Gut Microbes*. **2012**;3(4).
19. Baxter N.T., Schmidt A.W., Venkataraman A., Kim K.S., Waldron C., Schmidt T.M. Dynamics of human gut microbiota and short-chain fatty acids in response to dietary interventions with three fermentable fibers. *mBio*. **2019**;10(1).
20. Martens B.M.J., Flecher T., de Vries S., Schols H.A., Bruininx E., Gerrits W.J.J. Starch digestion kinetics and mechanisms of hydrolysing enzymes in growing pigs fed processed and native cereal-based diets. *British Journal of Nutrition*. **2019**;121(10):1124-1136.
21. Man J., Yang Y., Zhang C., Zhou X., Dong Y., Zhang F., Liu Q., Wei C. Structural changes of high-amylose rice starch residues following in vitro and in vivo digestion. *Journal of Agricultural & Food Chemistry*. **2012**;60(36):9332-9341.
22. Qin R., Wang J., Chao C., Yu J., Copeland L., Wang S., Wang S. RS5 produced more butyric acid through regulating the microbial community of human gut microbiota. *Journal of Agricultural & Food Chemistry*. **2021**;69(10):3209-3218.
23. Plongbunjong V., Graidist P., Bach Knudsen K.E., Wichienchot S. Starch-based carbohydrates display the bifidogenic and butyrogenic properties in pH-controlled faecal fermentation. *International Journal of Food Science & Technology*. **2017**;52(12):2647-2653.
24. Zhao X.H., Lin Y. Resistant starch prepared from high-amylose maize starch with citric acid hydrolysis and its simulated fermentation in vitro. *European Food Research and Technology*. **2009**;228(6):1015-1021.
25. Liu J., Liu F., Arıoğlu-Tuncil S., Xie Z., Fu X., Huang Q., Zhang B. In vitro fecal fermentation outcomes and microbiota shifts of resistant starch spherulites. *International Journal of Food Science & Technology*. **2022**;57(5).
26. Bui A.T., Williams B.A., Hoedt E.C., Morrison M., Mikkelsen D., Gidley M.J. High amylose wheat starch structures display unique fermentability characteristics, microbial community shifts and enzyme degradation profiles. *Food & Function*. **2020**;11(6):5635-5646.
27. Chang D., Ma Z., Li X., Hu X. Structural modification and dynamic in vitro fermentation profiles of precooked pea starch as affected by different drying methods. *Food & Function*. **2021**;12(24):12706-12723.
28. Minekus M., Smeets-Peters M., Bernalier A., Marol-Bonnin S., Havenaar R., Marteau P., Alric M., Fonty G., Huis in't Veld J.H. A computer-controlled system to simulate conditions of the large intestine with peristaltic mixing, water absorption and absorption of fermentation products. *Applied Microbiology & Biotechnology*. **1999**;53(1):108-114.
29. Baxter N.T., Lesniak N.A., Sinani H., Schloss P.D., Koropatkin N.M. The glucoamylase inhibitor acarbose has a diet-dependent and reversible effect on the murine gut microbiome. *mSphere*. **2019**;4(1).
30. El Kaoutari A., Armougom F., Gordon J.I., Raoult D., Henrissat B. The abundance and variety of carbohydrate-active enzymes in the human gut microbiota. *Nature Reviews Microbiology*. **2013**;11(7):497-504.
31. Drula E., Garron M.L., Dogan S., Lombard V., Henrissat B., Terrapon N. The carbohydrate-active enzyme database: functions and literature. *Nucleic Acids Research*. **2022**;50(D1):D571-D577.
32. Ze X., Duncan S.H., Louis P., Flint H.J. Ruminococcus bromii is a keystone species for the degradation of resistant starch in the human colon. *The ISME Journal*. **2012**;6(8):1535-1543.
33. Cerqueira F.M., Photenhauer A.L., Pollet R.M., Brown H.A., Koropatkin N.M. Starch digestion by gut bacteria: crowdsourcing for carbs. *Trends in Microbiology*. **2020**;28(2):95-108.

34. Photenhauer A.L., Cerqueira F.M., Villafuerte-Vega R., Armbruster K.M., Mareček G., Chen T., Wawrzak Z., Hopkins J.B., Vander Kooi C.W., Janeček S., Ruotolo B.T., Koropatkin N.M. The *Ruminococcus bromii* amylosome protein Sas6 binds single and double helical α -glucan structures in starch. *bioRxiv*. **2022**.
35. Bernabé A.M., Srikaeo K., Schlüter M. Resistant starch content, starch digestibility and the fermentation of some tropical starches in vitro. *Food Digestion*. **2011**;2:37-42.
36. Zhou Z., Cao X., Zhou J.Y.H. Effect of resistant starch structure on short-chain fatty acids production by human gut microbiota fermentation in vitro. *Starch-Starke*. **2013**;65(5-6):509-516.
37. Chang R., Jin Z., Lu H., Qiu L., Sun C., Tian Y. Type III resistant starch prepared from debranched starch: structural changes under simulated saliva, gastric, and intestinal conditions and the impact on short-chain fatty acid production. *Journal of Agricultural and Food Chemistry*. **2021**;69(8):2595-2602.
38. Giuberti G., Gallo A. In vitro evaluation of fermentation characteristics of type 3 resistant starch. *Heliyon*. **2020**;6(1):e03145.
39. Gu F., Li C., Hamaker B.R., Gilbert R.G., Zhang X. Fecal microbiota responses to rice RS3 are specific to amylose molecular structure. *Carbohydrate Polymers*. **2020**;243:116475.
40. Teichmann J., Cockburn D.W. In vitro fermentation reveals changes in butyrate production dependent on resistant starch source and microbiome composition. *Frontiers in Microbiology*. **2021**;12:640253.
41. Kaur A., Rose D.J., Rumpagaporn P., Patterson J.A., Hamaker B.R. In vitro batch fecal fermentation comparison of gas and short-chain fatty acid production using "slowly fermentable" dietary fibers. *Journal of Food Science*. **2011**;76(5):H137-142.
42. Wang S., Zhang B., Chen T., Li C., Fu X., Huang Q. Chemical cross-linking controls in vitro fecal fermentation rate of high-amylose maize starches and regulates gut microbiota composition. *Journal of Agricultural & Food Chemistry*. **2019**;67(49):13728-13736.
43. Endika M.F., Barnett D.J.M., Klostermann C.E., Schols H.A., Arts I.C.W., Penders J., Nauta A., Smidt H., Venema K. Microbiota-dependent influence of prebiotics on the resilience of infant gut microbiota to amoxicillin/clavulanate perturbation in an in vitro colon model *Frontiers in Microbiology*. **2023**;14:1456.
44. Poncheewin W., Hermes G.D.A., van Dam J.C.J., Koehorst J.J., Smidt H., Schaap P.J. NG-Tax 2.0: A semantic framework for high-throughput amplicon analysis. *Frontiers in Genetics*. **2020**;10:1366.
45. Quast C., Pruesse E., Yilmaz P., Gerken J., Schweer T., Yarza P., Peplies J., Glockner F.O. The SILVA ribosomal RNA gene database project: improved data processing and web-based tools. *Nucleic Acids Research*. **2013**;41(Database issue):D590-596.
46. Yilmaz P., Parfrey L.W., Yarza P., Gerken J., Pruesse E., Quast C., Schweer T., Peplies J., Ludwig W., Glockner F.O. The SILVA and "All-species Living Tree Project (LTP)" taxonomic frameworks. *Nucleic Acids Research*. **2014**;42(Database issue):D643-648.
47. McMurdie P.J., Holmes S. phyloseq: an R package for reproducible interactive analysis and graphics of microbiome census data. *PLoS One*. **2013**;8(4):e61217.
48. Lahti R., Shetty S. Microbiome r package: Tools for microbiome analysis in r. 2012-2019 [Available from: <https://github.com/microbiome/microbiome>].
49. Barnett D.J.M., Arts I.C.W., Penders J. microViz: an R package for microbiome data visualization and statistics. *Journal of Open Source Software*. **2021**;6(63):3201.
50. Chen J., Bittinger K., Charlson E.S., Hoffmann C., Lewis J., Wu G.D., Collman R.G., Bushman F.D., Li H. Associating microbiome composition with environmental covariates using generalized UniFrac distances. *Bioinformatics*. **2012**;28(16):2106-2113.
51. Crochet P., Beauxis-Lagrange T., Noel T.R., Parker R., Ring S.G. Starch crystal solubility and starch granule gelatinisation. *Carbohydrate Research*. **2005**;340(1):107-113.

52. Walker A.W., Ince J., Duncan S.H., Webster L.M., Holtrop G., Ze X., Brown D., Stares M.D., Scott P., Bergerat A., Louis P., McIntosh F., Johnstone A.M., Lobley G.E., Parkhill J., Flint H.J. Dominant and diet-responsive groups of bacteria within the human colonic microbiota. *The ISME Journal*. **2011**;5(2):220-230.
53. Klostermann C.E., Endika M.F., Ten Cate E., Buwalda P.L., de Vos P., Bitter J.H., Zoetendal E.G., Schols H.A. Type of intrinsic resistant starch type 3 determines *in vitro* fermentation by pooled adult faecal inoculum. *Accepted for publication in Carbohydrate Polymers*. **2023**.
54. Gu F., Borewicz K., Richter B., van der Zaal P.H., Smidt H., Buwalda P.L., Schols H.A. *In vitro* fermentation behavior of isomalto/malto-polysaccharides using human fecal inoculum indicates prebiotic potential. *Molecular Nutrition & Food Research*. **2018**;62(12):e1800232.
55. Leemhuis H., Dobruchowska J.M., Ebbelaar M., Faber F., Buwalda P.L., van der Maarel M.J., Kamerling J.P., Dijkhuizen L. Isomalto/malto-polysaccharide, a novel soluble dietary fiber made via enzymatic conversion of starch. *Journal of Agricultural and Food Chemistry*. **2014**;62(49):12034-12044.
56. Klostermann C.E., van der Zaal P.H., Schols H.A., Buwalda P.L., Bitter J.H. The influence of alpha-1,4-glucan substrates on 4,6-alpha-d-glucanotransferase reaction dynamics during isomalto/malto-polysaccharide synthesis. *International Journal of Biological Macromolecules*. **2021**;181:762-768.
57. Warren F.J., Fukuma N.M., Mikkelsen D., Flanagan B.M., Williams B.A., Lisle A.T., P O.C., Morrison M., Gidley M.J. Food starch structure impacts gut microbiome composition. *mSphere*. **2018**;3(3).
58. Belenguer A., Duncan S.H., Holtrop G., Anderson S.E., Lobley G.E., Flint H.J. Impact of pH on lactate formation and utilization by human fecal microbial communities. *Applied Environmental Microbiology*. **2007**;73(20):6526-6533.
59. Pokusaeva K., Fitzgerald G.F., van Sinderen D. Carbohydrate metabolism in Bifidobacteria. *Genes & Nutrition*. **2011**;6(3):285-306.
60. Ryan S.M., Fitzgerald G.F., van Sinderen D. Screening for and identification of starch-, amylopectin-, and pullulan-degrading activities in bifidobacterial strains. *Applied Environmental Microbiology*. **2006**;72(8):5289-5296.
61. Duncan S.H., Louis P., Thomson J.M., Flint H.J. The role of pH in determining the species composition of the human colonic microbiota. *Environmental Microbiology*. **2009**;11(8):2112-2122.
62. Shin M., Woo K., Seib P.A. Hot-water solubilities and water sorptions of resistant starches at 25°C. *Cereal Chemistry*. **2003**;80(5):495-633.

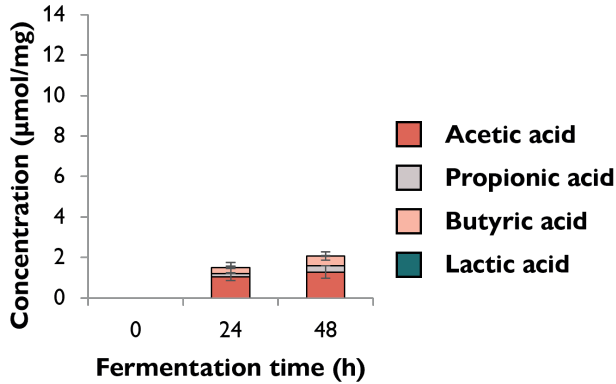
7. Supplementary information

Supplementary table 4.1. Starch recovery (%) in soluble and insoluble fractions of duplicate fermentations of different RS-3 preparations using pooled adult faecal inoculum during 48 h of incubation.

| Sample name | Time 0 h | | Time 24 h | | Time 48 h | |
|-------------|-------------|---------------|-------------|---------------|-------------|---------------|
| | Soluble (%) | Insoluble (%) | Soluble (%) | Insoluble (%) | Soluble (%) | Insoluble (%) |
| P14-A | 8.6 ± 0.0 | 83.6 ± 4.5 | 0.3 ± 0.0 | 13.7 ± 1.1 | 0.2 ± 0.0 | 1.4 ± 0.9 |
| P14-B | 29.7 ± 0.2 | 59.9 ± 1.1 | 0.8 ± 0.0 | 2.1 ± 0.1 | 0.6 ± 0.1 | 1.4 ± 0.1 |
| N15-B | 11.6 ± 5.0 | 76.8 ± 0.6 | 0.4 ± 0.1 | 9.8 ± 0.7 | 0.3 ± 0.2 | 4.0 ± 0.0 |
| P22-B | 13.1 ± 0.0 | 75.1 ± 3.2 | 0.0 ± 0.0 | 37.4 ± 0.8 | 0.3 ± 0.4 | 24.5 ± 1.3 |
| N18-A | 2.9 ± 0.2 | 87.7 ± 11.1 | 0.3 ± 0.0 | 72.5 ± 7.1 | 0.2 ± 0.0 | 30.9 ± 1.5 |
| N18-B | 10.7 ± 0.3 | 91.5 ± 0.5 | 0.0 ± 0.0 | 34.4 ± 2.8 | 0.1 ± 0.1 | 19.0 ± 3.4 |
| P40-B | 8.5 ± 1.6 | 92.1 ± 7.3 | 0.1 ± 0.0 | 69.0 ± 0.4 | 0.2 ± 0.1 | 61.4 ± 0.6 |
| N76-B | 1.2 ± 0.0 | 99.8 ± 4.5 | 0.1 ± 0.0 | 82.7 ± 8.4 | 0.4 ± 0.5 | 36.0 ± 0.3 |
| SPS | 83.3 ± 0.9 | n.a. | 0.6 ± 0.0 | n.a. | 0.3 ± 0.0 | n.a. |

Supplementary table 4.2. Starch recovery (%) in soluble and insoluble fractions of duplicate incubations of RS-3 preparations during 48 h.

| Sample name | Time 0 h | | Time 24 h | | Time 48 h | |
|-------------|--------------|---------------|-------------|---------------|-------------|---------------|
| | Soluble (%) | Insoluble (%) | Soluble (%) | Insoluble (%) | Soluble (%) | Insoluble (%) |
| P14-A | 8.3 ± 0.6 | 85.8 ± 3.9 | 28.2 ± 0.3 | 68.3 ± 3.0 | 28.0 ± 0.1 | 65.6 ± 2.0 |
| P14-B | 29.7 ± 0.1 | 62.8 ± 0.4 | 69.9 ± 1.8 | 27.8 ± 0.7 | 71.9 ± 4.3 | 28.0 ± 2.1 |
| N15-B | 15.1 ± 0.2 | 77.4 ± 1.5 | 32.4 ± 0.6 | 62.4 ± 2.6 | 31.4 ± 1.7 | 61.0 ± 1.5 |
| P22-B | 11.8 ± 0.4 | 86.6 ± 0.3 | 20.2 ± 0.5 | 76.2 ± 6.9 | 20.0 ± 0.8 | 79.3 ± 6.4 |
| N18-A | 1.9 ± 0.0 | 90.8 ± 5.4 | 6.5 ± 0.7 | 83.4 ± 9.1 | 6.7 ± 0.2 | 88.4 ± 2.7 |
| N18-B | 9.6 ± 0.3 | 94.0 ± 6.2 | 20.4 ± 1.4 | 81.9 ± 2.5 | 20.7 ± 0.8 | 79.1 ± 5.5 |
| P40-B | 10.2 ± 0.1 | 88.3 ± 4.2 | 15.3 ± 1.0 | 83.8 ± 5.7 | 15.7 ± 0.2 | 79.7 ± 13.7 |
| N76-B | 0.2 ± 0.0 | 94.7 ± 1.6 | 0.9 ± 0.3 | 101.3 ± 1.0 | 0.5 ± 0.1 | 98.9 ± 3.0 |
| SPS | 100.6 ± 12.0 | n.a. | 99.1 ± 0.9 | n.a. | 100.0 ± 1.3 | n.a. |



Supplementary figure 4.1. SCFA and lactic acid content ($\mu\text{mol}/\text{mg}$ substrate) during 48 h of incubation of the medium blank with pooled adult faecal inoculum. The average of biological duplicates is shown.

Supplementary table 4.3. PERMANOVA of RDS, SDS and RS on Aitchison distances of ASVs, Unweighted UniFrac and Generalized UniFrac distances on microbiota compositions of fermented RS-3 preparations after 24 h of incubation.

| Time 24 h | Variable | R ² | Pr |
|---------------------|----------|----------------|--------|
| Aitchison | RDS | 0.27226 | 1e-04 |
| | SDS | 0.12272 | 0.0288 |
| | RS | 0.1996 | 0.0017 |
| Unweighted UniFrac | RDS | 0.41345 | 1e-04 |
| | SDS | 0.18455 | 0.011 |
| | RS | 0.21107 | 0.0048 |
| Generalized UniFrac | RDS | 0.49388 | 3e-04 |
| | SDS | 0.13972 | 0.0568 |
| | RS | 0.37032 | 0.001 |

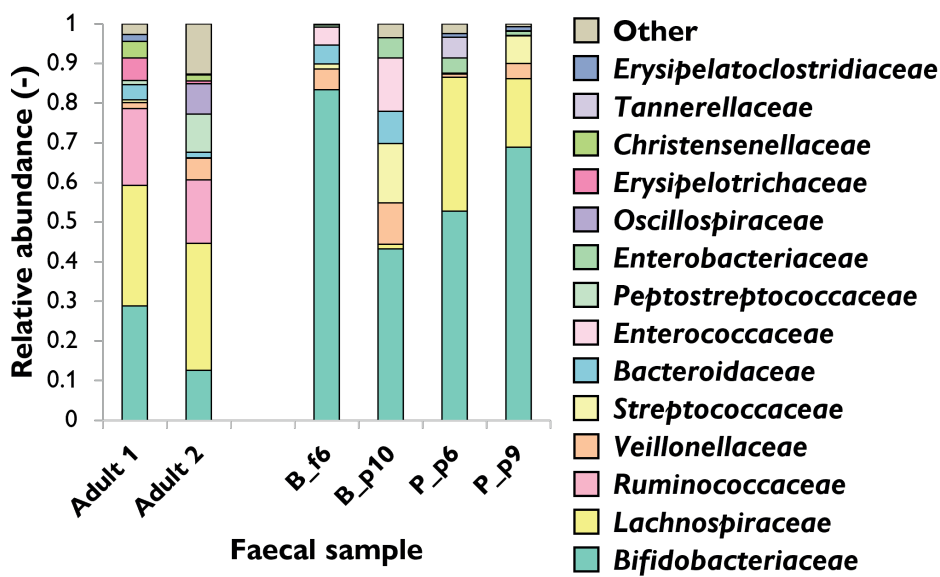
Supplementary table 4.4. PERMANOVA of RDS, SDS and RS on Aitchison distances of ASVs, Unweighted UniFrac and Generalized UniFrac distances on microbiota compositions of fermented RS-3 preparations after 48 h of incubation.

| Time 48 h | Variable | R ² | Pr |
|---------------------|----------|----------------|--------|
| Aitchison | RDS | 0.28846 | 2e-04 |
| | SDS | 0.10182 | 0.0636 |
| | RS | 0.19391 | 0.0018 |
| Unweighted UniFrac | RDS | 0.40323 | 1e-04 |
| | SDS | 0.23791 | 0.0023 |
| | RS | 0.19977 | 0.0059 |
| Generalized UniFrac | RDS | 0.39336 | 7e-04 |
| | SDS | 0.09752 | 0.1143 |
| | RS | 0.33754 | 2e-04 |

Supplementary information 4.1.

In vitro batch fermentations using individual faecal inocula were performed as previously described (Chapter 3) with minor differences. Individual faecal inocula were prepared by diluting faecal slurries to 10 mg/mL in mSIEM. N18-A and N76-B were weighed in duplicate in sterile 5 mL serum bottles (\pm 10 mg dry weight) and 1.8 mL mSIEM and 0.2 mL inoculum were added to reach final substrate concentrations of \pm 5 mg/mL. Also samples with SPS (at \pm 5 mg/mL), substrate blanks (\pm 5 mg/mL, without inoculum) and medium blanks (without additional substrate) were prepared. The serum bottles were capped with butyl rubber stoppers and incubated at 37 °C, 100 rpm for 0 and 48 h.

Sampling was performed as described in section 2.2. SCFAs were analysed according to Klostermann et al. as described in Chapter 3. The microbiota composition of the faecal samples was obtained as described in section 2.5 (Supplementary figure 4.2).



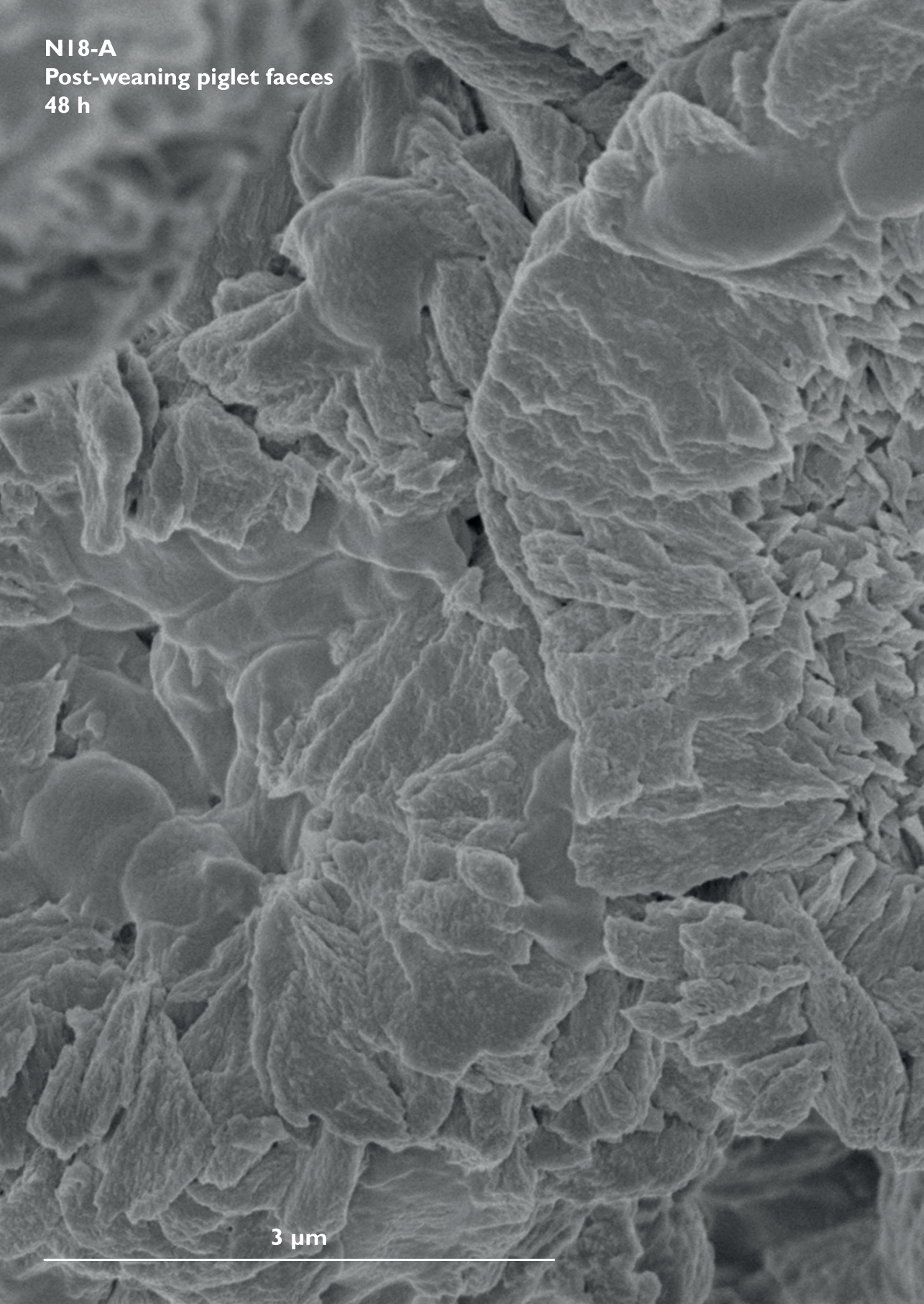
Supplementary figure 4.2. Microbiota composition (relative abundance) at family level of adult and infant faecal samples at 6 and 9-10 months old.

Supplementary table 4.5. SCFAs and other organic acids ($\mu\text{mol}/\text{mg}$ substrate) produced during 48 h of incubation of intrinsic RS-3 N18-A and N76-B, SPS and medium blank with different faecal inocula. The average of biological duplicates is shown.

| Inoculum | Substrate | Total SCFA ($\mu\text{mol}/\text{mg}$) | A : P : B | L ($\mu\text{mol}/\text{mg}$) | S ($\mu\text{mol}/\text{mg}$) |
|----------|--------------|---|-----------------|------------------------------------|------------------------------------|
| A1 | N18-A | 4.1 ± 0.2 | 0.5 : 0.1 : 0.3 | n.d. | 0.5 |
| | N76-B | 3.7 ± 0.4 | 0.5 : 0.2 : 0.3 | n.d. | n.d. |
| | SPS | 8.2 ± 0.1 | 0.9 : 0.0 : 0.1 | 2.9 | 0.4 |
| | Medium blank | 3.0 ± 0.1 | 0.5 : 0.2 : 0.3 | n.d. | n.d. |
| A2 | N18-A | 7.1 ± 1.1 | 0.5 : 0.1 : 0.4 | n.d. | n.d. |
| | N76-B | 6.1 ± 0.1 | 0.6 : 0.1 : 0.3 | 0.1 | n.d. |
| | SPS | 8.1 ± 0.0 | 0.9 : 0.0 : 0.1 | 3.5 | 0.1 |
| | Medium blank | 3.3 ± 0.2 | 0.6 : 0.2 : 0.2 | n.d. | n.d. |
| B_f6 | N18-A | 3.6 ± 0.1 | 0.6 : 0.4 : 0.0 | n.d. | n.d. |
| | N76-B | 1.9 ± 0.2 | 0.8 : 0.2 : 0.0 | n.d. | 0.2 |
| | SPS | 9.4 ± 0.1 | 0.9 : 0.1 : 0.0 | 0.0 | n.d. |
| | Medium blank | 2.0 ± 0.0 | 0.7 : 0.3 : 0.0 | n.d. | n.d. |
| B_p10 | N18-A | 3.4 ± 0.1 | 0.5 : 0.5 : 0.0 | n.d. | n.d. |
| | N76-B | 2.6 ± 0.0 | 0.5 : 0.5 : 0.0 | n.d. | n.d. |
| | SPS | 8.7 ± 0.4 | 0.7 : 0.3 : 0.0 | 0.1 | n.d. |
| | Medium blank | 2.4 ± 0.0 | 0.5 : 0.5 : 0.0 | n.d. | n.d. |
| P_p6 | N18-A | 2.7 ± 0.1 | 0.7 : 0.3 : 0.0 | 0.2 | 0.3 |
| | N76-B | 1.8 ± 0.1 | 0.7 : 0.3 : 0.0 | 0.1 | 0.2 |
| | SPS | 5.6 ± 0.2 | 1.0 : 0.0 : 0.0 | 3.9 | 0.4 |
| | Medium blank | 1.9 ± 0.1 | 0.7 : 0.3 : 0.0 | 0.1 | 0.1 |
| P_p9 | N18-A | 4.5 ± 0.3 | 0.5 : 0.4 : 0.1 | n.d. | n.d. |
| | N76-B | 3.4 ± 0.0 | 0.5 : 0.4 : 0.2 | n.d. | n.d. |
| | SPS | 2.4 ± 0.0 | 1.0 : 0.0 : 0.0 | 7.0 | n.d. |
| | Medium blank | 3.1 ± 0.0 | 0.5 : 0.3 : 0.2 | n.d. | n.d. |

A1 and A2 refer to adult faecal inocula, whereas B_f6 & B_p10 (infant B at 6 and 10 months old) and P_p6 & P_p9 (infant P at 6 and 9 months old) refer to infant faecal inocula. The initial microbiota compositions are shown in Supplementary figure 4.2. Total SCFAs include acetic, propionic and butyric acid, whereas A : P : B give the ratio between these acids. L and S refer to lactic and succinic acid, respectively. n.d. = non-detected.

NI8-A
Post-weaning piglet faeces
48 h



3 μm



Chapter 5

The prebiotic potential of RS-3
preparations for pre- and post-weaning
piglets

Cynthia E. Klostermann, T. Mignon. C. Quadens, Luis Silva Lagos,
Piet L. Buwalda †, Geert Bruggeman, Paul de Vos, Johannes H. Bitter,
Hauke Smidt, Bianca M.J. Martens, Henk A. Schols

Submitted

Abstract

Piglets undergo stress during the weaning period, resulting in an imbalance in gut microbial composition and activity, and potentially post-weaning diarrhoea. Supporting the maturation of the gut microbiota is a strategy to prepare piglets for weaning and prevention of diseases, and could be achieved by providing dietary fibres such as resistant starch in the creep feed. We investigated the prebiotic potential of four well-characterized retrograded starches (RS-3 preparations) for pre- and post-weaning piglets. These RS-3 preparations were fermented *in vitro* using pooled faecal inoculum of 3-week-old (pre-weaning) and 7-week-old (post-weaning) piglets. Depending on the physico-chemical characteristics, RS-3 preparations contain a digestible starch (DS) fraction. RS-3 preparations containing a high amount of DS ($\geq 75\%$) were fully fermented by both faecal inocula within 48 h. Such substrates generated mostly butyrate when fermented by pre-weaning piglet faecal inoculum, whereas mostly propionate was found during fermentation by post-weaning piglet faecal inoculum. Bacterial genera *Prevotella* and *Megasphaera* increased in relative abundance after fermentation by both inocula, whereas *Streptococcus* and *Selenomonas* increased in relative abundance when fermented by pre-weaning or post-weaning piglet faecal inocula, respectively. Highly resistant or so-called intrinsic RS-3 ($\geq 80\%$ RS) was hardly degraded by pre-weaning piglet faecal microbiota, whereas it was slowly fermented by post-weaning piglet faecal microbiota, stimulating specific phylotypes (ASVs) within *Prevotella* and *Roseburia*. This study shows that partially resistant RS-3 preparations might be beneficial dietary fibres for pre-weaning piglets by promoting short-chain fatty acid (SCFA) production, while intrinsic RS-3 was hardly fermentable. Intrinsic RS-3 substrates might be beneficial as a prebiotic for post-weaning piglets by stimulating potential health-beneficial *Prevotella* and *Roseburia*.

1. Introduction

In commercial pig husbandry, piglets are weaned around 3-4 weeks of age^[1], which is much younger than the age of 15-22 weeks in nature^[2]. This acute early weaning causes stress, since piglets are removed from the sow and need to adjust from an easily-digestible liquid milk diet to a more complex plant-based solid feed^[3]. Due to this acute change, feed intake usually decreases, resulting in undernutrition and weight loss^[4]. In addition, weaning could possibly cause a disbalance in gut microbiota composition, which gives the opportunity for enterotoxigenic *E. coli* (ETEC) to proliferate resulting in post-weaning diarrhoea (PWD), dehydration and even death^[5]. PWD can be overcome effectively by the use of antibiotics, such as colistin^[6], or therapeutic doses of zinc oxide^[7]. However, the preventive use of antibiotics and zinc oxide is forbidden in the EU^[8] due to increasing antibiotic resistance and environmental impact. Potential alternatives to decrease the post-weaning stress and potential incidence of PWD comprise nutritional strategies^[9] such as inclusion of probiotics^[10], prebiotics^[11-14], digestive enzyme cocktails^[15] or environmental changes such as enriched housing^[16, 17].

The gut microbiota composition of piglets during the first weeks of life changes dramatically when switching from sow's milk to a plant-based starter diet. Relative abundances of e.g. *Bacteroidaceae* and *Enterobacteriaceae* were shown to decline when changing to a starter diet, whereas *Lactobacillaceae*, *Ruminococcaceae*, *Veillonellaceae* and *Prevotellaceae* were shown to increase^[18]. Healthy 2-weeks post-weaning piglets were shown to have higher relative abundance of *Prevotellaceae*, *Lachnospiraceae*, *Ruminococcaceae* and *Lactobacillaceae*, compared to diarrheic piglets^[19]. Pre-weaning supplementation of prebiotics such as dietary fibres has been shown to support faster maturation of the gut microbiota and to have positive effects on intestinal barrier function, microbiota composition and production of short-chain fatty acids (SCFAs)^[9], compared to piglets not receiving such dietary fibres^[14]. A wide variety of dietary fibres have been tested *in vivo* for their prebiotic pre-weaning potential, such as inulin^[20], fructo-oligosaccharides^[21], galacto-oligosaccharides (GOS)^[22], arabinoxylans^[13] and β -glucans^[12] or a combination of dietary fibres^[14, 23]. It has also been suggested that resistant starch as a prebiotic may reduce the incidence of PWD and associated mortality^[24].

Starch is the main energy source of pigs and, depending on the source, is fully digested in the small intestine of growing pigs^[25] or partially fermented in the colon^[26]. Based on the Englyst *in vitro* digestion model, digestion kinetics can

divide starch into three different fractions: rapidly digestible starch, slowly digestible starch and resistant starch^[27]. Resistant starch is the starch fraction that is expected to escape digestion in the upper gastro-intestinal tract (GIT) and to be subject to fermentation in the ileum or colon of pigs. Although total tract digestibility of starch as measured in faeces is mostly complete in growing pigs, ileal digestibility differs depending on, among others, the botanical source^[28], processing^[25] and the amount of starch supplemented^[29]. Pancreatic α -amylase activity in piglets increases with age^[30] with a 6-fold increase in 3-week-old piglets compared to new-borns^[31]. Subsequently, the amylase activity increases further until similar activities were observed between 10-14 week-old pigs and 6-month-old pigs^[32]. Consequently, starch hydrolysis within the small intestine of piglets 0-10 days post-weaning was lower, compared to starch hydrolysis 14-28 days post-weaning, that was similar to growing pigs and sows^[33]. This indicates that the proportion of digestible starch as defined by Englyst et al. 1992^[27] reaching the ileum or colon depends on the age of the piglet, and consequently a proportion of digestible starch may be subject to fermentation in young piglets.

Different types of resistant starch exist of which RS-1 (starch locked due to a cell-wall matrix, such as in whole cereals) and RS-2 (native granules, such as high-amylose maize starch)^[34] are quite common in the pig diet^[35]. RS-3 refers to retrograded starch^[34] and can be prepared after starch gelatinization and cooling to recrystallize the starch molecules. RS-3 preparations, made by crystallizing α -1,4 glucans in a controlled way, may contain an *in vitro* digestible fraction, depending on physico-chemical parameters such as crystal type, chain length and molecular weight distribution (Chapter 2^[36]). Some RS-3 preparations made from short α -1,4 glucans were shown to be highly resistant to digestion (80-95 % RS)^[36, 37], therefore called “intrinsic RS-3”.

So far, no studies investigated the prebiotic potential of RS-3 (preparations) for pre- and post-weaning piglets. Raw potato starch (RS-2) was shown to increase colonic lactobacilli and *Bacteroides* in nursing piglets^[29], whereas high-amylose maize starches were shown to increase caecal and colonic *Bifidobacterium*^[38] and proximal colonic lactobacilli and bifidobacteria in nursing piglets^[39]. Nevertheless, in an *in vitro* study it was shown that faecal microbiota of pre-weaning piglets fermented raw potato starch (RS-2) poorly, whereas gelatinized potato starch was fermented properly^[40]. In contrast, in the same study, faecal microbiota obtained from adult pigs was able to ferment both raw and gelatinized potato starch^[40]. In adult pigs it was shown that a commercial RS-3 (≥ 50 % RS) was fully fermented in the caecum and positively influenced the

SCFA production and microbiota composition^[41]. However, the fermentability of RS-3 preparations by faecal inoculum of pre- and post-weaning piglets and the effects of such substrates on microbiota composition are unknown.

We investigated the prebiotic potential of four RS-3 preparations varying in physico-chemical characteristics and *in vitro* digestibility for pre- and post-weaning piglets. Faeces of pre- (3-week-old) and post- (7-week-old) weaning piglets was collected, pooled per age and used as inoculum for *in vitro* fermentation. The fermentation kinetics were followed over time by quantifying the remaining soluble and insoluble starch fractions and SCFAs generated. The changes in microbiota composition were evaluated after 16S ribosomal (rRNA) gene sequencing and the starch morphology during *in vitro* fermentation was visualized using scanning electron microscopy.

2. Materials and methods

2.1. Materials

All medium components used for the *in vitro* fermentation were obtained from Tritium Microbiologie (Eindhoven, The Netherlands). L-cysteine-hydrochloride, 2-(N-morpholino)ethanesulfonic acid and soluble potato starch (SPS) were obtained from Sigma-Aldrich (St. Louis, Missouri, USA).

2.1.1. RS-3 preparations

RS-3 preparations were prepared by crystallizing α -1,4 linked glucans obtained from either debranched highly branched potato starch (HBPS, Mw \pm 100 kDa, 8 % branch points, AVEBE (Veendam, The Netherlands)) (P14-A) or enzymatic synthesis (N18-A, N18-B, N32-B) as reported previously (Chapter 2^[36]). The physico-chemical characteristics and *in vitro* digestibility of the RS-3 preparations are summarized in Table 5.1 and discussed in the results section.

2.1.2. Faecal slurry

Faecal samples were obtained from cross-bred piglets (Danbred \times Piétrain; INNSOLPIG, Aalter, Belgium) of mixed gender (gilts and castrated boars) and normal weight that had not been exposed to antibiotics. From the age of 6 days piglets had ad-libitum availability to an experimental solid creep feed (Prestarter diet (Supplementary table 5.1), Nuscience Group, Apeldoorn, The Netherlands) until weaning at 19 \pm 2 days of age. From weaning until 40 days old, the piglets were fed an experimental weaning diet (Supplementary table 5.1, Nuscience

Group) followed by an experimental starter diet (Supplementary table 5.1, Nuscience Group). Pre-weaning faecal samples were collected from healthy piglets (3 castrated boars, 5 gilts) of different sows around 18 ± 2 days of age. Post-weaning piglet faecal samples were collected at 49 ± 2 days (3 castrated boars, 6 gilts). Seven of the piglets sampled pre-weaning were also sampled post-weaning. Faecal samples were obtained by stimulating the rectum with a sterile swap and collecting the faeces directly into a sterile 50 mL container with a filter screw cap (Greiner Bio-One CELLSTAR™ tube, Kremsmünster, Austria). The container was placed inside a pouch with a BD GasPak EZ anaerobe gas generating system with indicator (BD Diagnostics, Sparks, Maryland, USA) and transported cold, using cooling elements, to the laboratory and stored at 4 °C for maximum 24 h until processing. Equal masses of the faeces collected individually from either pre-weaning piglets or post-weaning piglets were pooled under anoxic conditions (4 % H₂, 15 % CO₂, 81 % N₂, Bactron 300, Sheldon Manufacturing, Corneliois, USA) and diluted to 25 % w/v using pre-reduced PBS-glycerol containing 10 % glycerol, 0.5 mg/L resazurin and 0.4 g/L L-cysteine-hydrochloride. The final faecal slurries were snap-frozen using liquid nitrogen and stored at -80 °C prior to use.

2.2. *In vitro* batch fermentation of RS-3 preparations

The culture medium was based on Standard Ileal Efflux Medium (SIEM)^[42] with minor modifications (0.592 g/L carbohydrates) as described in Chapter 3^[43] and referred to as mSIEM. The medium was stored overnight in an anaerobic chamber to remove the head-space oxygen. Culture medium containing 11.11 mg/mL soluble potato starch (mSIEM + SPS) was prepared as described previously (Chapter 3^[43]). Approximately 20 mg (dry weight) of the RS-3 preparations (Table 5.1) were weighed in duplicate in sterile 5 mL serum bottles for each individual sampling time and stored overnight in the anaerobic chamber. For the experiment using pre-weaning piglet faecal inoculum, we incubated P14-A, N18-A, N18-B and SPS, whereas we included one more intrinsic RS-3 (N32-B) using post-weaning faecal inoculum. From preliminary results it was observed that N32-B was hardly fermented by pre-weaning piglet faecal microbiota (data not shown).

In the anaerobic chamber, inoculum was prepared by diluting faecal slurry to 10 mg/mL faeces in mSIEM. An aliquot of 1.8 mL mSIEM or 1.8 mL mSIEM + SPS and 0.2 mL inoculum were added to the serum bottles to reach final substrate concentrations of ± 10 mg/mL. Medium blanks (without additional substrate, including mSIEM carbohydrates) and substrate blanks (without inoculum) were

also prepared. The serum bottles were capped with butyl rubber stoppers and incubated at 39 °C, 100 rpm for 0, 8, 24, 36 and 48 h.

At given time points, samples were collected as described previously (Chapter 3^[43]). Briefly, the serum bottles were decapped and the contents were transferred to Safe-Lock Eppendorf tubes (Eppendorf, Hamburg, Germany) and centrifuged at 4 °C, 20,000 × g for 10 min. The supernatant and pellet were separated and further processed as previously described (Chapter 3^[43]). The supernatant was heated in Safe-Lock Eppendorf tubes to 100 °C, 800 rpm for 10 min in an Eppendorf shaker and stored at -20 °C until analysis. The pellet was snap-frozen using liquid nitrogen and freeze-dried.

2.3. Total starch quantification

Starch was quantified in the supernatants and freeze-dried pellets obtained after *in vitro* fermentation using the Megazyme Total Starch Kit (AA/AMG) (Megazyme, Wicklow, Ireland) according to the company protocol and adjusted for smaller sample sizes as previously described (Chapter 3^[43]). Freeze-dried pellets containing N18-A and N32-B were solubilized using 1.7 M NaOH, whereas freeze-dried pellets containing P14-A and N18-B were solubilized by boiling, as described in Chapter 3^[43]. After appropriate neutralization, dilution and enzymatic hydrolysis of the solubilized starch, free glucose content was analysed using the GOPOD assay kit (Megazyme) as described previously (Chapter 3^[43]).

2.4. Short-chain fatty acids and other organic acids produced by fermentation

SCFAs, branched-chain fatty acids (BCFAs), lactic and succinic acid were analysed as described in Chapter 3^[43] using an HPLC-RI/UV (Dionex, Sunnyvale, California, USA) with an Aminex HPX-87H column (Bio-Rad laboratories Inc, Hercules, California, USA). Standard curves of acetic, propionic, butyric, isobutyric, isovaleric, lactic and succinic acid were prepared (0.05 – 2 mg/mL) for quantification.

2.5. Scanning Electron Microscopy

An aliquot of 20 µL of substrates P14-A, N18-B, N18-A and N32-B fermented by post-weaning piglet faecal inoculum were air-dried on 13 mm filters with 10 µm pores (Merck Isopore™ membrane filter (Merck, Burlington, Massachusetts, USA)) and attached to sample holders containing carbon adhesive tabs (EMS, Washington, USA) and sputter coated with 12 nm tungsten (EM SCD 500, Leica, Vienna, Austria). The samples were analysed using Scanning Electron

Microscopy (SEM) (Magellan 400, FEI, Eindhoven, The Netherlands) at the Wageningen Electron Microscopy Center. SEM images were recorded at an acceleration voltage of 2 kV and 13 pA and magnification of 10,000 and 25,000 times (Through Lens Detector). Unfortunately, we did not have fresh samples available for SEM analysis after *in vitro* fermentation of RS-3 preparations using pre-weaning piglet faecal microbiota.

2.6. Microbiota composition & data analysis

Microbiota composition was analysed in freeze-dried pellets obtained after *in vitro* fermentation, as described previously (Chapter 3^[43]). In short, DNA was isolated and duplicate PCRs were performed using purified DNA and the barcoded primer pair 515F^[44]-806R^[45] to amplify the V4 region of the 16S rRNA gene. The PCR products were pooled in equimolar amounts, together with a no-template control and two mock communities of known composition, and the libraries were sent for Illumina HiSeq2500 (2 × 150 bp) sequencing (Novogene, Cambridge, UK). Raw sequence data of the 16S rRNA gene amplicons was processed using the NG-Tax 2.0 pipeline and default settings^[46]. Taxonomy of each amplicon sequence variant (ASV) was assigned based on the SILVA database version 138.1^[47, 48]. Data was analysed using R version 4.1.0 and the R packages phyloseq version 1.38.0^[49], microbiome version 1.17.42^[50] and microViz version 0.10.1^[51]. Relative abundance of microbial taxa was calculated based on the 16S rRNA gene sequence read counts. Taxa with unidentified genus were renamed to the lowest classified taxonomic rank and sorted based on taxon abundance, e.g. the ASV of *Enterobacteriaceae* Family 01 is the most abundant ASV of unidentified genus of *Enterobacteriaceae*. Principle component analysis (PCA) and principle coordinate analysis (PCoA) were used to visualize the microbiota variation between substrates after centered-log-ratio (CLR) transformation of ASVs or Generalized UniFrac distances (i.e. taking phylogenetic relatedness and relative abundance of taxa into account, with an extra parameter α controlling the weight of abundant lineages^[52]) and Unweighted UniFrac distances (i.e. taking phylogenetic relatedness between taxa, but not relative abundance of taxa into account), respectively. The standard deviation obtained from two biological duplicates is shown in the figures.

3. Results

The *in vitro* fermentability of RS-3 preparations by pooled faecal inoculum obtained from pre-weaning (3-week-old, section 3.1) and post-weaning (7-week-old, section 3.2) piglets was studied. The RS-3 preparations differed in crystal type, Mw (DPn) and Mw distribution (PI) (Table 5.1) and were prepared previously (Chapter 2^[36]). The sample name were named after the physico-chemical characteristics: **P**: polydisperse; $PI \geq 1.3$, **N**: narrow disperse; $PI \leq 1.25$ - **DPn** and **crystal type** A/B. *In vitro* digestion using porcine pancreatin and amyloglucosidase revealed that these RS-3 preparations differed in the proportion of rapidly digestible (RDS), slowly digestible (SDS) and resistant starch content (RS) (Chapter 2^[36]) as defined by Englyst et al., 1992^[27]. P14-A and N18-B both contained a large proportion of *in vitro* digestible starch, whereas N18-A and N32-B were so-called intrinsic RS-3 ($\geq 80\%$ RS). In the *in vitro* fermentation experiments also fully rapidly digestible soluble potato starch (SPS) was taken along as positive control.

Table 5.1. Characteristics of RS-3 preparations and SPS used in this study, data obtained from Klostermann et al. (2021)^[36]

| Sample name | Reported in ref 36 | Crystal type | DPn | PI | RDS (%) | SDS (%) | RS (%) |
|-------------|--------------------|--------------|-----|------|----------------|----------------|----------------|
| SPS | | - | - | - | 100 | - | - |
| P14-A | dHBPS-A | A | 14 | 1.33 | 40.1 \pm 5.4 | 44.7 \pm 8.9 | 15.2 \pm 3.6 |
| N18-A | sG5-A | A | 18 | 1.21 | 12.4 \pm 9.1 | -0.3 \pm 6.1 | 88.0 \pm 3.8 |
| N18-B | sG5-B | B | 18 | 1.21 | 50.7 \pm 0.4 | 23.4 \pm 3.0 | 25.9 \pm 3.3 |
| N32-B | sG20-B | B | 32 | 1.14 | 7.9 \pm 7.6 | -2.8 \pm 5.0 | 94.9 \pm 2.7 |

DPn (number-based degree of polymerization) and PI (polydispersity index) were determined using HPSEC-RI, crystal type was determined using XRD and rapidly digestible starch (RDS), slowly digestible starch (SDS) and resistant starch (RS) were determined after digestion using pancreatin and amyloglucosidase^[36].

3.1. Fermentability of RS-3 preparations by pre-weaning piglet faecal microbiota

RS-3 preparations P14-A, N18-A and N18-B (Table 5.1) and SPS were incubated with pooled faecal inoculum obtained from pre-weaning piglets for 48 h. Starch degradation, SCFAs, BCFAs, lactic and succinic acid were quantified over time, and the changes in microbiota composition were evaluated.

The total starch degradation during *in vitro* fermentation of RS-3 preparations was evaluated (Figure 5.1) by quantifying the remaining soluble and insoluble starch fraction at given time points (Supplementary table 5.2). The total starch recovery at all time-points was normalized for starch recovery found at t0.

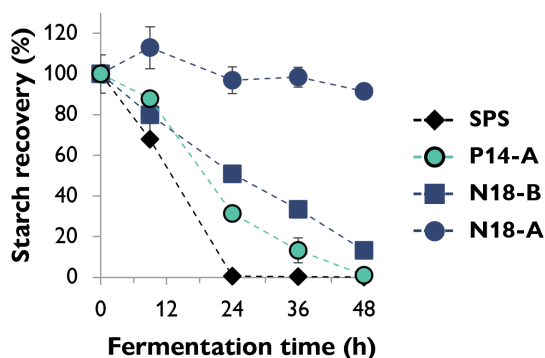


Figure 5.1. Starch recovery after *in vitro* batch fermentation of RS-3 preparations P14-A, N18-B and N18-A and SPS with pooled pre-weaning piglet faecal inoculum for 0, 8, 24, 36 and 48 h. All starch recovery values were normalized for starch recovery found at t0. The average of biological duplicates is shown, the error bars represent the standard deviation and might be smaller than the marker used.

Soluble potato starch (SPS) (0 % RS) was fully degraded by pre-weaning piglet faecal microbiota within 24 h of incubation (Figure 5.1). P14-A (polydisperse DPn 14 α -1,4 glucans in an A-type crystal (± 15 % RS)) and N18-B (narrow disperse DPn 18 α -1,4 glucans in a B-type crystal (± 26 % RS)) were degraded slower than SPS, with 30 % and 50 % starch remaining after 24 h. After 48 h of incubation, P14-A was fully degraded, whereas N18-B was degraded for ± 85 %. Intrinsic RS-3 N18-A, prepared from similar Mw α -1,4 glucans compared to N18-B but crystallized in an A-type crystal (± 88 % RS), was hardly degraded during 48 h of incubation and thus behaved differently than other RS-3 preparations in terms of *in vitro* fermentation by pre-weaning piglet faecal microbiota.

RS-3 preparations incubated without faecal inoculum (Supplementary table 5.3) showed that RS-3 preparations P14-A and N18-B partially solubilized during incubation (33.8 and 21.9 % at 24 h of incubation, respectively). However, after 24 h of incubation with faecal inoculum (Supplementary table 5.2), no soluble starch was detected anymore, indicating that soluble starch was fermented prior to insoluble starch.

After fermentation of RS-3 preparations and SPS by pre-weaning piglet faecal microbiota, the SCFAs, BCFAs, lactic and succinic acid were quantified at the given time points (Figure 5.2).

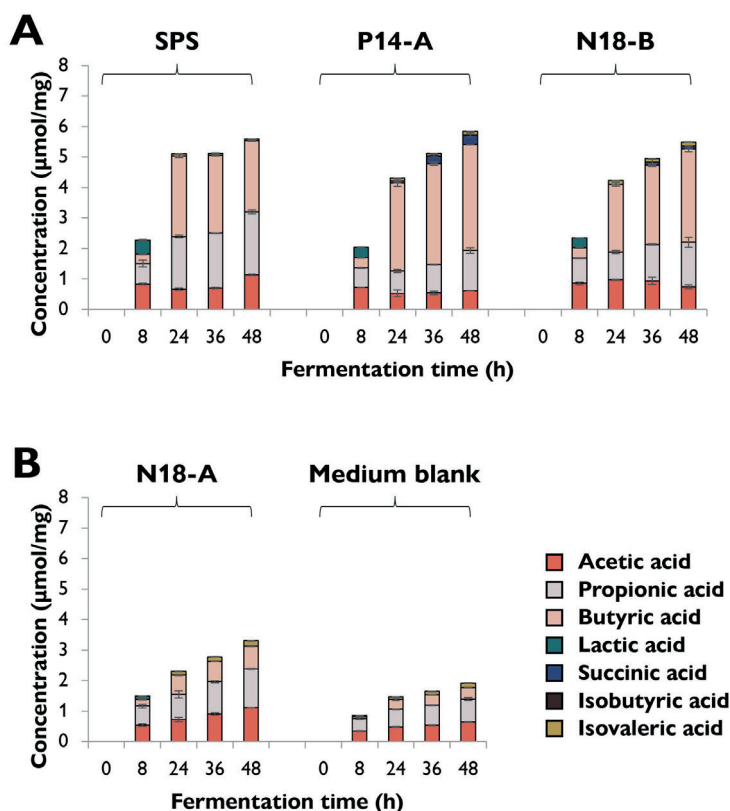


Figure 5.2. Short-chain fatty acids, branched-chain fatty acids, lactic and succinic acid formation (μmol/mg substrate) during 48 h of incubation of RS-3 preparations with pooled pre-weaning piglet faecal inoculum. A: SPS and RS-3 preparations P14-A and N18-B, B: Intrinsic RS-3 N18-A and the medium blank. The average of biological duplicates is shown, the error bars represent the standard deviation.

Fermentation of SPS, P14-A and N18-B generated a similar total amount of acids after 48 h of incubation (5.6, 5.8 and 5.9 μmol/mg substrate, respectively) (Figure 5.2-A), but the rate of acid production differed among the substrates, in line with differences in starch degradation rate (Figure 5.1). Furthermore, the ratio between acetate, propionate and butyrate after fermentation differed, with SPS generating relatively more propionate, whereas P14-A and N18-B generated more butyrate (ratio 1 : 1.8 : 2.1 (SPS), 1 : 2.1 : 5.6 (P14-A) and 1 : 2.0 : 4.1 (N18-B), after 48 h of incubation). Fermentation of P14-A also generated some succinate (0.3 μmol/mg substrate after 48 h), which was not observed after fermentation of N18-B. Intrinsic RS-3 N18-A generated a much lower total amount of acids (3.3 μmol/mg substrate after 48 h) compared to RS-3

preparations containing digestible starch (P14-A, N18-B) (Figure 5.2). Nevertheless, fermentation of N18-A generated slightly more acids than the medium blank (1.9 $\mu\text{mol}/\text{mg}$ substrate after 48 h), indicating some additional fermentation, although no clear starch degradation was demonstrated (Figure 5.1). The ratio of acetate, propionate and butyrate after 48 h of fermentation of N18-A was rather similar to that of the medium blank (N18-A: 1 : 1.1 : 0.7, vs medium blank: 1 : 1.2 : 0.6, after 48 h).

The results across treatments show that pre-weaning piglet faecal microbiota favoured to ferment the RS-3 preparations to relatively high amounts of butyrate. Additionally, minor amounts of isovaleric acid (max 0.18 $\mu\text{mol}/\text{mg}$ for N18-A) were generated, indicating slight proteolytic fermentation^[53].

Beta-diversity of microbiota compositions obtained after 0, 24 and 48 h of *in vitro* fermentation of RS-3 preparations was determined and CLR-PCA, Unweighted UniFrac-PCoA and Generalized UniFrac-PCoA showed that the pooled faeces and t0 clearly differed from the samples taken after 24 and 48 h of incubation (Supplementary figure 5.1), indicating that *in vitro* fermentation selectively stimulated microbial populations, compared to the inoculum. Furthermore, the results show that SPS and RS-3 preparations containing a digestible fraction (P14-A and N18-B) differed from intrinsic RS-3 N18-A and the medium blank (Supplementary figure 5.1). Especially Generalized UniFrac-PCoA showed slightly different microbial communities after 24 or 48 h of fermentation of P14-A and N18-B, indicating that the relative abundance of some taxa, already present at t24, especially changed during the second day of fermentation (Supplementary figure 5.1-C).

The microbiota compositions after 0, 24 and 48 h of *in vitro* fermentation of RS-3 preparations by pre-weaning piglet faecal microbiota were evaluated at family level (Figure 5.3) and the microbiota composition of all samples at t0 appeared similar to the initial microbiota composition of the pooled faeces, and consisted for the largest part of approximately 14 % *Oscillospiraceae*, 13 % *Lactobacillaceae*, 10 % *Clostridiaceae*, 9 % *Bacteroidaceae*, 8 % *Lachnospiraceae* and 7 % *Christensenellaceae*, among others. Fermentation of SPS, P14-A and N18-B by pre-weaning piglet microbiota resulted primarily in an increase in relative abundance of *Streptococcaceae* (± 45 %) (Figure 5.3-A). Fermentation of SPS and P14-A also caused an increase in relative abundance of *Clostridiaceae* (± 10 -20 %) and *Veillonellaceae* (± 20 %). Additionally, a slight increase in *Prevotellaceae* (± 15 %) after 48 h of fermentation of P14-A was observed. Fermentation of N18-B by pre-weaning piglet faecal microbiota caused, next to the increase in relative

abundance of *Streptococcaceae*, also an increase in *Prevotellaceae* ($\pm 30\%$) after 48 h of fermentation. Fermentation of N18-A by pre-weaning piglet microbiota increased the relative abundance of *Enterobacteriaceae*, *Prevotellaceae* and *Bacteroidaceae* (Figure 5.3-B), but did not result in pronounced differences compared to fermentation in the medium blank.

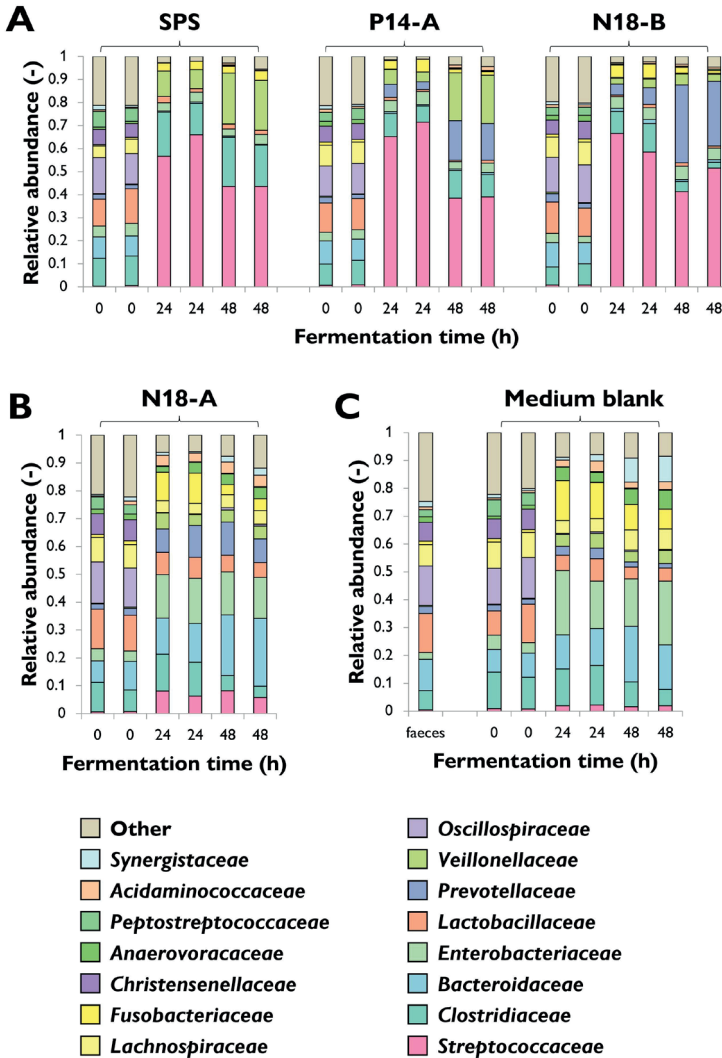


Figure 5.3. Microbiota composition in relative abundance at family level during 48 h of duplicate fermentations of RS-3 preparations by pooled pre-weaning piglet faecal microbiota. A: SPS and RS-3 preparations P14-A and N18-B. B: Intrinsic RS-3 N18-A. C: Medium blank and original pooled faeces. Results of both biological duplicates are indicated. The families shown are most abundantly present and contribute together to $\geq 80\%$ of the total relative abundance within a sample.

To have a deeper insight in microbiota composition after fermentation, we analysed the microbiota composition at ASV level. The heatmap shows the relative abundance of ASVs present $\geq 2\%$ within a fermented sample and in total explaining $\pm 80\%$ of the relative abundance (Supplementary figure 5.2). The relative abundances as shown at family level (Figure 5.3) were primarily explained by one ASV, with especially an increase of *Streptococcus* 01 after fermentation of SPS, P14-A and N18-B. All fermentations caused an increase of *Prevotella*_9 01 compared to the medium blank, except fermentation of SPS, lacking *Prevotella*_9 01 completely. For P14-A and P18-B, this increase in relative abundance of *Prevotella*_9 01 was primarily observed during the last 24 h of incubation. Fermentation of SPS and P14-A also caused an increase in relative abundance of *Megasphaera* 01 (*Veillonellaceae*), primarily during the last 24 h of incubation.

3.2. Fermentability of RS-3 preparations by post-weaning piglet faecal microbiota

The same RS-3 preparations were also incubated with pooled faecal inoculum obtained from post-weaning piglets, while one additional intrinsic RS-3 was included (N32-B; Table 5.1).

The total starch degradation was evaluated by quantifying the remaining soluble and insoluble starch fraction at given time points during incubation with (Figure 5.4; Supplementary table 5.4) and without faecal inoculum (Supplementary table 5.5).

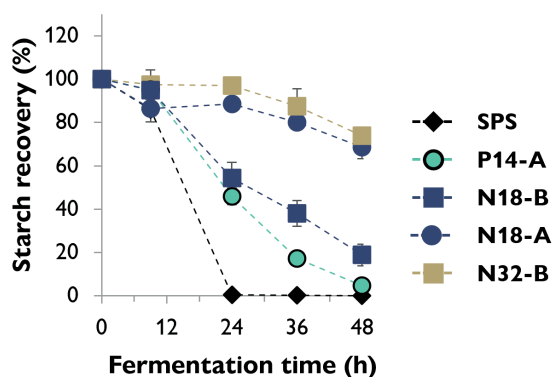


Figure 5.4. Starch recovery during *in vitro* batch fermentation of RS-3 preparations and soluble starch with pooled post-weaning piglet faecal inoculum for 0, 8, 24, 36 and 48 h. All starch recovery values were normalized for starch recovery found at t0. The average of biological duplicates is shown, the error bars represent the standard deviation and might be smaller than the marker used.

Complete degradation of SPS occurred during the first 24 h of incubation with post-weaning piglet faecal microbiota (Figure 5.4), similar to results obtained for pre-weaning piglet faecal microbiota (Figure 5.1). Approximately 50 % of P14-A and N18-B were degraded within the first 24 h of incubation, after which P14-A was fully degraded, whereas N18-B was degraded for ± 80 % during the second 24 h of incubation (Figure 5.4). P14-A and N18-B were degraded similarly by post- and pre-weaning piglet faecal microbiota (Figure 5.4 vs Figure 5.1), with a slightly higher degradation rate of P14-A compared to N18-B by both faecal inocula. In contrast, post-weaning piglet faecal microbiota degraded intrinsic RS-3 N18-A especially during the last 24 h of incubation for ± 32 % (Figure 5.4), whereas no clear degradation was observed by pre-weaning piglet faecal microbiota (Figure 5.1). We also incubated another intrinsic RS-3 substrate, N32-B with a B-type crystal, using post-weaning piglet faecal microbiota, and also here we found clear degradation of the substrate for ± 25 % during 48 h of incubation (Figure 5.4). Although post-weaning faecal microbiota clearly degraded intrinsic RS-3, the degradation rate was much lower compared to more digestible starches SPS, P14-A and N18-B.

The SCFAs, BCFAs, lactic and succinic acid were quantified for different time points (Figure 5.5). Fermentation of SPS by post-weaning piglet faecal microbiota generated acetate, propionate and butyrate to similar levels after 24 and 48 h of incubation, (6.1 $\mu\text{mol}/\text{mg}$ substrate) (Figure 5.5-A), with a ratio of acetate, propionate and butyrate of 1 : 1.8 : 1.5 after 48 h. Fermentation of P14-A and N18-B was more gradual with total acids of 4.5 and 6.1 $\mu\text{mol}/\text{mg}$ substrate (P14-A) and 4.1 and 7.3 $\mu\text{mol}/\text{mg}$ substrate (N18-B) after 24 and 48 h of fermentation and differed in acetate, propionate and butyrate ratio (1 : 1.9 : 1.3 for P14-A and 1 : 1.8 : 0.5 for N18-B, at 48 h). N18-B thus generated more propionate, compared to SPS and P14-A. Fermentation of these substrates by pre-weaning piglet faecal microbiota caused similar total amounts of acids formed, but generally generated more butyrate.

Fermentation of intrinsic RS-3 substrates N18-A and N32-B generated lower amounts of acids (± 3.5 and $3.3 \mu\text{mol}/\text{mg}$ substrate after 48 h, respectively) (Figure 5.5-B), compared to partially digestible RS-3 substrates, in line with the starch recovery (Figure 5.4). Nevertheless, these intrinsic RS-3 substrates generated slightly more acids compared to fermentation of the medium blank (2.0 $\mu\text{mol}/\text{mg}$), with an acetate, propionate and butyrate ratio of 1 : 1 : 0.5 (N18-A), 1 : 0.9 : 0.5 (N32-B) and 1 : 0.5 : 0.4 (medium blank) after 48 h of incubation. Comparing *in vitro* fermentation of intrinsic RS-3 N18-A by pre- vs post-weaning piglet faecal microbiota (Figure 5.2-B vs Figure 5.5-B), a similar total acid level

(3.3 vs 3.5 $\mu\text{mol}/\text{mg}$ substrate) with approximately similar ratios between SCFA, indicating a rather similar microbial activity. Nevertheless, intrinsic RS-3 was clearly degraded more by post- compared to pre-weaning piglet faecal microbiota (Figure 5.1 vs Figure 5.4).

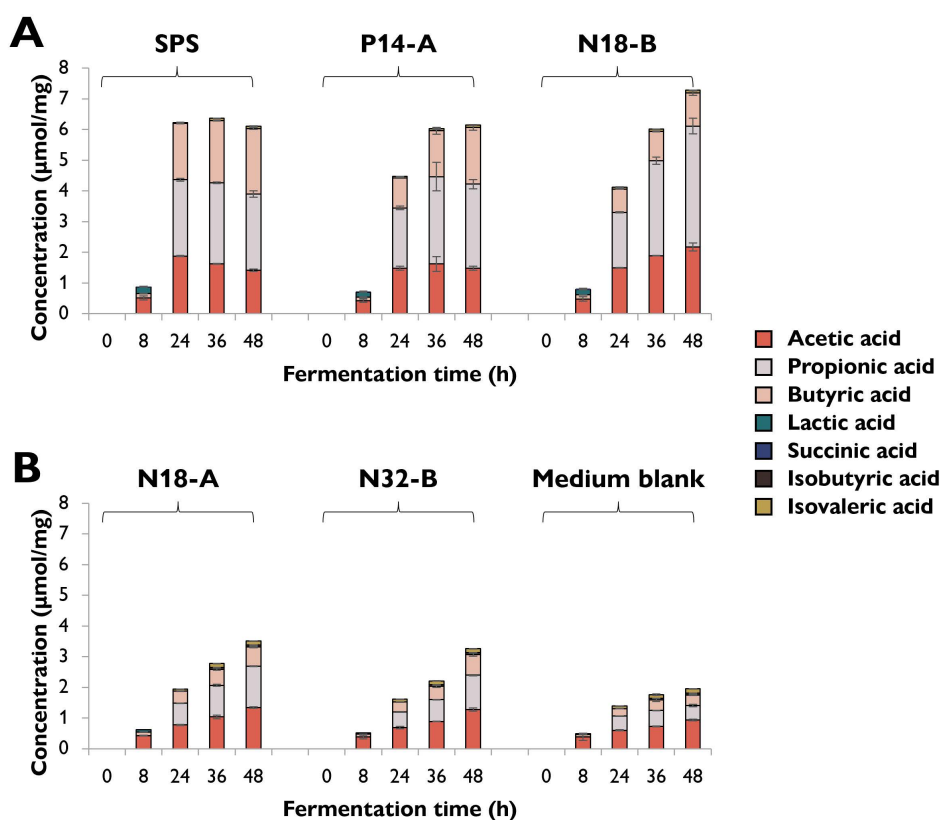


Figure 5.5. Short-chain fatty acid, branched-chain fatty acid, lactic and succinic acid formation ($\mu\text{mol}/\text{mg}$ substrate) during 48 h of incubation of RS-3 preparations with pooled post-weaning piglet faecal inoculum. A: RS-3 preparations containing > 70 % digestible starch. B: Intrinsic RS-3 and the medium blank. The average of biological duplicates is shown, the error bars represent the standard deviation.

The microbiota composition obtained after 0, 24 and 48 h of *in vitro* fermentation of RS-3 preparations by post-weaning-piglet faecal microbiota was visualized using PCA of CLR-transformed relative abundances of ASVs and PCoA using Unweighted and Generalized UniFrac distances (Supplementary figure 5.3) and indicated that the pooled faeces and t0 clearly differed from the samples taken

after 24 and 48 h of incubation. Distinction between substrates based on β -diversity was much less clear for post-weaning piglet faecal microbiota, compared to pre-weaning piglet faecal microbiota (Supplementary figure 5.1). Unweighted UniFrac-PCoA showed clear clustering of SPS, P14-A and N18-B both after 24 and 48 h of fermentation (Supplementary figure 5.3-B), indicating similar presence of unique taxa among these substrates at both time-points. Interestingly, Unweighted UniFrac distances of fermented intrinsic RS-3 N18-A, N32-B and medium blank differed between 24 and 48 h, indicating different unique taxa among these substrates between 24 and 48 h of incubation.

The microbiota compositions after 0, 24 and 48 h of *in vitro* fermentation of RS-3 preparations by post-weaning piglet faecal microbiota were evaluated at family level (Figure 5.6) and the microbiota composition of all samples at t0 appeared similar to the initial microbiota composition of the pooled faeces and consisted of approximately 21 % *Clostridiaceae*, 18 % *Prevotellaceae*, 9 % *Lactobacillaceae*, 7 % *Lachnospiraceae*, 6 % *Ruminococcaceae* and 5 % *Oscillospiraceae*, among others. Fermentation of SPS caused an increase in relative abundance to \pm 30-40 % *Prevotellaceae*, \pm 10 % *Selenomonadaceae* and \pm 10-20 % *Veillonellaceae* (Figure 5.6-A). Fermentation of P14-A and N18-B resulted in rather similar microbiota compositions with 40 % (P14-A) or \pm 20-30 % (N18-B) *Selenomonadaceae*, and \pm 20 % (P14-A) or 40 % (N18-B) *Prevotellaceae* after 48 h of fermentation. Fermentation of intrinsic RS-3 N18-A and N32-B by pooled post-weaning piglet faecal microbiota resulted in a slightly different microbiota composition compared to the medium blank (Figure 5.6-B, C). Especially after 48 h of fermentation, an increase in relative abundance of *Prevotellaceae* to \pm 45 % (\pm 23 % in medium blank) and *Lachnospiraceae* to \pm 10-15 % (\pm 4 % in medium blank) was observed for intrinsic RS-3 N18-A and N32-B. Such pronounced increase in *Lachnospiraceae* was not observed after fermentation of starches containing a digestible starch fraction SPS, P14-A and N18-B (Figure 5.6-A).

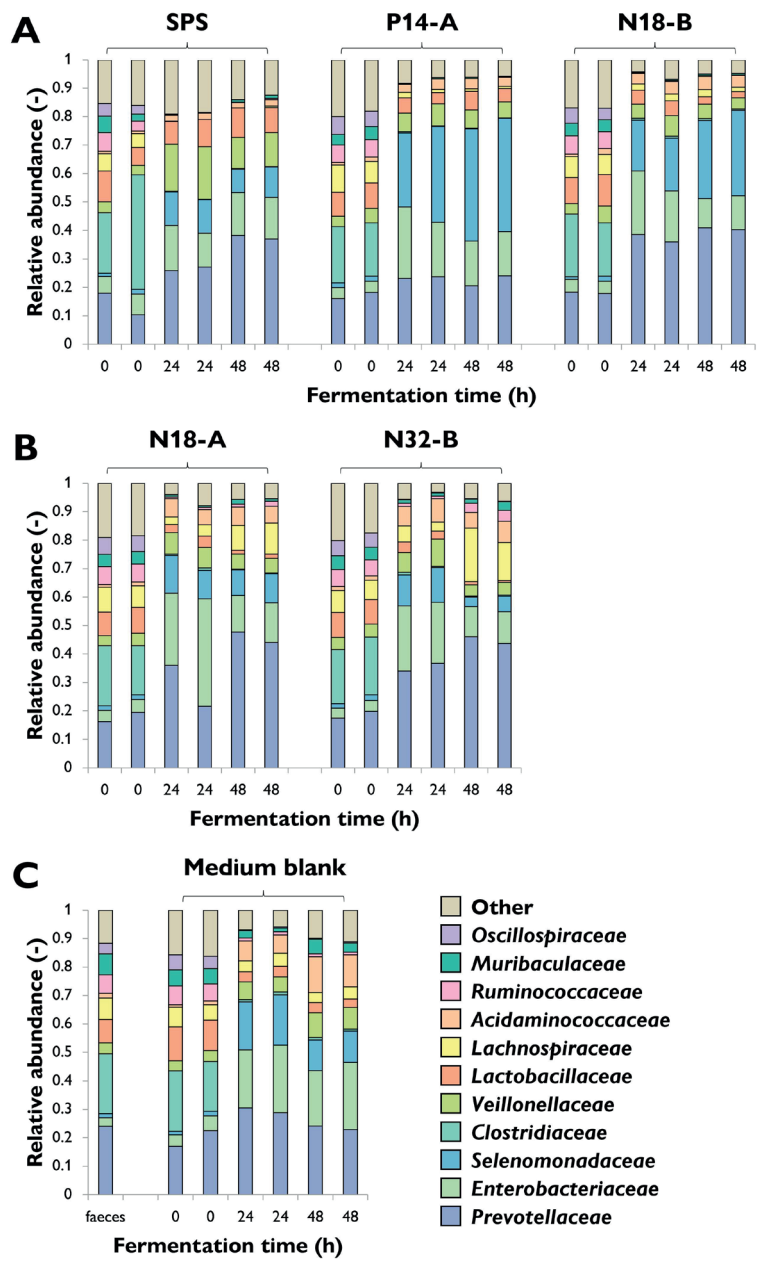


Figure 5.6. Microbiota composition in relative abundance at family level during 48 h of duplicate fermentations of RS-3 preparations by pooled post-weaning piglet faecal microbiota. A: RS-3 preparations containing > 70 % digestible starch. B: Intrinsic RS-3. C: Initial pooled faeces and the medium blank. Results of both biological duplicates are indicated. The families shown are most abundantly present and contribute together to ≥ 80 % of the total relative abundance within a sample.

To further investigate the differences in microbiota composition after 24 and 48 h of fermentation of RS-3 preparations by pooled post-weaning piglet faecal microbiota, we analysed the microbiota composition at ASV level, showing taxa contributing $\geq 2\%$ of the total relative abundance within a sample (Supplementary figure 5.4). The increase in relative abundance of *Selenomonadaceae* as shown for fermented P14-A and N18-B (Figure 5.6-A) was primarily explained by ASV *Selenomonas* 1. *Prevotellaceae* consisted of at least five different ASVs. *Prevotella*_9 01 was present in all fermented RS-3 substrates, whereas *Prevotella*_7 01 increased especially in relative abundance during the last 24 h of fermentation of SPS. Especially *Prevotella*_9 03 increased in relative abundance after 48 h of fermentation of intrinsic RS-3 N18-A and N32-B. Within the same timeframe also an increase in relative abundance of *Roseburia* 1 (*Lachnospiraceae*) was found for N18-A and N32-B.

3.3. Visual inspection of starch degradation by post-weaning piglet faecal microbiota

As we observed pronounced degradation of RS-3 preparations by post-weaning piglet faecal microbiota, we conducted SEM analysis to provide some preliminary insights in the degradation approach of insoluble starch by gut microbiota (Figure 5.7).

The SEM image of the initial P14-A substrate shows that P14-A consisted of quite roughly clustered particles (Figure 5.7-A1) of around 10-15 μm . After 24 h of fermentation, the particles were covered by a biofilm (oval) with bacteria attached to the substrate (white arrows) (Figure 5.7-A2, A3). The SEM image of the initial N18-B substrate shows that N18-B consisted of regularly shaped spheres of around 3 μm (Figure 5.7-B1). After 24 h of fermentation, holes appeared within those spheres (black arrow) and additionally, bacterial cells were attached to the N18-B spheres (white arrow) (Figure 5.7-B2, B3). The SEM image of the initial N18-A substrate shows that N18-A consisted of elongated particles that were clustered together in spheres (Figure 5.7-C1). After 48 h of fermentation, these elongated crystals could be observed much better (Figure 5.7-C2), probably due to degradation of an easier-accessible fraction. In addition, some bacteria were recognizable attached to the N18-A substrate (white arrow) (Figure 5.7-C3). The SEM image of the initial N32-B substrate shows that N32-B consisted of quite regularly shaped spheres of around 3-7 μm (Figure 5.7-D1). After 48 h of fermentation some holes within the substrate appeared (black arrow). In addition, the surface of the N32-B spheres was rougher when

compared to the initial substrate and some attached bacteria could be observed (white arrow) (Figure 5.7-D2, D3).

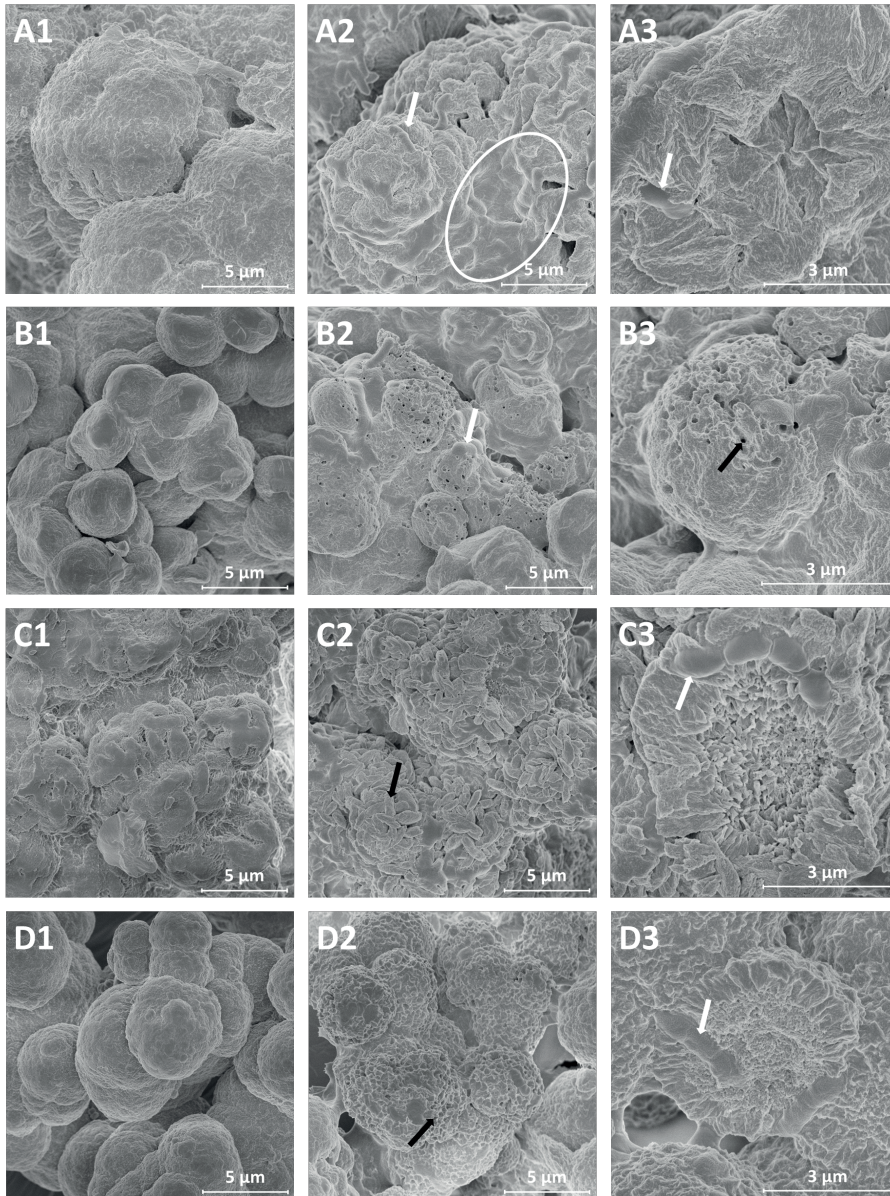


Figure 5.7. Scanning Electron Microscope images of RS-3 preparations fermented by post-weaning piglet faecal microbiota. Figure A, B, C and D refer to P14-A, N18-B, N18-A and N32-B, respectively. Image 1 refers to the initial substrate, whereas image 2 and 3 refer to the substrate after 24 h of incubation (P14-A, N18-B) or 48 h of incubation (N18-A, N32-B). White arrows point towards bacteria, black arrows point towards specific starch structures, the white oval highlights the presence of biofilm.

4. Discussion

Weaning is a stressful period for piglets, often causing a disbalance in gut microbiota composition^[1], which might result in post-weaning diarrhoea. By *in vitro* fermentation of RS-3 preparations differing in crystal type, α -1,4 glucan chain length and resistant starch content, we evaluated the prebiotic potential of such substrates for pre- and post-weaning piglets. Four RS-3 preparations (P14-A, N18-B, N18-A and N32-B) were incubated with inocula obtained by pooling faeces of pre- or post-weaning piglets and subsequently, starch degradation, organic acid production and changes in microbiota composition upon fermentation were analysed. It should be noted that the pre-weaning piglets already had ad-libitum availability to creep-feed from 6 days of age, which could have influenced the microbiota composition of the faeces used as inoculum.

RS-3 preparations P14-A and N18-B contained a large digestible starch fraction (Table 5.1, Chapter 2^[36]). Although the digestible starch is subjected to digestion in the small intestine, such substrates may partially be subject to fermentation in pre-weaning piglets due to lower amylase activities in such piglets^[30]. In addition, Wang et al. (2019) found high relative abundance of starch-utilizing enzymes being encoded within the metagenome of faecal microbiota of even up to 4 weeks post-weaning piglets consuming wheat starch and suggested that digestible starch is a major carbohydrate source for colonic microbiota^[54]. In contrast to digestible starches which only conditionally reach the colon, starches that contain a high amount of RS ($\geq 80\%$)^[36] will certainly transit to the colon largely intact. However, such starches require microbes for degradation that express amylases with carbohydrate binding modules (CBMs), able to bind to the insoluble substrate^[55]. That such microbes should be targeted and specialized to degrade undigestible starches was demonstrated in our study where N18-A ($\pm 88\%$ RS) was hardly fermentable by pooled pre-weaning piglet gut microbiota, simply because the appropriate bacteria were not present at noticeable abundances. This was similar to a previous *in vitro* study showing that raw potato starch (RS-2) was poorly fermented by pre-weaning piglet faecal microbiota^[40]. Indeed, it has been shown that among others, genes encoding for starch degrading enzymes were lower in the bacterial metagenome of nursing compared to weaned piglets^[18]. Together this suggests that highly RS-containing substrates might not be beneficial for pre-weaning piglets, simply because the specialized starch-degrading microbes are not (yet) present at high abundances. If intrinsic RS-3 is eventually fermentable by pre-weaning piglet faecal microbiota using elongated fermentation time, requires further investigation.

For pre-weaning piglets, more easily fermentable dietary fibres, such as GOS^[56] or partially digestible starch might be more beneficial, let aside that such starch is not fully hydrolysed in time by pancreatic amylase in the upper GIT. Previously, it has been shown that waxy maize and normal maize starch, varying in amylose to amylopectin ratio, differently influenced the ileal and caecal gut microbiota composition of growing pigs^[57], indicating that such digestible starch is subject to fermentation, even in growing pigs.

To the best of our knowledge, not many studies investigated the *in vitro* fermentability of dietary fibres using pre-weaning piglet faecal microbiota. Previously, it has been shown that wheat starch (containing digestible starch) was fermented slower by faecal microbes of 4-week-old pre-weaning piglets, compared to more readily fermentable dietary fibres inulin and lactulose^[58]. Here, we showed that pre-weaning piglet faecal microbiota fermented partially resistant starch slower than purely digestible starch, but still fermentation was almost complete within 48 h of incubation (Figure 5.1). The observed increase in relative abundance in *Streptococcaceae* in our fermentation digesta (Figure 5.3-A) was also found previously, when cooked digestible wheat starch was fermented using faecal inoculum of growing pigs^[59]. In the same study, fermentation of granular wheat starch did not result in an increase in relative abundance of *Streptococcaceae*^[59], suggesting that only easily fermentable starch was targeted by these bacteria. Indeed, some *Streptococcus* species are known to efficiently degrade soluble and raw maize starch and ferment it to lactate in mono-culture^[60]. *Streptococcus* could thus have contributed to the digestible starch degradation by pre-weaning piglet faecal microbiota in our study, producing lactate that could have been further metabolized to acetate, propionate and butyrate. Fermentation of partially digestible starch by pre-weaning piglet faecal microbiota in our study yielded primarily butyrate, together with an increase in relative abundance of *Megasphaera*. *Megasphaera* produces acetate, propionate and butyrate directly from lactate^[61] and is additionally able to produce butyrate via the 4-aminobutyrate pathway^[62], and could therefore have contributed to the SCFA production and composition found. Fermentation of partially resistant P14-A and N18-B by pre-weaning piglet faecal microbiota also resulted in an increased relative abundance of *Prevotella*, primarily after 48 h of fermentation. *Prevotella* harbours species with many carbohydrate degrading enzymes encoded on polysaccharide utilization loci (PUL)^[63, 64]. *Prevotella* species, such as *P. copri*, are able to produce succinate and acetate, but lack the ability to produce propionate^[65]. Since *Prevotella_9 01* only increased in relative abundance after the soluble starch was fully fermented by pre-weaning piglet faecal inoculum, it might be responsible for the

degradation of the insoluble and resistant fraction of P14-A and N18-B preparations. Nevertheless, such abilities have not been described for *Prevotella* species before. In contrast, a recent study showed that specifically *P. copri* strains were only slightly growing on soluble starch, much worse than known starch degrading members of *Bacteroidetes* species *B. ovatus* and *B. thetaiotaomicron*^[66]. Partially resistant starches such as P14-A and N18-B are likely degradable by many different gut microbes and therefore it is hard to predict the prebiotic potential of such substrates for pre-weaning piglets. Nevertheless, these partially resistant starches surely behaved like regular, beneficial dietary fibres for pre-weaning piglets, by promoting SCFA production.

As indicated, and depending on the digestion kinetics, partially resistant starches such as P14-A and N18-B may be subject to ileal or colonic fermentation in post-weaning piglets. Both RS-3 preparations were fermented slower than purely digestible starch SPS by pre- and post-weaning piglet faecal inocula, both stimulating individually different microbial populations in pre- vs post-weaning faecal inocula. This indeed indicates that many different gut microbes can ferment substrates like P14-A and N18-B.

Intrinsic RS-3 substrates N18-A and N32-B are different from partially resistant RS-3 preparations P14-A and N18-B, since they are > 85 % undigestible by pancreatic α -amylase (Chapter 2^[36]). The overall gut microbiome possesses more different α -amylases^[67, 68], compared to the number of host α -amylases and therefore intrinsic RS-3 might be degradable by specific bacterial α -amylases, whereas not degradable by host α -amylases. Previously, we have shown that intrinsic RS-3 is much slower fermented than digestible starch (Chapter 3^[43] and Chapter 4^[69]) and by distinct microbial populations.

Intrinsic RS-3 substrates N18-A and N32-B were slowly fermented by post-weaning piglet faecal microbiota, and starch degradation was especially observed between 24 – 48 h of incubation (Figure 5.4), similarly to what we found using human adult faecal inoculum (Chapter 3^[43]). After 48 h of fermentation, a pronounced increase in relative abundance of *Prevotella*_9 03 and *Roseburia* 1 to \pm 5 – 15 % was found, which were almost absent after 24 h. *Roseburia* 1 was fully absent after fermentation of all other starches and the medium blank, whereas *Prevotella*_9 03 was present at a relative abundance of 0 – 1 %. This indicates that intrinsic RS-3 specifically stimulated *Prevotella*_9 03 and *Roseburia* 1 using post-weaning piglet faecal inoculum. Other bacteria such as *Bifidobacterium adolescentis* and *Ruminococcus bromii* that harbour specialized RS-degrading machineries, are considered to be primary RS-degraders^[70]. However, we did not observe ASVs similar to *R. bromii* and *B. adolescentis*,

indicating that also other gut microbes such as *Prevotella* and *Roseburia* species might be able to degrade intrinsic RS-3. This would be in agreement with an earlier statement, that *R. bromii* does not fulfil a key-stone degrading role in weaning piglets consuming wheat starch^[54]. These authors concluded that the metabolism of starch fermentation by pig faecal microbiota is dependent on cooperation between *Firmicutes* and *Bacteroidetes*^[54], to which *Roseburia* and *Prevotella* belong, respectively.

Increased relative abundance of *Roseburia* was also shown when weaned piglets were fed 5 % raw potato starch^[71]. *Roseburia* produces butyrate from carbohydrates and is more often shown to be increased during *in vitro* fermentation of resistant starch^[72]. Some *Roseburia* species harbour a single α -amylase with multiple CBMs (CBM82^[73], CAZy database^[74]) within the same protein^[67], that could bind to insoluble starch. To the best of our knowledge, direct RS-degrading capabilities have not yet been shown for *Roseburia* species, although these bacteria are suggested to be secondary degraders of RS, that are likely able to bind and degrade partially pre-degraded RS^[55]. *Prevotella* has a starch utilization system-like (Sus-like) multiprotein complex as found for *B. thetaiotaomicron*^[63]. However, *B. thetaiotaomicron* is unable to degrade RS on its own and relies on primary RS-degraders^[55] and additionally, *P. copri* was found to ferment soluble starch worse than *B. ovatus* and *B. thetaiotaomicron*^[66]. Nevertheless, it has been reported that some *Prevotella* strains harbour a CBM74-containing amylase^[75], together with a CBM26 domain being encoded in their genome^[76]. Such complex present in *Prevotella* might be of importance to bind to insoluble starch as recently shown by Photenhauer and co-authors (2022) for keystone degrader *R. bromii*^[76]. Since *Roseburia* 1 and *Prevotella*_9 03 ASVs specifically increased in relative abundance after incubation with intrinsic RS-3 and clear degradation of these substrates was shown using SEM (Figure 5.7), it might be of interest to investigate *Prevotella* and *Roseburia* species for their intrinsic RS-3 degrading capability.

5. Conclusions

We studied the fermentability of RS-3 preparations by pre- and post-weaning piglet faecal microbiota. Fermentation of RS-3 preparations by pre-weaning and post-weaning piglet faecal microbiota caused differences in microbial activity and composition. Both inocula fermented partially resistant RS-3 preparations quickly, whereas intrinsic RS-3 was only fermentable by post-weaning piglet faecal microbiota. Fermentation of RS-3 preparations by pre-weaning piglet faecal microbiota stimulated butyrate production and caused an increase in relative abundance of *Prevotella*, *Streptococcus* and *Megasphaera*. In contrast, post-weaning piglet microbiota fermented partially resistant RS-3 preparations to mostly propionate while stimulating *Prevotella* and *Selenomonas*. Intrinsic RS-3 fermentation by post-weaning piglet faecal microbiota resulted in an increase in relative abundance of specific phylotypes (ASVs) within *Prevotella* and *Roseburia*, which likely contributed to an appropriate insoluble starch degradation and fermentation. Partially resistant RS-3 preparations may not have prebiotic potential for pre-weaning piglets, but might provide the common benefits of all dietary fibres by stimulating SCFA production. Intrinsic RS-3 may have prebiotic potential in post-weaning piglets by stimulating more specific microbes, which requires further investigation.

6. References

1. Gresse R., Chaucheyras-Durand F., Fleury M.A., Van de Wiele T., Forano E., Blanquet-Diot S. Gut microbiota dysbiosis in postweaning piglets: understanding the keys to health. *Trends in Microbiology*. **2017**;25(10):851-873.
2. Jensen P., Stangel G. Behaviour of piglets during weaning in a semi-natural enclosure. *Applied Animal Behaviour Science*. **1992**;33:227-238.
3. Guevarra R.B., Lee J.H., Lee S.H., Seok M.J., Kim D.W., Kang B.N., Johnson T.J., Isaacson R.E., Kim H.B. Piglet gut microbial shifts early in life: causes and effects. *Journal of Animal Science and Biotechnology*. **2019**;10:1.
4. Lallès J.-P., Boudry G., Favier C., Le Floc N., Luron I., Montagne L., Oswald I.P., Pié S., Piel C., Sève B. Gut function and dysfunction in young pigs: physiology. *Animal Research*. **2004**;53(4):301-316.
5. Sun Y., Kim S.W. Intestinal challenge with enterotoxigenic *Escherichia coli* in pigs, and nutritional intervention to prevent postweaning diarrhea. *Animal Nutrition*. **2017**;3(4):322-330.
6. Rhouma M., Fairbrother J.M., Beaudry F., Letellier A. Post weaning diarrhea in pigs: risk factors and non-colistin-based control strategies. *Acta Veterinaria Scandinavica*. **2017**;59(1):31.
7. Bonetti A., Tugnoli B., Piva A., Grilli E. Towards zero zinc oxide: feeding strategies to manage post-weaning diarrhea in piglets. *Animals (Basel)*. **2021**;11(3).
8. Regulation (EU) 2019/6 of the European Parliament and of the Council of 11 December 2018 on veterinary medicinal products and repealing Directive 2001/82/EC.
9. Huting A.M.S., Middelkoop A., Guan X., Molist F. Using nutritional strategies to shape the gastrointestinal tracts of suckling and weaned piglets. *Animals (Basel)*. **2021**;11(2).
10. Bogere P., Choi Y.J., Heo J. Probiotics as alternatives to antibiotics in treating post-weaning diarrhoea in pigs: Review paper. *South African Journal of Animal Science*. **2019**;49(3):403-416.
11. Bai Y., Wang Z., Zhou X., Zhang Y., Ye H., Wang H., Pi Y., Lian S., Han D., Wang J. Ingestion of xylooligosaccharides during the suckling period improve the feed efficiency and hindgut fermentation capacity of piglets after weaning. *Food & Function*. **2021**;12(21):10459-10469.
12. de Vries H., Geervliet M., Jansen C.A., Rutten V., van Hees H., Groothuis N., Wells J.M., Savelkoul H.F.J., Tijhaar E., Smidt H. Impact of yeast-derived beta-glucans on the porcine gut microbiota and immune system in early life. *Microorganisms*. **2020**;8(10).
13. Van Hees H., Maes D., Millet S., Den Hartog L., Van Kempen T., Janssens G. Fibre supplementation to pre-weaning piglet diets did not improve the resilience towards a post-weaning enterotoxigenic *E. coli* challenge. *Journal of Animal Physiology and Animal Nutrition*. **2021**;105(2):260-271.
14. Choudhury R., Middelkoop A., Boekhorst J., Gerrits W.J.J., Kemp B., Bolhuis J.E., Kleerebezem M. Early life feeding accelerates gut microbiome maturation and suppresses acute post-weaning stress in piglets. *Environmental Microbiology*. **2021**;23(11):7201-7213.
15. Slupecka M., Wolinski J., Prykhodko O., Ochniewicz P., Gruijic D., Fedkiv O., Westrom B.R., Pierzynowski S.G. Stimulating effect of pancreatic-like enzymes on the development of the gastrointestinal tract in piglets. *Journal of Animal Science*. **2012**;90 Suppl 4:311-314.
16. Saladrigas-Garcia M., D'Angelo M., Ko H.L., Traserra S., Nolis P., Ramayo-Caldas Y., Folch J.M., Vergara P., Llonch P., Perez J.F., Martin-Orue S.M. Early socialization and environmental enrichment of lactating piglets affects the caecal microbiota and metabolomic response after weaning. *Scientific Reports*. **2021**;11(1):6113.
17. Wen C., van Dixhoorn I., Schokker D., Woelders H., Stockhofe-Zurwieden N., Rebel J.M.J., Smidt H. Environmentally enriched housing conditions affect pig welfare, immune system and gut microbiota in early life. *Animal Microbiome*. **2021**;3(1):52.
18. Frese S.A., Parker K., Calvert C.C., Mills D.A. Diet shapes the gut microbiome of pigs during nursing and weaning. *Microbiome*. **2015**;3:28.
19. Dou S., Gadonna-Widehem P., Rome V., Hamoudi D., Rhazi L., Lakhal L., Larcher T., Bahi-Jaber N., Pinon-Quintana A., Guyonvarch A., Huerou-Luron I.L., Abdennebi-Najar L. Characterisation of early-life fecal microbiota in susceptible and healthy pigs to post-weaning diarrhoea. *PLoS One*. **2017**;12(1):e0169851.

20. Li B., Schroyen M., Lebloy J., Wavreille J., Soyeurt H., Bindelle J., Everaert N. Effects of inulin supplementation to piglets in the suckling period on growth performance, postleal microbial and immunological traits in the suckling period and three weeks after weaning. *Archives of Animal Nutrition*. **2018**;72(6):425-442.
21. Schokker D., Fledderus J., Jansen R., Vastenhout S.A., de Bree F.M., Smits M.A., Jansman A. Supplementation of fructooligosaccharides to suckling piglets affects intestinal microbiota colonization and immune development. *Journal of Animal Science*. **2018**;96(6):2139-2153.
22. Tian S., Wang J., Yu H., Wang J., Zhu W. Effects of galacto-oligosaccharides on growth and gut function of newborn suckling piglets. *Journal of Animal Science and Biotechnology*. **2018**;9:75.
23. Wu Y., Zhang X., Han D., Ye H., Tao S., Pi Y., Zhao J., Chen L., Wang J. Short administration of combined prebiotics improved microbial colonization, gut barrier, and growth performance of neonatal piglets. *ACS Omega*. **2020**;5(32):20506-20516.
24. Tan F.P.Y., Beltranena E., Zijlstra R.T. Resistant starch: Implications of dietary inclusion on gut health and growth in pigs: a review. *Journal of Animal Science and Biotechnology*. **2021**;12(1):124.
25. Martens B.M.J., Flecher T., de Vries S., Schols H.A., Bruininx E., Gerrits W.J.J. Starch digestion kinetics and mechanisms of hydrolysing enzymes in growing pigs fed processed and native cereal-based diets. *British Journal of Nutrition*. **2019**;121(10):1124-1136.
26. Van Erp R.J.J., De Vries S., Van Kempen T.A.T.G., Den Hartog L.A., Gerrits W.J.J. Feed intake patterns nor growth rates of pigs are affected by dietary resistant starch, despite marked differences in digestion. *Animal*. **2020**;14(7):1402-1412.
27. Englyst H.N., Kingman S.M., Cummings J.H. Classification and measurement of nutritionally important starch fractions. *European Journal of Clinical Nutrition*. **1992**;46 Suppl 2:S33-50.
28. Wiseman J. Variations in starch digestibility in non-ruminants. *Animal Feed Science and Technology*. **2006**;130(1-2):66-77.
29. Bhandari S.K., Nyachoti C.M., Krause D.O. Raw potato starch in weaned pig diets and its influence on postweaning scours and the molecular microbial ecology of the digestive tract. *Journal of Animal Science*. **2009**;87(3):984-993.
30. Wiseman J., Pickard J., Zarkadas L. Starch digestion in piglets. In: Varley M.A., Wiseman J., editors. The weaner pig: nutrition and management proceedings of a British society of animal science occasional meeting, University of Nottingham, UK, September 2000. University of Nottingham, UK2000.
31. Pond W.G., Snook J.T., McNeill D., Snyder W.I., Stillings B.R. Pancreatic enzyme activities of pigs up to three weeks of age. *Journal of Animal Science*. **1971**;33(6):1270-1273.
32. Westrom B.R., Ohlsson B., Karlsson B.W. Development of porcine pancreatic hydrolases and their isoenzymes from the fetal period to adulthood. *Pancreas*. **1987**;2(5):589-596.
33. Bach Knudsen K.E., Hedemann M.S., Laerke H.N. The role of carbohydrates in intestinal health of pigs. *Animal Feed Science and Technology*. **2012**;173(1-2):41-53.
34. Birt D.F., Boylston T., Hendrich S., Jane J.L., Hollis J., Li L., McClelland J., Moore S., Phillips G.J., Rowling M., Schalinske K., Scott M.P., Whitley E.M. Resistant starch: promise for improving human health. *Advances in Nutrition*. **2013**;4(6):587-601.
35. Aumiller T., Mosenthin R., Weiss E. Potential of cereal grains and grain legumes in modulating pigs' intestinal microbiota – A review. *Livestock Science*. **2015**;172:16-32.
36. Klostermann C.E., Buwalda P.L., Leemhuis H., de Vos P., Schols H.A., Bitter J.H. Digestibility of resistant starch type 3 is affected by crystal type, molecular weight and molecular weight distribution. *Carbohydrate Polymers*. **2021**;265:118069.
37. Cai L.M., Shi Y.C. Self-assembly of short linear chains to A- and B-type starch spherulites and their enzymatic digestibility. *Journal of Agricultural and Food Chemistry*. **2013**;61(45):10787-10797.
38. Fohse J.M., Ganzle M.G., Regmi P.R., van Kempen T.A., Zijlstra R.T. High amylose starch with low in vitro digestibility stimulates hindgut fermentation and has a bifidogenic effect in weaned pigs. *Journal of Nutrition*. **2015**;145(11):2464-2470.
39. Bird A.R., Vuaran M., Brown I., Topping D.L. Two high-amylose maize starches with different amounts of resistant starch vary in their effects on fermentation, tissue and digesta mass accretion, and bacterial populations in the large bowel of pigs. *British Journal of Nutrition*. **2007**;97(1):134-144.

40. Bauer E., Williams B.A., Voigt C., Mosenthin R., Verstegen M.W.A. Microbial activities of faeces from unweaned and adult pigs, in relation to selected fermentable carbohydrates. *Animal Science*. **2001**;73:313-322.
41. Haenen D., Zhang J., Souza da Silva C., Bosch G., van der Meer I.M., van Arkel J., van den Borne J.J., Perez Gutierrez O., Smidt H., Kemp B., Muller M., Hooiveld G.J. A diet high in resistant starch modulates microbiota composition, SCFA concentrations, and gene expression in pig intestine. *Journal of Nutrition*. **2013**;143(3):274-283.
42. Minekus M., Smeets-Peters M., Bernalier A., Marol-Bonnin S., Havenaar R., Marteau P., Alric M., Fonty G., Huis in't Veld J.H. A computer-controlled system to simulate conditions of the large intestine with peristaltic mixing, water absorption and absorption of fermentation products. *Applied Microbiology & Biotechnology*. **1999**;53(1):108-114.
43. Klostermann C.E., Endika M.F., Ten Cate E., Buwalda P.L., de Vos P., Bitter J.H., Zoetendal E.G., Schols H.A. Type of intrinsic resistant starch type 3 determines in vitro fermentation by pooled adult faecal inoculum. *Accepted for publication in Carbohydrate Polymers*. **2023**.
44. Parada A.E., Needham D.M., Fuhrman J.A. Every base matters: assessing small subunit rRNA primers for marine microbiomes with mock communities, time series and global field samples. *Environmental Microbiology*. **2016**;18(5):1403-1414.
45. Apprill A., McNally S., Parsons R., Weber L. Minor revision to V4 region SSU rRNA 806R gene primer greatly increases detection of SAR11 bacterioplankton. *Aquatic Microbial Ecology*. **2015**;75(2):129-137.
46. Poncheewin W., Hermes G.D.A., van Dam J.C.J., Koehorst J.J., Smidt H., Schaap P.J. NG-Tax 2.0: A semantic framework for high-throughput amplicon analysis. *Frontiers in Genetics*. **2020**;10:1366.
47. Quast C., Priesse E., Yilmaz P., Gerken J., Schweer T., Yarza P., Peplies J., Glockner F.O. The SILVA ribosomal RNA gene database project: improved data processing and web-based tools. *Nucleic Acids Research*. **2013**;41(Database issue):D590-596.
48. Yilmaz P., Parfrey L.W., Yarza P., Gerken J., Priesse E., Quast C., Schweer T., Peplies J., Ludwig W., Glockner F.O. The SILVA and "All-species Living Tree Project (LTP)" taxonomic frameworks. *Nucleic Acids Research*. **2014**;42(Database issue):D643-648.
49. McMurdie P.J., Holmes S. phyloseq: an R package for reproducible interactive analysis and graphics of microbiome census data. *PLoS One*. **2013**;8(4):e61217.
50. Lahti R., Shetty S. Microbiome r package: Tools for microbiome analysis in r. 2012-2019 [Available from: <https://github.com/microbiome/microbiome>].
51. Barnett D.J.M., Arts I.C.W., Penders J. microViz: an R package for microbiome data visualization and statistics. *Journal of Open Source Software*. **2021**;6(63):3201.
52. Chen J., Bittiger K., Charlson E.S., Hoffmann C., Lewis J., Wu G.D., Collman R.G., Bushman F.D., Li H. Associating microbiome composition with environmental covariates using generalized UniFrac distances. *Bioinformatics*. **2012**;28(16):2106-2113.
53. Macfarlane G.T., Gibson G.R., Beatty E., Cummings J.H. Estimation of short-chain fatty acid production from protein by human intestinal bacteria based on branched-chain fatty acid measurements *FEMS Microbiology Ecology*. **1992**;202:81-88.
54. Wang W., Hu H., Zijlstra R.T., Zheng J., Ganzle M.G. Metagenomic reconstructions of gut microbial metabolism in weanling pigs. *Microbiome*. **2019**;7(1):48.
55. Cerqueira F.M., Photenhauer A.L., Pollet R.M., Brown H.A., Koropatkin N.M. Starch digestion by gut bacteria: crowdsourcing for carbs. *Trends in Microbiology*. **2020**;28(2):95-108.
56. Difilippo E., Pan F., Logtenberg M., Willems R.H., Braber S., Fink-Gremmels J., Schols H.A., Gruppen H. In Vitro Fermentation of Porcine Milk Oligosaccharides and Galacto-oligosaccharides Using Piglet Faecal Inoculum. *Journal of Agricultural & Food Chemistry*. **2016**;64(10):2127-2133.
57. Luo Y.H., Yang C., Wright A.D., He J., Chen D.W. Responses in ileal and cecal bacteria to low and high amylose/amylopectin ratio diets in growing pigs. *Applied Microbiology and Biotechnology*. **2015**;99(24):10627-10638.
58. Awati A., Bosch M.W., Tagliapietra F., Williams B.A., Verstegen M.W.A. Difference in in vitro fermentability of four carbohydrates and two diets, using ileal and faecal inocula from unweaned piglets. *Journal of the Science of Food and Agriculture*. **2006**;86(4):573-582.

59. Bui A.T., Williams B.A., Hoedt E.C., Morrison M., Mikkelsen D., Gidley M.J. High amylose wheat starch structures display unique fermentability characteristics, microbial community shifts and enzyme degradation profiles. *Food & Function*. **2020**;11(6):5635-5646.
60. Narita J., Nakahara S., Fukuda H., Kondo A. Efficient production of L-(+)-lactic acid from raw starch by *Streptococcus bovis* 148. *Journal of Bioscience and Bioengineering*. **2004**;97(6):423-425.
61. Duncan S.H., Louis P., Flint H.J. Lactate-utilizing bacteria, isolated from human feces, that produce butyrate as a major fermentation product. *Applied Environmental Microbiology*. **2004**;70(10):5810-5817.
62. Anand S., Kaur H., Mande S.S. Comparative In silico analysis of butyrate production pathways in gut commensals and pathogens. *Frontiers in Microbiology*. **2016**;7:1945.
63. Accetto T., Avgustin G. Polysaccharide utilization locus and CAZYme genome repertoires reveal diverse ecological adaptation of *Prevotella* species. *Systematic and Applied Microbiology*. **2015**;38(7):453-461.
64. Galvez E.J.C., Iljazovic A., Amend L., Lesker T.R., Renault T., Thiemann S., Hao L., Roy U., Gronow A., Charpentier E., Strowig T. Distinct polysaccharide utilization determines interspecies competition between intestinal *Prevotella* spp. *Cell Host Microbe*. **2020**;28(6):838-852 e836.
65. Franke T., Deppenmeier U. Physiology and central carbon metabolism of the gut bacterium *Prevotella copri*. *Molecular Microbiology*. **2018**;109(4):528-540.
66. Fehlner-Peach H., Magnabosco C., Raghavan V., Scher J.U., Tett A., Cox L.M., Gottsegen C., Watters A., Wiltshire-Gordon J.D., Segata N., Bonneau R., Littman D.R. Distinct polysaccharide utilization profiles of human intestinal *Prevotella copri* isolates. *Cell Host Microbe*. **2019**;26(5):680-690 e685.
67. Ramsay A.G., Scott K.P., Martin J.C., Rincon M.T., Flint H.J. Cell-associated alpha-amylases of butyrate-producing Firmicute bacteria from the human colon. *Microbiology (Reading)*. **2006**;152(Pt 11):3281-3290.
68. Mukhopadhyay I., Morais S., Laverde-Gomez J., Sheridan P.O., Walker A.W., Kelly W., Klieve A.V., Ouwerkerk D., Duncan S.H., Louis P., Koropatkin N., Cockburn D., Kibler R., Cooper P.J., Sandoval C., Crost E., Juge N., Bayer E.A., Flint H.J. Sporulation capability and amylosome conservation among diverse human colonic and rumen isolates of the keystone starch-degrader *Ruminococcus bromii*. *Environmental Microbiology*. **2018**;20(1):324-336.
69. Klostermann C.E., Endika M.F., Buwalda P.L., de Vos P., Zoetendal E.G., Bitter J.H., Schols H.A. Presence of digestible starch impacts in vitro fermentation of resistant starch. *In preparation for submission*. **2023**.
70. Ze X., Duncan S.H., Louis P., Flint H.J. *Ruminococcus bromii* is a keystone species for the degradation of resistant starch in the human colon. *The ISME Journal*. **2012**;6(8):1535-1543.
71. Yi S.W., Lee H.G., So K.M., Kim E., Jung Y.H., Kim M., Jeong J.Y., Kim K.H., Oem J.K., Hur T.Y., Oh S.I. Effect of feeding raw potato starch on the composition dynamics of the piglet intestinal microbiome. *Animal Bioscience*. **2022**;35(11):1698-1710.
72. Wang S., Dhital S., Wang K., Fu X., Zhang B., Huang Q. Side-by-side and exo-pitting degradation mechanism revealed from in vitro human fecal fermentation of granular starches. *Carbohydrate Polymers*. **2021**;263:118003.
73. Cockburn D.W., Suh C., Medina K.P., Duvall R.M., Wawrzak Z., Henrissat B., Koropatkin N.M. Novel carbohydrate binding modules in the surface anchored alpha-amylase of *Eubacterium rectale* provide a molecular rationale for the range of starches used by this organism in the human gut. *Molecular Microbiology*. **2018**;107(2):249-264.
74. Drula E., Garron M.L., Dogan S., Lombard V., Henrissat B., Terrapon N. The carbohydrate-active enzyme database: functions and literature. *Nucleic Acids Research*. **2022**;50(D1):D571-D577.
75. Valk V., Lammerts van Bueren A., van der Kaaij R.M., Dijkhuizen L. Carbohydrate-binding module 74 is a novel starch-binding domain associated with large and multidomain alpha-amylase enzymes. *FEBS Journal*. **2016**;283(12):2354-2368.
76. Photenhauer A.L., Cerqueira F.M., Villafuerte-Vega R., Armbruster K.M., Mareček G., Chen T., Wawrzak Z., Hopkins J.B., Vander Kooi C.W., Janeček S., Ruotolo B.T., Koropatkin N.M. The *Ruminococcus bromii* amylosome protein Sas6 binds single and double helical α -glucan structures in starch. *bioRxiv*. **2022**.

7. Supplementary information

Supplementary table 5.1. Feed compositions of weaning, starter and pre-started diet used in this study.

| Ingredient | Weaning diet G | Starter diet G | Prestarter Diet |
|---|----------------|----------------|-----------------|
| Grains (wheat, barley, maize and oatmeal) | 665 | 729 | 365 |
| Protein sources (soy, potato) | 212 | 218 | 196 |
| Milk derivatives (whey) | 63 | - | 224 |
| Soy bean oil | 14.2 | 10 | 50 |
| Amino acids | 8.4 | 12.7 | 6,5 |
| Salt | 4.6 | 5.5 | - |
| Sugars | 10.0 | - | 90 |
| Premix* | 22.8 | 24.8 | 68.5 |

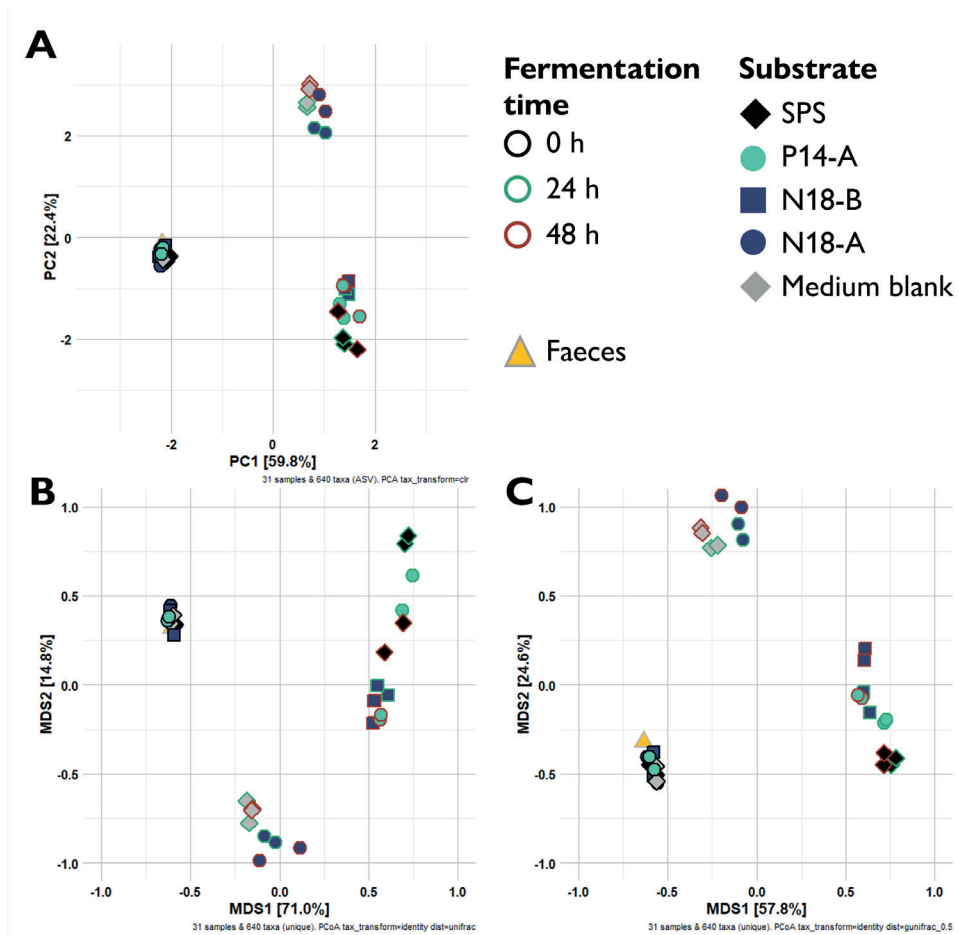
* Premix includes aroma's, minerals and trace minerals, vitamins, acids, enzymes, antioxidants

Supplementary table 5.2. Starch recoveries during 48 h of incubation of RS-3 preparations with pooled faecal inoculum of pre-weaning piglets.

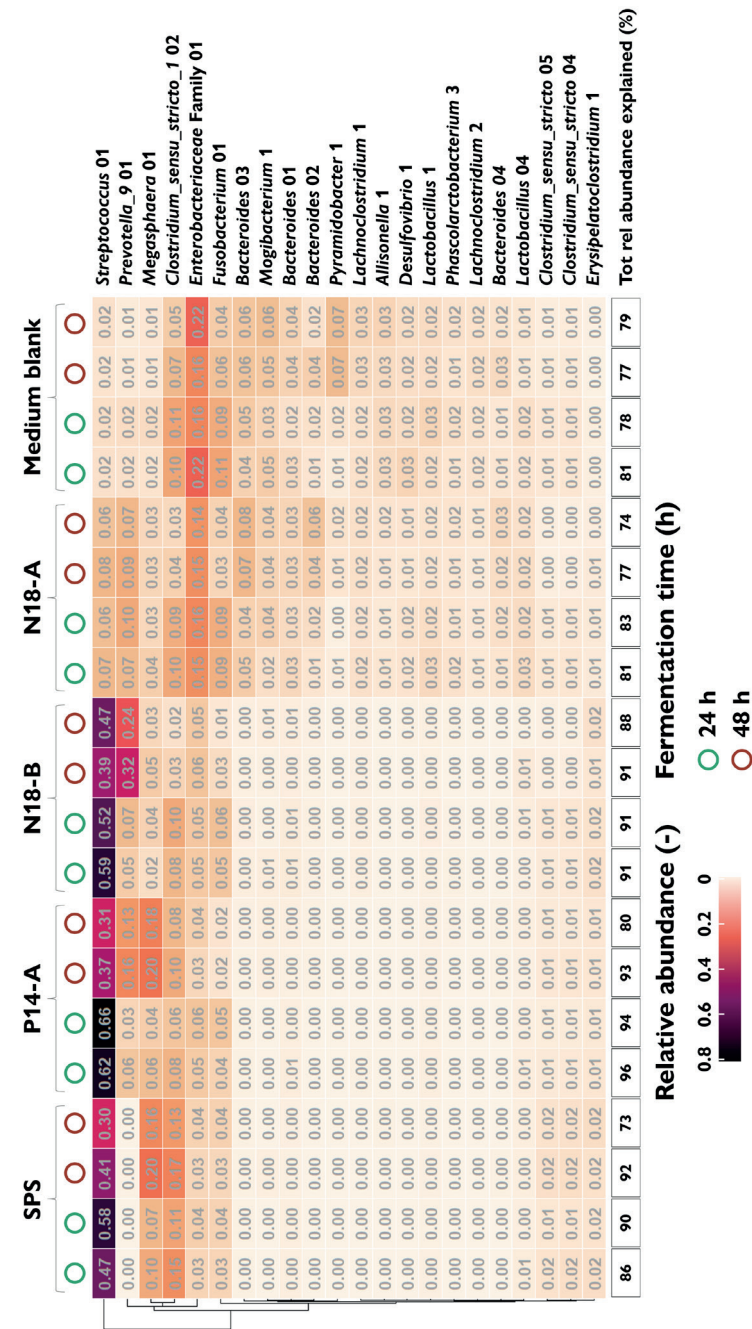
| Time | | SPS | P14-A | N18-A | N18-B |
|------|---------------|------------|-------------|--------------|------------|
| 0 h | Soluble (%) | 86.7 ± 8.2 | 9.8 ± 0.0 | 1.5 ± 4.2 | 10.5 ± 0.8 |
| | Insoluble (%) | | 102.1 ± 5.2 | 95.5 ± 4.2 | 87.8 ± 1.3 |
| 8 h | Soluble (%) | 58.9 ± 1.1 | 15.1 ± 0.3 | 0.1 ± 0.1 | 7.3 ± 0.0 |
| | Insoluble (%) | | 83.2 ± 0.8 | 109.5 ± 10.0 | 71.4 ± 9.7 |
| 24 h | Soluble (%) | 0.5 ± 0.0 | 0.2 ± 0.2 | 0.1 ± 0.0 | 0.1 ± 0.1 |
| | Insoluble (%) | | 34.9 ± 3.1 | 94.0 ± 6.3 | 49.9 ± 1.6 |
| 36 h | Soluble (%) | 0.3 ± 0.0 | 0.3 ± 0.1 | 0.2 ± 0.1 | 0.1 ± 0.1 |
| | Insoluble (%) | | 14.6 ± 6.8 | 95.3 ± 4.6 | 32.9 ± 1.5 |
| 48 h | Soluble (%) | 0.2 ± 0.1 | 0.2 ± 0.0 | 0.1 ± 0.1 | 0.2 ± 0.1 |
| | Insoluble (%) | | 1.0 ± 0.0 | 88.6 ± 1.6 | 12.9 ± 3.8 |

Supplementary table 5.3. Starch recoveries during 48 h of incubation of RS-3 preparations without pre-weaning piglet faecal microbiota.

| Time | | SB SPS | SB P14-A | SB N18-A | SB N18-B |
|------|---------------|-------------|------------|-------------|------------|
| 0 h | Soluble (%) | 96.9 ± 3.0 | 11.0 ± 0.6 | 3.5 ± 2.5 | 9.5 ± 0.1 |
| | Insoluble (%) | | 94.3 ± 0.5 | 78.4 ± 4.6 | 79.5 ± 0.9 |
| 8 h | Soluble (%) | 101.3 ± 5.5 | 26.2 ± 1.1 | 5.2 ± 0.0 | 19.0 ± 1.5 |
| | Insoluble (%) | | 77.4 ± 5.7 | 85.7 ± 0.6 | 76.3 ± 3.3 |
| 24 h | Soluble (%) | 99.4 ± 8.8 | 33.8 ± 0.8 | 7.9 ± 0.0 | 21.9 ± 0.8 |
| | Insoluble (%) | | 68.5 ± 3.3 | 73.3 ± 8.6 | 76.1 ± 3.6 |
| 36 h | Soluble (%) | 95.4 ± 3.1 | 37.7 ± 0.1 | 7.9 ± 0.3 | 22.6 ± 0.0 |
| | Insoluble (%) | | 66.2 ± 2.5 | 75.3 ± 14.6 | 67.7 ± 8.0 |
| 48 h | Soluble (%) | 92.4 ± 1.1 | 40.1 ± 2.3 | 7.6 ± 2.9 | 25.6 ± 0.7 |
| | Insoluble (%) | | 66.3 ± 1.5 | 79.8 ± 15.2 | 70.0 ± 4.2 |



Supplementary figure 5.1. Beta-diversities of microbiota composition after 0, 24 and 48 h of *in vitro* fermentation of RS-3 preparations and medium blank using pre-weaning piglet faecal microbiota. Figure A, B and C show PCA of CLR-transformed ASVs and PCoA of Unweighted and Generalized UniFrac distances, respectively.



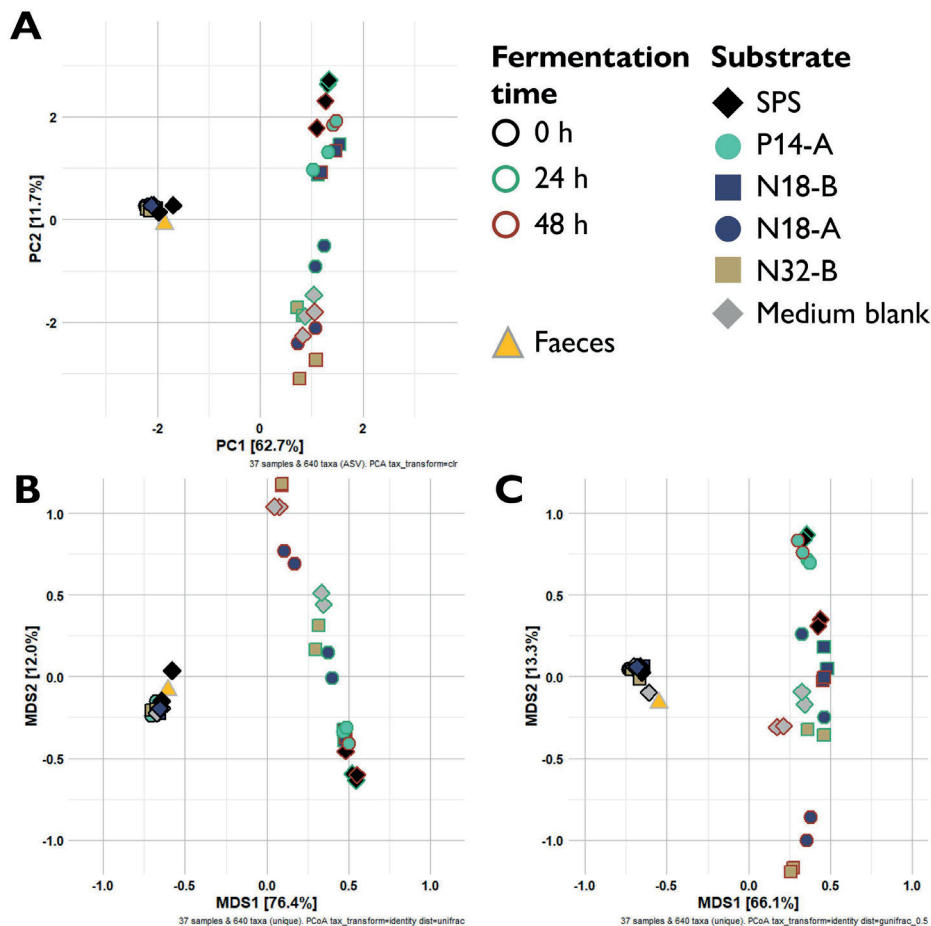
Supplementary figure 5.2. Heatmap showing ASVs contributing $\geq 2\%$ to the total relative abundance within a sample after 24 and 48 h of fermentation of SPS, P14-A, N18-B, N18-A and medium blank using pooled pre-weaning piglet faecal inoculum. The total relative abundance explained (%) is also provided. The taxa are sorted by hierarchical clustering of Euclidean distances.

Supplementary table 5.4. Starch recoveries during 48 h of incubation of RS-3 preparations with pooled faecal inoculum of post-weaning piglets.

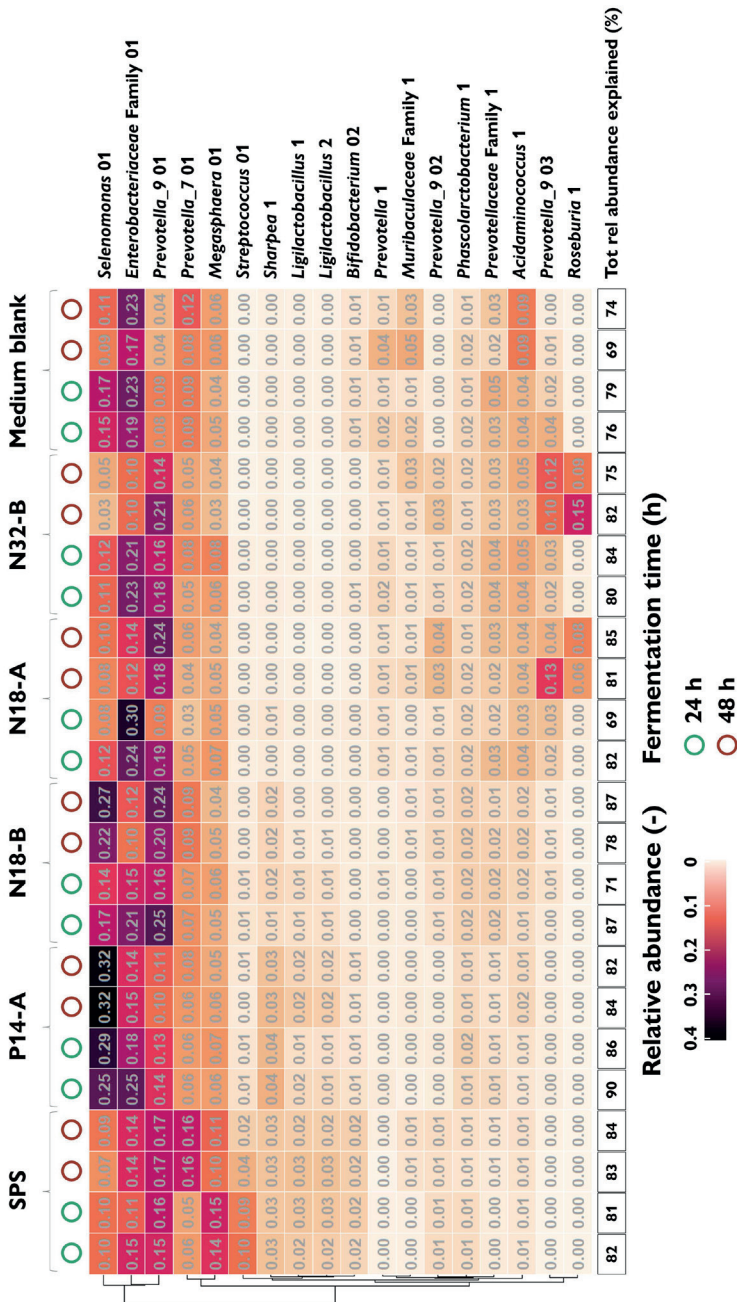
| Time | | SPS | P14-A | N18-A | N18-B | N32-B |
|------|---------------|------------|------------|------------|------------|------------|
| 0 h | Soluble (%) | 82.2 ± 2.3 | 5.4 ± 0.1 | 2.6 ± 1.1 | 7.3 ± 0.3 | 1.0 ± 0.0 |
| | Insoluble (%) | | 82.9 ± 1.4 | 88.7 ± 0.6 | 83.4 ± 3.2 | 87.0 ± 1.7 |
| 8 h | Soluble (%) | 70.8 ± 2.2 | 10.4 ± 0.0 | 0.6 ± 0.1 | 9.9 ± 0.0 | 0.3 ± 0.0 |
| | Insoluble (%) | | 73.8 ± 1.2 | 78.3 ± 5.8 | 76.3 ± 2.9 | 85.5 ± 5.9 |
| 24 h | Soluble (%) | 0.3 ± 0.1 | 0.1 ± 0.0 | 0.1 ± 0.0 | 0.1 ± 0.0 | 0.0 ± 0.0 |
| | Insoluble (%) | | 40.4 ± 3.3 | 80.9 ± 2.9 | 49.2 ± 6.7 | 85.5 ± 1.2 |
| 36 h | Soluble (%) | 0.1 ± 0.1 | 0.5 ± 0.7 | 0.1 ± 0.0 | 0.1 ± 0.0 | 0.0 ± 0.0 |
| | Insoluble (%) | | 14.6 ± 2.4 | 73.1 ± 0.8 | 34.4 ± 5.4 | 77.1 ± 7.0 |
| 48 h | Soluble (%) | 0.1 ± 0.1 | 0.6 ± 0.6 | 0.0 ± 0.0 | 0.1 ± 0.1 | 0.0 ± 0.0 |
| | Insoluble (%) | | 3.6 ± 1.0 | 62.6 ± 4.7 | 17.0 ± 4.4 | 65.1 ± 1.2 |

Supplementary table 5.5. Starch recoveries during 48 h of incubation of RS-3 preparations without post-weaning piglet faecal microbiota.

| Time | | SB SPS | SB P14-A | SB N18-A | SB N18-B | SB N32-B |
|------|---------------|------------|------------|-------------|------------|-------------|
| 0 h | Soluble (%) | 84.6 ± 1.8 | 7.0 ± 0.1 | 2.0 ± 0.1 | 6.6 ± 0.2 | 0.8 ± 0.1 |
| | Insoluble (%) | | 82.2 ± 0.8 | 88.9 ± 6.7 | 84.0 ± 2.3 | 78.1 ± 18.7 |
| 8 h | Soluble (%) | 84.6 ± 1.5 | 15.0 ± 0.9 | 3.9 ± 0.3 | 13.4 ± 0.2 | 1.6 ± 0.1 |
| | Insoluble (%) | | 70.6 ± 3.5 | 86.8 ± 1.5 | 74.6 ± 1.0 | 89.3 ± 0.2 |
| 24 h | Soluble (%) | 84.2 ± 1.5 | 21.0 ± 0.0 | 5.5 ± 0.2 | 15.3 ± 0.6 | 2.4 ± 0.2 |
| | Insoluble (%) | | 59.6 ± 3.8 | 83.3 ± 3.6 | 73.9 ± 0.0 | 85.9 ± 1.1 |
| 36 h | Soluble (%) | 84.2 ± 0.7 | 22.4 ± 1.1 | 5.7 ± 0.4 | 16.7 ± 0.8 | 2.7 ± 0.8 |
| | Insoluble (%) | | 59.9 ± 7.6 | 99.6 ± 14.9 | 73.8 ± 1.7 | 86.5 ± 1.5 |
| 48 h | Soluble (%) | 86.2 ± 0.8 | 24.6 ± 1.5 | 5.9 ± 0.1 | 16.0 ± 0.3 | 2.7 ± 0.1 |
| | Insoluble (%) | | 63.6 ± 0.1 | 84.6 ± 4.7 | 73.7 ± 0.6 | 82.6 ± 2.5 |

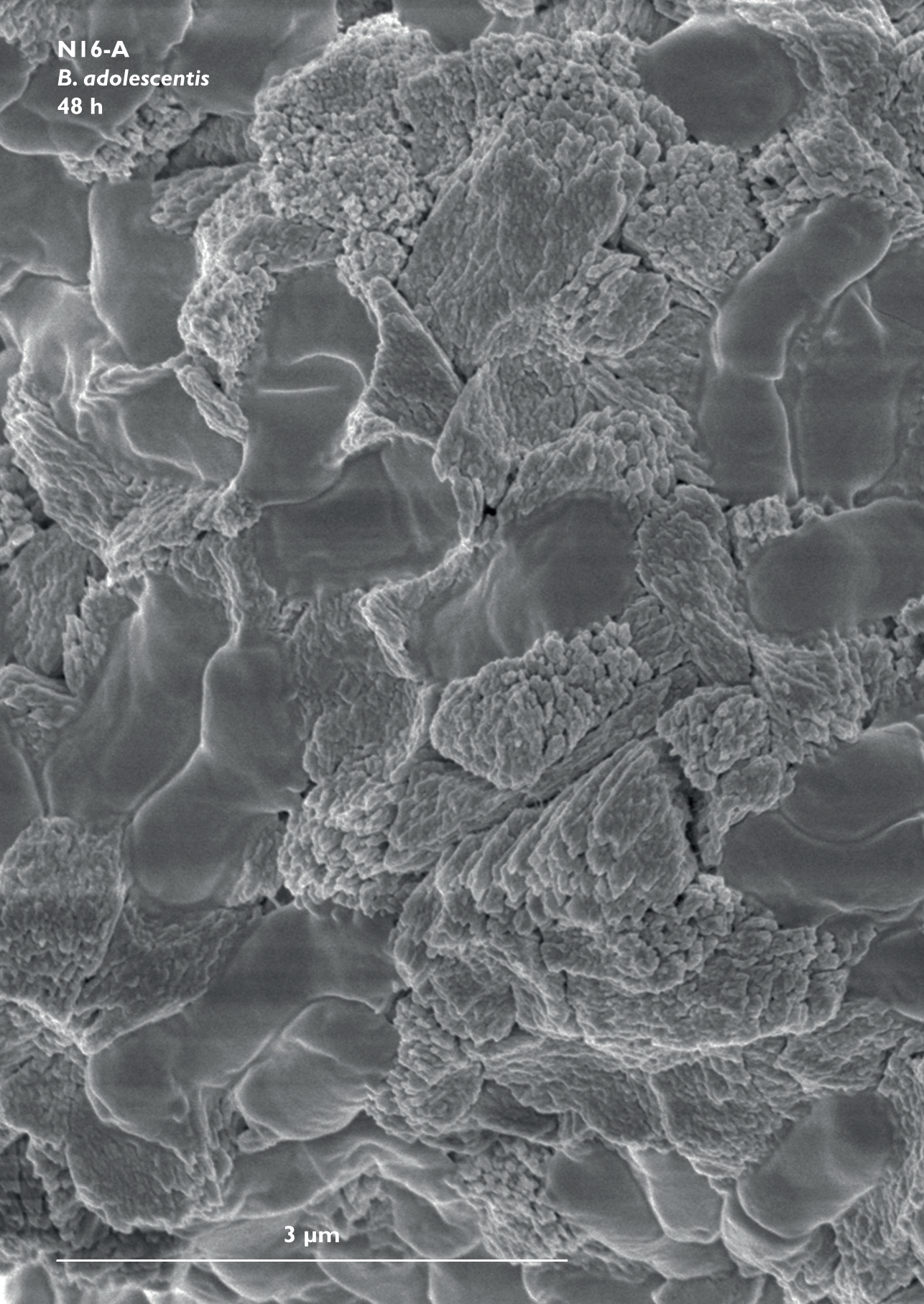


Supplementary figure 5.3. Beta-diversities of microbiota composition after 0, 24 and 48 h of *in vitro* fermentation of RS-3 preparations and medium blank using post-weaning piglet faecal microbiota. Figure A, B and C show PCA of CLR-transformed ASVs and PCoA of Unweighted and Generalized UniFrac distances, respectively.



Supplementary figure 5.4. Heatmap showing ASVs contributing $\geq 2\%$ to the total relative abundance within a sample after 24 and 48 h of fermentation of SPS, P14-A, N18-B, N18-A, N32-B and medium blank using pooled post-weaning piglet faecal inoculum. The total relative abundance explained (%) is also provided. The taxa are sorted by hierarchical clustering of Euclidean distances.

N16-A
B. adolescentis
48 h



3 μ m

A scanning electron micrograph (SEM) showing a dense cluster of starch crystals. The crystals exhibit a highly textured, layered, and somewhat fibrous appearance, with varying shades of gray highlighting their three-dimensional structure. The overall shape is roughly spherical but irregular, with many small facets and protrusions.

Chapter 6

Degradation of intrinsic resistant starch
type 3 crystals by gut microbes

B. adolescentis and *R. bromii*

Voor Piet

Cynthia E. Klostermann, Marina Fassarella,

Erwin G. Zoetendal, Henk A. Schols

To be submitted

Abstract

Intrinsic resistant starch type 3 (RS-3) is retrograded starch that is highly resistant to pancreatic digestion ($\geq 80\%$ RS) and will therefore transit to the colon largely intact. Two gut microbes, known as RS degraders, *Ruminococcus bromii* and *Bifidobacterium adolescentis* were studied for their ability to degrade intrinsic RS-3 with defined crystal type and chain length (A-type, degree of polymerization (DP_n) 16 or DP_n 21; B-type, DP_n 32 or DP_n 76). The insoluble RS-3 degradation was quantified and visualized by Scanning Electron Microscopy (SEM) over time and compared to degradation of granular maize and potato starch. *R. bromii* was not limited by any specific physico-chemical starch characteristic and degraded all substrates gradually to primarily maltose and glucose, although these sugars were not further fermented. In contrast, *B. adolescentis* was unable to degrade B-type intrinsic RS-3 and only slightly fermented A-type intrinsic RS-3 to acetate, whereas granular maize and potato starch were fermented readily to acetate and lactate. The elaborate use of SEM in this study revealed the unique morphology of the RS-3 structures and the difference in degradation approach by the two gut microbes. It can be concluded that efficient degradation of intrinsic RS-3 requires microbes with specific enzyme machineries such as those present in *R. bromii*.

1. Introduction

Resistant starch is an insoluble dietary fibre that is associated with many health-benefits^[1], among others, since it is efficiently fermented by gut microbiota into short-chain fatty acids (SCFAs)^[2]. Degradation of resistant starch occurs by primary degraders^[3], that provide substrates to secondary utilizers via cross-feeding, resulting in e.g. enhanced butyrate production^[4]. Butyrate has been associated with many health-benefits, such as providing energy to colonocytes^[5]. Supplementation of resistant starch in the diet could potentially improve human health by modulating the gut microbiota and enhance butyrate production in the colon. Several intervention studies showed effective modulation of the gut microbiota after resistant starch supplementation, although results were highly variable^[6-9]. These intervention studies investigated primarily the impact of resistant starch type 2 (RS-2), such as raw potato starch^[6-8].

Resistant starch type 3 (RS-3) is retrograded starch that escapes digestion in the upper gastro-intestinal tract (GIT) and therefore will transit to the colon. RS-3 preparations can be prepared from debranched starches followed by controlled crystallization^[10] and in most cases contain a digestible fraction^[11], that most probably will be hydrolysed in the upper GIT. To increase resistance to digestion, RS-3 preparations can be made by crystallization of α -1,4 glucans with a defined molecular weight (Mw) into A- or B-type crystals^[12-14]. Alpha-1,4 linked glucans of different Mw can be obtained by debranching (waxy) starches of different botanical sources^[15] or by enzymatic synthesis using amylosucrase^[16] or α -glucan phosphorylase^[17]. Previously, it was shown that specific RS-3 substrates prepared from α -glucan phosphorylase synthesized α -1,4 glucans with a narrow disperse Mw distribution were very resistant to *in vitro* digestion (Chapter 2^[12]). Especially RS-3 preparations of degree of polymerization (DPn) ~15-20 with an A-type crystal, or RS-3 preparations of DPn ~30-75 with a B-type crystal were ≥ 80 % resistant to *in vitro* digestion (Chapter 2^[12]) and are therefore considered “intrinsic RS-3”. *In vitro* fermentation of these specific RS-3 structures by pooled faecal inoculum of adults showed that all intrinsic RS-3 structures, independent of crystal type or Mw, were fermented to acetate and butyrate and stimulated *Lachnospiraceae*, that harbours many butyrate-producing bacteria^[18], and *Ruminococcus* and *Bifidobacterium* (Chapter 3^[19]).

Ruminococcus bromii and *Bifidobacterium adolescentis* are known primary degraders of resistant starch^[3]. The two bacterial species have been shown to increase in relative abundance *in vivo* after a diet containing resistant starch^[7, 8], or *in vitro* after fermentation using faecal inoculum^[2]. Furthermore, in mono-

culture both *R. bromii* and *B. adolescentis* were able to degrade Novelose® 330^[20], a commercial RS-3 ingredient with a B-type polymorph^[21]. *R. bromii* is a strict-anaerobic Gram-positive, spore-forming^[22] bacterium belonging to the *Firmicutes* phylum. It was shown to be a key-stone starch degrading bacterium in the human gut^[20]. Recently, some studies focussed on discovering the full starch degrading mechanism of *R. bromii*^[22-29]. The genome of *R. bromii* strains obtained from human faeces encode 17 glycoside hydrolase (GH) Family 13 enzymes^[22]. Some of these GH13 enzymes work together in a starch-degrading machinery called amylosome, which is anchored in the bacterial cell-wall^[22, 23]. Due to the presence of dockerin modules that bind to specific cohesins, the amylosome complex is very stable^[3]. Recently, a highly flexible starch-binding protein able to bind to starch granules was discovered to be present within the amylosome complex^[25]. Additionally, another starch-binding protein Sas6, was found to contain a carbohydrate binding module (CBM) 26 that binds to short malto-oligosaccharides, as well as a CBM74 able to bind to single or double helical α -glucans and these CBMs work together to bind to insoluble starch granules^[29]. The amylosome complex, together with other amylases present on the cell-wall of *R. bromii* are responsible for efficient degradation of resistant starch.

In contrast to *R. bromii* the starch-degrading specialist, *B. adolescentis* has a broader substrate preference^[30, 31]. *B. adolescentis* is an anaerobic Gram-positive, non-motile and non-spore forming bacterium belonging to the *Actinobacteria* phylum^[32]. Some *B. adolescentis* strains are known to possess GH13 enzymes able to degrade starch^[30, 33], although not automatically being able to degrade insoluble resistant starch^[34]. *B. adolescentis* genes are predicted to encode components of ABC-transporters that are able to transport maltodextrins and maltose into the cell^[30]. Once in the cell, the malto-oligosaccharides are further fermented to acetate and lactate via the bifid shunt^[35]. The exact starch degrading mechanism of *B. adolescentis* is not fully discovered yet, although it is known that the RS degrading enzymes are anchored in the cell-wall and possess CBMs 25, 26 and 74^[33] that are associated with insoluble starch binding^[36].

Next to these primary RS degraders, also secondary degraders of RS are described in literature^[37]. Secondary degraders can degrade soluble starch^[38] using extracellular amylases, but require primary degraders to initiate resistant starch degradation^[20]. One secondary degrader described is *Agathobacter rectalis* (previously known as *Eubacterium rectale*), a butyrate producing bacterium within the *Lachnospiraceae* family, which was shown to possess one single amylase anchored in its cell-wall^[39]. *A. rectalis* was shown to bind efficiently to both regular and high amylose maize starch granules using five CBMs among

which CBM82 and CBM83, although low binding to potato starch granules was observed^[39]. Previously, it was shown that *A. rectalis* was able to degrade RS-3 preparations, containing up to 40 % RS, and that these were fermented to acetate, propionate and butyrate^[40].

Earlier, we found an increase in relative abundance of primarily *Lachnospiraceae*, *Ruminococcus* and *Bifidobacterium* during *in vitro* fermentation of intrinsic RS-3 using a pooled faecal inoculum of healthy adults (Chapter 3^[19]). Depending on the RS-3 characteristics, the relative abundances of these taxa after *in vitro* fermentation differed, which might indicate that specific characteristics of intrinsic RS-3 substrates determine the degradation capability by such gut microbiota. To investigate if intrinsic RS-3 substrates differing in physico-chemical characteristics are fermentable by known primary RS-degraders, we incubated *R. bromii* and *B. adolescentis* with two A-type intrinsic RS-3 substrates (DPn 16, Polydispersity index (PI) 1.23; DPn 21, PI 1.59) and two B-type intrinsic RS-3 substrates (DPn 32, PI 1.14; DPn 76, PI 1.07) and compared their fermentability over time with that of native maize and potato starch granules. We analysed the starch degradation and product formation quantitatively, and followed changes in starch morphology by SEM visualization in time.

2. Materials and methods

2.1. Materials

Native potato starch granules and highly branched potato starch from potato (Mw \pm 100 kDa, 8 % branch points) were obtained from AVEBE (Veendam, The Netherlands), whereas regular maize starch was obtained from Roquette (Nord-Pas-de-Calais, France). *Ruminococcus bromii* ATCC27255 (ATCC, Manassas, Virginia, USA) was obtained from the Laboratory of Microbiology (Wageningen University & Research, Wageningen, The Netherlands) and *Bifidobacterium adolescentis* strain L2-32 was obtained from BEI resources (ATCC).

2.1.1. RS-3 preparations

RS-3 preparations were prepared by crystallizing debranched waxy rice starch or enzymatically synthesized α -glucans as described in Chapter 2^[12]. The specific physico-chemical characteristics and *in vitro* digestibility of these RS-3 preparations are summarized in Table 6.1, and were described in Klostermann et al. (2021)^[12]. The sample name is named after the RS-3 physico-chemical

characteristics with **N**: narrow disperse, **P**: polydisperse, **number**: DP_n, **A**: A-type crystal, **B**: B-type crystal.

Table 6.1. Crystal type, chain length, Mw distribution and *in vitro* digestibility of poly- and narrow disperse RS-3 preparations used in this study, as described in Klostermann et al. (2021)^[12].

| Sample name | Reported as ^[12] | Crystal type | DP _n _{crystal} | PI _{crystal} | <i>In vitro</i> digestibility (120 min) (%) |
|-------------|-----------------------------|--------------|------------------------------------|-----------------------|---|
| N16-A | sG2-A | A | 16 | 1.23 | 20 |
| P21-A | dWRS-A | A | 21 | 1.59 | 21 |
| N32-B | sG20-B | B | 32 | 1.14 | 5 |
| N76-B | sG65-B | B | 76 | 1.07 | 6 |

DP_n (number-based degree of polymerization) and PI (polydispersity index) were determined using HPSEC-RI, crystal type was determined using XRD and *in vitro* digestion was performed using pancreatin and amyloglucosidase^[12]. The sample name has been recoded compared to Klostermann et al., 2021.

2.2. *In vitro* batch fermentation of RS-3 preparations

2.2.1. Culture medium

B. adolescentis L2-32 was pre-cultured in modified clostridial broth (MCR) at pH 6.8, containing per L: 10 g tryptose, 10 g meat peptone, 3 g yeast extract, 5 g glucose, 5 g NaCl, 1 g soluble starch, 0.5 g L-cysteine-hydrochloride, 3 g sodium acetate and 1 mL resazurin solution (500 mg/L). Fermentation experiments were performed using modified simulated ileal efflux medium (mSIEM), containing per L: 3 g bactopectone, 3 g casein, 0.05 g ox-bile, 2.5 g K₂HPO₄·3H₂O, 4.5 g NaCl, 0.45 g CaCl₂·2H₂O, 0.005 g FeSO₄·7H₂O and 0.01 g haemin, 0.5 g MgSO₄ (Tritium Microbiologie, Eindhoven, The Netherlands) and 0.4 g L-cysteine-hydrochloride (Sigma-Aldrich, St. Louis, Missouri, USA). A vitamin mix was added with a final concentration of 1 µg/L menadione, 2 µg/L biotin, 0.5 µg/L vitamin B12, 10 µg/L pantothenate, 5 µg/L nicotinamide, 5 µg/L para-aminobenzoic acid, 4 µg/L thiamine (Tritium Microbiologie). The medium was buffered using 0.1 M sodium phosphate buffer at pH 5.8.

R. bromii ATCC27255 was pre-cultured in modified Gifu Anaerobic Medium broth (mGAM) (HyServe GmbH, Uffing, Germany) at pH 7.3 with the addition of 1 mL resazurin solution (500 mg/L) per L of medium. For fermentation experiments, the medium was diluted twice and supplemented with 0.25 g/L L-cysteine-hydrochloride. The expected soluble starch content in the twice diluted mGAM broth was 2.5 mg/mL, according to the supplier.

All media were pre-reduced according to Aguirre et al. (2015)^[41]. Briefly, media were boiled for 20 seconds to remove O₂ and cooled under nitrogen flow after

which L-cysteine-hydrochloride was added, pH adjusted and nitrogen influx continued for 10 more minutes until the colour conversion of resazurin was observed. Subsequently, the medium was transferred to serum bottles and capped with butyl rubber stoppers and aluminium caps. The headspace was exchanged using 100 % N₂ and the serum bottles were autoclaved.

2.2.2. *In vitro* fermentation

B. adolescentis L2-32 (MRC broth) and *R. bromii* ATCC27255 (mGAM broth) were pre-cultured at 37 °C without shaking for 20-24 h.

Approximately 5-6 mg (dry weight) of all substrates was weighed in duplicate in sterile 5 mL serum bottles and transferred to the anaerobic chamber for gas exchange overnight (gas composition: 4 % H₂, 15 % CO₂, 81 % N₂; Bactron 300, Sheldon Manufacturing, Cornelius, Oregon, USA). To the weighed starches, 1.9 mL medium was added followed by 0.1 mL pre-cultured *B. adolescentis* L2-32 or *R. bromii* ATCC27255 (5 % v/v inoculum). Samples without additional substrate (all time points) or samples without inoculum (only t = 48 h) were prepared as blank. The serum bottles were capped using butyl rubber stoppers and aluminium caps and incubated at 37 °C without shaking for 0, 24, 48 and 72 h.

At each time point, the assigned serum bottles were taken out of the incubator. The serum bottles were decapped and the contents were transferred to Safe-Lock Eppendorf tubes (Eppendorf, Hamburg, Germany). The tubes were centrifuged at 4 °C, 10,000 x g for 10 min and 0.55 mL of supernatant was separated and immediately heated at 100 °C, 800 rpm for 10 min (Eppendorf shaker, Eppendorf). Another 1.1 mL of supernatant was collected in another tube and stored at 4 °C until further use. From the serum bottles containing some remaining substrate particles, 25 µL was used for SEM (section 2.6). Subsequently, 1.5 mL of autoclaved milliQ was used to wash the serum bottles and transferred to the Safe-Lock Eppendorf tubes containing the pellet and mixed. The tubes were centrifuged once more and 1 mL of supernatant was discarded. The tubes containing pellet were immediately frozen using liquid N₂ and subsequently freeze-dried.

2.3. Starch quantification

Starch was quantified in the supernatant and in the freeze-dried pellets obtained after fermentation using the Megazyme Total Starch Kit (AA/AMG) (Megazyme, Wicklow, Ireland), according to the company protocol and adjusted for smaller sample sizes as described in Chapter 3^[19]. Briefly, insoluble starch was solubilized using 1.7 M NaOH and after proper neutralization, dilution and

enzymatic hydrolysis, the free glucose content was analysed using the GOPOD assay kit (Megazyme). In the supernatant, both free glucose and total glucose after enzymatic hydrolysis were determined using the GOPOD assay kit.

Soluble oligosaccharides present in the supernatant after fermentation of the starch substrates by *R. bromii* were analysed using High Performance Anion Exchange Chromatography with Pulsed Amperometric Detection (HPAEC-PAD). The supernatants were diluted 20 times with milliQ water, centrifuged (20,000 × g, 10 min) and 10 µL of the supernatants were injected on a CarboPac PA-1 (2 × 250 mm) column, with a CarboPac PA-1 guard column (Dionex, Sunnyvale, California, USA), using an ICS-6000 HPAEC system from ThermoFisher Scientific (Waltham, Massachusetts, USA). The oligosaccharides were detected using a Pulsed Electrochemical Detector in the PAD mode. The eluents used were 0.1 M NaOH solution (eluent A) and 1 M NaOAc in 0.1 M NaOH (eluent B). The gradient used was 2.5 - 25 % B (0-30 min), followed by 25 - 100 % B (30-40 min), 100 % B (40-50 min) and re-equilibration at 2.5 % B (50-65 min). Elution was performed with 0.3 mL/min at 25 °C. A standard curve of malto-oligosaccharides (DP 1 – DP 7) was prepared for quantification (concentration 5 - 25 µg/mL). Data analysis was performed with Chromeleon™ 7.3 software from ThermoFisher Scientific.

2.4. Metabolite quantification

Organic acid and ethanol quantification was performed using HPLC-RI/UV (Dionex) with an Aminex HPX-87H column (Bio-Rad laboratories Inc, Hercules, California, USA) as described in Chapter 3^[19]. For *R. bromii* standard curves of 0.05 – 2 mg/mL acetic acid, formic acid and ethanol were used, as representative metabolites of *R. bromii* growth^[42]. For *B. adolescentis* standard curves of 0.05 – 2 mg/mL acetic acid and lactic acid were included as representative metabolites of *B. adolescentis* growth^[43].

2.5. Extracellular α -amylase activity using Ceralpha kit

Activity of the extracellular α -amylases secreted in the supernatant during fermentation of the starches by *R. bromii* and *B. adolescentis* was analysed in mono using the Ceralpha method (Megazyme), according to the suppliers manual, adjusted for smaller sample sizes. In short, supernatants obtained after 24 – 72 h of fermentation by *R. bromii* were diluted 10 times with a buffer containing 0.1 M maleic acid pH 6.5 and supplemented with 0.1 M sodium chloride and 2 mM calcium chloride dihydrate. Supernatants obtained after 0 h of fermentation by *R. bromii* and all time points of fermentation by *B. adolescentis* were non-diluted

and used as such. An aliquot of 50 μ L per analysis of the Megazyme Amylase HR reagent was incubated at 40 °C for 5 min. The (diluted) supernatant was also heated to 40 °C for 5 min. To each tube containing the Amylase HR reagent, 50 μ L of the (diluted) supernatant was added. The mixture was incubated at 40 °C, 800 rpm, for 10 min (Eppendorf shaker). Exactly after 10 min of incubation, 750 μ L of stopping reagent was added (20 % tri-sodium phosphate solution, pH ~11, Megazyme). The absorbance was measured at 400 nm against distilled water. The final activities were corrected for background absorbance obtained in the mSIEM or mGAM media.

2.6. Scanning Electron Microscopy

Fermentation samples were dried on 13 mm filters with 10 μ m holes (Merck Isopore™ membrane filter (Merck, Burlington, Massachusetts, USA)), in a flow cabinet, attached to sample holders containing carbon adhesive tabs (EMS, Washington, USA) and coated with 12 nm tungsten (EM SCD 500, Leica, Vienna, Austria). The samples were analysed with SEM (Magellan 400, FEI, Eindhoven, The Netherlands) at the Wageningen Electron Microscopy Center. SEM images were recorded at an acceleration voltage of 2 kV and 13 pA and magnification of 5,000 (Everhart-Thornley detector) and 25,000 (Through Lens Detector) times.

3. Results

3.1. Insoluble starch degradation

The fermentability of intrinsic RS-3 by two well-known primary resistant starch degraders *Bifidobacterium adolescentis* L2-32 and *Ruminococcus bromii* ATC27255 was investigated. The intrinsic RS-3 substrates consisted of two with an A-type polymorph (N16-A, P21-A) and two with a B-type polymorph (N32-B and N76-B) (Chapter 2^[12]). N16-A, N32-B and N76-B were prepared from narrow disperse enzymatically synthesized α -1,4 glucans, whereas P21-A was prepared from polydisperse debranched waxy rice starch.

N16-A, P21-A, N32-B and N76-B were incubated over time with *R. bromii* and *B. adolescentis* in mono-culture, and well-studied substrates native regular maize and potato starch granules were included as well. After incubation, the remaining insoluble starch was quantified (Figure 6.1). Total starch recovery, including the insoluble and soluble starch fraction, and the recovery in the substrate blanks can be found in Supplementary table 6.1 and 6.2.

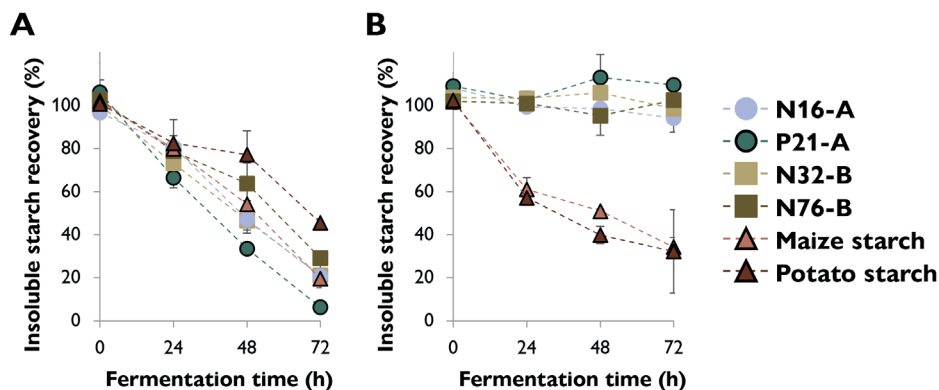


Figure 6.1. Insoluble starch recovery in time during 72 h of incubation of intrinsic RS-3 and native maize and potato starch granules with A: *R. bromii* ATCC27255 and B: *B. adolescentis* L2-32. The average of biological duplicates is shown, the error bars represent the standard deviation and might be smaller than the marker used.

The results show that the insoluble starch recovery decreased quite constantly over time, for all substrates individually during incubation with *R. bromii* (Figure 6.1-A). Small differences were observed in degradation rate among the substrates. In contrast, during incubation of insoluble starch with *B. adolescentis*, the insoluble starch recovery only decreased obviously for maize and potato starch (Figure 6.1-B) and indicated no degradation of intrinsic RS-3 substrates N16-A, P21-A, N32-B and N76-B. Potato and maize starch granules were effectively degraded by *B. adolescentis* during 72 h of incubation, although the degradation rate decreased over time. Together, these results indicate that *R. bromii* enzymes degraded all intrinsic RS-3 and granular starches, whereas *B. adolescentis* enzymes only degraded granular starches.

3.2. Metabolite production

To study the metabolites produced during incubation of intrinsic RS-3 and granular starches with *R. bromii* and *B. adolescentis*, acetic acid, lactic acid and ethanol were quantified (Figure 6.2), together with quantification of these products in the positive control HBPS and the medium blank. No formic acid was detected in the spent medium.

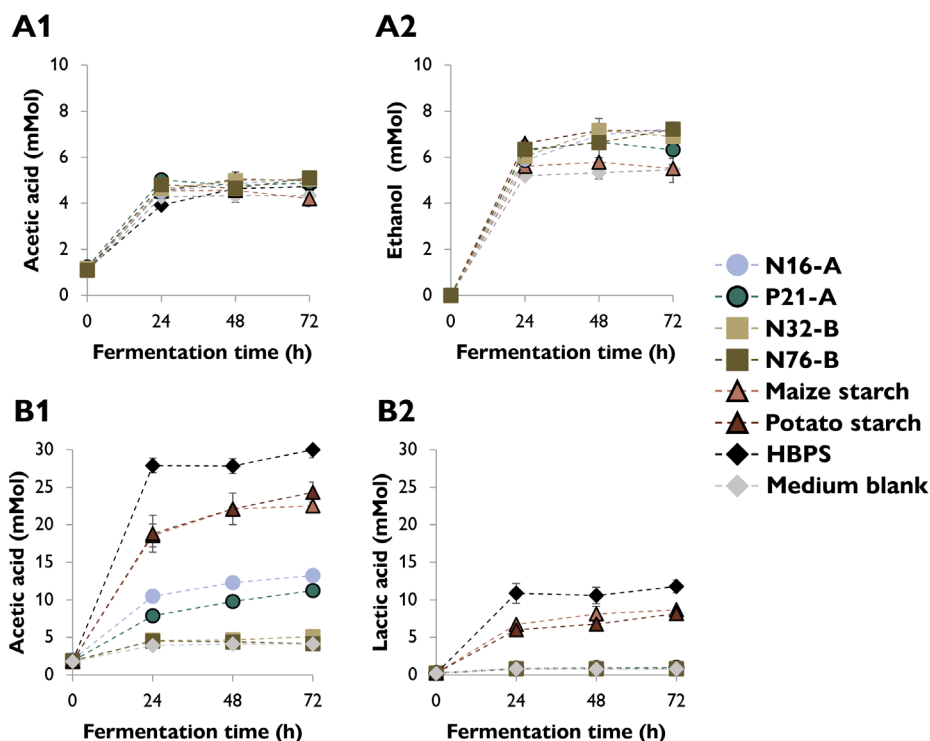


Figure 6.2. A: Acetic acid and ethanol produced by *R. bromii* ATCC27255 and B: acetic and lactic acid produced by *B. adolescentis* L2-32 during fermentation of intrinsic RS-3, native granules, HBPS and a medium blank. The average of biological duplicates is shown, the error bars represent the standard deviation and might be smaller than the marker used.

The results show that acetate production by *R. bromii* increased from approximately 1 mMol at t_0 to approximately 4 mMol at t_{24} for all substrates (Figure 6.2-A1). After 24 h of fermentation, the acetate content did not increase anymore. For ethanol production, something similar was observed, increasing from 0 mMol at t_0 to 6 mMol at t_{24} for all substrates and remaining at that concentration for the following 48 h of fermentation (Figure 6.2-A2). Since we did not observe clear differences in acetate and ethanol production between the medium blank and the substrates during incubation with *R. bromii*, these results indicate that *R. bromii* did not ferment starches. Some compounds present within the medium were fermented by *R. bromii* causing the slight increase in acetate and ethanol during the first 24 h of incubation.

The results show that acetate production by *B. adolescentis* increased from approximately 2 mMol at t_0 to different values for all substrates (Figure 6.2-B1). HBPS, a fully soluble highly branched starch, was fermented rapidly during the

first 24 h, yielding 28 mMol acetate, which only slightly increased thereafter. During fermentation of maize and potato starch this was very similar, with acetate increasing rapidly to 18 mMol at t24 and slowly increasing afterwards to 22 mMol after 72 h. In contrast, fermentation of intrinsic RS-3 substrates N16-A and P21-A by *B. adolescentis* generated only 10 and 8 mMol acetate, during the first 24 h, with a final concentration of 12 and 10 mMol after 72 h, respectively. Acetate formation during incubation of intrinsic B-type RS-3 substrates with *B. adolescentis* was similar to the medium blank, only increasing from 2 mMol at t0 to 4 mMol at 24 h and remaining at that concentration till 72 h. The results show that lactate production by *B. adolescentis* increased during fermentation of HBPS from 0 mMol at t0 to 10 mMol at 24 h and remaining at a similar concentration for the following 48 h (Figure 6.2-B2). Also during fermentation of maize and potato starch lactate production increased, whereas no lactate production was observed during incubation of intrinsic RS-3 with *B. adolescentis*. The production of acetate and lactate during fermentation of HBPS, maize and potato starches indicates that *B. adolescentis* degraded and fermented these substrates. The slight production of acetate, but no lactate, during incubation of intrinsic A-type RS-3 substrates with *B. adolescentis* indicates that *B. adolescentis* can only slightly ferment these substrates, which might be related to the digestible fraction present (Table 6.1). For the B-type intrinsic RS-3 substrates we did not observe any acetate and lactate production, indicating, together with the full insoluble starch recovery, that *B. adolescentis* L2-32 cannot degrade and ferment B-type intrinsic RS-3 substrates.

R. bromii degraded all substrates during 72 h of fermentation (Figure 6.1-A), which did not result in additional acetate and ethanol production (Figure 6.2-A). Instead, soluble starch including glucose, was found within the spent medium (Figure 6.3), which was not observed for *B. adolescentis* (Supplementary table 6.1). The soluble oligomers found in the spent medium of starches incubated with *R. bromii* were further identified using HPAEC-PAD analysis (Figure 6.4).

For incubations of starches with *R. bromii* we used mGAM broth, which already contained some soluble starch. The results show that *R. bromii* fermented the soluble starch present within the medium for ± 50 % during the first 24 h of incubation, after which the soluble starch recovery stabilized, indicating no further fermentation of starch (Figure 6.3), probably because *R. bromii* reached the stationary phase. *R. bromii* hydrolysed the soluble starch present within the medium to primarily glucose and maltose (Figure 6.4-A). Incubation of fully soluble HBPS with *R. bromii* resulted in a decrease in soluble starch recovery

during the first 24 h (Figure 6.3). Already at 24 h of incubation all HBPS and soluble starch present within the medium was hydrolysed to glucose, maltose and maltotriose (Figure 6.4-A). Longer incubation of HBPS with *R. bromii* resulted in a slight decrease in soluble starch content and the maltotriose present at 24 h was further hydrolysed to glucose and maltose (Figure 6.4-A).

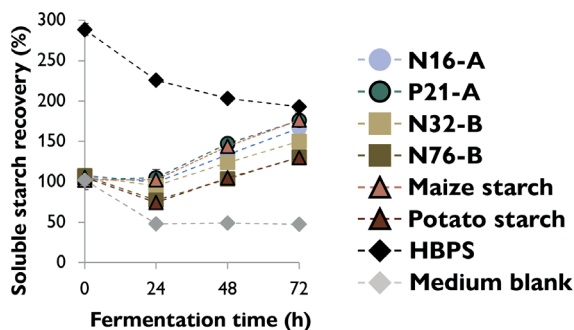


Figure 6.3. Soluble starch recovery as found during incubation of starches with *R. bromii*. The starch in the medium blank (mGAM) at t_0 is set at 100 % for all samples tested. The average of biological duplicates is shown, the error bars represent the standard deviation and might be smaller than the marker used.

For the insoluble potato starch granules and insoluble intrinsic RS-3 N76-B, a slight decrease in soluble starch recovery was observed during the first 24 h (Figure 6.3), indicating fermentation of starch present within the medium, after which the soluble starch recovery increased, indicating degradation of the insoluble substrates to soluble glucose and maltose (Figure 6.4-B,D). For the insoluble maize granules and insoluble intrinsic RS-3 N16-A, P21-A and N32-B no clear decrease in soluble starch recovery during the first 24 h of incubation was observed (Figure 6.3), potentially because *R. bromii* already degraded more insoluble substrate to soluble oligomers within these starches (Figure 6.4).

The results indicate that *R. bromii* enzymes hydrolysed all starches to primarily glucose and maltose (Figure 6.4). Furthermore, the results of the medium blank indicate that around 50 % of the soluble starch initially present was fermented within 24 h by *R. bromii* to acetate and ethanol (Figure 6.2-A). Increased starch degradation by *R. bromii* did not result in additional acetate and ethanol production, resulting in accumulation of glucose and maltose in the spent medium.

As a preliminary test we examined the amylase activity within the cell-free medium and the results showed a lack of amylase activity for *B. adolescentis* in

all samples (Supplementary table 6.3), whereas for *R. bromii* we observed some amylase activity, although quite low and no substantial differences among the different substrates were observed (Supplementary table 6.4).

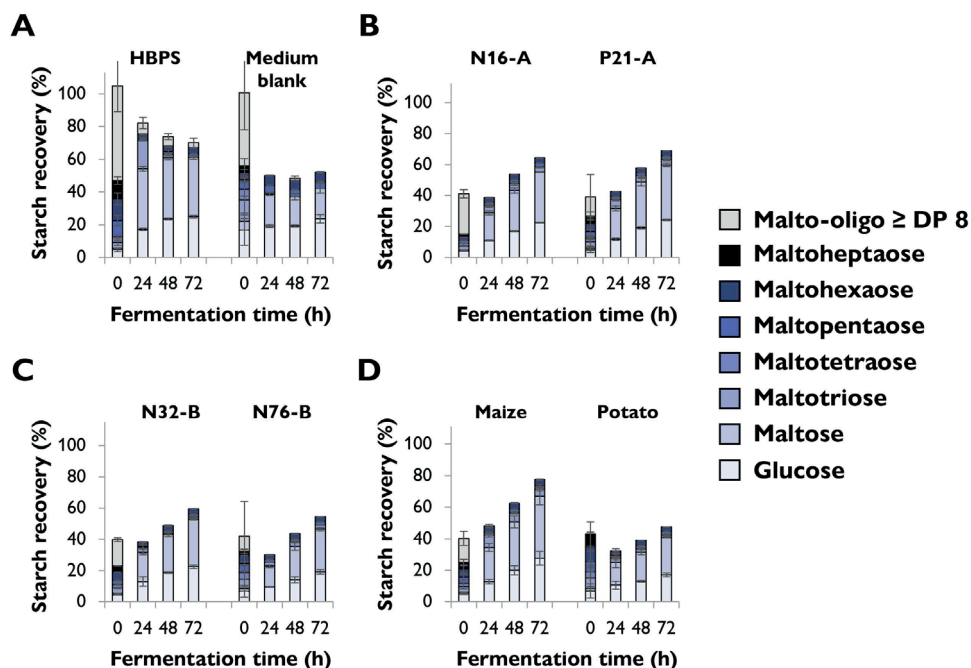


Figure 6.4. Composition of the soluble starch fraction of total starch recovered during 72 h of incubation of starches with *R. bromii*. Figures represent A: HBPS and medium blank, B: intrinsic A-type RS-3 substrates, C: intrinsic B-type RS-3 substrates and D: native granules. Malto-oligomers were quantified using HPAEC-PAD, in combination with Megazyme GOPOD assay before and after enzymatic hydrolysis. The average of biological duplicates is shown, the error bars represent the standard deviation.

3.3. Changes in starch morphology during degradation by primary degraders

Scanning Electron Microscopy can be used to study the changes in starch morphology due to degradation by gut microbes. Here, we compare substrate degradation of our intrinsic RS-3 N16-A by primary degraders *R. bromii* and *B. adolescentis* (Figure 6.5-6.7). Furthermore, we compare degradation of N32-B and N76-B, two B-type intrinsic RS-3 substrates differing in α -1,4 glucan chain length, by *R. bromii* (Figure 6.8-6.10). SEM images of all substrates incubated over time with *R. bromii* or *B. adolescentis* can be found in the supplementary information (Supplementary figure 6.1-6.12).

In our previous studies we observed slight solubilization ($\pm 10\%$) of N16-A after 24 h of incubation (Chapter 3^[19]). Also when incubated in mSIEM for 48 h, $\pm 10\%$ of N16-A solubilized (Supplementary table 6.1). The SEM images of N16-A immediately after incubation with *R. bromii* or *B. adolescentis* (t0) and the images after 48 h incubation in mGAM or mSIEM were identical (Figure 6.5-A,B), indicating that solubilization did not affect the morphology of N16-A. N16-A consisted of small rectangular blocks of $\pm 1.5 \times 0.5 \mu\text{m}$ that were connected to each other in spherical particles with a diameter of $\pm 3\text{--}5 \mu\text{m}$. Detailed images clearly show how the rectangular blocks were connected to each other in a dense spherical particle (Figure 6.5-C). In the middle of the particle, the fibres seem less aligned (Figure 6.5-C1).

Incubation of N16-A dramatically changed the shape of N16-A over time, especially when incubated with *R. bromii* (Figure 6.6-RB). After 24 h of incubation with *R. bromii*, the spherical shape of N16-A was still recognizable, including the rectangular blocks, although the structure became more loose. After 48 h, the spherical shape of N16-A was completely lost and the rectangular blocks changed to more spiky structures. After 72 h of incubation with *R. bromii*, these spikes were still recognizable at some spots whereas at other spots also this spiky structure was lost and a less clear microstructure was obtained.

When incubated with *B. adolescentis*, the structure of N16-A changed less dramatically (Figure 6.6-BA) and after 24 h, the rectangular blocks that together formed the spherical particle were very clearly recognizable. Compared to N16-A at t0, it seems that *B. adolescentis* especially removed an amorphous layer that was covering the N16-A intrinsic RS-3, making the structure much better visible. After 48 and 72 h of incubation with *B. adolescentis*, the spherical structure of N16-A was still recognizable and many bacteria were attached to the surface of the N16-A substrate.

The images give an overall view on N16-A degradation by *R. bromii* and *B. adolescentis*. Also from these images it is clear that *R. bromii* degraded the substrate much further, compared to *B. adolescentis* during 72 h of incubation, as already indicated by quantifying remaining insoluble starch over time (Figure 6.1). Quantification of the remaining insoluble starch during incubation of N16-A with *B. adolescentis* was not conclusive, since we found a similar insoluble starch recovery in the incubated N16-A with and without *B. adolescentis* (Supplementary table 6.1). From these SEM images (Figure 6.6-BA) it is clear that *B. adolescentis* degraded N16-A partially, confirming the acetate generated during incubation (Figure 6.2) and potentially even degraded the substrate more than the digestible part only.

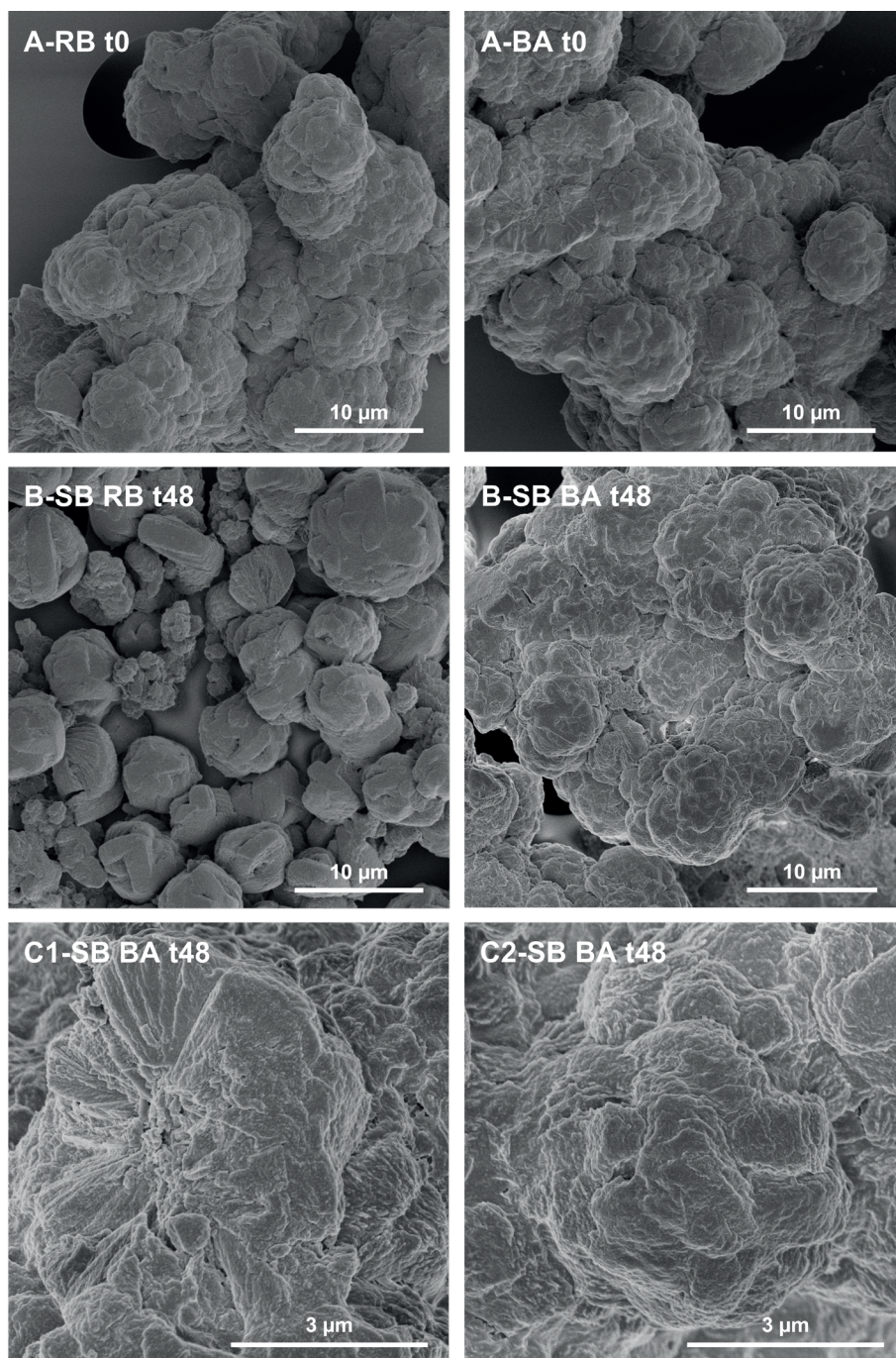


Figure 6.5. SEM images (5000 \times & 25,000 \times magnified) of A: Intrinsic RS-3 N16-A with *R. bromii* (RB) or *B. adolescentis* (BA) at t0 and B: incubated N16-A without RB (in mGAM) or BA (in mSIEM) for 48 h, C: incubated N16-A without BA for 48 h.

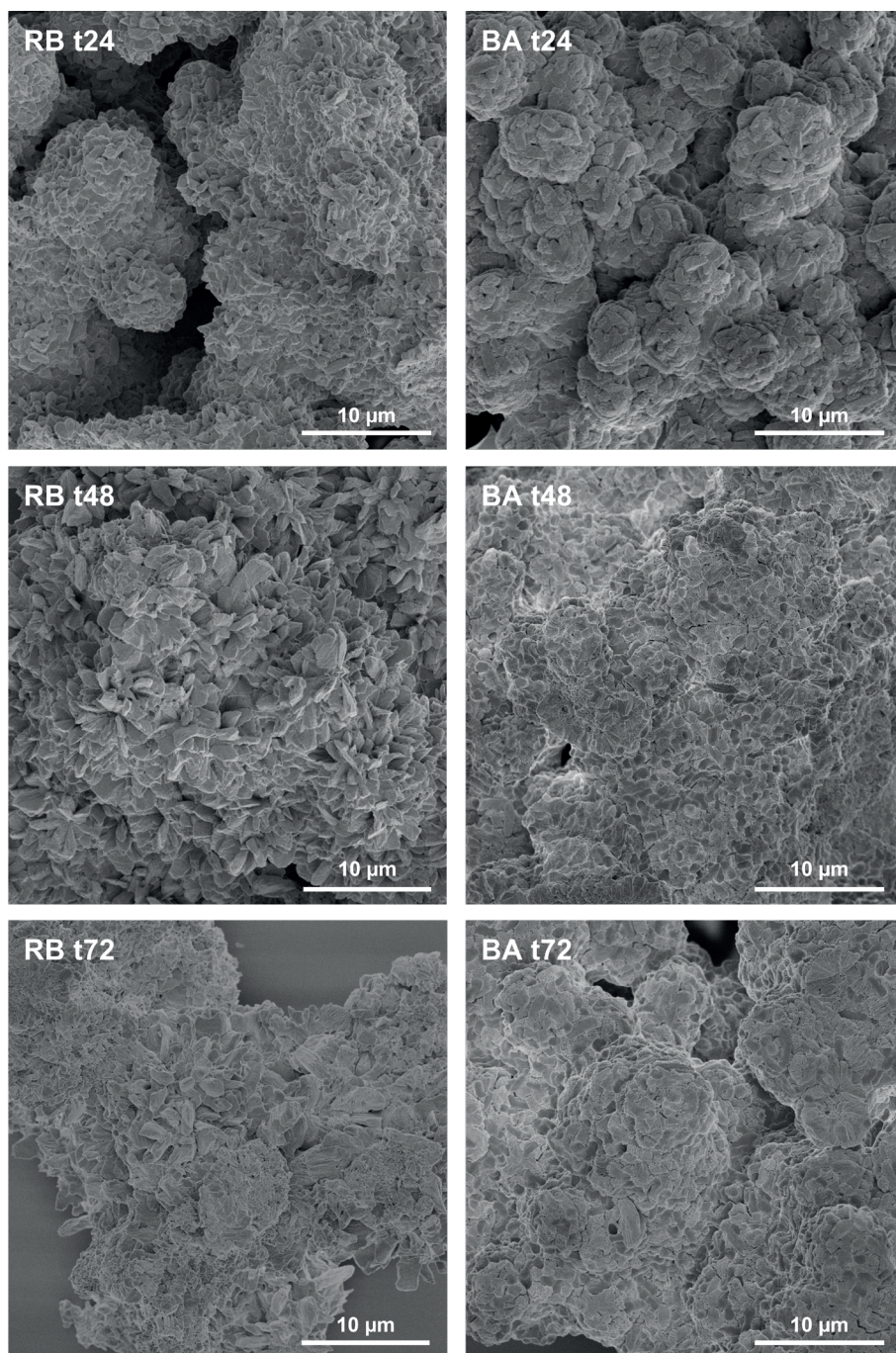


Figure 6.6. SEM images (5000 × magnified) of intrinsic RS-3 N16-A with *R. bromii* (RB) or *B. adolescentis* (BA) at 24, 48 and 72 h of incubation.

More detailed images of N16-A incubated with *R. bromii* and *B. adolescentis* over time, clearly show the bacteria (Figure 6.7 - white arrows). *R. bromii* is a tiny coccus-shaped bacterium of $\pm 0.5 \mu\text{m}$, sometimes present as diplococcus or in a chain of cocci. Over time, it can be observed that *R. bromii* cells were attached all over the substrate, in between the rectangular blocks (black arrow, t24) and the spiky structures (t48) (Figure 6.7-RB). After 72 h of incubation, less *R. bromii* cells were recognizable, probably related to the *R. bromii* growth curve, and also here, it is clear that the initial structure of N16-A was completely lost. Incubation of another A-type intrinsic RS-3 (P21-A) with *R. bromii* also resulted in complete loss of the initial structure after 72 h of incubation (Supplementary figure 6.3).

Such detailed images of N16-A incubated with *B. adolescentis* over time clearly show rod-shaped bacteria of $\pm 0.8 \mu\text{m}$ attached to the N16-A substrate (Figure 6.7-BA-t24). The structure of the rectangular blocks became clearly visible and seem to consist of long aligned fibres that together formed such a rectangular block (black arrow). After 48 h of incubation with *B. adolescentis*, still some bacterial cells were recognizable attaching to the N16-A substrate (white arrows), but these cells were more hidden within cavities. Additionally, some tiny empty cavities ($1\text{--}2 \mu\text{m}$) were visible (black arrows), probably resulting from hydrolysis of N16-A by *B. adolescentis*. After 72 h of incubation with *B. adolescentis*, less bacterial cells were visible, probably completely hidden within the partially degraded N16-A structure. A close look on the starch structure shows that the N16-A rectangular blocks became more spiky (black arrow). Degradation of N16-A by *B. adolescentis* was very different from degradation by *R. bromii*, since the initial N16-A structure after 72 h of incubation with *B. adolescentis* was still somewhat recognizable. Although slightly less degraded, similar results were obtained during incubation of another A-type intrinsic RS-3 (P21-A) with *B. adolescentis* (Supplementary figure 6.4).

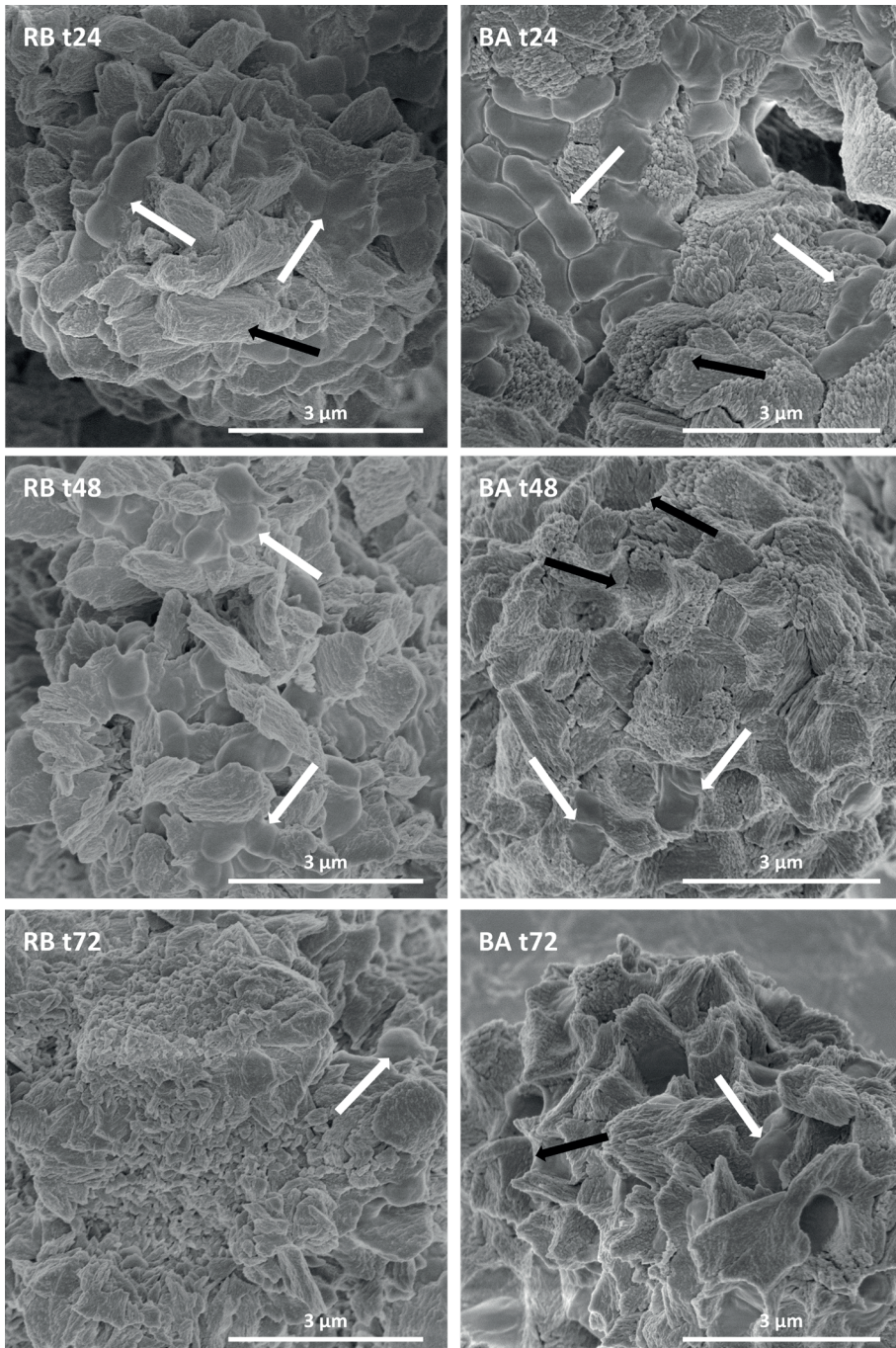


Figure 6.7. Detailed SEM images (25,000 x magnified) of intrinsic RS-3 N16-A with *R. bromii* (RB) or *B. adolescentis* (BA) at 24, 48 and 72 h of incubation. The white arrows point towards bacteria and the black arrows to specific starch structures.

We also investigated the morphology of two B-type intrinsic RS-3 substrates N32-B and N76-B. N32-B consisted of spherical particles of $\pm 3\text{--}7\text{ }\mu\text{m}$ with a quite smooth surface (Figure 6.8-N32-B). The spheres were partially connected to each other and a clear interconnection was visible. N76-B, prepared from longer chain length α -1,4 glucans, consisted of smaller particles of $\pm 2\text{--}3\text{ }\mu\text{m}$ with a much rougher surface compared to N32-B, which were also interconnected to each other (Figure 6.8 – N76-B). Also for these substrates, we confirmed that incubation in medium without bacteria did not change the starch morphology (Supplementary figure 6.5, Supplementary figure 6.6).

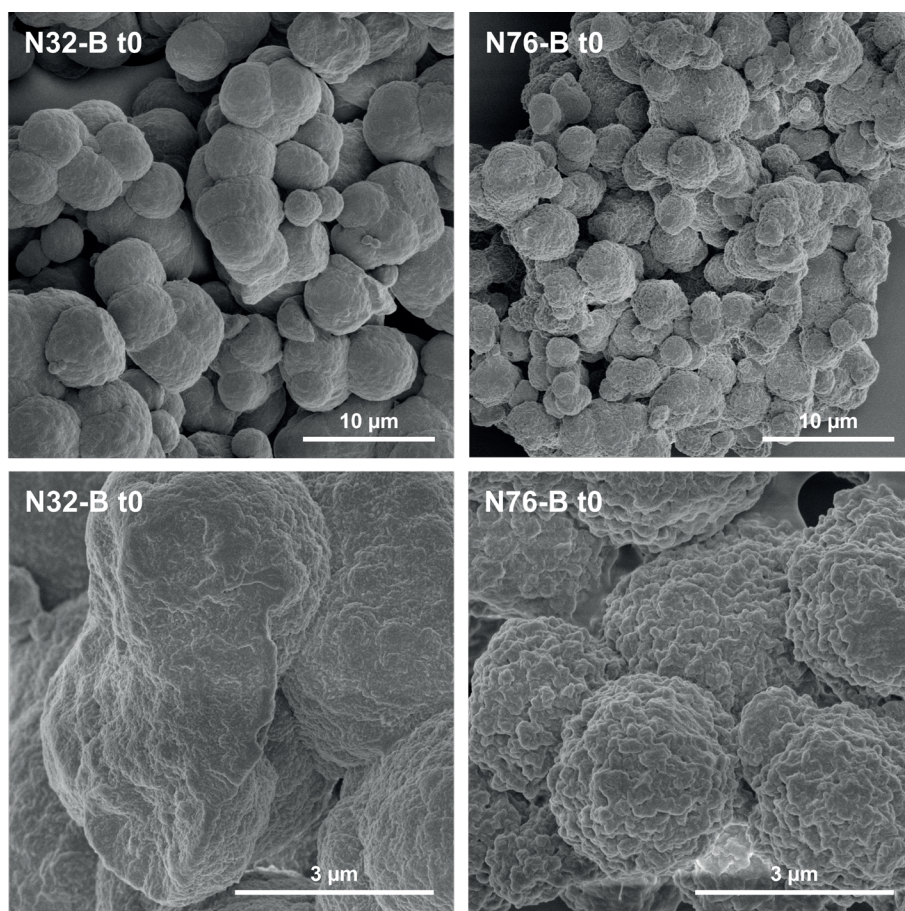


Figure 6.8. SEM images (5000 or 25,000 \times magnified) of intrinsic RS-3 N32-B and N76-B with *R. bromii* at t0.

B. adolescentis was unable to degrade B-type intrinsic RS-3, as confirmed by the lack of acetate and lactate generated (Figure 6.2) and the lack of changes in starch morphology during 72 h of incubation of N32-B and N76-B (Supplementary figure 6.7). Additionally, no clear attachment of *B. adolescentis* cells to B-type intrinsic RS-3 was observed (Supplementary figure 6.7). In contrast, *R. bromii* degraded both N32-B and N76-B, hydrolysing these substrates to primarily glucose and maltose (Figure 6.4).

During incubation of N32-B with *R. bromii*, the initial spherical structure could be recognized at all time points (Figure 6.9-N32-B). Nevertheless, changes in the surface were visible over incubation time. After 24 h of incubation with *R. bromii*, the surface of the initially rather smooth N32-B structure, became more rough, which was even better visible after 48 h of incubation. After 72 h of incubation of *R. bromii* with N32-B, tiny holes within the substrate were recognizable. In contrast, incubation of N76-B with *R. bromii* over time, did not result in major changes of the overall initial N76-B structure (Figure 6.9-N76-B).

Coccus-shaped bacteria were recognizable on more detailed images of N32-B and N76-B during incubation with *R. bromii* (Figure 6.10 – white arrows). After 24 h of incubation with *R. bromii*, the initial smooth structure of N32-B was lost (Figure 6.10-N32-B). The surface of the N32-B spheres became more rough and spiky, whereas at other spots the inside of an N32-B became visible (black arrows). For other N32-B spots, the spiky and rough outer layer was already lost, whereas after 48 h of incubation with *R. bromii* the N32-B spheres completely lacked the spiky and rough outer layer. Interestingly, after 48 h of incubation of N32-B with *R. bromii*, bacterial cells were mostly visible on the interconnection between two spheres. Already at 48 h of incubation, tiny holes of 80-90 nm within the N32-B spheres were recognizable, which were better visible after 72 h of incubation (black arrow). Here, coccus-shaped bacteria were fully embedded within the fully changed N32-B structure.

In contrast to incubation of N32-B with *R. bromii*, the morphology of N76-B did not change dramatically when incubated with *R. bromii* (Figure 6.10-N76-B). As also observed for N32-B, after 24 h of incubation, coccus-shaped bacteria were clearly recognizable (white arrows) attached to the N76-B spherical particles. After 48 h of incubation with *R. bromii*, coccus-shaped bacteria were again mostly visible on the interconnection between two N76-B spheres, similar to N32-B, and the N76-B structure became somewhat more spiky, compared to the surface of the initial N76-B spheres (Figure 6.8-N76-B).

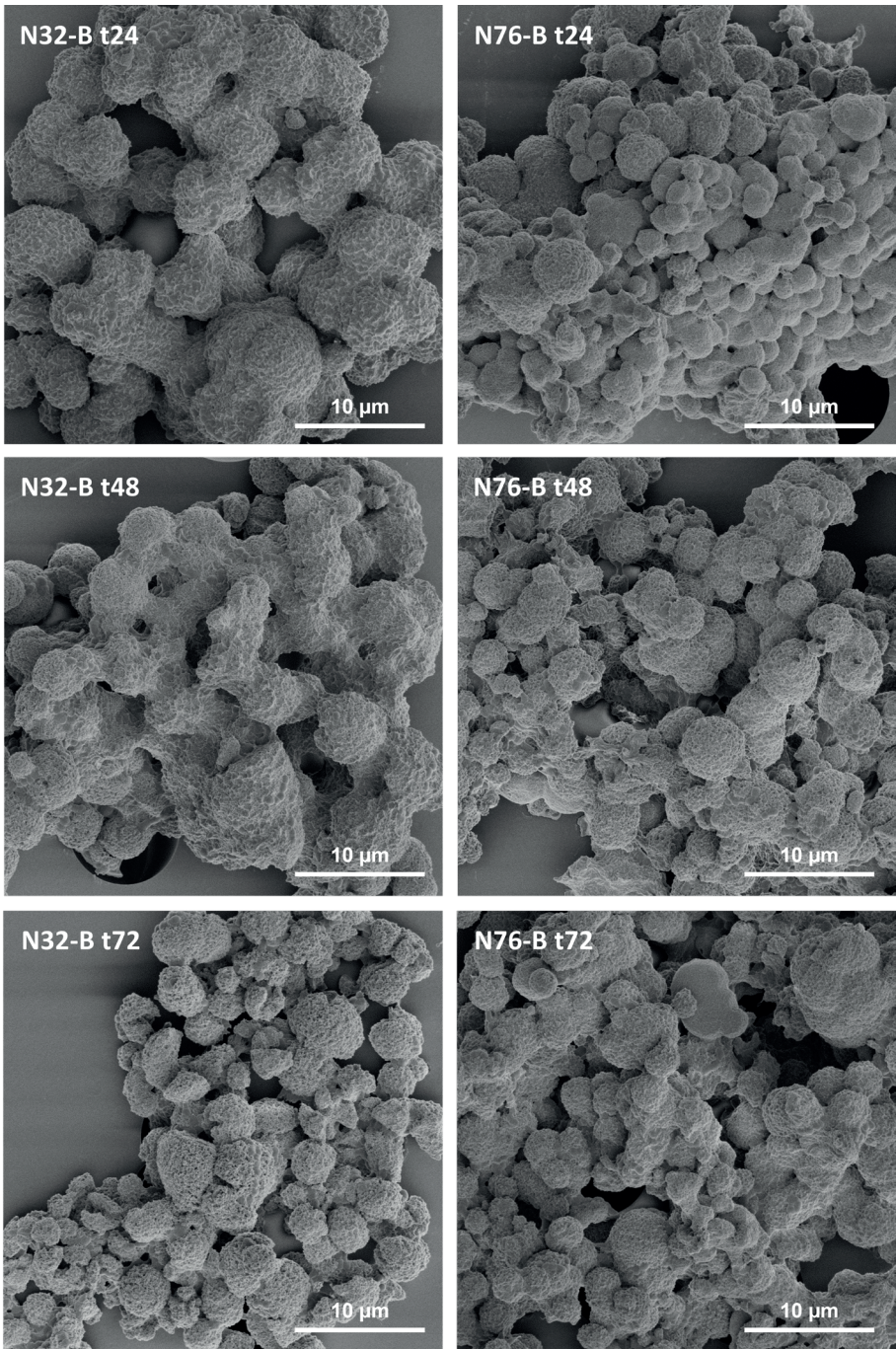


Figure 6.9. SEM images (5000 x magnified) of intrinsic RS-3 N32-B or N76-B with *R. bromii* at 24, 48 and 72 h of incubation.

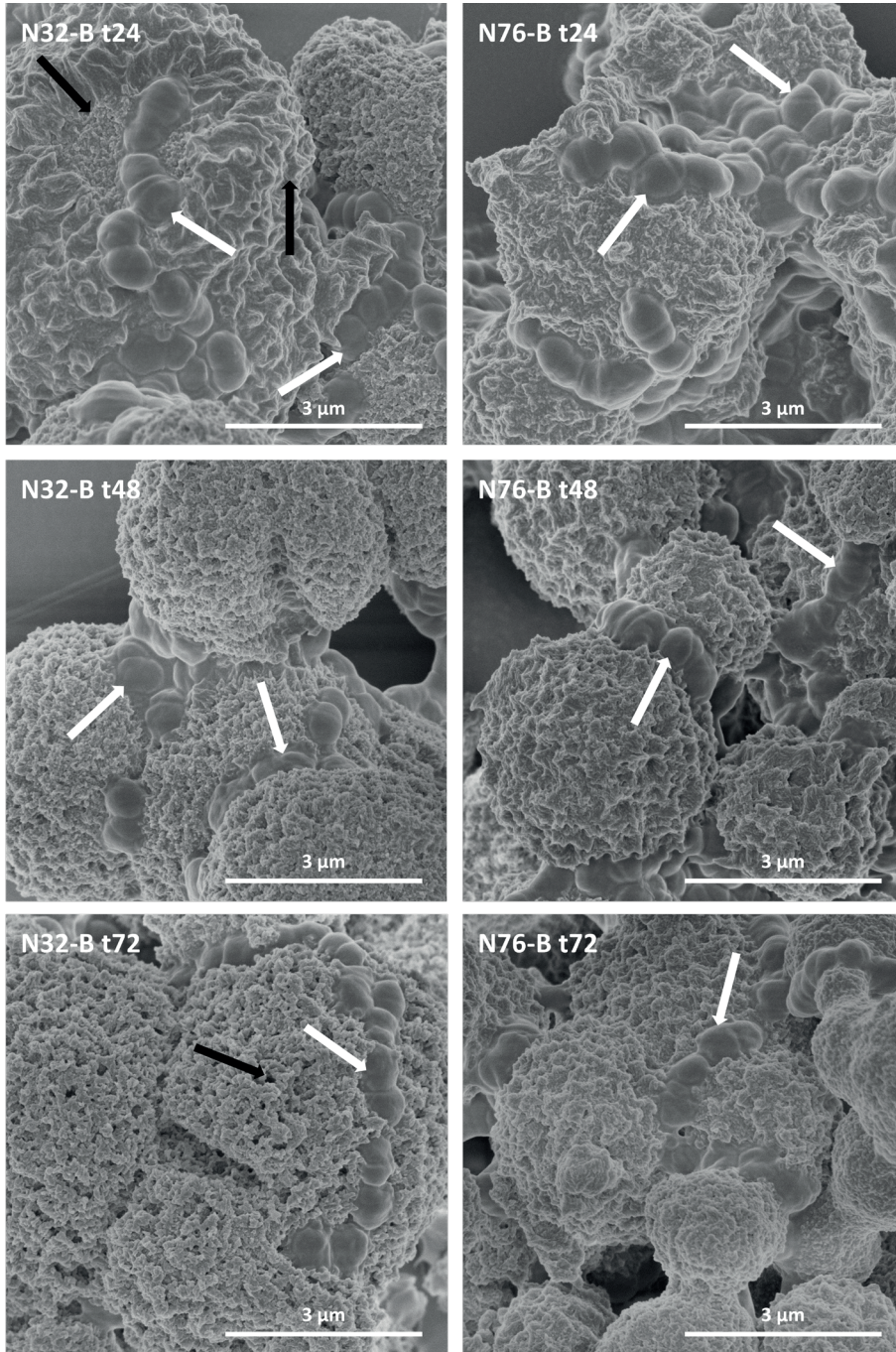


Figure 6.10. SEM images (25,000 × magnified) of intrinsic RS-3 N32-B or N76-B with *R. bromii* at 24, 48 and 72 h of incubation. The white arrows point towards bacteria and the black arrows to specific starch structures.

Although N32-B and N76-B were both prepared from narrow disperse α -1,4 glucans, crystallized in a B-type crystal polymorph and only differed in the α -1,4 glucan chain length (DPn 32 vs DPn 76), their change in morphology due to degradation by *R. bromii* differed. N32-B apparently consisted of spheres of two unique structures, one dense outer structure that first had to be degraded by *R. bromii* resulting in a spiky layer, under which a more smooth inner particle became visible. In contrast, these two unique layers were not detected in N76-B. Furthermore, after 72 h of incubation with *R. bromii*, much more tiny holes within the N32-B spheres, compared to N76-B spheres, were detected. For both N32-B and N76-B, *R. bromii* especially attached to the interconnection between two spherical particles.

Comparing initial intrinsic B-type RS-3 N32-B and N76-B with intrinsic A-type intrinsic RS-3 N16-A, many differences in morphology were visible. N16-A consisted of rectangular blocks that were connected to each other in a sphere, whereas N32-B and N76-B did not have a suborder and just consisted of spheres. After 72 h of incubation with *R. bromii* the initial structure of N16-A was completely lost, whereas for N32-B and N76-B the overall initial spherical particles could still be recognized, although in the case of N32-B fully pierced with tiny holes.

Both *B. adolescentis* and *R. bromii* degraded native maize and potato starch granules as shown by quantitative analysis and as confirmed by SEM images (Supplementary figure 6.8-6.11). During incubation of N16-A, P21-A, maize and potato granules with *B. adolescentis*, a potential biofilm was formed (Supplementary figure 6.12), clearly visible on some images.

4. Discussion

R. bromii and *B. adolescentis* are both recognized as primary degraders of resistant starch in the gut, although they have a quite different starch degrading machinery^[3]. *R. bromii* degrades starch to malto-oligomers, maltose and glucose and generates acetate, ethanol, formate and propanol^[44]. *B. adolescentis* degrades starch and takes up malto-oligomers via ABC-transporters and ferments them via the bifid shunt to acetate and lactate^[35]. In this research, we studied the ability of *R. bromii* and *B. adolescentis* to degrade and ferment novel intrinsic RS-3 substrates with specific physico-chemical characteristics. We found that *R. bromii* was able to degrade all four intrinsic RS-3 substrates, differing in crystal type and α -1,4 glucan chain length, to a major extent (Figure 6.1-A). In contrast,

B. adolescentis was only able to degrade A-type intrinsic RS-3 to a minor extent (Figure 6.1-B, Figure 6.6).

R. bromii degraded all intrinsic RS-3 and native granules efficiently, but degradation rates slightly differed among the substrates. The *R. bromii* enzymes hydrolysed the insoluble starch to primarily glucose and maltose, released into the spent medium (Figure 6.4). Such release of glucose and maltose in the spent medium was also observed previously, when *R. bromii* was incubated with native^[20] or retrograded high-amylose maize starch^[44], likely because *R. bromii* produces more of these products than it requires to grow. It is known that *R. bromii* cannot ferment glucose, is able to utilize maltose slightly, whereas it is able to utilize maltotriose, maltotetraose and fructose equally well^[20] and was shown to utilize galactose too in strains obtained from humans^[22]. Due to the lack of glucose utilization and restricted maltose utilization, *R. bromii* cross-feeds other bacteria such as *A. rectalis*^[20] that utilize these released sugars for the production of e.g. butyrate^[45]. We detected only a minor amount of ethanol and acetate in the spent medium of *R. bromii* incubated with intrinsic RS-3, maize and potato granules or fully soluble HBPS, primarily produced during the first 24 h, whereas we did not detect any formate (Figure 6.2-A). Previously, low levels of formate (2-3 mM), ethanol (8-10 mM) and acetate (30 mM) were detected during the exponential phase of *R. bromii* growth, with increased levels in the stationary phase, both when incubated with soluble starch or retrograded high-amylose maize starch^[44]. Additionally, these authors reported minor propanol production (0.4-0.8 mM) by *R. bromii*, especially in the stationary phase, which did not elute within our HPLC run time and could have been formed in our study as well. The lower levels of acetate detected in our study, compared to Crost et al. (2018)^[44] could be explained by the other strain (*R. bromii* L2-36) and conditions used by these authors. Our results and that of others^[20, 44] indicate that *R. bromii* still continued to degrade insoluble starch to soluble glucose and maltose, even when it was not utilizing these sugars anymore, thereby releasing easily fermentable sugars that via cross-feeding can be further utilized to produce SCFAs.

B. adolescentis only degraded A-type intrinsic RS-3 to a minor extent, whereas it rapidly degraded maize and potato starch within the first 24 h, after which fermentation slowed down (Figure 6.1-B). The fast initial degradation followed by slowing down can likely be explained by the growth curve of *B. adolescentis*. We did not observe any amylase activity in the spent cell-free medium (Supplementary table 6.3), potentially confirming that *B. adolescentis* RS-degrading enzymes are cell-wall anchored^[33]. *B. adolescentis* fermented HBPS and maize starch to lactate and acetate in a ratio of 0.4, whereas potato starch

and A-type intrinsic RS-3 were fermented to ratios of 0.3 and 0.1, respectively (Figure 6.2-B). *B. adolescentis* fermented A-type RS-3 thus very differently compared to HBPS and maize starch. It is known that bifidobacteria ferment carbohydrates to different ratios of acetate and lactate, depending on the species, the substrate^[46] and the growth rate^[47]. In a recent study based on metabolic models, it was shown that bifidobacteria tend to lean towards lactate production in the case of polysaccharides, whereas the balance acetate and lactate is more 1-to-1 in the case of monosaccharides^[31]. Although that might be true for easily fermentable substrates, this seems not to be the case for our complex insoluble RS-3. Previously, it was shown that due to a limit in energy *B. breve* would change from lactate production towards acetyl phosphate to maximise ATP synthesis^[48]. Probably, catalytic activity by the *B. adolescentis* enzymes towards intrinsic A-type RS-3 was so slow, that there was a limit in energy and therefore a lack of lactate production. Also O'Callaghan and Van Sinderen (2016) reported in their review that less lactate is produced by bifidobacteria when the energy source is consumed at a slow rate^[35].

For *R. bromii* we found slight differences in the rate of insoluble starch degradation for various substrates (Figure 6.1-A) and also the mechanism of degradation seemed different as indicated by the SEM images where intrinsic B-type RS-3 was pierced with tiny holes after fermentation, which was not recognized with A-type intrinsic RS-3 (Figure 6.7, Figure 6.10). We observed low amylase activity in the spent cell-free medium and no pronounced differences among the substrates (Supplementary table 6.4), which might confirm a previous finding where most of the amylase activity was detected in the cell pellet, rather than in the spent medium, indicating that the amylases are cell-associated^[23]. Substrate specificity differs among *R. bromii* strains and within a strain, with e.g. faster degradation of cooked high-amylose maize starch, compared to cooked (partially digestible) Novelose® 330^[22]. *R. bromii* possesses a starch-degrading machinery called amylosome, able to degrade starch substrates of many sources^[23], not yet found for any other species. The amylosome is thought to be anchored in the *R. bromii* cell-wall, and consists of four GH13 enzymes called Amy4 (amylase), Amy9 (amylase), Amy10 (pullulanase) and Amy12 (pullulanase), and containing dockerin and cohesin modules that provide stability to the amylosome complex^[22, 23]. Additionally, cell-free amylosome complexes have also been proposed to form between Amy4, Amy9, Amy10, Amy12 and Amy16 (amylase) and structural proteins containing cohesin domains (scaffoldin 3 or scaffoldin 4)^[22]. The presence of such cell-free amylosome complexes could explain the tiny holes obtained in B-type intrinsic RS-3, likely produced by extracellular amylases excreted in the medium.

Recently, it was shown that another amylase (Amy5), not being part of the amylosome complex, but present on the cell-surface of *R. bromii* did not contain any CBM and preferred binding of short α -1,4 glucans^[26]. This amylase produced primarily maltose from among others amylose, amylopectin and soluble starch with lower levels of glucose^[28]. Activity such as shown for Amy5 could explain why we primarily found maltose and glucose in the spent medium. However, how *R. bromii* exactly degraded these intrinsic RS-3 substrates remains to be discovered.

It is remarkable that *B. adolescentis* was unable to degrade B-type intrinsic RS-3 and only degraded A-type intrinsic RS-3 slowly, but easily degraded native maize and potato starch granules. Utilization of potato granules by another *B. adolescentis* strain was also shown previously^[8]. *B. adolescentis* L2-32 encodes seven extracellular starch-specific GH13 enzymes^[30, 49], including multiple CBMs of which one CBM74, associated with insoluble starch binding^[29, 36]. Recently, it was shown that other *B. adolescentis* strains (DSM 20083, previously not indicated as RS-degrading strain^[34], and DSM 24849) degraded highly resistant RS-3 preparations with varying amount of α -1,6 branch points for $\pm 20 - 80 \%$ ^[50]. Nevertheless, these RS-3 preparations, having a B-type polymorph, were prepared from much longer α -1,4 glucans (3.46×10^4 Da)^[50] and were probably less crystalline than ours. Why *B. adolescentis* L2-32 was unable to degrade B-type intrinsic RS-3 and fermented A-type intrinsic RS-3 only slightly and if other *B. adolescentis* strains can utilize intrinsic RS-3, remains to be discovered in the future.

It has been shown by Nagara et al. (2022) that when both *R. bromii* and *B. adolescentis* were present in the faecal microbiome, especially *B. adolescentis* increased in relative abundance when subjects consumed raw potato starch^[8], together with increased acetate levels in the faeces. In contrast, subjects that did not harbour *B. adolescentis*, but *R. bromii* and *A. rectalis* in their microbiome, showed increases in relative abundance of primarily *A. rectalis*, together with its metabolite butyrate, after the intervention. These authors suggested that *B. adolescentis* is more competitive than *R. bromii* and could even take over the surface of potato starch granules when first *R. bromii* fully covered this surface *in vitro*^[8]. Since raw potato starch is efficiently degraded by both primary degraders *R. bromii* and *B. adolescentis* (Figure 6.1), it is considered to be a non-specific dietary fibre^[51]. In contrast, intrinsic RS-3 might be more specific, promoting primarily *R. bromii*, even when subjects have both *R. bromii* and *B. adolescentis* in their microbiome. Supplementation of intrinsic RS-3 might thus be beneficial, since *R. bromii* could cross-feed to other microbes including butyrate

producers such as *A. rectalis*. If co-culture of these species with intrinsic RS-3 results in efficient butyrate production remains to be investigated.

5. Conclusions

This research is the first to study the fermentability of intrinsic RS-3 with specific physico-chemical characteristics by primary resistant starch degrading gut microbes *R. bromii* and *B. adolescentis*. *R. bromii* was able to degrade all intrinsic RS-3 substrates and hydrolysed these to primarily maltose and glucose, although it did not benefit from the released sugars and needed components from the medium to sustain its growth. Using SEM, *R. bromii* cells were clearly detected attached to the substrates. After 48 and 72 h of incubation, tiny holes were found within B-type intrinsic RS-3, but not within A-type intrinsic RS-3, potentially indicating a different degradation mechanism. *B. adolescentis* was unable to degrade B-type intrinsic RS-3 and was only slightly able to degrade A-type intrinsic RS-3. *B. adolescentis* cells clearly attached to A-type intrinsic RS-3, whereas this was not observed for B-type intrinsic RS-3. It can be concluded that a highly specific enzyme machinery, such as expressed by *R. bromii*, is required to be able to ferment intrinsic RS-3 in the gut. Future studies are needed to reveal the exact enzymatic pathways of intrinsic RS-3 degradation by *R. bromii* and *B. adolescentis*. The basic research performed in this study provides valuable information on primary degradation of RS-3, which could support future studies on the prebiotic potential of intrinsic RS-3.

6. Acknowledgement

The following reagent was obtained through BEI Resources, NIAID, NIH as part of the Human Microbiome Project: *Bifidobacterium adolescentis*, Strain L2-32, HM-633.

7. References

1. Lockyer S., Nugent A.P. Health effects of resistant starch. *Nutrition Bulletin*. **2017**;42(1):10-41.
2. Teichmann J., Cockburn D.W. In vitro fermentation reveals changes in butyrate production dependent on resistant starch source and microbiome composition. *Frontiers in Microbiology*. **2021**;12:640253.
3. Cerqueira F.M., Photenhauer A.L., Pollet R.M., Brown H.A., Koropatkin N.M. Starch digestion by gut bacteria: crowdsourcing for carbs. *Trends in Microbiology*. **2020**;28(2):95-108.
4. Flint H.J., Duncan S.H., Scott K.P., Louis P. Interactions and competition within the microbial community of the human colon: links between diet and health. *Environmental Microbiology*. **2007**;9(5):1101-1111.
5. Fu X., Liu Z., Zhu C., Mou H., Kong Q. Nondigestible carbohydrates, butyrate, and butyrate-producing bacteria. *Critical Reviews in Food Science & Nutrition*. **2019**;59(sup1):S130-S152.
6. Venkataraman A., Sieber J.R., Schmidt A.W., Waldron C., Theis K.R., Schmidt T.M. Variable responses of human microbiomes to dietary supplementation with resistant starch. *Microbiome*. **2016**;4(1):33.
7. Baxter N.T., Schmidt A.W., Venkataraman A., Kim K.S., Waldron C., Schmidt T.M. Dynamics of human gut microbiota and short-chain fatty acids in response to dietary interventions with three fermentable fibers. *mBio*. **2019**;10(1).
8. Nagara Y., Fujii D., Takada T., Sato-Yamazaki M., Odani T., Oishi K. Selective induction of human gut-associated acetogenic/butyrogenic microbiota based on specific microbial colonization of indigestible starch granules. *The ISME Journal*. **2022**.
9. Walker A.W., Ince J., Duncan S.H., Webster L.M., Holtrop G., Ze X., Brown D., Stares M.D., Scott P., Bergerat A., Louis P., McIntosh F., Johnstone A.M., Lobley G.E., Parkhill J., Flint H.J. Dominant and diet-responsive groups of bacteria within the human colonic microbiota. *The ISME Journal*. **2011**;5(2):220-230.
10. Cai L.M., Shi Y.C. Self-assembly of short linear chains to A- and B-type starch spherulites and their enzymatic digestibility. *Journal of Agricultural and Food Chemistry*. **2013**;61(45):10787-10797.
11. Kiatpongarp W., Tongta S., Rolland-Sabate A., Buleon A. Crystallization and chain reorganization of debranched rice starches in relation to resistant starch formation. *Carbohydrate Polymers*. **2015**;122:108-114.
12. Klostermann C.E., Buwalda P.L., Leemhuis H., de Vos P., Schols H.A., Bitter J.H. Digestibility of resistant starch type 3 is affected by crystal type, molecular weight and molecular weight distribution. *Carbohydrate Polymers*. **2021**;265:118069.
13. Cai L.M., Shi Y.C. Preparation, structure, and digestibility of crystalline A- and B-type aggregates from debranched waxy starches. *Carbohydrate Polymers*. **2014**;105:341-350.
14. Adra H.J., Zhi J., Luo K., Kim Y.R. Facile preparation of highly uniform type 3 resistant starch nanoparticles. *Carbohydrate Polymers*. **2022**;294:119842.
15. Cai L.M., Shi Y.C. Structure and digestibility of crystalline short-chain amylose from debranched waxy wheat, waxy maize, and waxy potato starches. *Carbohydrate Polymers*. **2010**;79(4):1117-1123.
16. Potocki-Veronese G., Putaux J.L., Dupeyre D., Albenne C., Remaud-Simeon M., Monsan P., Buleon A. Amylose synthesized in vitro by amylsucrase: morphology, structure, and properties. *Biomacromolecules*. **2005**;6(2):1000-1011.
17. Ohdan K., Fujii K., Yanase M., Takaha T., Kuriki T. Enzymatic synthesis of amylose. *Biocatalysis and Biotransformation*. **2006**;24(1-2):77-81.
18. Vital M., Howe A.C., Tiedje J.M. Revealing the bacterial butyrate synthesis pathways by analyzing (meta)genomic data. *mBio*. **2014**;5(2):e00889.

19. Klostermann C.E., Endika M.F., Ten Cate E., Buwalda P.L., de Vos P., Bitter J.H., Zoetendal E.G., Schols H.A. Type of intrinsic resistant starch type 3 determines in vitro fermentation by pooled adult faecal inoculum. *Accepted for publication in Carbohydrate Polymers*. **2023**.
20. Ze X., Duncan S.H., Louis P., Flint H.J. Ruminococcus bromii is a keystone species for the degradation of resistant starch in the human colon. *The ISME Journal*. **2012**;6(8):1535-1543.
21. Aravind N., Sissons M., Fellows C.M., Blazek J., Gilbert E.P. Optimisation of resistant starch II and III levels in durum wheat pasta to reduce in vitro digestibility while maintaining processing and sensory characteristics. *Food Chemistry*. **2013**;136(2):1100-1109.
22. Mukhopadhyaya I., Morais S., Laverde-Gomez J., Sheridan P.O., Walker A.W., Kelly W., Klieve A.V., Ouwerkerk D., Duncan S.H., Louis P., Koropatkin N., Cockburn D., Kibler R., Cooper P.J., Sandoval C., Crost E., Juge N., Bayer E.A., Flint H.J. Sporulation capability and amylosome conservation among diverse human colonic and rumen isolates of the keystone starch-degrader Ruminococcus bromii. *Environmental Microbiology*. **2018**;20(1):324-336.
23. Ze X., Ben David Y., Laverde-Gomez J.A., Dassa B., Sheridan P.O., Duncan S.H., Louis P., Henrissat B., Juge N., Koropatkin N.M., Bayer E.A., Flint H.J. Unique organization of extracellular amylases into amylosomes in the resistant starch-utilizing human colonic Firmicutes bacterium Ruminococcus bromii. *mBio*. **2015**;6(5):e01058-01015.
24. Zeng F., Chen F.Q., Kong F.S., Gao Q.Y., Aadil R.M., Yu S.J. Structure and digestibility of debranched and repeatedly crystallized waxy rice starch. *Food Chemistry*. **2015**;187:348-353.
25. Cerqueira F.M., Photenhauer A.L., Doden H.L., Brown A.N., Abdel-Hamid A.M., Morais S., Bayer E.A., Wawrzak Z., Cann I., Ridlon J.M., Hopkins J.B., Koropatkin N.M. Sas20 is a highly flexible starch-binding protein in the Ruminococcus bromii cell-surface amylosome. *Journal of Biological Chemistry*. **2022**;298(5):101896.
26. Cockburn D.W., Cerqueira F.M., Bahr C., Koropatkin N.M. The structures of the GH13_36 amylases from Eubacterium rectale and Ruminococcus bromii reveal subsite architectures that favor maltose production. *Amylase*. **2020**;4(1):24-44.
27. Cockburn D.W., Kibler R., Brown H.A., Duvall R., Morais S., Bayer E., Koropatkin N.M. Structure and substrate recognition by the Ruminococcus bromii amylosome pullulanases. *Journal of Structural Biology*. **2021**;213(3):107765.
28. Jung J.H., An Y.K., Son S.Y., Jeong S.Y., Seo D.H., Kim M.K., Park C.S. Characterization of a novel extracellular alpha-amylase from Ruminococcus bromii ATCC 27255 with neopullulanase-like activity. *International Journal of Biological Macromolecules*. **2019**;130:605-614.
29. Photenhauer A.L., Cerqueira F.M., Villafuerte-Vega R., Armbruster K.M., Mareček G., Chen T., Wawrzak Z., Hopkins J.B., Vander Kooi C.W., Janeček S., Ruotolo B.T., Koropatkin N.M. The Ruminococcus bromii amylosome protein Sas6 binds single and double helical α -glucan structures in starch. *bioRxiv*. **2022**.
30. Duranti S., Turrioni F., Lugli G.A., Milani C., Viappiani A., Mangifesta M., Gioiosa L., Palanza P., van Sinderen D., Ventura M. Genomic characterization and transcriptional studies of the starch-utilizing strain Bifidobacterium adolescentis 22L. *Applied Environmental Microbiology*. **2014**;80(19):6080-6090.
31. Devika N.T., Raman K. Deciphering the metabolic capabilities of Bifidobacteria using genome-scale metabolic models. *Scientific Reports*. **2019**;9(1):18222.
32. Ventura M., Canchaya C., Tauch A., Chandra G., Fitzgerald G.F., Chater K.F., van Sinderen D. Genomics of Actinobacteria: tracing the evolutionary history of an ancient phylum. *Microbiology and Molecular Biology Reviews*. **2007**;71(3):495-548.
33. Jung D.H., Seo D.H., Kim Y.J., Chung W.H., Nam Y.D., Park C.S. The presence of resistant starch-degrading amylases in Bifidobacterium adolescentis of the human gut. *International Journal of Biological Macromolecules*. **2020**;161:389-397.
34. Jung D.H., Kim G.Y., Kim I.Y., Seo D.H., Nam Y.D., Kang H., Song Y., Park C.S. Bifidobacterium adolescentis P2P3, a human gut bacterium having strong non-gelatinized

- resistant starch-degrading activity. *Journal of Microbiology and Biotechnology*. **2019**;29(12):1904-1915.
35. O'Callaghan A., Van Sinderen D. Bifidobacteria and their role as members of the human gut microbiota. *Frontiers in Microbiology*. **2016**;7:925.
 36. Valk V., Lammerts van Bueren A., van der Kaaij R.M., Dijkhuizen L. Carbohydrate-binding module 74 is a novel starch-binding domain associated with large and multidomain alpha-amylase enzymes. *FEBS Journal*. **2016**;283(12):2354-2368.
 37. Dobranowski P.A., Stintzi A. Resistant starch, microbiome, and precision modulation. *Gut Microbes*. **2021**;13(1):1926842.
 38. Desai M.S., Seekatz A.M., Koropatkin N.M., Kamada N., Hickey C.A., Wolter M., Pudlo N.A., Kitamoto S., Terrapon N., Muller A., Young V.B., Henrissat B., Wilmes P., Stappenbeck T.S., Nunez G., Martens E.C. A dietary fiber-deprived gut microbiota degrades the colonic mucus barrier and enhances pathogen susceptibility. *Cell*. **2016**;167(5):1339-1353 e1321.
 39. Cockburn D.W., Suh C., Medina K.P., Duvall R.M., Wawrzak Z., Henrissat B., Koropatkin N.M. Novel carbohydrate binding modules in the surface anchored alpha-amylase of *Eubacterium rectale* provide a molecular rationale for the range of starches used by this organism in the human gut. *Molecular Microbiology*. **2018**;107(2):249-264.
 40. Purwani E.Y., Purwadaria T., Suhartono M.T. Fermentation RS3 derived from sago and rice starch with *Clostridium butyricum* BCC B2571 or *Eubacterium rectale* DSM 17629. *Anaerobe*. **2012**;18(1):55-61.
 41. Aguirre M., Eck A., Koenen M.E., Savelkoul P.H., Budding A.E., Venema K. Evaluation of an optimal preparation of human standardized fecal inocula for in vitro fermentation studies. *Journal of Microbiological Methods*. **2015**;117:78-84.
 42. Moore W.E.C., Cato E.P., Holdeman L.V. *Ruminococcus bromii* sp. n. and Emendation of the Description of *Ruminococcus Sijpesteijn*. *International Journal of Systematic and Evolutionary Microbiology*. **1972**;22(2):78-80.
 43. Pokusaeva K., Fitzgerald G.F., van Sinderen D. Carbohydrate metabolism in Bifidobacteria. *Genes & Nutrition*. **2011**;6(3):285-306.
 44. Crost E.H., Le Gall G., Laverde-Gomez J.A., Mukhopadhyay I., Flint H.J., Juge N. Mechanistic insights into the cross-feeding of *Ruminococcus gnavus* and *Ruminococcus bromii* on host and dietary carbohydrates. *Frontiers in Microbiology*. **2018**;9:2558.
 45. Pryde S.E., Duncan S.H., Hold G.L., Stewart C.S., Flint H.J. The microbiology of butyrate formation in the human colon. *FEMS Microbiology Letters*. **2002**;217(2):133-139.
 46. Palframan R.J., Gibson G.R., Rastall R.A. Carbohydrate preferences of Bifidobacterium species isolated from the human gut. *Current Issues in Intestinal Microbiology*. **2003**;4(2):71-75.
 47. De Vuyst L., Leroy F. Cross-feeding between bifidobacteria and butyrate-producing colon bacteria explains bifidobacterial competitiveness, butyrate production, and gas production. *International Journal of Food Microbiology*. **2011**;149(1):73-80.
 48. Degnan B.A., Macfarlane G.T. Effect of dilution rate and carbon availability on Bifidobacterium breve fermentation. *Biotechnology*. **1994**;40:800-805.
 49. Crittenden R.G., Morris L.F., Harvey M.L., Tran L.T., Mitchell H.L., Playne M.J. Selection of a Bifidobacterium strain to complement resistant starch in a synbiotic yoghurt. *Journal of Applied Microbiology*. **2001**;90(2):268-278.
 50. Ryu H.J., Jung D.H., Yoo S.H., Tuncil Y.E., Lee B.H. Bifidogenic property of enzymatically synthesized water-insoluble α -glucans with different α -1,6 branching ratio. *Food Hydrocolloids*. **2022**;133.
 51. Cantu-Jungles T.M., Hamaker B.R. New view on dietary fiber selection for predictable shifts in gut microbiota. *mBio*. **2020**;11(1).

8. Supplementary information

Supplementary table 6.1. Insoluble and soluble (incl. glucose) starch recovery during incubation of starch with *B. adolescentis* L2-32

| Sample name | Time point (h) | Insoluble starch (%) | Soluble starch (%) |
|---------------|----------------|----------------------|--------------------|
| N16-A | 0 | 98.4 ± 3.3 | 1.4 ± 0.3 |
| | 24 | 90.4 ± 0.9 | 0.8 ± 0.2 |
| | 48 | 88.8 ± 4.8 | 0.7 ± 0.1 |
| | 72 | 85.5 ± 5.3 | 0.6 ± 0.0 |
| | SB 48 | 83.5 ± 0.5 | 11.4 ± 0.2 |
| P21-A | 0 | 99.1 ± 1.4 | 1.8 ± 0.5 |
| | 24 | 92.5 ± 3.6 | 0.9 ± 0.1 |
| | 48 | 103.0 ± 10.5 | 1.0 ± 0.1 |
| | 72 | 99.5 ± 1.5 | 0.7 ± 0.2 |
| | SB 48 | 81.6 ± 13.2 | 8.9 ± 0.2 |
| N32-B | 0 | 99.7 ± 5.1 | 1.8 ± 0.2 |
| | 24 | 99.4 ± 3.6 | 1.0 ± 0.1 |
| | 48 | 101.8 ± 4.2 | 1.0 ± 0.0 |
| | 72 | 95.0 ± 5.7 | 0.7 ± 0.2 |
| | SB 48 | 92.4 ± 1.8 | 8.8 ± 0.2 |
| N76-B | 0 | 98.7 ± 1.3 | 0 |
| | 24 | 97.6 ± 2.6 | 1.1 ± 0.2 |
| | 48 | 91.5 ± 9.4 | 1.7 ± 0.8 |
| | 72 | 99.2 ± 7.6 | 1.3 ± 0.6 |
| | SB 48 | 94.6 ± 4.0 | 1.2 ± 0.6 |
| Maize starch | 0 | 100.8 ± 3.4 | 0.1 ± 0.1 |
| | 24 | 57.0 ± 8.2 | 1.6 ± 0.0 |
| | 48 | 61.8 ± 10.8 | 1.3 ± 0.5 |
| | 72 | 28.4 ± 7.7 | 1.8 ± 0.3 |
| | SB 48 | 96.5 ± 4.7 | 0.8 ± 1.0 |
| Potato starch | 0 | 94.6 ± 2.3 | 0 |
| | 24 | 60.2 ± 4.8 | 0.9 ± 0.4 |
| | 48 | 39.8 ± 5.9 | 0.8 ± 0.1 |
| | 72 | 43.1 ± 14.8 | 0.6 ± 0.1 |
| | SB 48 | 90.8 ± 6.2 | 0.6 ± 0.0 |
| HBPS | 0 | n.a. | 101.9 ± 0.9 |
| | 24 | n.a. | 14.9 ± 5.6 |
| | 48 | n.a. | 4.5 ± 2.1 |
| | 72 | n.a. | 3.0 ± 0.1 |
| | SB 48 | n.a. | 102 ± 8.1 |

Supplementary table 6.2. Insoluble, soluble (excl. glucose) and glucose recovery during incubation of starch with *R. bromii* ATCC27255

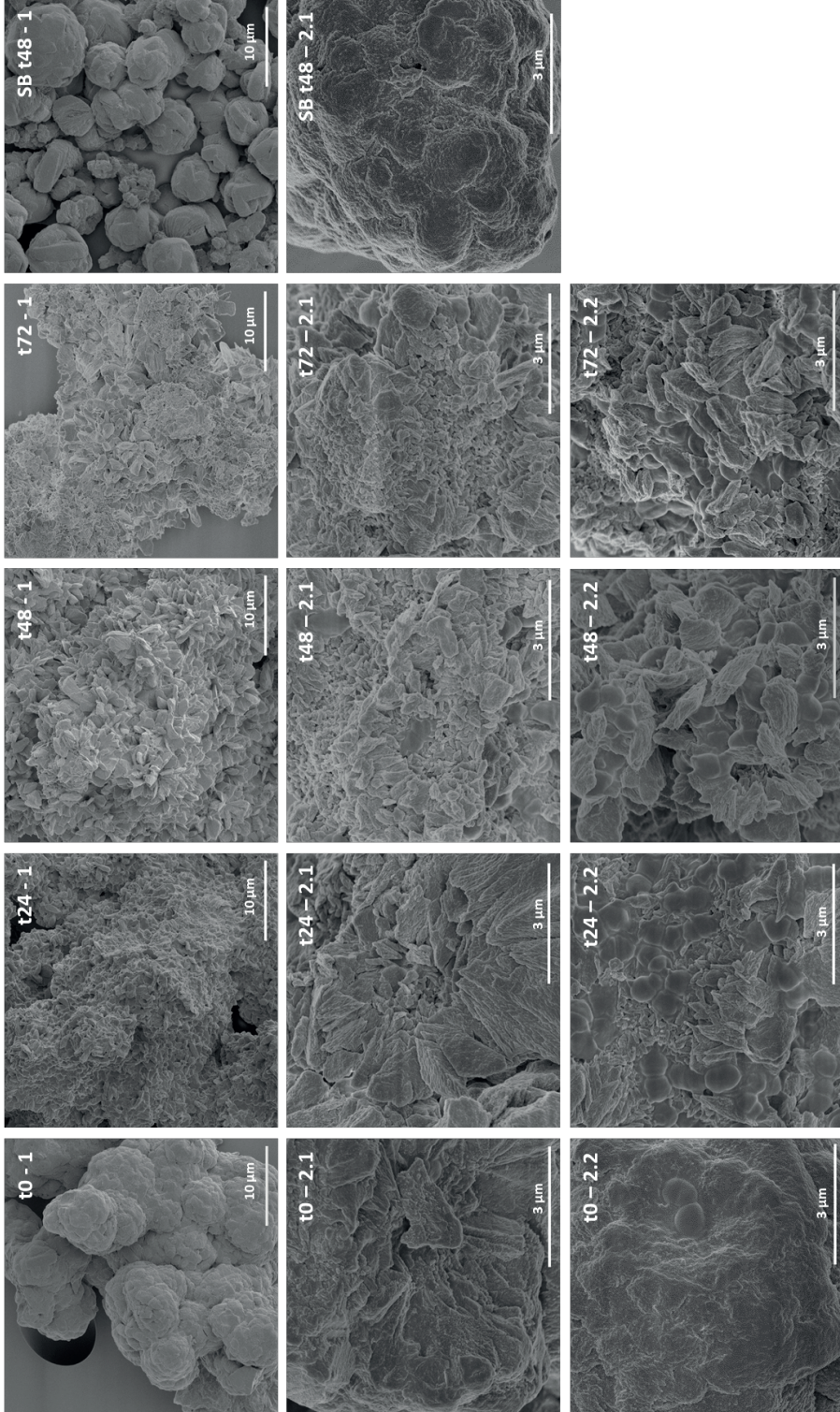
| Sample name | Time point (h) | Insoluble starch (%) | Soluble starch (%) | Glucose (%) |
|---------------------------|----------------|----------------------|--------------------|-------------|
| N16-A | 0 | 55.9 ± 1.0 | 36.9 ± 2.4 | 4.2 ± 0.1 |
| | 24 | 46.6 ± 3.0 | 31.0 ± 4.9 | 10.9 ± 0.4 |
| | 48 | 27.2 ± 3.6 | 27.0 ± 5.1 | 17.0 ± 0.4 |
| | 72 | 11.9 ± 3.1 | 30.4 ± 1.9 | 22.5 ± 0.2 |
| | SB 48 | 59.6 ± 1.5 | 39.5 ± 2.9 | 4.0 ± 0.3 |
| P21-A | 0 | 61.1 ± 63.5 | 34.3 ± 0.6 | 4.8 ± 1.5 |
| | 24 | 39.7 ± 2.8 | 32.7 ± 3.4 | 11.7 ± 0.7 |
| | 48 | 20.1 ± 0.8 | 28.3 ± 3.1 | 19.1 ± 0.7 |
| | 72 | 3.8 ± 0.0 | 32.6 ± 4.8 | 24.2 ± 0.4 |
| | SB 48 | 56.0 ± 4.5 | 36.9 ± 1.0 | 4.5 ± 1.4 |
| N32-B | 0 | 61.5 ± 2.8 | 35.3 ± 0.3 | 4.5 ± 0.1 |
| | 24 | 44.9 ± 3.1 | 27.9 ± 2.7 | 13.0 ± 3.1 |
| | 48 | 28.6 ± 2.7 | 22.5 ± 0.6 | 18.7 ± 0.5 |
| | 72 | 13.0 ± 1.7 | 26.1 ± 1.5 | 22.6 ± 1.1 |
| | SB 48 | 61.2 ± 7.3 | 33.2 ± 1.9 | 4.2 ± 0.6 |
| N76-B | 0 | 62.4 ± 1.3 | 35.3 ± 0.6 | 6.7 ± 3.8 |
| | 24 | 47.8 ± 1.6 | 27.6 ± 0.5 | 9.5 ± 0.3 |
| | 48 | 38.7 ± 5.8 | 20.7 ± 1.3 | 14.2 ± 1.9 |
| | 72 | 17.7 ± 0.7 | 24.2 ± 0.9 | 19.3 ± 1.4 |
| | SB 48 | 59.0 ± 0.4 | 32.5 ± 1.9 | 4.0 ± 0.1 |
| Maize starch | 0 | 63.1 ± 1.8 | 35.2 ± 4.3 | 5.0 ± 0.3 |
| | 24 | 49.4 ± 0.5 | 31.4 ± 4.1 | 12.9 ± 1.5 |
| | 48 | 33.6 ± 0.9 | 27.5 ± 5.1 | 19.9 ± 2.8 |
| | 72 | 12.1 ± 2.2 | 31.8 ± 0.9 | 27.7 ± 4.2 |
| | SB 48 | 60.7 ± 2.0 | 30.5 ± 3.5 | 5.5 ± 2.4 |
| Potato starch | 0 | 63.3 ± 2.2 | 31.0 ± 4.3 | 6.9 ± 4.5 |
| | 24 | 51.8 ± 6.9 | 23.8 ± 3.7 | 10.5 ± 2.5 |
| | 48 | 48.5 ± 7.0 | 16.2 ± 1.5 | 13.1 ± 0.6 |
| | 72 | 28.5 ± 1.3 | 21.2 ± 0.0 | 17.1 ± 1.2 |
| | SB 48 | 62.3 ± 1.7 | 32.3 ± 0.2 | 4.3 ± 0.6 |
| HBPS | 0 | n.a. | 100.3 ± 3.7 | 4.6 ± 1.1 |
| | 24 | n.a. | 81.9 ± 1.5 | 17.2 ± 0.7 |
| | 48 | n.a. | 65.0 ± 0.8 | 23.6 ± 0.6 |
| | 72 | n.a. | 57.4 ± 1.7 | 25.0 ± 0.9 |
| | SB 48 | n.a. | 90.0 ± 5.2 | 5.1 ± 0.3 |
| <i>R. bromii</i> blank | 0 | n.a. | 83.9 ± 7.1 | 16.7 ± 9.2 |
| | 24 | n.a. | 58.8 ± 0.9 | 19.3 ± 0.9 |
| | 48 | n.a. | 28.1 ± 1.0 | 19.3 ± 0.7 |
| | 72 | n.a. | 27.9 ± 1.6 | 23.6 ± 2.5 |
| | SB 48 | n.a. | 88.6 ± 4.6 | 10.8 ± 1.5 |

Supplementary table 6.3. Extracellular α -amylase activity, secreted in the supernatant by *B. adolescentis* L2-32 during 72 h of incubation. The average of two biological duplicates is given. One Ceralpha unit of activity is the amount of enzyme required to release one micromole of p-nitrophenol from BPNG7 per minute, per mL fermentation medium.

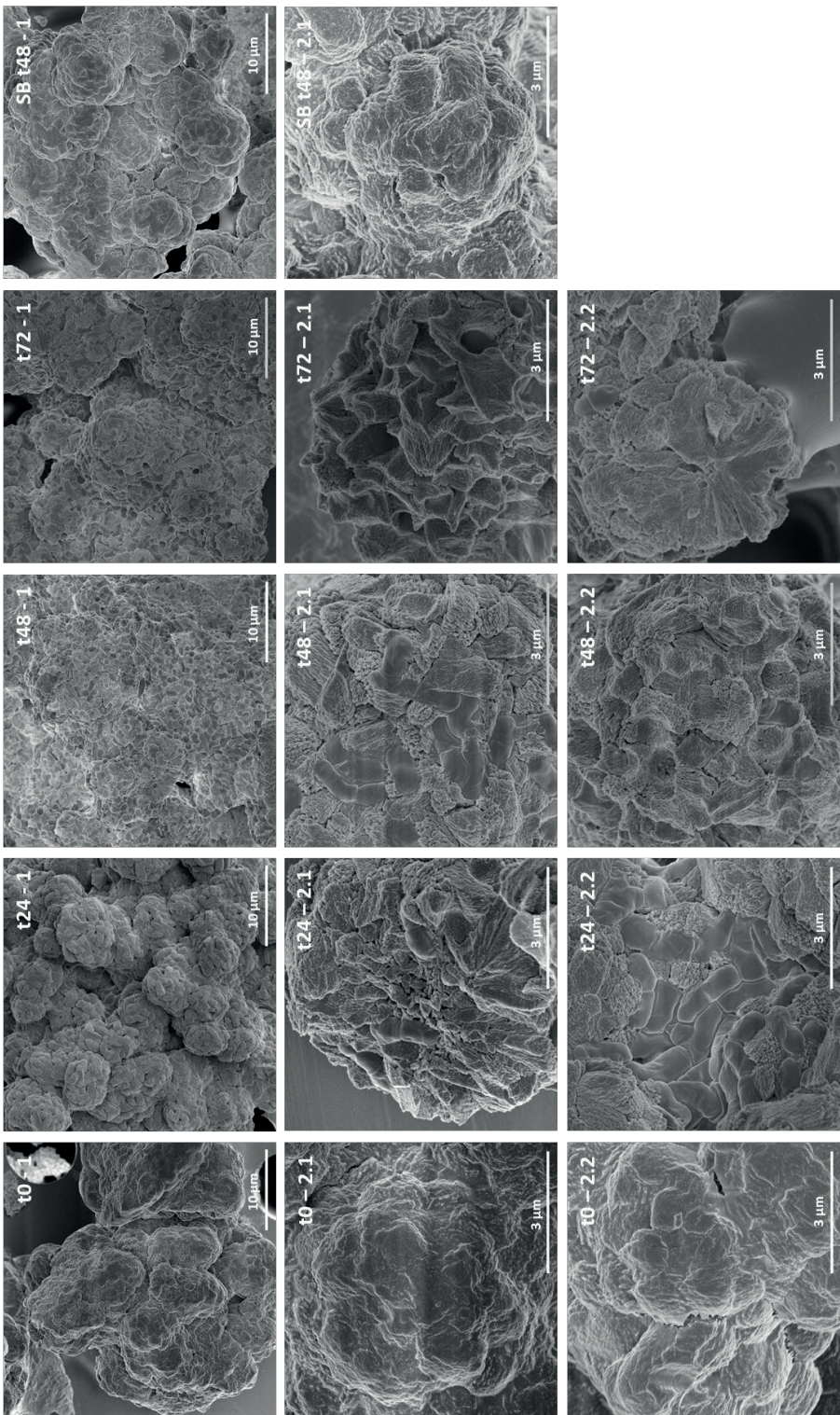
| Sample name | t0 | t24 | t48 | t72 |
|------------------------------|---------|---------|---------|---------|
| sG2A | 0.0001 | 0.0040 | 0.0048 | 0.0043 |
| P21-A | 0.0001 | 0.0035 | 0.0035 | 0.0038 |
| N32-B | 0.0000 | 0.0015 | 0.0021 | 0.0019 |
| N76-B | 0.0001 | 0.0016 | 0.0014 | 0.0013 |
| Maize | 0.0000 | 0.0070 | 0.0052 | 0.0054 |
| Potato | 0.0001 | 0.0068 | 0.0066 | 0.0063 |
| HBS | -0.0001 | -0.0012 | -0.0008 | -0.0016 |
| <i>B. adolescentis</i> blank | 0.0001 | 0.0013 | 0.0016 | 0.0015 |

Supplementary table 6.4. Extracellular α -amylase activity, secreted in the supernatant by *R. bromii* ATCC27255 during 72 h of incubation. The average of two biological duplicates is given. One Ceralpha unit of activity is the amount of enzyme required to release one micromole of p-nitrophenol from BPNG7 per minute, per mL fermentation medium.

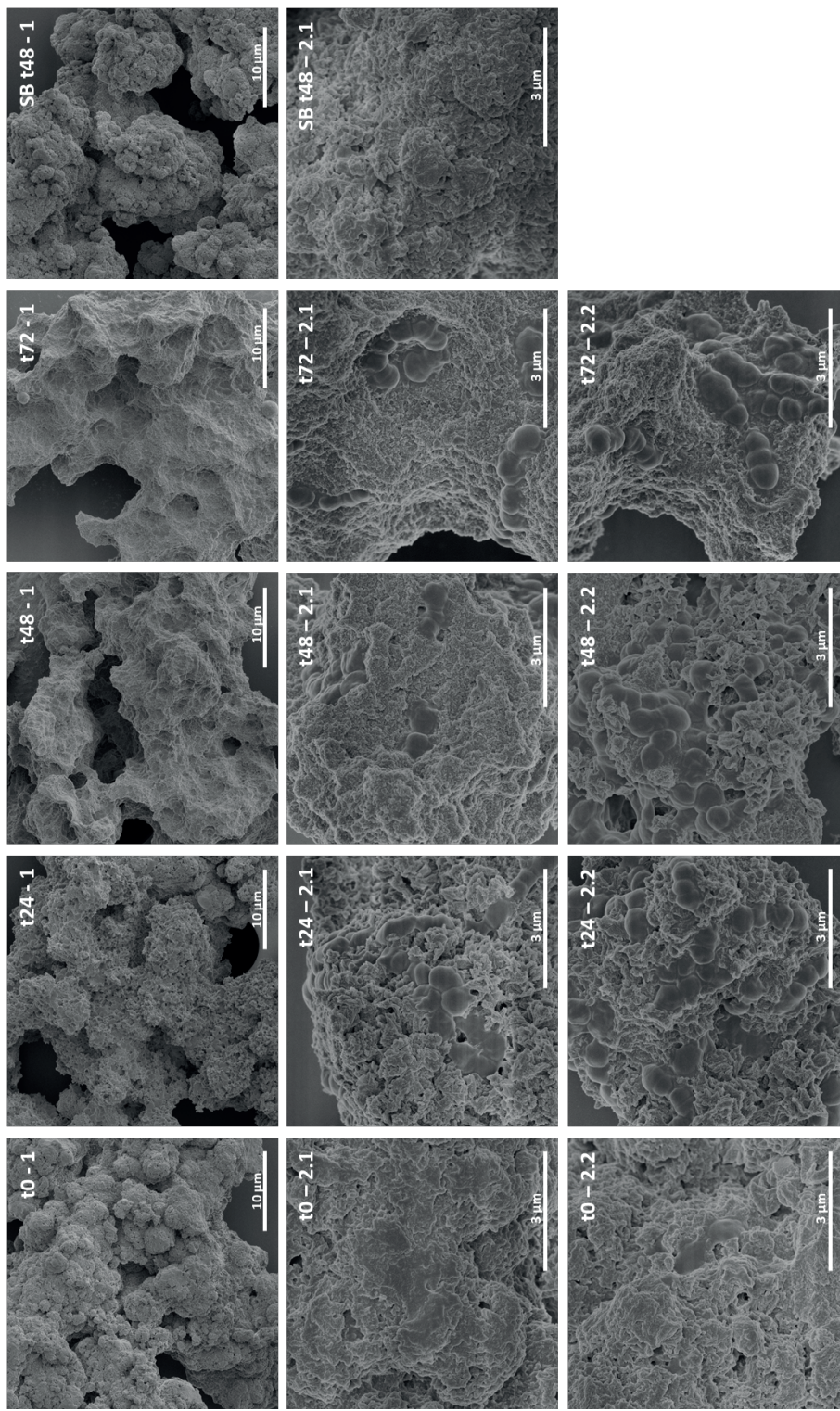
| Sample name | t 0 h | t 24 h | t 48 h | t 72 h |
|------------------------|--------|--------|--------|--------|
| N16-A | 0.0013 | 0.1231 | 0.1456 | 0.1625 |
| P21-A | 0.0010 | 0.1136 | 0.1306 | 0.1432 |
| N32-B | 0.0008 | 0.1157 | 0.1301 | 0.1451 |
| N76-B | 0.0008 | 0.1104 | 0.1207 | 0.1446 |
| Maize | 0.0008 | 0.1219 | 0.1404 | 0.1404 |
| Potato | 0.0011 | 0.1383 | 0.1752 | 0.1808 |
| HBPS | 0.0007 | 0.1185 | 0.1507 | 0.1526 |
| <i>R. bromii</i> blank | 0.0007 | 0.1325 | 0.1442 | 0.1216 |



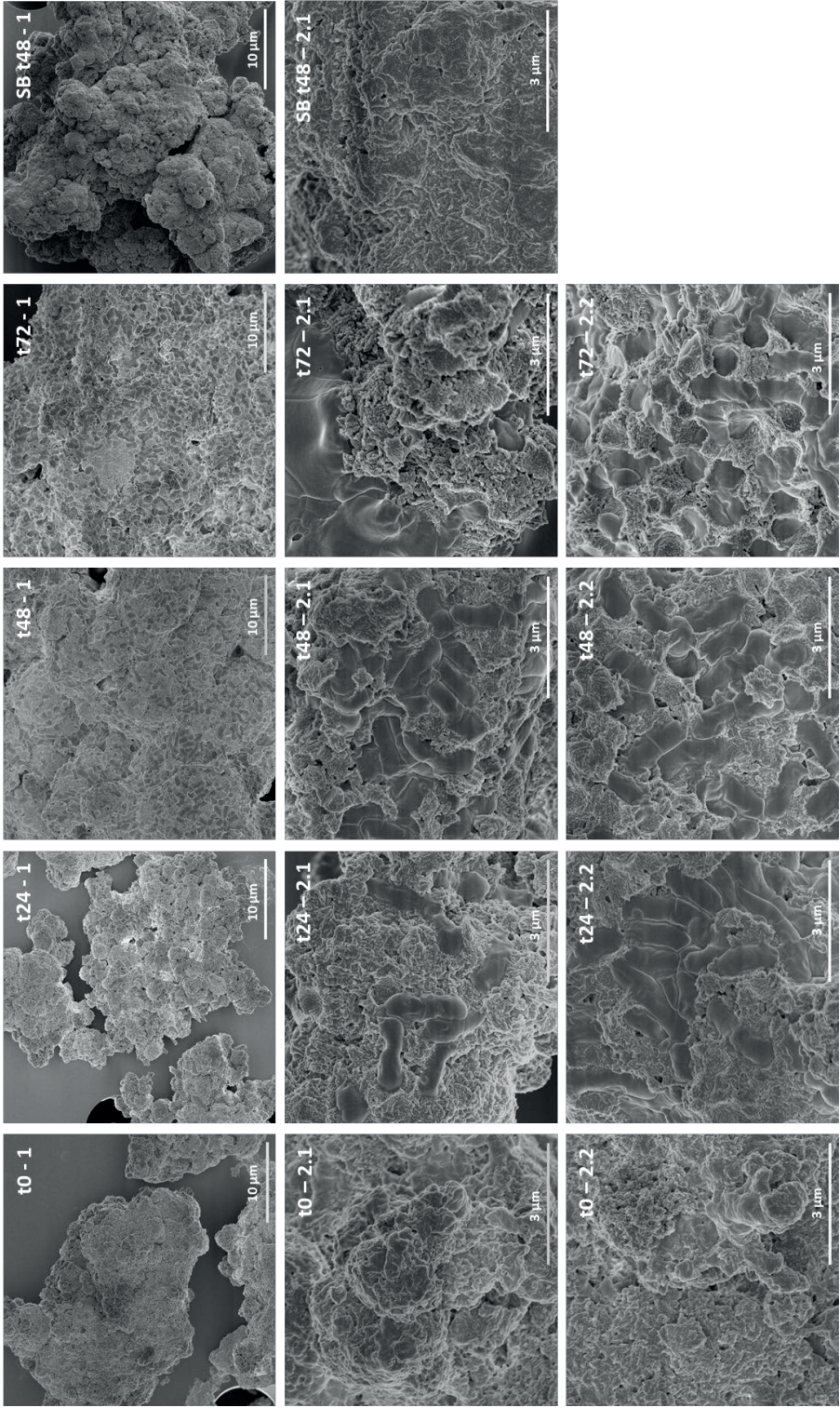
Supplementary figure 6.1. SEM images of N16-A degradation by *R. bromii* during 72 h of fermentation, including incubation of the substrate without bacteria at t48 (SB). Image 1 is 5000 x magnified, whereas 2.1 and 2.2 are duplicates at 25,000 x magnification.



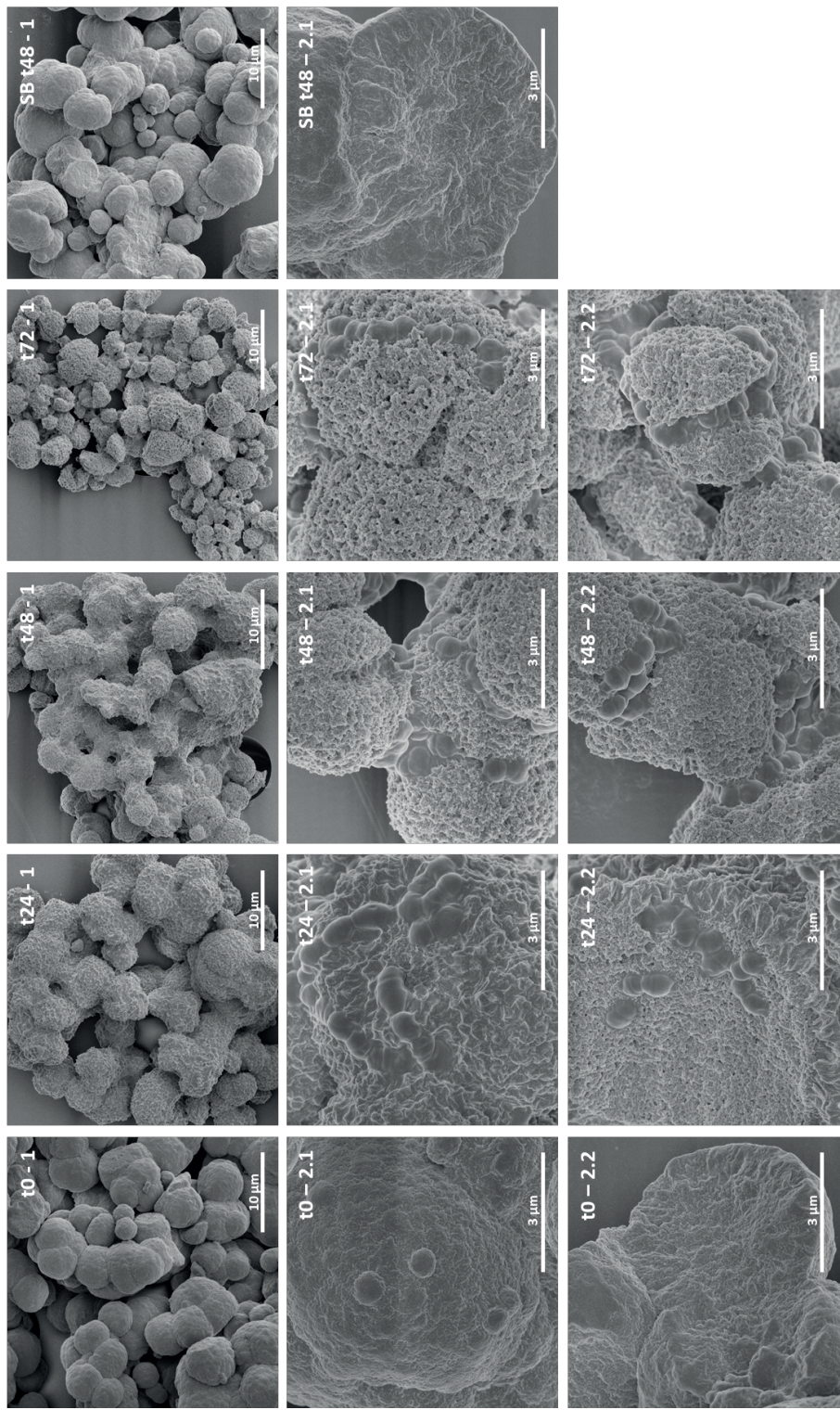
Supplementary figure 6.2. SEM images of N16-A degradation by *B. adolescentis* during 72 h of fermentation, including incubation of the substrate without bacteria at t48 (SB). Image 1 is 5000 x magnified, whereas 2.1 and 2.2 are duplicates at 25,000 x magnification.



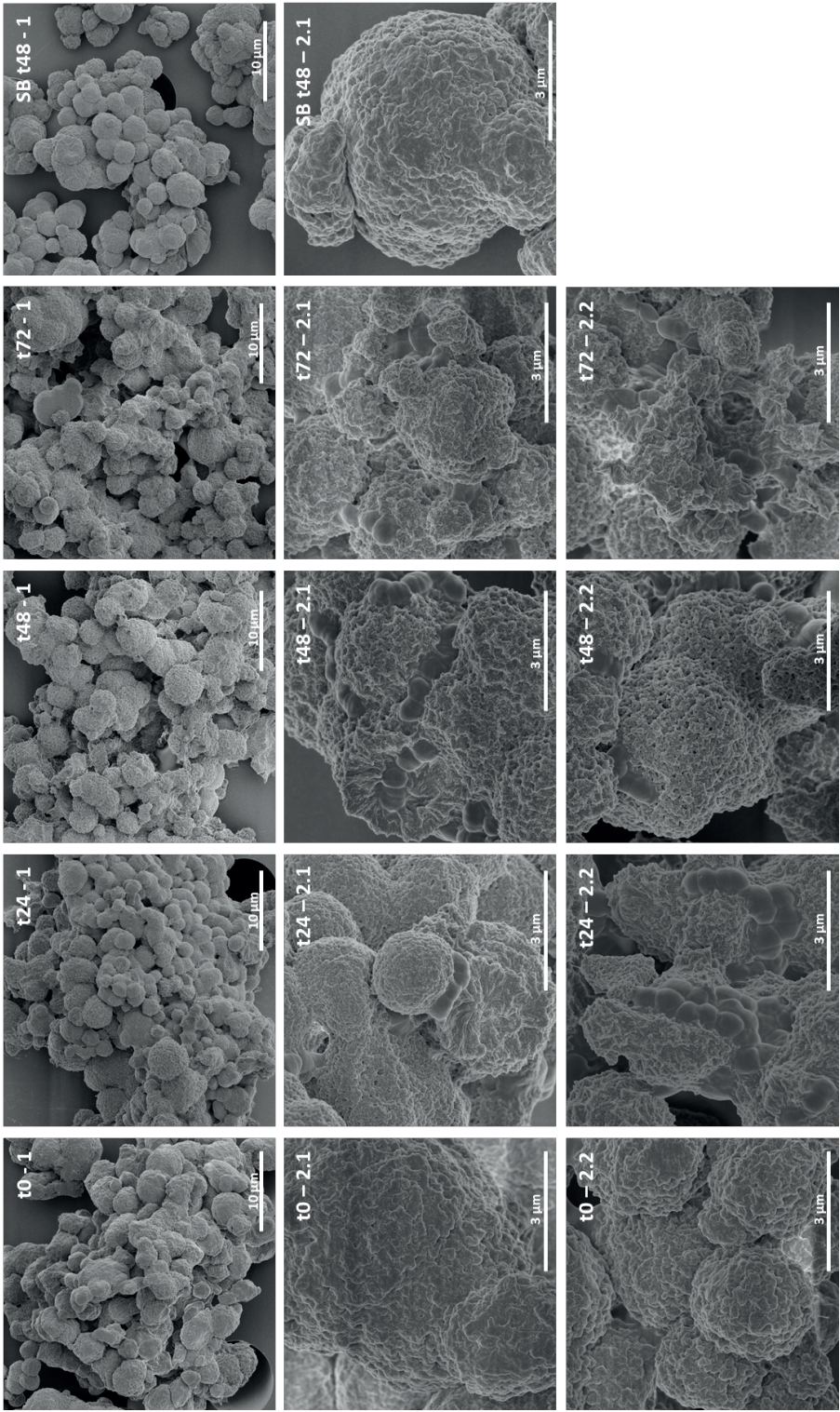
Supplementary figure 6.3. SEM images of P21-A degradation by *R. bromii* during 72 h of fermentation, including incubation of the substrate without bacteria at t48 (SB). Image 1 is 5000 x magnified, whereas 2.1 and 2.2 are duplicates at 25,000 x magnification.



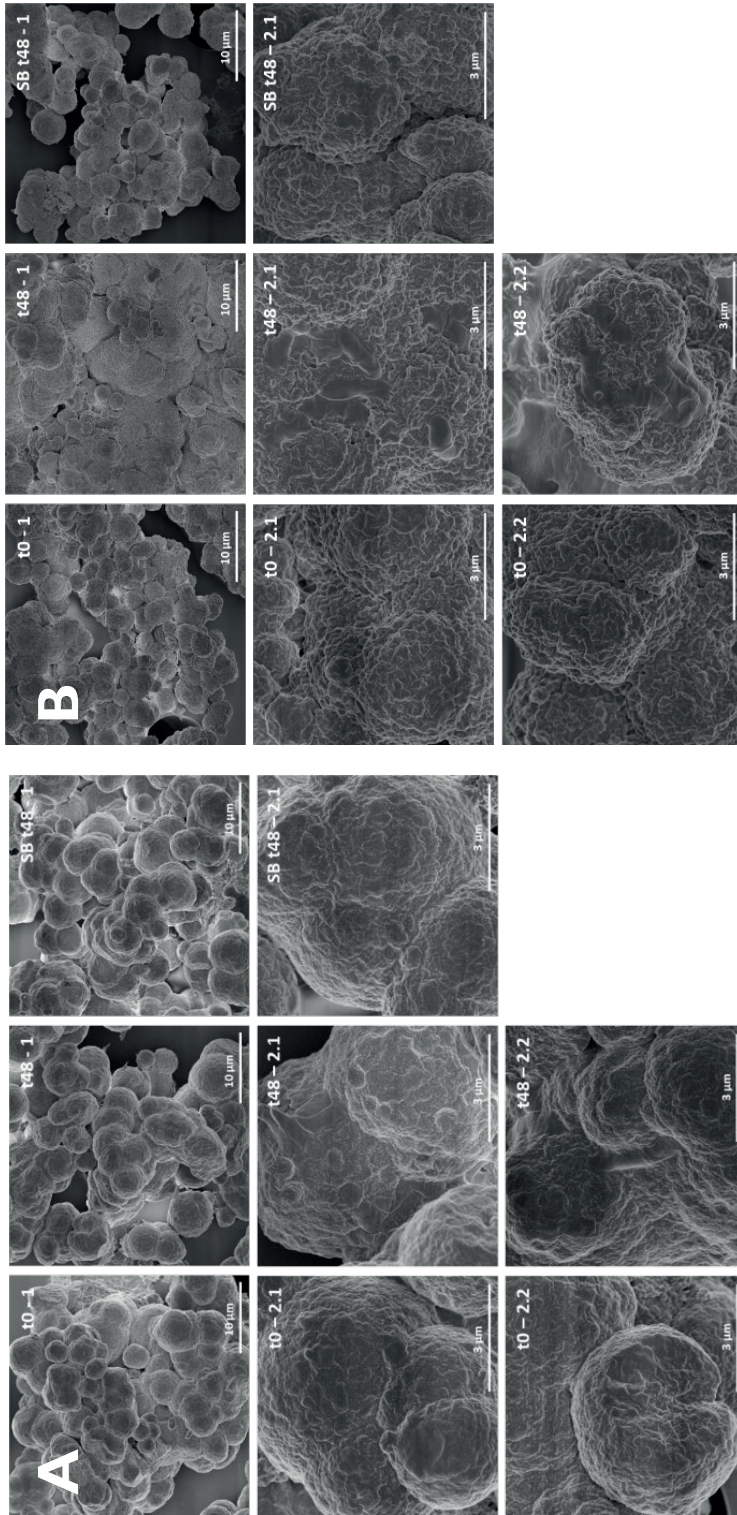
Supplementary figure 6.4. SEM images of P21-A degradation by *B. adolescentis* during 72 h of fermentation, including incubation of the substrate without bacteria at t48 (SB). Image 1 is 5000 x magnified, whereas 2.1 and 2.2 are duplicates at 25,000 x magnification.



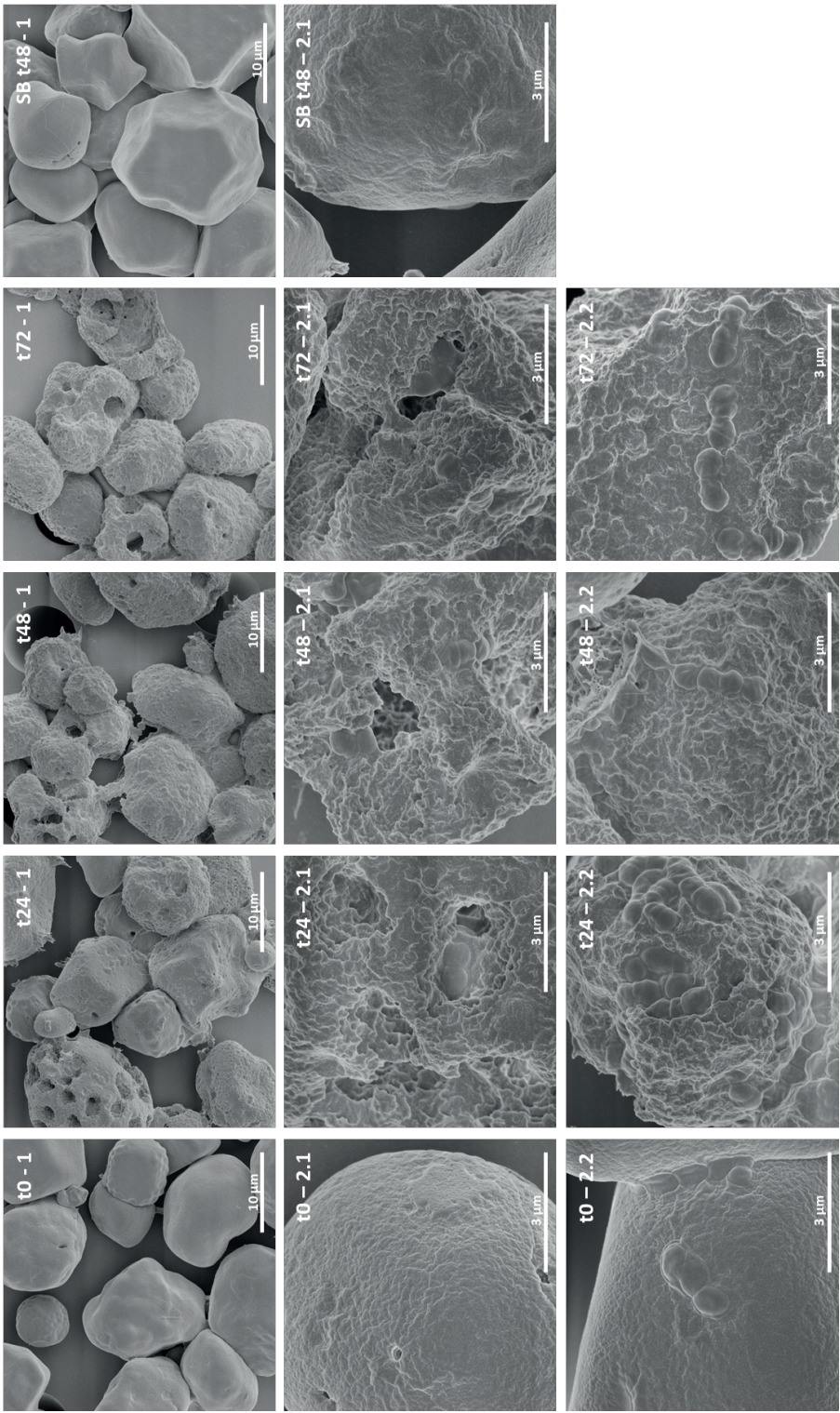
Supplementary figure 6.5. SEM images of N32-B degradation by *R. bromii* during 72 h of fermentation, including incubation of the substrate without bacteria at t48 (SB). Image 1 is 5000 x magnified, whereas 2.1 and 2.2 are duplicates at 25,000 x magnification.



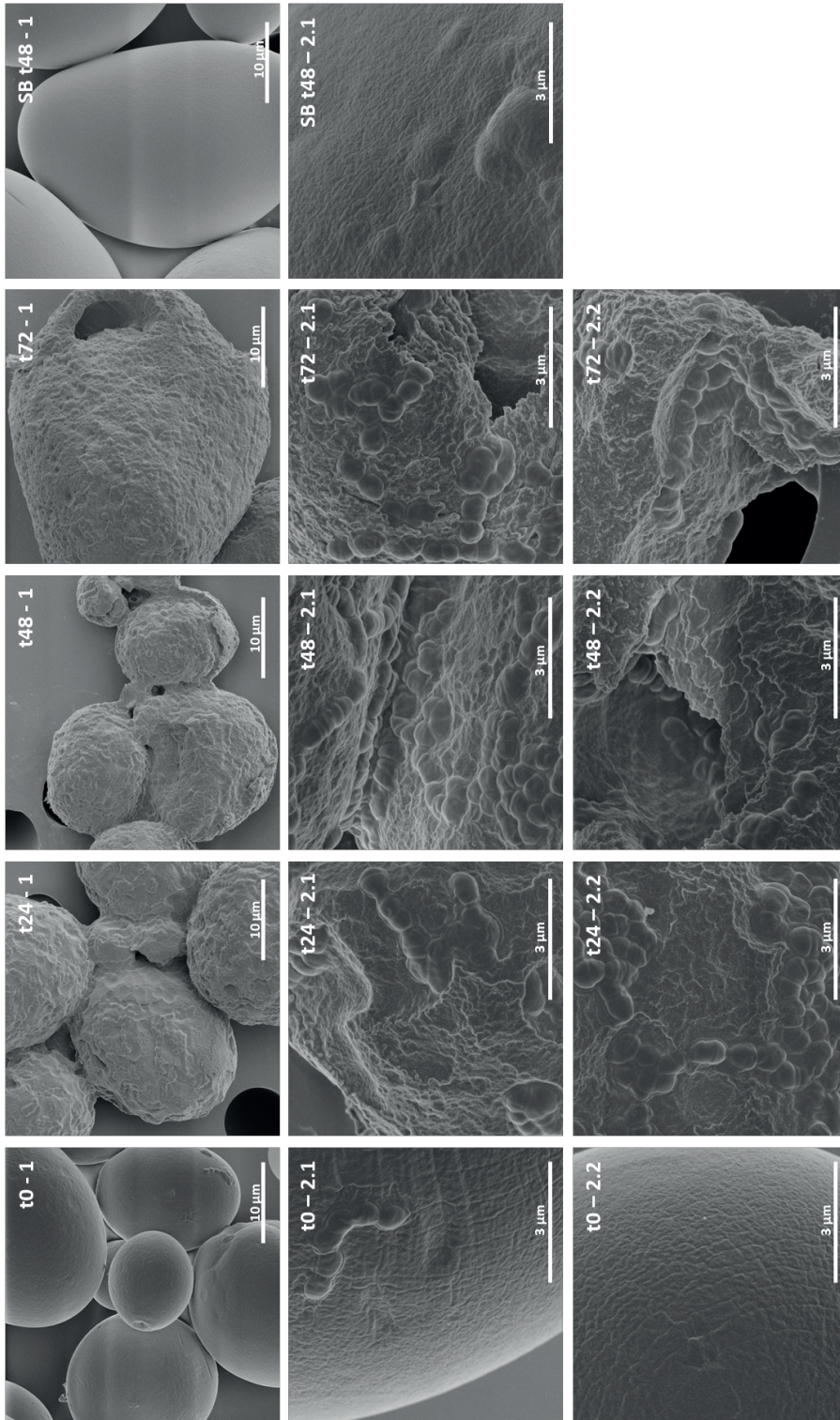
Supplementary figure 6.6. SEM images of N76-B degradation by *R. bromii* during 72 h of fermentation, including incubation of the substrate without bacteria at t48 (SB). Image 1 is 5000 x magnified, whereas 2.1 and 2.2 are duplicates at 25,000 x magnification.



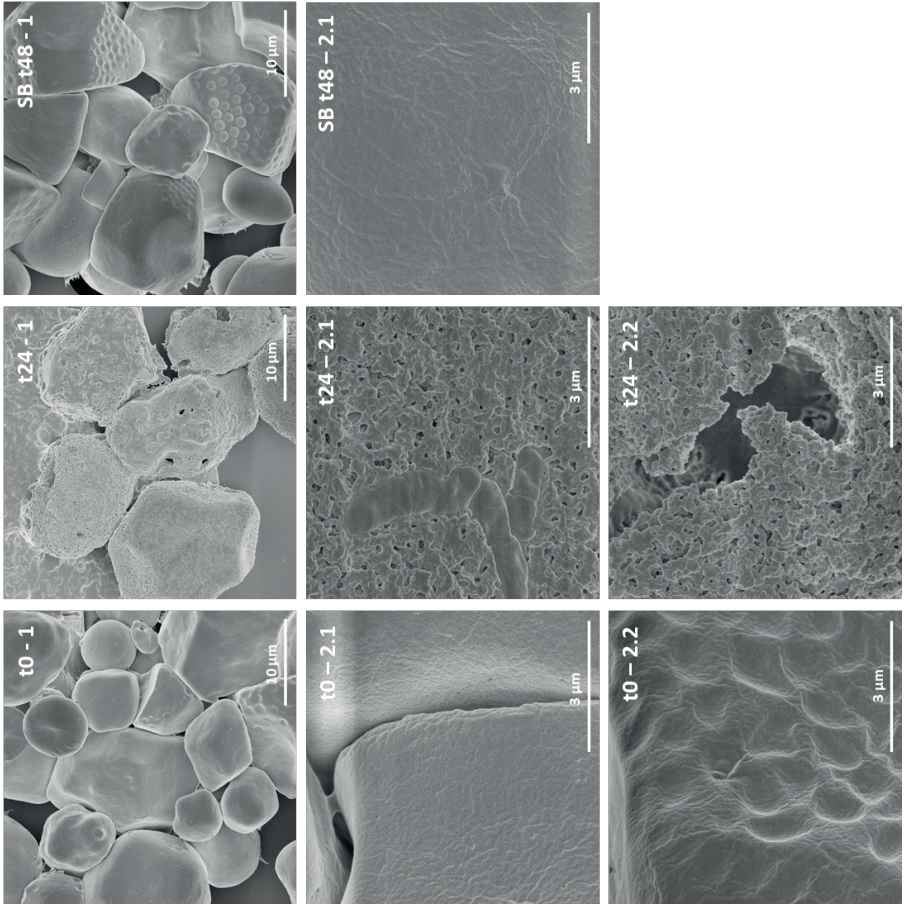
Supplementary figure 6.7. SEM images of A: N32-B and B: N76-B by *B. adolescentis* during 48 h of fermentation, including incubation of the substrate without bacteria at t48 (SB). Image 1 is 5000 x magnified, whereas 2.1 and 2.2 are duplicates at 25,000 x magnification.



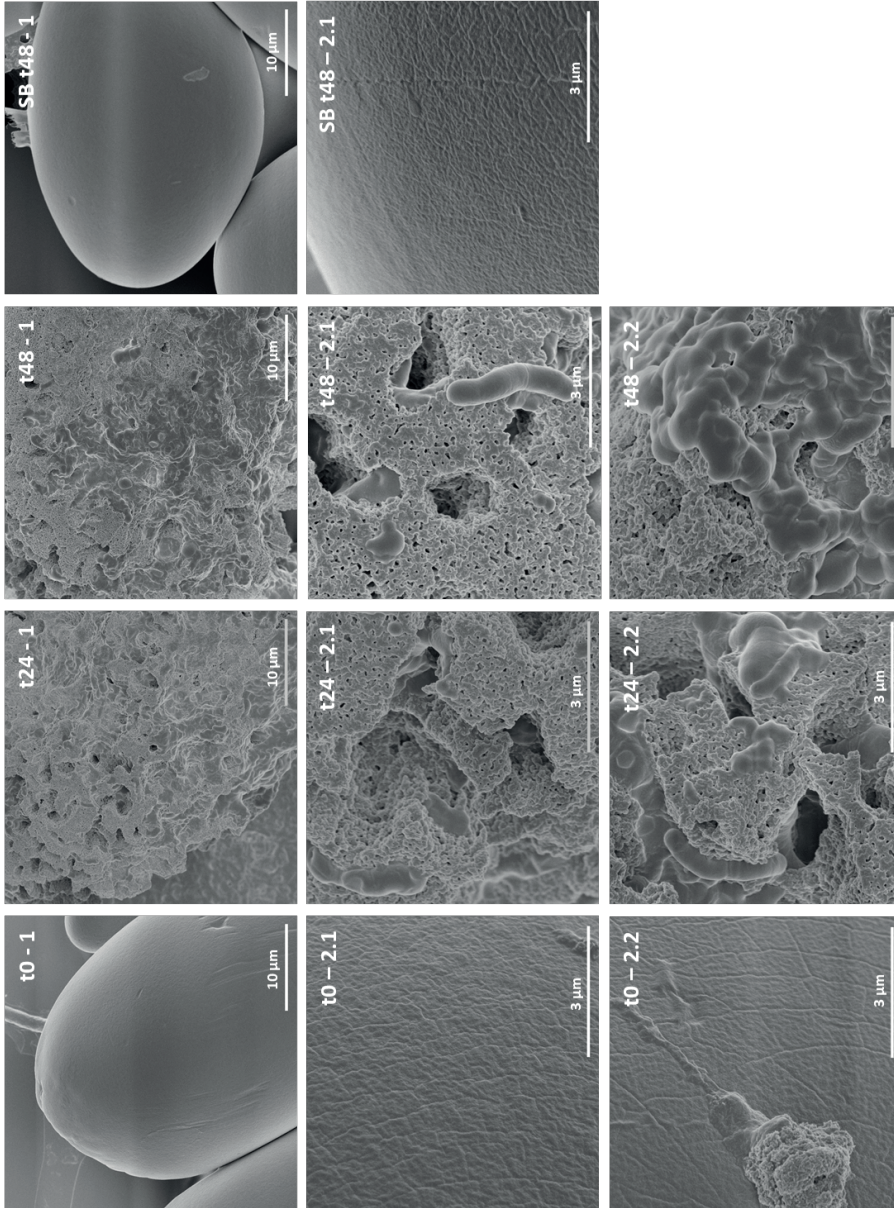
Supplementary figure 6.8. SEM images of maize starch degradation by *R. bromii* during 72 h of fermentation, including incubation of the substrate without bacteria at t48 (SB). Image 1 is 5000 x magnified, whereas 2.1 and 2.2 are duplicates at 25,000 x magnification.



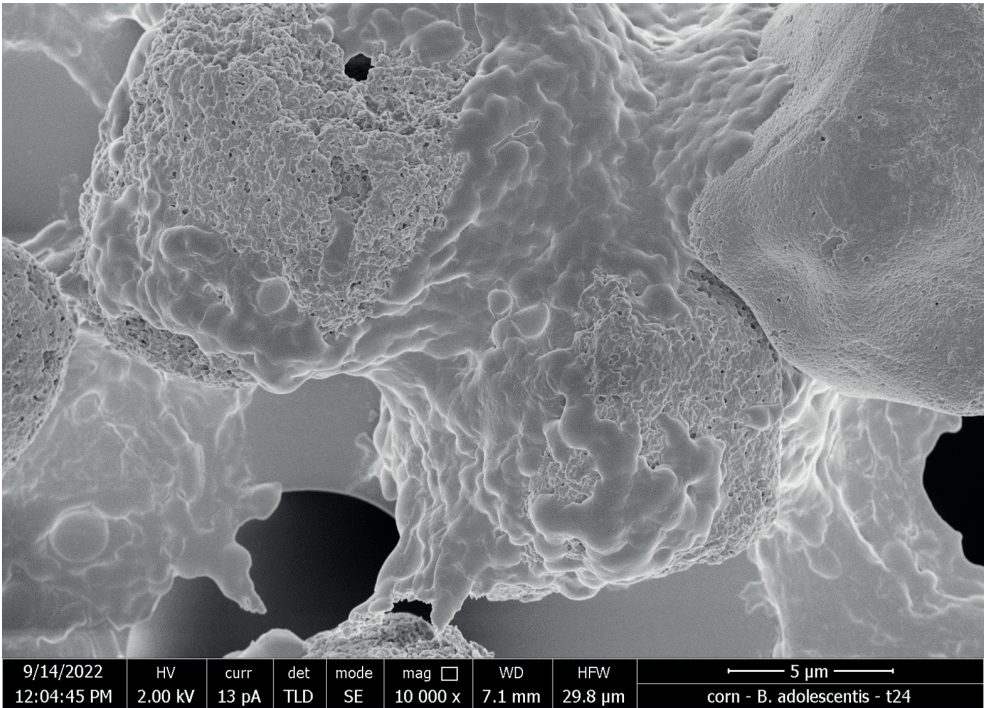
Supplementary figure 6.9. SEM images of potato starch degradation by *R. bromii* during 72 h of fermentation, including incubation of the substrate without bacteria at t48 (SB). Image 1 is 5000 x magnified, whereas 2.1 and 2.2 are duplicates at 25,000 x magnification.



Supplementary figure 6.10. SEM images of maize starch degradation by *B. adolescentis* after 24 h of fermentation, including incubation of the substrate without bacteria at t48 (SB). Image 1 is 5000 x magnified, whereas 2.1 and 2.2 are duplicates at 25,000 x magnification.

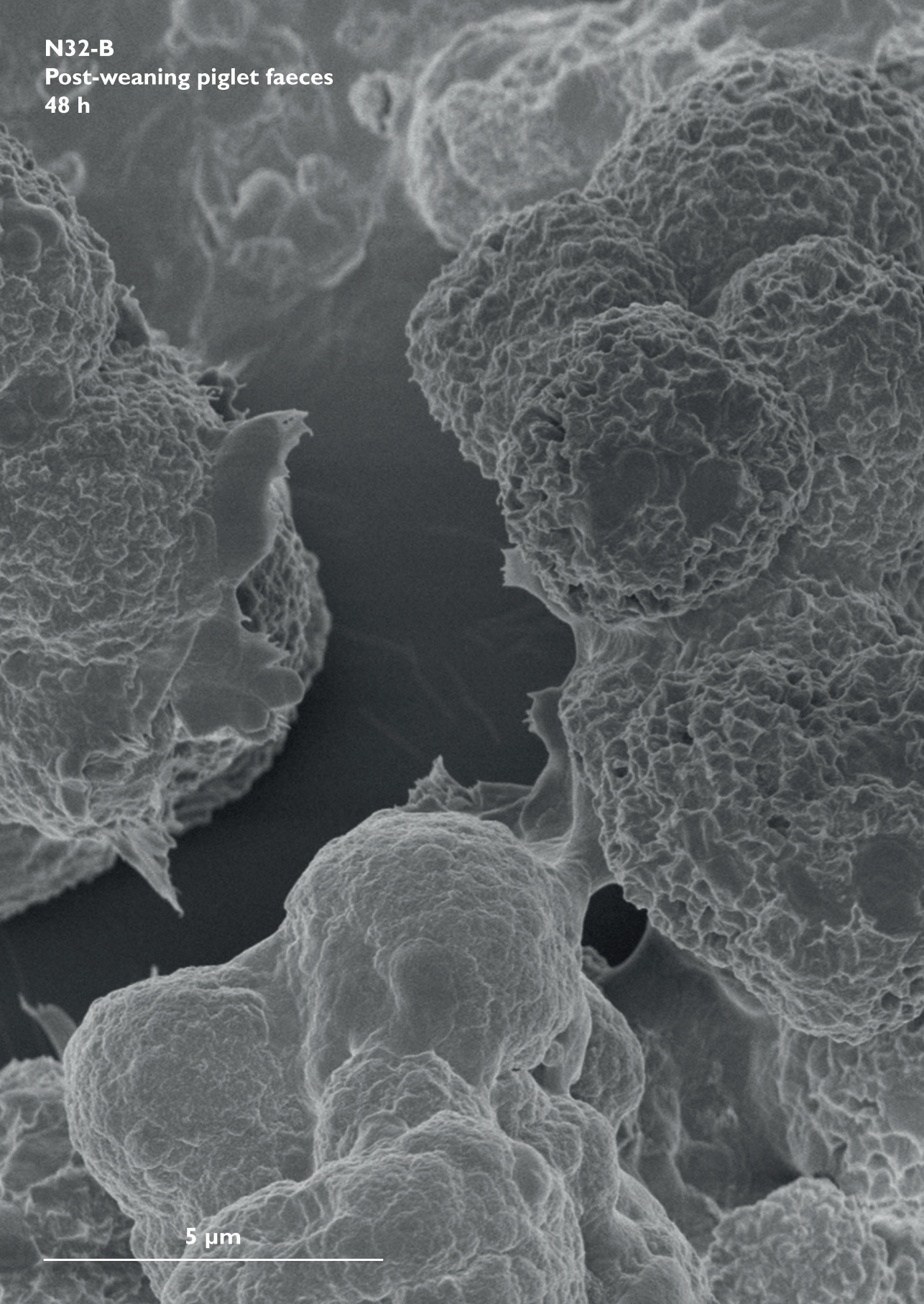


Supplementary figure 6.11. SEM images of potato starch degradation by *B. adolescentis* during 72 h of fermentation, including incubation of the substrate without bacteria at t48 (SB). Image 1 is 5000 x magnified, whereas 2.1 and 2.2 are duplicates at 25,000 x magnification.



Supplementary figure 6.12. SEM images of maize starch by *B. adolescentis* after 24 h of fermentation, showing the formation of a biofilm.

N32-B
Post-weaning piglet faeces
48 h



5 μ m

A scanning electron micrograph (SEM) showing a highly porous, cellular structure. The material consists of numerous interconnected, rounded, and elongated cells with a textured, almost honeycomb-like surface. The cells are densely packed, creating a complex, three-dimensional network. The lighting highlights the intricate details of the cell walls and the voids between them, giving the material a soft, organic appearance. The overall color is a monochromatic grey, typical of SEM images.

Chapter 7

General discussion

1. Research aim and main findings

The aim of this research was to investigate how to improve the resistant starch content within resistant starch type 3 (RS-3) preparations by the use of defined physico-chemical properties and if and how such highly resistant RS-3 substrates were fermented by faecal microbiota of various subjects. An overview of the physico-chemical characteristics of the RS-3 preparations as made and characterized in this project, their *in vitro* digestibility and their fermentability by the various faecal inocula, as presented in detail in the experimental chapters, is shown in Table 7.1.

1.1. Preparation of RS-3 counterparts

As elaborated in **Chapter 1**, already before the start of this project researchers investigated the effect of Mw and crystal type of RS-3 preparations on *in vitro* digestion^[1-3], but the *in vitro* fermentability of such RS-3 preparations was largely unknown. Furthermore, the effect of Mw distribution on RS-3 formation and subsequent *in vitro* digestion and fermentation was not yet taken into account. Within this project, we designed twelve RS-3 preparations in such a way that they all had a counterpart with only one physico-chemical property different (α -1,4 glucan chain length, Mw distribution, crystal type) (Table 7.1) (**Chapter 2**). This allowed us to study the effect of chain length, Mw distribution and crystal type of RS-3 preparations on *in vitro* digestion and fermentation.

1.2. *In vitro* digestion of RS-3 preparations

As explained in detail in **Chapter 2**, especially crystal type was determinant for the resistance to *in vitro* digestion, with RS-3 preparations having an A-type crystal being much more resistant than B-type counterparts (Table 7.1), as also observed previously^[1]. However, when prepared from longer chain length α -1,4 glucans, also B-type RS-3 preparations were very resistant to digestion. Six of the twelve RS-3 preparations were found to be highly resistant to digestion (intrinsic RS-3, 80-95 % RS) (**Chapter 2**^[4]). These six intrinsic RS-3 substrates comprised three samples with an A-type polymorph (average degree of polymerization (DPn) 16-22) and three with a B-type polymorph (average DPn 32-76). The other six RS-3 preparations contained a varying RS content (0-70 %) and comprised of one sample with an A-type polymorph (DPn 14) and five with a B-type polymorph (DPn 14-40) (Table 7.1).

Table 7.1. Overview of the results obtained in this project. Substrates defined as intrinsic RS-3 are underlined. For details: see the experimental chapters.

| Sample name | Crystal type | DPn | PI | RS (%) | | Degraded/Fermented | | | | | | (Faecal) inoculum |
|--|--------------|------|------|---------|---------|--------------------|---|---|---|---|--|-------------------|
| | | | | 120 min | 360 min | 2 | 3 | 4 | 5 | 6 | | |
| Chapter | | | | | | | | | | | | |
| SPS/HBPS | - | - | - | 0 | 0 | | | | | | | |
| dHBPS-A ^a /P14-A ^b | A | 14.3 | 1.33 | 15 | 0 | | | | | | | |
| dHBPS-B ^a /P14-B ^b | B | 14.0 | 1.35 | 0 | 0 | | | | | | | |
| sG2-A ^a /N16-A ^b | A | 15.6 | 1.23 | 80 | 77 | | | | | | | |
| sG2-B ^a /N16-B ^b | B | 15.2 | 1.25 | 11 | 11 | | | | | | | |
| dWRS-A ^a /P21-A ^b | A | 21.4 | 1.59 | 79 | 80 | | | | | | | |
| dWRS-B ^a /P22-B ^b | B | 21.9 | 1.59 | 20 | 9 | | | | | | | |
| P22-B-pd ^b | B | | | | | | | | | | | |
| sG5-A ^a /N18-A ^b | A | 18.0 | 1.21 | 88 | 87 | | | | | | | |
| sG5-B ^a /N18-B ^b | B | 18.0 | 1.21 | 26 | 19 | | | | | | | |
| dWPS-B ^a /P40-B ^b | B | 39.9 | 2.11 | 74 | 67 | | | | | | | |
| P40-B-pd ^b | B | | | | | | | | | | | |
| sG20-B ^a /N32-B ^b | B | 31.6 | 1.14 | 95 | 97 | | | | | | | |
| dAMPS-B ^a /P53-B ^b | B | 53.0 | 1.67 | 91 | 88 | | | | | | | |
| sG65-B ^a /N76-B ^b | B | 75.6 | 1.07 | 94 | 92 | | | | | | | |

Fermented/Degraded was based on starch degradation and/or SCFA formation after 48 h of incubation. The sample name was derived from a) (Chapter 2) the α -1,4 glucan used and crystal type, or b) (Chapter 3), the physico-chemical characteristics of the RS-3 preparations with P/N: polydisperse/narrow disperse, Number: DPn, A/B: crystal type. SPS/HBPS is purely digestible starch and used as reference material.

It is quite remarkable that P14-A and N16-A only differed minorly in chain length and Mw distribution, but behaved very differently in terms of *in vitro* digestion (Table 7.1), with N16-A being highly resistant to pancreatic digestion and P14-A following a typical starch digestion pattern (**Chapter 2**). Apparently, RS-3 preparations made of DPn 14.3 α -1,4 glucans are less stable than ones made of DPn 15.6, resulting in this major difference in terms of *in vitro* digestion.

1.3. *In vitro* fermentation of RS-3 preparations

In vitro fermentation of the twelve RS-3 preparations revealed that intrinsic RS-3 (80-95 % RS) was fermented distinctly different from RS-3 preparations that contained a digestible fraction (0 - 70 % RS) (**Chapter 3 & 4**). Intrinsic RS-3 substrates were fermented slowly to acetate and butyrate by pooled adult faecal inoculum, whereas RS-3 preparations containing a digestible fraction were fermented rapidly to acetate and lactate using the same inoculum. Digestible starch was fermentable by all faecal inocula tested, whereas this was not the case for intrinsic RS-3 (Table 7.1).

1.3.1. Intrinsic RS-3, a novel dietary fibre?

Generally, we observed that intrinsic RS-3 (80-95 % RS) was hardly fermented or very slowly fermented by faecal microbiota as described in **Chapter 3-5** (Table 7.1). Next to the fermentability of intrinsic RS-3 by the faecal inocula listed, we also incubated intrinsic RS-3 with faecal inocula of other subjects (pre- and post-weaning piglets, 6- and 9-month old infants) and generally observed low fermentability of intrinsic RS-3. Using pooled adult faecal inoculum, we observed that ± 60 % of intrinsic RS-3 was fermented within 48 h of incubation, already quite long for such an *in vitro* experiment^[5] (**Chapter 3**), whereas ± 25 % was degraded within the same time frame using pooled post-weaning piglet faecal inoculum (**Chapter 5**). Intrinsic RS-3 is thus a rather difficult-to-degrade dietary fibre and likely specialized bacteria with advanced enzymatic machineries are required to achieve degradation of such substrates. This was also shown indirectly by the limited RS-3 degrading capacity of pooled pre-weaning piglet faecal inoculum and individual faecal inocula obtained from infants and one adult, likely not harbouring such specific gut microbes (**Chapter 4-5**). The difficult-to-degrade nature of intrinsic RS-3 certainly has drawbacks, since such intrinsic RS-3 might be unfermentable by different subjects, either due to the lack of these specialized bacteria within the gut microbiome or due to too fast transit in which these RS-3 substrates are defecated untouched. Nevertheless, the difficult-to-degrade nature of intrinsic RS-3 also has opportunities, since such intrinsic RS-3 has the potential to arrive in the distal

colon. Furthermore, intrinsic RS-3 might have prebiotic potential by stimulating specific health-beneficial gut microbes.

1.3.2. Intrinsic RS-3 and gut microbiota

After *in vitro* fermentation of intrinsic RS-3 using pooled adult faecal inoculum, we observed increases in relative abundance of specific phylotypes (ASVs) within *Lachnospiraceae* and *Ruminococcus*, whereas using pooled post-weaning piglet faecal inoculum, we observed specific increases in relative abundance of *Prevotella* and *Roseburia*. Known primary RS degraders *Ruminococcus bromii* and *Bifidobacterium adolescentis* were shown to have a similar degrading capacity towards resistant starch type 2 (RS-2) (raw potato starch), whereas this was different for intrinsic RS-3 (**Chapter 6**). *R. bromii* efficiently degraded intrinsic RS-3 to glucose and maltose, whereas *B. adolescentis* was hardly able to degrade A-type intrinsic RS-3 and was unable to degrade B-type intrinsic RS-3. Intrinsic RS-3 might therefore be considered as a dietary fibre that is only degradable by specific gut microbes, which need to be present within the gut microbiome to achieve degradation.

1.4. Morphology of RS-3 and its microbial degradation revealed by SEM

We used scanning electron microscopy (SEM) as a tool to observe the effect of chain length, Mw distribution and crystal type on morphology of the obtained RS-3 preparations and on the change in morphology due to degradation by gut microbes. In **Chapter 2**, we showed that RS-3 preparations made from narrow disperse α -1,4 glucans crystallized in much more narrow disperse particles, compared to RS-3 made from polydisperse α -1,4 glucans, that crystallized in large blocks. A- and B-type RS-3 counterparts had similar particle size, but especially the surface morphology differed, in contrast to a study by Cai & Shi (2013)^[3]. The high resolution SEM used, allowed us to study the surface of RS-3 particles and their degradation by gut microbes in more detail than ever reported (**Chapter 3 & 5**). Especially the degradation by *R. bromii* and *B. adolescentis* (**Chapter 6**) taught us about the interesting morphology of these insoluble dietary fibres.

2. Redefining resistant starch: intrinsic and kinetic RS, food for specialists versus generalists

2.1. Intrinsic and kinetic RS differ in digestibility

Currently, resistant starch is considered as the fraction of starch that is undigested in the small intestine and transits to the colon^[6], where it is subject to fermentation. This is a purely physiological definition and does not explain why this starch fraction is not digested in the upper gastro-intestinal tract (GIT), neither on the absolute digestibility among individuals, nor on the physico-chemical properties and structure required to reach the colon and be effectively fermented. Starch that arrives in the colon simply because it is kinetically not digested by the upper GIT enzymes differs from starch that arrives in the colon because those enzymes are physically unable to degrade it. The latter one can be considered a dietary fibre as such, similar to non-digestible carbohydrates pectin or inulin. In contrast, (partially) digestible starches cannot be considered dietary fibres as such, since the amount of digestible starch arriving in the colon is hard to predict and largely depends on the individual consuming it^[7].

2.2. Digestible starch is food for generalists

The gut microbiota composition is very host-specific and therefore varies immensely among individuals^[8]. Nevertheless, among individuals the overall metabolic function of the gut microbiome is rather similar^[8], resulting in similar fermentation capabilities of the two gut microbiotas of two individuals, while the responsible microbes might differ completely. Based on the fermentation characteristics among individuals, dietary fibres can be divided into two groups: those that are fermentable by a wide range of bacteria in the gut (non-specific fibres), and those that are fermentable by only a few specialized bacteria (specific fibres), due to their chemical and physical characteristics^[9]. The gut microbiota encodes many carbohydrate-active enzymes, of which glycoside hydrolase family 13 (GH13), the largest starch-active enzyme family, is represented the most^[10]. The fact that many gut microbes encode GH13 enzymes^[11], suggests that starch is an important substrate for obtaining glucose or malto-oligosaccharides as energy source. We have shown that soluble potato starch was fermentable by many different faecal inocula (**Chapter 3-5**), and, depending on the botanical source, autoclaved starches might even stimulate different microbial populations^[12]. Nevertheless, it has been shown that digestible starch supplementation did not change the faecal microbiota composition of individuals, both when supplemented in a low or a high dose^[13]. These examples

suggest that (partially hydrolysed) digestible starch -if arriving in the colon- is fermentable by many different gut microbes and therefore a non-specific “fibre”, since no special enzyme machineries are required to hydrolyse such starch.

2.3. RS-2 and intrinsic RS-3 are food for specialists

Other starches, such as raw granular starch from potato or high-amylose maize are slower digested by upper GIT enzymes and thus contain a larger proportion of resistant starch^[14] according to the Englyst model^[15]. Most of the gut microbes cannot degrade such granular starches, but e.g. *Ruminococcus bromii* and *Bifidobacterium adolescentis* have been shown to efficiently degrade raw potato (Chapter 6) and high-amylose maize starch^[16]. In recent *in vivo* studies investigating the effect of raw potato starch (RS-2) on the faecal microbiota composition, it was observed that the changes in microbiota composition were highly variable among individuals^[13, 17, 18]. After the intervention, it was observed that either *Bifidobacterium* increased in relative abundance, or *Ruminococcus* with *Agathobacter rectalis* [*Eubacterium rectale*] increased in relative abundance, or no changes in microbiota composition were observed at all^[13, 17, 18]. The high variability among individuals after the intervention indicates that RS-2 from potato is not a very specific dietary fibre^[9]. Raw potato starch can be effectively degraded by, among others, the well-studied primary RS-degraders *R. bromii* and *B. adolescentis* (Chapter 6), with *B. adolescentis* dominating when both are present^[17]. Nevertheless, in most cases, supplementation of RS-2 from potato did change the faecal microbiota composition of individuals after the intervention^[13, 17, 18], making it a dietary fibre that is much more specific than e.g. digestible starch.

In this project, we studied the fermentability of intrinsic RS-3 (80-95 % RS) by different faecal inocula (Chapter 3-6). Only 1 of the individual faecal inocula tested was clearly able to ferment intrinsic RS-3 within 48 h, and from the pooled faecal inocula tested only faecal inoculum obtained from adults was convincingly able to ferment intrinsic RS-3 efficiently. Especially intrinsic RS-3 prepared from narrow disperse α -1,4 glucans was found to increase the relative abundance of *Ruminococcus* (Chapter 3) and indeed we showed that *R. bromii* ATCC27255 could degrade these substrates (Chapter 6). In contrast, *B. adolescentis* L2-32, a known RS-degrading strain^[16, 19], was unable to degrade such intrinsic RS-3. Assuming that intrinsic RS-3 is also resistant to hydrolysis by other *B. adolescentis* strains, intrinsic RS-3 could be considered an even more specific dietary fibre, compared to raw potato starch (RS-2), making it food for

real specialists such as *R. bromii*, and a potential useful health-beneficial ingredient.

3. *In vitro* fermentation of intrinsic versus partially digestible or pre-digested RS-3 preparations

During this project, more research was published on the fermentability of RS-3 preparations^[20-28]. Several studies focused on the preparation and characterization of RS-3 spherulites, followed by *in vitro* fermentation^[21, 23, 27], whereas others focussed on the changes in microbiota composition without full characterization of the RS-3 preparations^[22, 25, 28]. Some studies included a pre-digestion treatment^[20-25], whereas others reported the RS content but fermented the RS-es without further pre-digestion^[26] or did not report the RS content nor performed pre-digestion^[27, 28]. Some studies freeze-dried their pre-digested RS-3 substrates prior to *in vitro* fermentation^[21, 28, 29], although it was shown previously that freeze-drying majorly impacted the RS-content of RS-3 substrates^[30]. Such major differences in experimental set-up and characterization make it difficult to compare our results to the ones obtained in recent studies.

3.1. The effect of Mw distribution

Published research on the digestibility and fermentability of RS-3 (preparations) used (partially) debranched amylopectins^[20, 23, 24, 27] or starches of various (botanical) sources^[21, 22, 25], exploiting all a polydisperse Mw distribution. In this project, we also took the effect of Mw distribution into account by enzymatic synthesis of narrow disperse α -1,4 glucans crystallized into RS-3 preparations. Our results showed that Mw distribution minorly affected the *in vitro* digestion of RS-3 preparations of similar chain length and crystal type (**Chapter 2**). However, within intrinsic RS-3 (≥ 80 % RS), Mw distribution seemed an important factor steering for specific microbial populations, such as higher relative abundance of *Lachnospiraceae* for RS-3 preparations of polydisperse Mw distribution and higher relative abundance of *Ruminococcus* for RS-3 preparations of narrow disperse Mw (**Chapter 3**).

To elaborate further on the effect of Mw distribution of RS-3 preparations on *in vitro* fermentation, we also studied the fermentability of an RS-3 preparation with an even broader Mw distribution compared to dWPS-B (= P40-B, PI 2.11, Table 7.1), namely partially pullulanase debranched waxy potato starch crystallized in a B-type polymorph (ppdWPS-B). Both polydisperse dWPS-B and

ppdWPS-B contained a digestible fraction ($\pm 30\%$ (Table 7.1) and $\pm 50\%$, respectively) that was partially removed prior to *in vitro* fermentation to obtain RS enriched substrates dWPS-B-pd and ppdWPS-B-pd. These pre-digested substrates showed a typical B-type polymorph (Figure 7.1-A). The typical bimodal M_w distribution of fully isoamylase debranched waxy potato starch (dWPS-B-pd) was recognizable within partially pullulanase debranched ppdWPS-B-pd (Figure 7.1-B), although the latter showed a much broader M_w distribution. N32-B, prepared from enzymatically synthesized α -1,4 glucans, obviously had a much more narrow M_w distribution compared to both debranched starches.

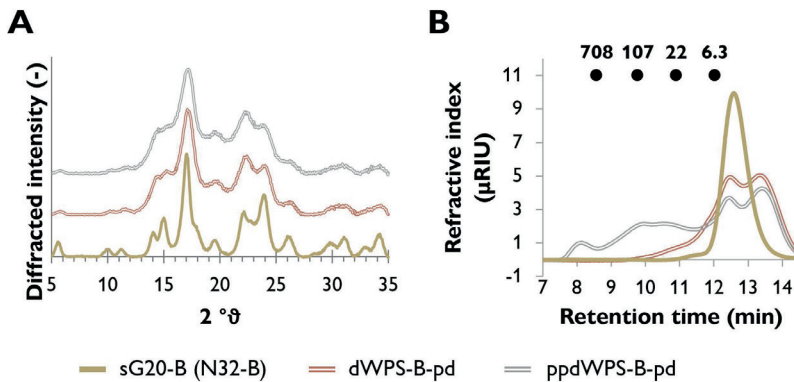


Figure 7.1. Figure A: XRD diffractograms of dWPS-B-pd (P40-B-pd) and partially pullulanase debranched waxy potato starch (ppdWPS-B-pd) after pre-digestion using pancreatin and sG20-B (N32-B). Figure B: High-performance size exclusion chromatogram of dWPS-B-pd, ppdWPS-B-pd and sG20-B. The numbers indicate the M_w (kDa) of pullulan standards at the representative retention times.

N32-B, dWPS-B-pd and ppdWPS-B-pd were *in vitro* fermented using pooled adult faecal inoculum and total starch recovery, short-chain fatty acids (SCFAs) and lactic acid and changes in microbiota composition were evaluated (Figure 7.2), using similar protocols and methods as described in **Chapter 3** and **4**.

All starches were fermented at an approximately similar rate, with $\pm 60\%$ of starch degraded after 48 h (Figure 7.2-A), while generating acetate and butyrate, with low levels of propionate and lactate (Figure 7.2-B). Analyses of the microbiota composition after 48 h of *in vitro* fermentation indicated that all starches stimulated rather similar microbial populations, with ± 30 -40 % *Bifidobacterium* and 30-40 % *Lachnospiraceae* (Figure 7.2-C). However,

fermentation of N32-B and dWPS-B-pd also caused an increase in relative abundance of *Ruminococcus*, whereas this was not observed for ppdWPS-B-pd. The results seem to suggest that the more narrow the Mw distribution, the higher the relative abundance of *Ruminococcus*.

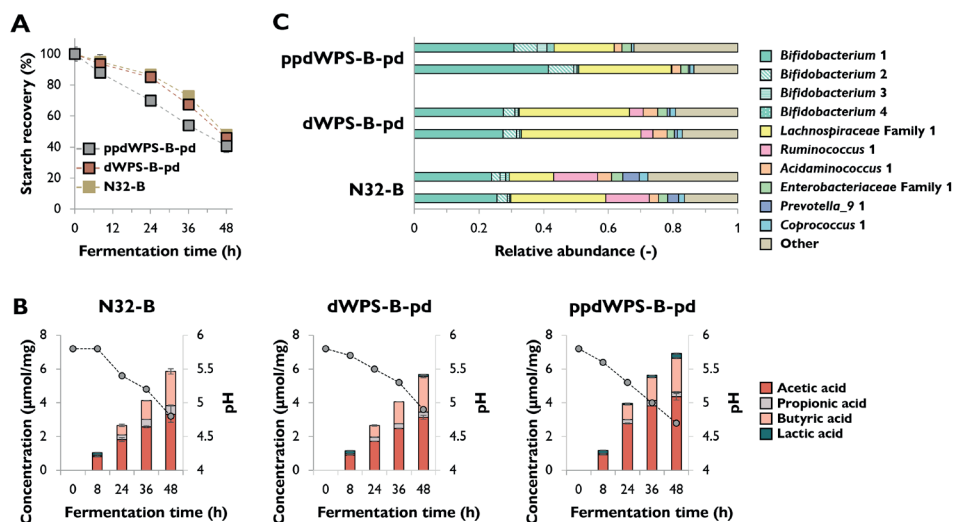


Figure 7.2. Incubation of dWPS-B-pd (P40-B-pd), ppdWPS-B-pd and N32-B with pooled adult faecal inoculum during 48 h of incubation. The average of biological duplicates is shown. Figure A: total starch recovery. Figure B: SCFAs and lactic acid produced (μmol/mg substrate). Figure C: Microbiota composition after 48 h of fermentation of the ASVs representing $\geq 2\%$ of the total relative abundance, results of both biological duplicates are indicated.

The morphology of these RS-3 substrates greatly differed, with N32-B consisting of quite dense spherical particles, whereas more polydisperse substrates formed much larger blocks without a clear microstructure (Figure 7.3). Interestingly, to both substrates from polydisperse α -1,4 glucans primarily rod-shaped bacteria were attached, whereas for N32-B we observed primarily coccus-shaped bacteria (Figure 7.3). It is likely that more narrow disperse α -1,4 glucans crystallize in a more ordered way, resulting in a more ordered microstructure. Such ordered microstructure is potentially more difficult to degrade, resulting in the need for specialized enzyme machineries to achieve degradation. These results and our findings as described in **Chapter 3**, suggest that RS-3 formed from polydisperse α -1,4 glucans result in better accessible structures, whereas RS-3 formed from narrow disperse α -1,4 glucans result in more dense structures, and are thus potentially more specific dietary fibres, than polydisperse RS-3 counterparts. However, the synthesis of narrow disperse α -1,4 glucans is much more costly than debranching waxy starches. Whether such dense structures can also be

formed from polydisperse α -1,4 glucans by optimizing the crystallization parameters, requires further investigation.

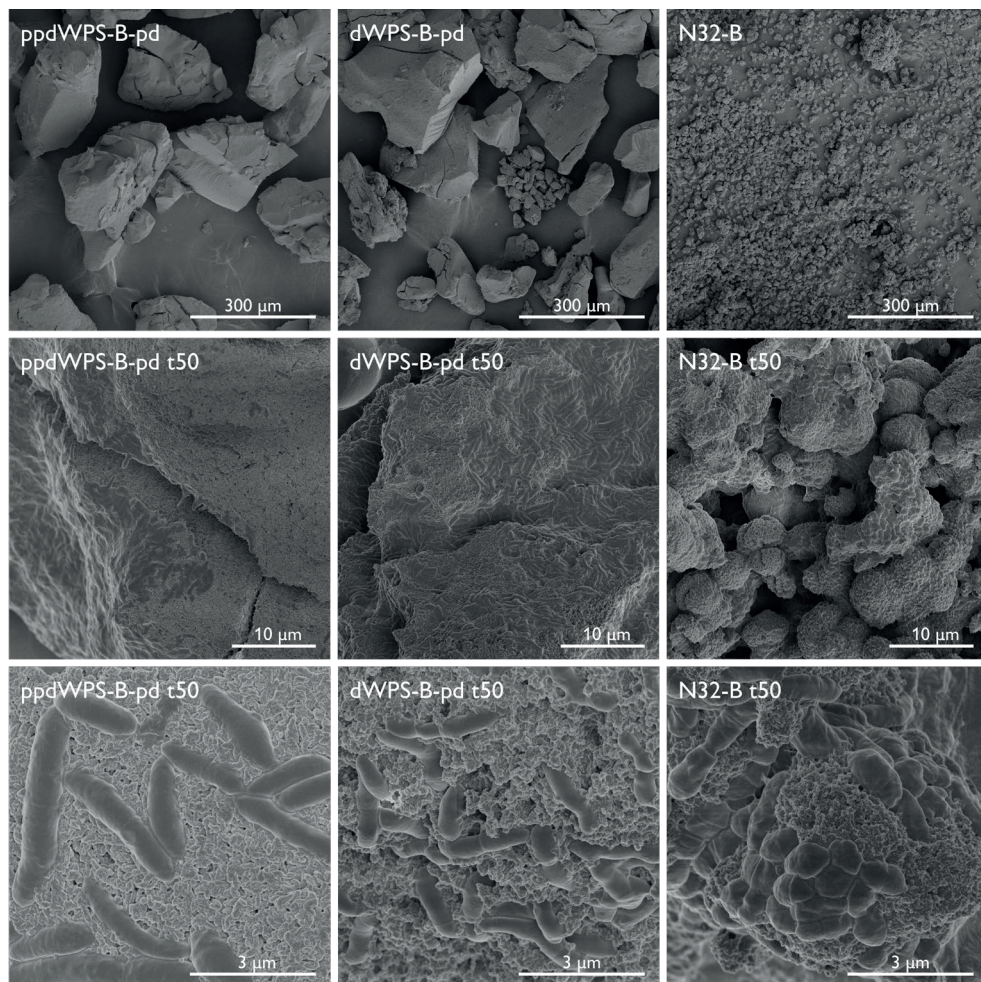


Figure 7.3. SEM images of pre-digested ppdWPS-B-pd and dWPS-B-pd and intrinsic RS-3 N32-B before (300 μ m) and after 48 h of incubation with pooled adult faecal inoculum (10 and 3 μ m).

3.2. The effect of crystal type and chain length

As elaborated, crystal type had a major influence on resistance to digestion of RS-3 preparations, with A-type RS-3 much more resistant than B-type RS-3 counterparts (**Chapter 2**), e.g. P21-A vs P22-B (Table 7.1). Due to the larger amount of digestible starch present within B-, compared to A-type RS-3 counterparts, we could not make a direct comparison in fermentability of A- and

B-type RS-3. In a recent study though, Liu et al. (2022) fermented starch spherulites prepared from debranched waxy maize starch in an A- or B-type polymorph^[27], essentially allowing to study the effect of crystal type on e.g. microbiota composition. Although Liu et al. did not report the digestibility of their RS spherulites, nor performed a pre-digestion prior to *in vitro* fermentation, they found similar fermentation rates but distinct microbial populations after fermentation of RS-3 spherulites of A- vs B-type polymorph^[27]. Especially A-type RS-3 preparations promoted the abundance of butyrogenic bacteria like *Roseburia faecis* and *Lachnospiraceae*, similar to our findings, whereas B-type RS-3 preparations promoted more propionate producing bacteria like *Prevotella copri*^[27]. In contrast, when comparing A- and B-type RS-3 counterparts in our study, we always observed distinct differences in fermentation rate, SCFA production and microbiota composition, when fermented by various inocula, due to the presence of digestible starch within B-type counterparts (**Chapter 3-5**). When the digestible starch fraction was (partially) removed, we observed a rather similar fermentation rate, SCFA production and microbiota composition during fermentation of A- and B-type RS-3 counterparts (**Chapter 3**). Also Chang et al. (2021) investigated the fermentability of A-type RS-3 prepared from debranched waxy maize starch and found enhanced butyrate production, similar to our study, but did not study changes in microbiota composition^[23]. Our results as described in **Chapter 6** showed that *Bifidobacterium adolescentis* was somewhat able to ferment A-type intrinsic RS-3, whereas unable to ferment B-type intrinsic RS-3. However, these A- and B-type intrinsic RS-3 substrates also differed in chain length, making it impossible to conclude on crystal type as a single parameter. Based on our findings, we can conclude that crystal type is highly determinant for resistance to digestion of RS-3 counterparts, but does not majorly affect fermentability within highly resistant RS-3.

No other studies reported the effect of chain length on fermentability of RS-3 and we observed a similar fermentation rate and SCFA production of RS-3 counterparts differing in α -1,4 glucan chain length (**Chapter 3**). After fermentation of both A- (N16-A and N18-A) and B-type (N32-B and N76-B) counterparts differing in chain length we observed slightly higher relative abundance of *Ruminococcus* with intrinsic RS-3 prepared from longer chain length α -1,4 glucans. In **Chapter 6**, it was shown that N76-B (longer chain length) was degraded slightly slower by *R. bromii* compared to N32-B, and the changes in morphology due to degradation, as observed on the SEM images, distinctly differed among the two substrates. However, all differences observed regarding chain length were minor and therefore, it can be concluded that also α -1,4 glucan

chain length is more determinant for RS formation than for steering *in vitro* fermentation within highly resistant RS-3.

4. The prebiotic/synbiotic potential of intrinsic RS-3 and *R. bromii*

One of the aims of this project was to design highly resistant RS-3 that would stimulate butyrate production, as was achieved by e.g. our substrate P21-A, being highly resistant to *in vitro* digestion and stimulating microbial populations that resulted in the highest butyrate-acetate ratio among the incubations performed (**Chapter 3**). However, next to the dietary fibre, especially the initial microbiota composition determines the production and composition of SCFAs during *in vitro* fermentation^[31]. Nevertheless, it has been shown that butyrate-producing bacteria from the *Clostridium* cluster XIVa, such as *Roseburia* and *Agathobacter rectalis* [*Eubacterium rectale*], increased in relative abundance in responding individuals when consuming RS^[13, 17, 32], making RS indeed of interest to enhance butyrate production in the colon.

As elaborated, in studies providing raw potato starch (RS-2) to subjects, the outcomes on faecal microbiota composition and enhanced butyrate production were highly variable among individuals^[13, 18] with either increased relative abundance of *B. adolescentis* and its metabolite acetate or increased *R. bromii* with *A. rectalis* and enhanced butyrate^[17]. *Bifidobacterium* is already long described as a probiotic^[33], but in a recent *in vivo* study investigating the effect of raw potato starch supplementation on microbiota composition, a lack of butyrate production was observed when *B. adolescentis* increased in relative abundance, also when both *R. bromii* (RS-degrader) and *A. rectalis* (butyrate producer) were both present^[17]. Moreover, when *B. adolescentis* and *A. rectalis* were both present, *A. rectalis* did not increase in relative abundance during the intervention^[17], potentially indicating that *A. rectalis* did not benefit from primary degradation by *B. adolescentis*. This suggests that for increasing butyrate production in the colon, it might be more beneficial to have a resistant starch that is specifically degradable by e.g. *R. bromii* and butyrate-producers like *A. rectalis*, and not by *B. adolescentis*, to avoid the competitive nature of *Bifidobacterium*. Since we showed that *B. adolescentis* strain L2-32, a known RS-degrading strain^[16, 19], was hardly able to degrade intrinsic RS-3, whereas *R. bromii* ATCC27255 efficiently degraded this substrate (**Chapter 6**), intrinsic RS-3 could be such a specific resistant starch. Therefore, supplementation of intrinsic RS-3 in the diet might potentially result in degradation of such substrates by *R. bromii*, also when

R. bromii and *B. adolescentis* are both present within the gut microbiome. Due to the observed slow degradation of intrinsic RS-3 in mono-culture and in faecal inocula, intrinsic RS-3 might transit to the distal colon, be degraded by *R. bromii*, thereby potentially cross-feeding butyrate-producing secondary degraders as shown in *in vivo* studies on RS-2^[13, 17] and promote butyrate production in the distal colon.

However, supplementation of intrinsic RS-3 to promote butyrate production is obviously only beneficial when subjects harbour *R. bromii*, since otherwise efficient degradation might be limited, as shown by a study of Walker et al. (2011) who provided 14 overweight men with RS-3 and found two non-responders that still had > 60 % of the starch remaining in their faeces^[32]. A follow-up study investigating the faecal samples of the same men showed a low increase in relative abundance of *R. bromii* in 6 out of 14 men, including the non-responders^[34], indicating that also other primary degraders might have degraded the RS-3 in responding men. Interestingly, when *Bifidobacterium* was absent or decreased, *R. bromii* increased in all subjects (except for the non-responders), potentially confirming the competition between *R. bromii* and *B. adolescentis*^[34]. Nagara et al. (2022) showed that 4 out of 10 healthy men harboured *R. bromii* within their microbiome, of which two also harboured *B. adolescentis* and all subjects harboured *A. rectalis*^[17], whereas Walker et al. showed that 8 out of 14 men increased in relative abundance of *R. bromii* after RS-3 supplementation^[32]. Together, these studies illustrate that 40 – 60 % of the subjects harbour *R. bromii* in their microbiome^[17, 34]. In case subjects do not possess *R. bromii* within their gut microbiome, they could potentially benefit from supplementation with *R. bromii* together with intrinsic RS-3 as a synbiotic to achieve efficient degradation and potential enhanced butyrate production in the distal colon. Indeed, recently *R. bromii* was included in a list of so-called next-generation probiotics, for its ability to degrade resistant starch^[35].

5. Other potential RS degraders

Especially *Ruminococcus bromii* and *Bifidobacterium adolescentis* are recognized as primary degraders of RS in the gut^[36] and, as elaborated, various studies reported increases in relative abundance of *R. bromii* or *B. adolescentis* after a diet high in RS-2 (raw potato starch)^[13, 17]. *R. bromii* was reported as key-stone degrader, since individuals lacking this species did not degrade RS-3^[32], whereas when the faecal inoculum of such individual was supplemented with *R. bromii*, RS-3 degradation was restored^[16]. These primary degraders have substrate

specific preferences^[16, 19, 37], with *B. adolescentis* being more competitive than *R. bromii* when fermenting e.g. raw potato starch^[17].

Although currently primarily *R. bromii* and *B. adolescentis* are described as primary degraders of RS, such capabilities were also shown recently for other species, such as *Ruminococcoides bili* obtained from human bile^[38] or *Ruminococcus* species FMB-CY1 closely related to *R. bromii*^[39]. In our study, we found increased relative abundance of *Roseburia* and of a specific *Prevotella_9* ASV when intrinsic RS-3 was incubated with pooled post-weaning piglet faecal inoculum (**Chapter 5**). Furthermore, when intrinsic RS-3 was incubated with pooled adult faecal inoculum, we found an increase of a certain, but different *Prevotella_9* ASV (**Chapter 3**). Although it has been shown that *Prevotella* increased in relative abundance when rats were fed high RS diets, *Prevotella* was not associated with RS degradation in that study^[40]. We also found an increase in relative abundance of *Lachnospiraceae* (**Chapter 3**), that might have contributed to RS degradation and fermentation in our study. Other researchers reported *Clostridium leptum* as a potential degrader^[13], but so far no supporting literature was found.

5.1. Binding to starch

The ability to degrade RS is likely related to the ability to bind to insoluble starches. *B. adolescentis* and *R. bromii* were both shown to attach to insoluble RS (**Chapter 6**), likely because they both express several carbohydrate binding modules (CBMs). Although not fully revealed yet, their starch-degrading and binding mechanisms differ. *R. bromii* binds and degrades insoluble RS using its amylosome^[41], which is highly conserved among *R. bromii* strains^[37]. The amylosome complex consists of starch-degrading GH13 enzymes^[37] and starch binding proteins and is highly stabilized due to the presence of various cohesins that bind to dockerins^[36]. Recent research revealed that the different binding proteins within the *R. bromii* amylosome have unique binding features^[42, 43], with e.g. starch adherence system 6 (Sas6) consisting of a CBM26 and a CBM74 that have proposed binding to short malto-oligosaccharides, and single and double helical α -glucans, respectively^[43]. In contrast, the ability to utilize insoluble resistant starch is not conserved among *B. adolescentis* strains, although some strains can efficiently ferment high-amylose maize starch^[19], whereas others were shown to utilize highly resistant (>90 %) RS-3 substrates^[44]. RS-degrading *B. adolescentis* strains express three extracellular RS-degrading α -amylases, that have various CBMs and have different activity towards high-amylose maize starch^[45]. Binding proteins such as the various CBMs, seem necessary to allow binding to insoluble (raw) starches and enhance hydrolysis by the α -amylases.

Recently, it has been shown that especially CBM74 increased in relative abundance when highly resistant high-amylose maize starch and raw potato starch were incubated with faecal inoculum from 1 healthy adult donor, whereas overall relative abundance of GH13 enzymes increased in all fermentations, including less resistant starches^[28]. These authors suggested that such CBM74 might be necessary to bind to complex insoluble RS, whereas such CBM is unnecessary for more accessible starches^[28]. CBM74 is a large module that was indeed shown to bind to insoluble starches^[46]. Recently, Photenhauer et al. (2022) reported many bacteria with a CBM74 encoded in their genome, of which most had one or more other CBMs (20, 25 or 26) appended to it^[43]. Ravi et al. reported that CBM74 was encoded in several species after fermentation of RS-2, such as *R. bromii* and newly detected species *Blautia hennigii*, *Ruminococcus anthropic*, *Cohabitan norwichensis*^[28] and indeed also some *B. adolescentis* strains were shown to encode such CBM74^[45]. Furthermore, it has been shown that some *Prevotella* species from human faeces encode a putative α -amylase with a CBM74 and a CBM26 in their genome^[43]. This, together with the observed increase in relative abundance of *Prevotella* ASVs in our *in vitro* work (**Chapter 3 & 5**) make such *Prevotella* species of interest to investigate for their RS binding and degrading capability.

Also gut microbes that are not known to encode a CBM74 in their genome might be RS degraders, such as the *Roseburia* ASV and potentially the *Lachnospiraceae* ASV that increased in relative abundance when intrinsic RS-3 was incubated with pooled post-weaning piglet or pooled adult faecal inoculum, respectively (**Chapter 5, 3**). Some of these *Clostridium* cluster XIVa bacteria are known butyrate producers and secondary degraders of starch, that possess one extracellular cell-wall anchored α -amylase that includes one or more CBMs to support binding to insoluble starch^[36, 47]. For example, *Roseburia inulinivorans*, has been reported as secondary degrader of starch^[36], harbouring one cell-surface anchored α -amylase/neopullulanase^[48]. Interestingly, this species was shown to upregulate genes for the synthesis of a flagellin, especially during growth on starch, possibly indicating that it can move towards insoluble starch^[49]. Also *Agathobacter rectalis* [*Eubacterium rectale*] was shown to possess one extracellular cell-wall anchored α -amylase that binds starch via five CBMs belonging to families 26, 41, 82 and 83^[47]. Although *A. rectalis* has not been shown to directly degrade resistant starch granules, it was found to increase in abundance when *R. bromii* partially degraded the starch first^[16] and thus may benefit from primary degradation of RS by *R. bromii*^[36], thereby promoting butyrate production.

The ability to degrade highly resistant starch is not limited to known RS-degrading gut microbes *R. bromii* and *B. adolescentis*. However, fermentation of intrinsic RS-3 in our study was more efficient using pooled adult faecal inoculum (with specific *Ruminococcus* ASV), compared to pooled post-weaning piglet faecal inoculum (specific *Roseburia* and *Prevotella_9* ASVs) (**Chapter 3, 5**), which might indicate that efficient degradation of intrinsic RS-3 requires specialized enzyme machineries such as present in *R. bromii*. Whether intrinsic RS-3 is thus efficiently degraded by other potential RS-degrading gut microbes than *R. bromii* requires further investigation.

6. Digestible starch for one is kinetically resistant starch for another

The results obtained within this project indicated that many faecal inocula, such as that of infants and pre-weaning piglets, were hardly able to ferment intrinsic RS-3 within the incubation time tested (Table 7.1 and data not shown). As elaborated, the difficult-to-degrade nature of intrinsic RS-3 likely requires gut microbes with specialized enzymatic machineries to achieve efficient degradation, which might not (yet) be present in pre-weaning piglet or infant microbiota. Such subjects could benefit from supplementation of more easily fermentable fibres, such as galacto-oligosaccharides or isomalto-oligosaccharides^[50, 51]. Depending on the individual, also slowly digestible starch might be considered a dietary fibre for particular individuals, that have e.g. lowered starch digestive capacities such as young mammals like infants^[52] and pre-weaning piglets^[53]. P14-A is an RS-3 preparation that was slower digested by pancreatic α -amylase, compared to soluble starch, and contained a small resistant starch fraction based on the Englyst model^[15], although fully digestible with extended incubation times (**Chapter 2**, Table 7.1). Such substrate might be partially fermented in the colon of individuals that have lower α -amylase activity in their upper GIT. Here, we compare results obtained after *in vitro* fermentation of P14-A using three individual faecal inocula of 6-month-old infants (Figure 7.4). Fermentation of P14-A by pooled pre- and post-weaning piglet faecal inoculum and pooled adult faecal inoculum as described in **Chapter 5** and **Chapter 4**, respectively, is shown as reference. The gut microbiota composition of the three 6-month old infant faecal inocula used was typically rich in *Bifidobacterium* (Figure 7.4-A) as reported before^[54] and is shown as reference at family level.

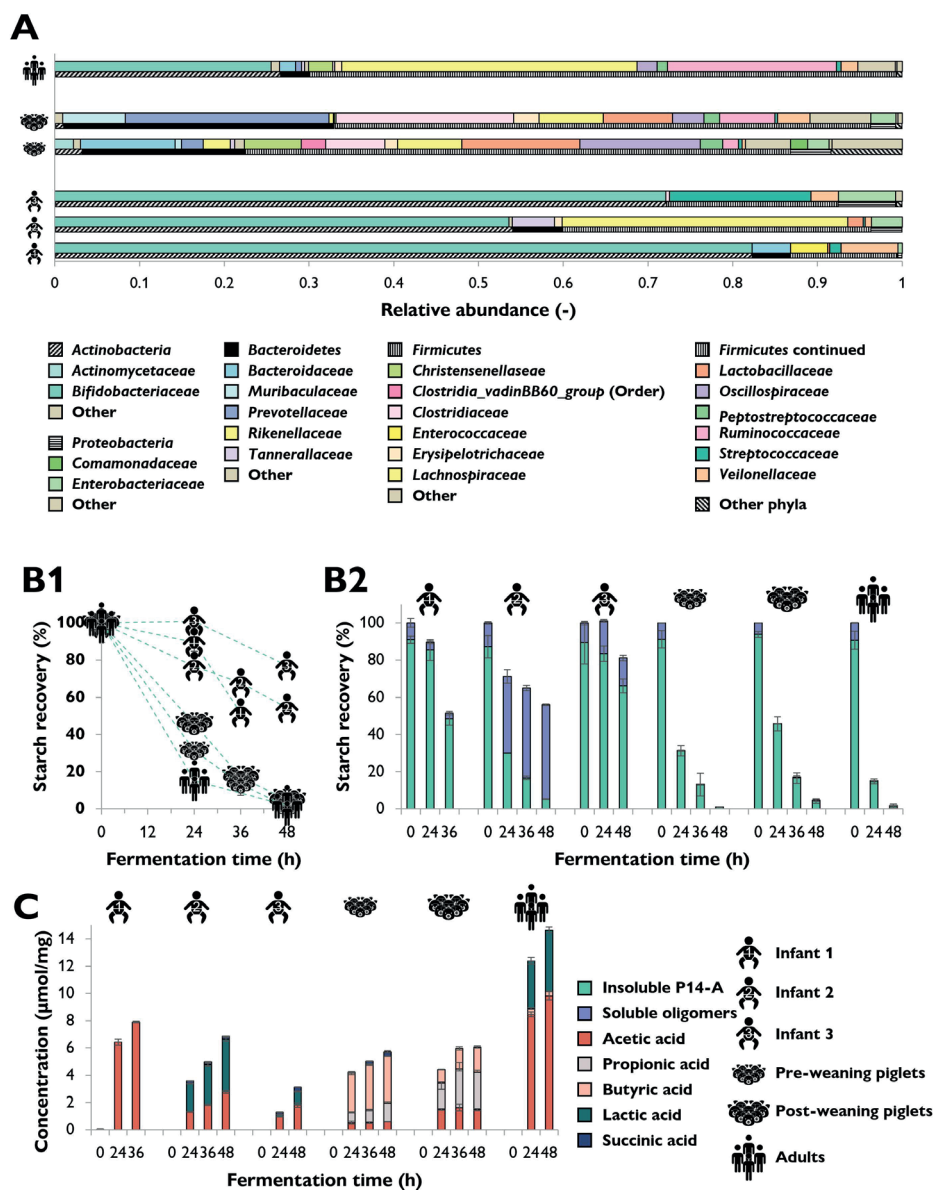


Figure 7.4. Comparison of *in vitro* fermentation of P14-A by faecal inocula of 6-month-old infants and pooled faecal inocula of pre- and post-weaning piglets and adults. Methods were as described in Chapter 3, 4 and 5. Figure A: Microbiota composition in relative abundance (Family) of faecal microbiota. Figure B1: Total starch recovery during 48 h of *in vitro* fermentation of P14-A by the respective faecal inocula. Figure B2: Starch recovery in the insoluble and soluble (incl. glucose) fraction. Figure C: SCFAs, lactic and succinic acid ($\mu\text{mol/mg}$ substrate) formed during *in vitro* fermentation of P14-A. Infant 1 and infant 2 are the same as B_f6 and P_p6 in Chapter 4.

Degradation of P14-A by individual faecal inocula obtained from 6-month-old infants was slow and incomplete within 36 h of fermentation (Figure 7.4-B1). Among the 6-month old infants, the faecal microbiota of infant 1 was most efficient in degrading P14-A, whereas especially that of infant 3 was almost unable to degrade P14-A. Interestingly, around 60 % of the total starch was remaining after 48 h of fermentation of P14-A by faecal microbiota of infant 2, whereas a closer look to the starch composition (Figure 7.4-B2) indicates that the (partially) insoluble P14-A was almost fully degraded to soluble oligomers (primarily maltose and maltotriose, data not shown). Pooled human adult and pre- and post-weaning piglet faecal inocula almost fully degraded P14-A within 36 h (Figure 7.4-B1). Pre- and post-weaning piglet and human adult faecal microbiota fermented P14-A to SCFAs and lactate, whereas that of infant 2 did not fully convert the released maltose and maltotriose further to SCFAs and lactate (Figure 7.4-C). This indicates that microbes within the faecal microbiota of infant 2 were able to express the desired α -amylases to degrade such RS-3 preparations, but further conversion of small malto-oligomers to SCFAs was limited. These results thus illustrate that among 6-month-old infants the degradation capabilities of the gut microbiota towards an “easily” fermentable substrate like partially digestible starch greatly differ. Furthermore, these results illustrate the importance of quantifying the remaining starch after fermentation in both a soluble and insoluble fraction, since sometimes bacterial enzymes are present that can degrade the substrate, but further conversion to SCFAs is hindered (infant 2), whereas in other cases the appropriate bacterial enzymes may be absent (infant 3).

The faecal inocula of the various subjects fermented P14-A to different amounts of SCFAs, lactate and succinate (Figure 7.4-C). Infant 1 (Bf_6) only produced acetate, similar to fermentation of soluble potato starch (SPS) as shown in **Chapter 4**. Faecal inocula obtained from pre- and post-weaning piglets and adults all fully fermented P14-A, but the conversion to SCFAs differed both in composition and in amount (Figure 7.4-C). SCFAs are often quantified as a measure for fermentability. Here we show that pooled piglet faecal microbiota fermented the same substrate to lower amounts of SCFAs compared to pooled human adult faecal microbiota, whereas the amount of substrate utilized was the same. A lower amount of SCFAs for pig versus human faecal inocula, while a similar amount of substrate was utilized, was also observed previously, when pig(let) and human faecal inocula were used to ferment a variety of dietary fibers^[50, 55]. In contrast, others observed a similar total SCFA production with similar substrate utilization using pig and human faecal inocula^[56, 57]. The major difference in total amount of SCFAs produced in our study can likely be

explained by the increase in relative abundance of *Bifidobacterium* using pooled adult faecal inoculum as described in **Chapter 4**. *Bifidobacterium* is very efficient in theoretically fermenting 1 mol glucose to 1.5 mol acetate and 1 mol lactate via the bifid shunt^[58] and was not present in piglet faecal inoculum (**Chapter 5**).

7. Considerations for pre-digestion assays when studying the prebiotic potential of resistant starch

We have shown that the digestible starch fraction is fermented differently than the resistant starch fraction within resistant starch preparations (**Chapter 3-4**). Most resistant starches or resistant starch preparations contain both a digestible and a more resistant fraction^[14, 59, 60]. Such starches, including commercial ingredients such as C*Actistar™ and Novelose® 330, need to be pre-digested to obtain the RS fraction and to enable a study towards their prebiotic potential *in vitro*. However, *in vitro* digestion assays are developed to quantify the amount of RS and not necessarily as a pre-treatment for obtaining the RS fraction. For studying the prebiotic potential of RS-es, it is needed to use a method that removes the digestible fraction prior to *in vitro* fermentation, without any effect on the physico-chemical properties of the remaining resistant starch.

Previous studies on *in vitro* fermentation of (resistant) starches that included a pre-digestion step, used different methods (Table 7.2). The method of pre-digestion is essential, since methods are differently efficient in removing the digestible fraction and thus may affect the *in vitro* fermentability as was shown by Tuncil et al., 2018^[61]. Commonly, a combination of porcine pancreatic α -amylase and amyloglucosidase (AMG) is used for pre-digestion (Table 7.2). Pancreatic α -amylase is used because it is considered the main starch hydrolysing enzyme in the small intestine, whereas fungal amyloglucosidase is used to mimic the effect of brush-border α -glucosidases. However, the use of AMG for the recovery of the resistant starch fraction might be less preferable than expected.

Table 7.2. A selection of *in vitro* pre-digestion methods used in literature to obtain the resistant starch fraction for *in vitro* fermentation.

| Starch source | Enzymes used | Removal/inactivation of hydrolysed substances | Drying method | Ref. |
|---------------|---|---|-----------------------------|-----------|
| RS-2 | Salivary α -amylase, porcine pepsin, porcine pancreatin | Dialysis | Dried, method not specified | [62] |
| RS-3 | Salivary α -amylase, porcine pancreatin and amyloglucosidase | Washed and centrifuged | Oven-dried | [23] |
| RS-3 | Salivary α -amylase, porcine pancreatin and amyloglucosidase | Heated to 100 °C, dialysis | Freeze-dried | [29] |
| RS-2, RS-3 | Pancreatin and amyloglucosidase | Washed, centrifuged, ethanol treatment | Not dried | [22] |
| RS-2 | Pepsin, pancreatic α -amylase and amyloglucosidase | Ethanol precipitation, washing, centrifuged | Air-dried | [63] |
| RS-3 | Salivary, gastric and pancreatic enzymes, not specified | Centrifugation | Not specified | [64] |
| RS-2, RS-3 | Porcine pancreatic α -amylase | Addition of 0.3 M Na ₂ CO ₃ , washing, centrifugation | Rotary evaporation | [25] |
| RS-3 | Thermostable α -amylase, amyloglucosidase | Centrifugation, washing with water and ethanol | Oven dried | [65] |
| RS-3 | Porcine pancreatin | Centrifugation, washing with water | Oven dried | Chapter 3 |

7.1. The use of fungal amyloglucosidase re-considered

In the upper GIT, several brush-border α -glucosidases are present that primarily hydrolyse soluble dextrans released by pancreatic α -amylase to glucose^[66]. Previously, it has been shown that brush-border α -glucosidases enhance starch hydrolysis when incubated with pancreatic α -amylase, compared to hydrolysis by pancreatic α -amylase alone^[67], clearly illustrating that the activity of these α -glucosidases is not neglectable. Nevertheless, the majority of the starch digestion models either ignore the activity of brush-border α -glucosidases (e.g. INFOGEST)^[68] or replace them with fungal amyloglucosidases (AMG) (e.g. Englyst^[15])^[69], for the purpose of quantification^[7]. When AMG is used together with pancreatic α -amylase, soluble starch is fully hydrolysed to glucose, similar

to the *in vivo* situation. Both AMG and brush-border α -glucosidases are active on granular starches^[70], but affinity among substrates differs^[71], with AMG generally being more active towards raw starches^[70] and partially pancreatic α -amylase digested starches^[72]. Next to being active on native granules^[73], AMG alone was also active on intrinsic RS-3 (unpublished own results). This is likely because AMG from *Aspergillus niger* has a CBM20^[74] that binds strongly to raw starches and was shown to be highly important for AMG activity on granular starches^[75, 76]. Due to the strong binding of AMG to insoluble starches, it seems almost impossible to fully remove AMG after a pre-digestion treatment without changing the starch structure. This, in combination with the overdose often used^[7], might make that AMG remains active during *in vitro* fermentation, releasing easily fermentable glucose residues and therefore influencing the real fermentability of resistant starches, while not even fully resembling the activity of brush-border α -glucosidases. Therefore, it is recommended for future research to avoid using AMG during *in vitro* digestion as pre-treatment for obtaining the RS fraction.

7.2. Inactivation of the digestive enzymes

Most of the studies as presented in Table 7.2 did not use any method to inactivate the digestive enzymes. Although applied by some^[29], heating should be avoided, since it may (partially) solubilize the starch and therefore introduce newly formed digestible starch. Many studies washed the digested substrate several times with water and/or ethanol or used dialysis to remove the hydrolysed oligomers and digestive enzymes (Table 7.2). Previously, it was shown that pancreatic α -amylase binds to retrograded starch directly^[77], implying the difficulty of simply removing pancreatic α -amylase by repeated washing cycles. To elaborate on this difficulty, we incubated our P40-B substrate with pancreatin, performed 4 cycles of washing with milliQ and subsequently oven-dried the pre-digested substrate (P40-B-pd). Successively, we incubated the P40-B-pd substrate in mSIEM for 48 h and analysed the solubilized fraction. Here, we observed slight activity of remaining pancreatic α -amylase as illustrated by the chromatograms and quantitative analysis of released malto-oligomers over time (Figure 7.5). Although the remaining activity is minor, as shown by the presence of malto-oligomers > DP 5 after 48 h of incubation, these results also indicate that pancreatic α -amylase cannot be fully washed away and this thus indicates a need for proper inactivation methods of digestive enzymes prior to *in vitro* fermentation. Warren et al. (2018) treated the substrates after pre-digestion with 0.3 M Na₂CO₃ to stop hydrolysis followed by three washing cycles^[25]. Such

treatment may be a good option, left aside that it does not affect the physico-chemical characteristics of the RS-3 substrates.

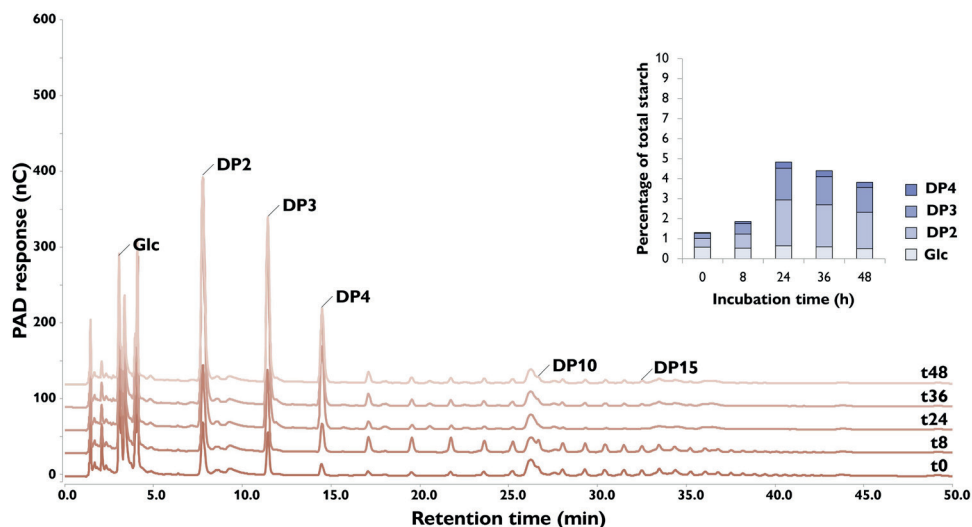


Figure 7.5. High-performance anion exchange chromatograms of pre-digested P40-B incubated for 48 h in modified simulated ileal efflux medium (mSIEM). The malto-oligomers are identified within the chromatogram. The inset presents the quantification of glucose, maltose, maltotriose and maltotetraose within these samples as percentage of total starch.

A new protocol for *in vitro* batch fermentation of foods suggests to add 10 % of the supernatant obtained after pre-digestion to the *in vitro* batch fermentation^[5]. This includes the enzymes used for pre-digestion, since they will be fermented by the microbes too^[5], which would obviously inhibit their activity. Although such addition of supernatant after pre-digestion may better reflect the *in vivo* situation than fully removing the released oligosaccharides and digestive enzymes, for studying the prebiotic potential of resistant starches, it is recommended to avoid having an easily digestible fraction as elaborated on in **Chapter 4**.

7.3. The way of drying might induce newly formed digestible starch

In most studies the pre-digested starches were dried prior to *in vitro* fermentation (Table 7.2). Previously, it has been shown that the drying method used affected the digestibility of RS-3 preparations^[30] and the fermentability of precooked pea starches^[78]. Newly formed digestible starch can be introduced by the drying method, of which the fraction may be larger when choosing freeze-drying over air-drying^[30]. Freeze-drying, as proposed by Lebet et al. (1998)^[79],

should be avoided, since it was shown to decrease crystallinity and therewith increase the fraction of digestible starch^[30]. Air- or oven-drying is mostly used (Table 7.2), but also using oven-drying, newly formed digestible starch may be introduced as shown by the presence of soluble oligomers at t0 (Figure 7.5).

Future research is thus required to obtain pre-digested starches that mimic upper GIT digestion, in which the enzymes are properly removed, the starch fraction is not changed due to heating and no newly formed digestible starch is introduced due to drying.

8. Concluding remarks and future perspectives

Butyrate is found to be essential for gut health^[80] and supplementation of resistant starch in the diet has been associated with increased butyrate levels in the gut^[81]. RS-3 is retrograded starch that is formed in cooked and cooled foods, but can also be prepared as a food ingredient. RS-3 is usually heat-stable and therefore has potential as a health-beneficial ingredient that can be added as such to foods. To enable transit to the colon and potentially promote butyrate production over there, it is essential that RS-3 is highly resistant to pancreatic α -amylase. Here, we prepared highly resistant RS-3 from α -1,4 glucans of varying chain length, retrograded into A- (DPn 16 - 22) or B-type (DPn 32 - 76) crystals. These intrinsic RS-3 substrates (80-95 % RS) were shown to promote butyrate production and/or butyrate producing bacteria during *in vitro* fermentation. To achieve degradation of intrinsic RS-3 in the gut, it is likely that specific gut microbes are required to be present within the gut microbiota, unlike other starches that are degradable by many gut microbes. Intrinsic RS-3 therefore clearly differs from gelatinized or granular starches and RS-3 as found in cooked and cooled foods and is potentially stimulating more specific starch-degrading bacteria in the gut, compared to gelatinized or granular starches.

Intrinsic RS-3 (80-95 % RS) can be prepared from narrow disperse α -1,4 glucans, crystallized in spherical particles with an A-type crystal (short chain length) or B-type crystal (long chain length). Enzymatic synthesis of narrow disperse α -1,4 glucans using glucose-1-phosphate is very costly, but could potentially be avoided. This could be done by either optimizing crystallization parameters to obtain spherical and dense particles from debranched waxy starches directly, or by enzymatic treatment of such debranched waxy starches to obtain a more narrow disperse Mw distribution, followed by crystallization. Obviously, such treatments are only valuable when they still result in RS-3 with high resistance to digestion (≥ 80 % RS).

We have observed that many faecal inocula were unable to degrade intrinsic RS-3 efficiently within the incubation time tested, and if degraded, the degradation rate was quite slow. The slow degradation of intrinsic RS-3 might cause transit to the distal colon. In the distal colon, intrinsic RS-3 might be specifically degraded by e.g. RS-degrading specialists such as *Ruminococcus bromii*, that could cross-feed with butyrate-producing *Lachnospiraceae* and therefore enhance butyrate production. When *Ruminococcus bromii* is not present within the microbiome, intrinsic RS-3 might be defecated untouched. In such case, subjects could benefit from intrinsic RS-3 with *R. bromii* supplementation as a synbiotic. If intrinsic RS-3 is efficiently degraded within the transit and results in enhanced butyrate production *in vivo*, requires further investigation.

Our results suggest that degradation of intrinsic RS-3 requires specific gut microbes with specific enzymatic machineries. Intrinsic RS-3 might therefore be considered as a very specific dietary fibre. To confirm that intrinsic RS-3 is such a specific dietary fibre, future research should investigate its specificity using individual faecal inocula from different subjects, and quantify the starch degradation and determine the changes in microbiota composition after incubation. These individual faecal inocula should also be supplemented with *R. bromii* to study if *R. bromii* could enable butyrate production from intrinsic RS-3 in subjects that do not harbour *R. bromii*. Furthermore, it is recommended to study the intrinsic RS-3 degrading capacity of other *B. adolescentis* strains than tested in this project and of other potential RS-degrading species, such as *Prevotella* and *Roseburia*. If intrinsic RS-3 is indeed considered such a specific dietary fibre by specifically being degradable by *R. bromii* and promoting butyrate production *in vitro*, its abilities to promote butyrate production *in vivo* should be studied. This research thus indicates that intrinsic RS-3 has the potential to be a beneficial ingredient by potentially promoting butyrate production in the distal colon and therewith promoting a healthy gut.

9. References

1. Cai L.M., Shi Y.C. Preparation, structure, and digestibility of crystalline A- and B-type aggregates from debranched waxy starches. *Carbohydrate Polymers*. **2014**;105:341-350.
2. Cai L.M., Shi Y.C. Structure and digestibility of crystalline short-chain amylose from debranched waxy wheat, waxy maize, and waxy potato starches. *Carbohydrate Polymers*. **2010**;79(4):1117-1123.
3. Cai L.M., Shi Y.C. Self-assembly of short linear chains to A- and B-type starch spherulites and their enzymatic digestibility. *Journal of Agricultural and Food Chemistry*. **2013**;61(45):10787-10797.
4. Klostermann C.E., Buwalda P.L., Leemhuis H., de Vos P., Schols H.A., Bitter J.H. Digestibility of resistant starch type 3 is affected by crystal type, molecular weight and molecular weight distribution. *Carbohydrate Polymers*. **2021**;265:118069.
5. Perez-Burillo S., Molino S., Navajas-Porras B., Valverde-Moya A.J., Hinojosa-Nogueira D., Lopez-Maldonado A., Pastoriza S., Rufian-Henares J.A. An in vitro batch fermentation protocol for studying the contribution of food to gut microbiota composition and functionality. *Nature Protocols*. **2021**;16(7):3186-3209.
6. Birt D.F., Boylston T., Hendrich S., Jane J.L., Hollis J., Li L., McClelland J., Moore S., Phillips G.J., Rowling M., Schalinske K., Scott M.P., Whitley E.M. Resistant starch: promise for improving human health. *Advances in Nutrition*. **2013**;4(6):587-601.
7. Dhital S., Warren F.J., Butterworth P.J., Ellis P.R., Gidley M.J. Mechanisms of starch digestion by alpha-amylase-structural basis for kinetic properties. *Critical Reviews in Food Science and Nutrition*. **2017**;57(5):875-892.
8. Human Microbiome Project C. Structure, function and diversity of the healthy human microbiome. *Nature*. **2012**;486(7402):207-214.
9. Cantu-Jungles T.M., Hamaker B.R. New view on dietary fiber selection for predictable shifts in gut microbiota. *mBio*. **2020**;11(1).
10. El Kaoutari A., Armougom F., Gordon J.I., Raoult D., Henrissat B. The abundance and variety of carbohydrate-active enzymes in the human gut microbiota. *Nature Reviews Microbiology*. **2013**;11(7):497-504.
11. White B.A., Lamed R., Bayer E.A., Flint H.J. Biomass utilization by gut microbiomes. *Annual Reviews Microbiology*. **2014**;68:279-296.
12. Long C., de Vries S., Venema K. Polysaccharide source altered ecological network, functional profile, and short-chain fatty acid production in a porcine gut microbiota. *Beneficial Microbes*. **2020**;11(6):591-610.
13. Baxter N.T., Schmidt A.W., Venkataraman A., Kim K.S., Waldron C., Schmidt T.M. Dynamics of human gut microbiota and short-chain fatty acids in response to dietary interventions with three fermentable fibers. *mBio*. **2019**;10(1).
14. Martens B.M.J., Gerrits W.J.J., Bruininx E., Schols H.A. Amylopectin structure and crystallinity explains variation in digestion kinetics of starches across botanic sources in an in vitro pig model. *Journal of Animal Science and Biotechnology*. **2018**;9:91.
15. Englyst H.N., Kingman S.M., Cummings J.H. Classification and measurement of nutritionally important starch fractions. *European Journal of Clinical Nutrition*. **1992**;46 Suppl 2:S33-50.
16. Ze X., Duncan S.H., Louis P., Flint H.J. *Ruminococcus bromii* is a keystone species for the degradation of resistant starch in the human colon. *The ISME Journal*. **2012**;6(8):1535-1543.
17. Nagara Y., Fujii D., Takada T., Sato-Yamazaki M., Odani T., Oishi K. Selective induction of human gut-associated acetogenic/butyrogenic microbiota based on specific microbial colonization of indigestible starch granules. *The ISME Journal*. **2022**.

18. Venkataraman A., Sieber J.R., Schmidt A.W., Waldron C., Theis K.R., Schmidt T.M. Variable responses of human microbiomes to dietary supplementation with resistant starch. *Microbiome*. **2016**;4(1):33.
19. Jung D.H., Kim G.Y., Kim I.Y., Seo D.H., Nam Y.D., Kang H., Song Y., Park C.S. Bifidobacterium adolescentis P2P3, a human gut bacterium having strong non-gelatinized resistant starch-degrading activity. *Journal of Microbiology and Biotechnology*. **2019**;29(12):1904-1915.
20. Sorndech W.R., S.; Blennow, A.; Tongta, S. Impact of resistant maltodextrins and resistant starch on human gut microbiota and organic acids production. *Starch-Starke*. **2019**;71(5-6):1800231.
21. Cui W., Ma Z., Li X., Hu X. Structural rearrangement of native and processed pea starches following simulated digestion in vitro and fermentation characteristics of their resistant starch residues using human fecal inoculum. *International Journal of Biological Macromolecules*. **2021**;172:490-502.
22. Teichmann J., Cockburn D.W. In vitro fermentation reveals changes in butyrate production dependent on resistant starch source and microbiome composition. *Frontiers in Microbiology*. **2021**;12:640253.
23. Chang R., Jin Z., Lu H., Qiu L., Sun C., Tian Y. Type III resistant starch prepared from debranched starch: structural changes under simulated saliva, gastric, and intestinal conditions and the impact on short-chain fatty acid production. *Journal of Agricultural and Food Chemistry*. **2021**;69(8):2595-2602.
24. Giuberti G., Gallo A. In vitro evaluation of fermentation characteristics of type 3 resistant starch. *Heliyon*. **2020**;6(1):e03145.
25. Warren F.J., Fukuma N.M., Mikkelsen D., Flanagan B.M., Williams B.A., Lisle A.T., P O.C., Morrison M., Gidley M.J. Food starch structure impacts gut microbiome composition. *mSphere*. **2018**;3(3).
26. Liang D., Li N., Dai X., Zhang H., Hu H. Effects of different types of potato resistant starches on intestinal microbiota and short-chain fatty acids under *in vitro* fermentation. *International Journal of Food Science & Technology*. **2021**;56:2432-2442.
27. Liu J., Liu F., Arıoğlu-Tuncil S., Xie Z., Fu X., Huang Q., Zhang B. In vitro fecal fermentation outcomes and microbiota shifts of resistant starch spherulites. *International Journal of Food Science & Technology*. **2022**;57(5).
28. Ravi A., Troncoso-Rey P., Ahn-Jarvis J., Corbin K.R., Harris S., Harris H., Aydin A., Kay G.L., Le Viet T., Gilroy R., Pallen M.J., Page A.J., O'Grady J., Warren F.J. Hybrid metagenome assemblies link carbohydrate structure with function in the human gut microbiome. *Communications Biology*. **2022**;5(1):932.
29. Gu F., Li C., Hamaker B.R., Gilbert R.G., Zhang X. Fecal microbiota responses to rice RS3 are specific to amylose molecular structure. *Carbohydrate Polymers*. **2020**;243:116475.
30. Zeng F., Zhu S.M., Chen F.Q., Gao Q.Y., Yu S.J. Effect of different drying methods on the structure and digestibility of short chain amylose crystals. *Food Hydrocolloids*. **2016**;52:721-731.
31. van Trijp M.P.H., Rosch C., An R., Keshtkar S., Logtenberg M.J., Hermes G.D.A., Zoetendal E.G., Schols H.A., Hooiveld G. Fermentation kinetics of selected dietary fibers by human small intestinal microbiota depend on the type of fiber and subject. *Molecular Nutrition and Food Research*. **2020**;64(20):e2000455.
32. Walker A.W., Ince J., Duncan S.H., Webster L.M., Holtrop G., Ze X., Brown D., Stares M.D., Scott P., Bergerat A., Louis P., McIntosh F., Johnstone A.M., Lobley G.E., Parkhill J., Flint H.J. Dominant and diet-responsive groups of bacteria within the human colonic microbiota. *The ISME Journal*. **2011**;5(2):220-230.
33. Russell D.A., Ross R.P., Fitzgerald G.F., Stanton C. Metabolic activities and probiotic potential of bifidobacteria. *International Journal of Food Microbiology*. **2011**;149(1):88-105.

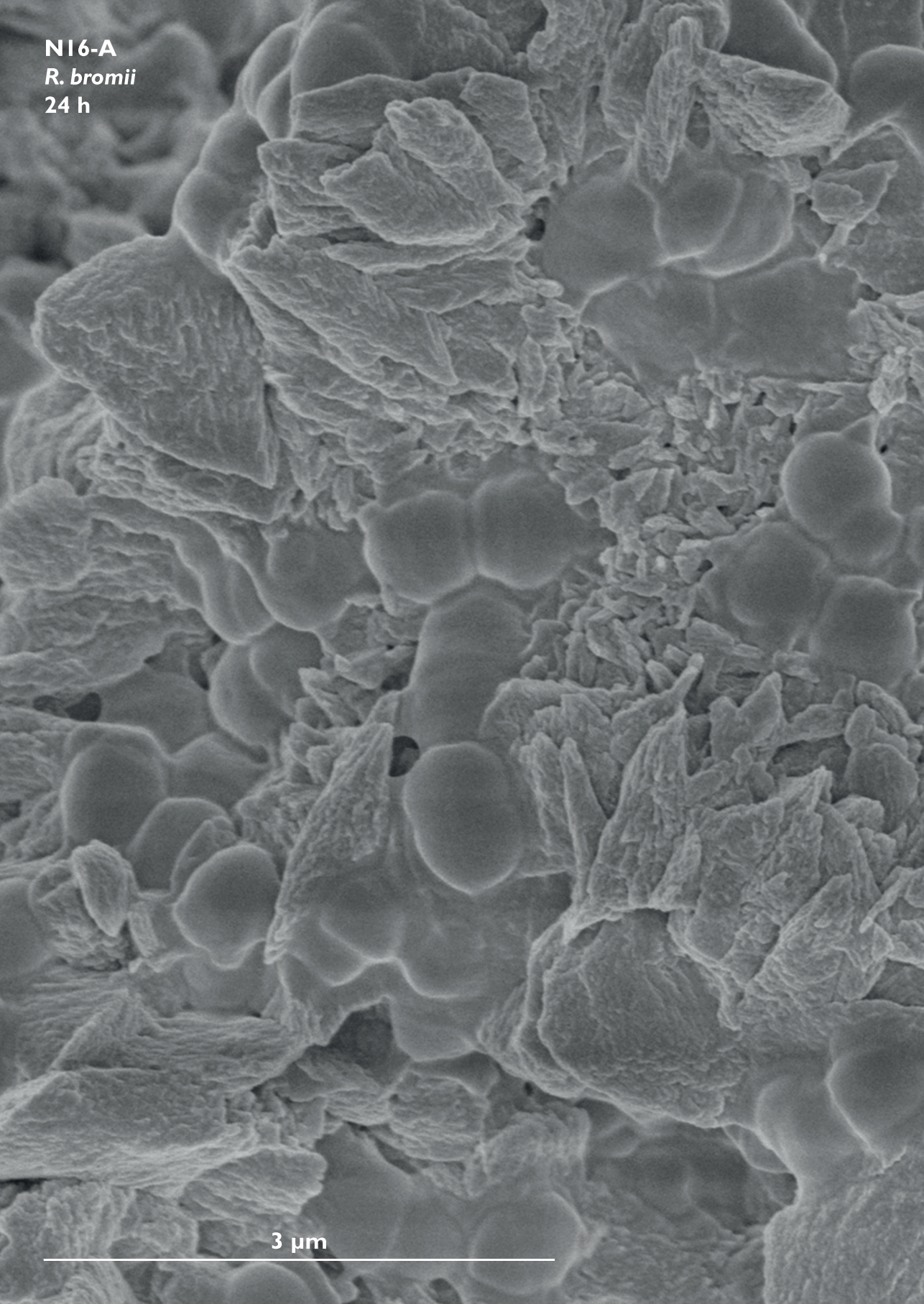
34. Salonen A., Lahti L., Salojärvi J., Holtrop G., Korpela K., Duncan S.H., Date P., Farquharson F., Johnstone A.M., Lobley G.E., Louis P., Flint H.J., de Vos W.M. Impact of diet and individual variation on intestinal microbiota composition and fermentation products in obese men. *The ISME Journal*. **2014**;8(11):2218-2230.
35. Kumari M., Singh P., Nataraj B.H., Kokkiligadda A., Naithani H., Azmal Ali S., Behare P.V., Nagpal R. Fostering next-generation probiotics in human gut by targeted dietary modulation: An emerging perspective. *Food Research International*. **2021**;150(Pt A):110716.
36. Cerqueira F.M., Potenhauer A.L., Pollet R.M., Brown H.A., Koropatkin N.M. Starch digestion by gut bacteria: crowdsourcing for carbs. *Trends in Microbiology*. **2020**;28(2):95-108.
37. Mukhopadhyay I., Morais S., Laverde-Gomez J., Sheridan P.O., Walker A.W., Kelly W., Klieve A.V., Ouwerkerk D., Duncan S.H., Louis P., Koropatkin N., Cockburn D., Kibler R., Cooper P.J., Sandoval C., Crost E., Juge N., Bayer E.A., Flint H.J. Sporulation capability and amylosome conservation among diverse human colonic and rumen isolates of the keystone starch-degrader *Ruminococcus bromii*. *Environmental Microbiology*. **2018**;20(1):324-336.
38. Molinero N., Conti E., Sánchez B., Walker A.W., Margolles A., Duncan S.H., Delgado S. *Ruminococcoides bili* gen. nov., sp. nov., a bile-resistant bacterium from human bile with autolytic behavior. *International Journal of Systematic and Evolutionary Microbiology*. **2021**;71(8):004960.
39. Hong Y.S., Jung D.H., Chung W.H., Nam Y.D., Kim Y.J., Seo D.H., Park C.S. Human gut commensal bacterium *Ruminococcus* species FMB-CY1 completely degrades the granules of resistant starch. *Food Science and Biotechnology*. **2022**;31(2):231-241.
40. Bendiks Z.A., Guice J., Coulon D., Raggio A.M., Page R.C., Carvajal-Aldaz D.G., Luo M., Welsh D.A., Marx B.D., Taylor C.M., Hussender C., Keenan M.J., Marco M.L. Resistant starch type 2 and whole grain maize flours enrich different intestinal bacteria and metatranscriptomes. *Journal of Functional Foods*. **2022**;90:104982.
41. Ze X., Ben David Y., Laverde-Gomez J.A., Dassa B., Sheridan P.O., Duncan S.H., Louis P., Henrissat B., Juge N., Koropatkin N.M., Bayer E.A., Flint H.J. Unique organization of extracellular amylases into amylosomes in the resistant starch-utilizing human colonic Firmicutes bacterium *Ruminococcus bromii*. *mBio*. **2015**;6(5):e01058-01015.
42. Cerqueira F.M., Potenhauer A.L., Doden H.L., Brown A.N., Abdel-Hamid A.M., Morais S., Bayer E.A., Wawrzak Z., Cann I., Ridlon J.M., Hopkins J.B., Koropatkin N.M. Sas20 is a highly flexible starch-binding protein in the *Ruminococcus bromii* cell-surface amylosome. *Journal of Biological Chemistry*. **2022**;298(5):101896.
43. Potenhauer A.L., Cerqueira F.M., Villafuerte-Vega R., Armbruster K.M., Mareček G., Chen T., Wawrzak Z., Hopkins J.B., Vander Kooi C.W., Janeček S., Ruotolo B.T., Koropatkin N.M. The *Ruminococcus bromii* amylosome protein Sas6 binds single and double helical α -glucan structures in starch. *bioRxiv*. **2022**.
44. Ryu H.J., Jung D.H., Yoo S.H., Tuncil Y.E., Lee B.H. Bifidogenic property of enzymatically synthesized water-insoluble α -glucans with different α -1,6 branching ratio. *Food Hydrocolloids*. **2022**;133.
45. Jung D.H., Seo D.H., Kim Y.J., Chung W.H., Nam Y.D., Park C.S. The presence of resistant starch-degrading amylases in *Bifidobacterium adolescentis* of the human gut. *International Journal of Biological Macromolecules*. **2020**;161:389-397.
46. Valk V., Lammerts van Bueren A., van der Kaaij R.M., Dijkhuizen L. Carbohydrate-binding module 74 is a novel starch-binding domain associated with large and multidomain α -amylase enzymes. *FEBS Journal*. **2016**;283(12):2354-2368.
47. Cockburn D.W., Suh C., Medina K.P., Duvall R.M., Wawrzak Z., Henrissat B., Koropatkin N.M. Novel carbohydrate binding modules in the surface anchored α -amylase of *Eubacterium rectale* provide a molecular rationale for the range of starches used by this organism in the human gut. *Molecular Microbiology*. **2018**;107(2):249-264.

48. Ramsay A.G., Scott K.P., Martin J.C., Rincon M.T., Flint H.J. Cell-associated alpha-amylases of butyrate-producing Firmicute bacteria from the human colon. *Microbiology (Reading)*. **2006**;152(Pt 11):3281-3290.
49. Scott K.P., Martin J.C., Chassard C., Clerget M., Potrykus J., Campbell G., Mayer C.D., Young P., Rucklidge G., Ramsay A.G., Flint H.J. Substrate-driven gene expression in Roseburia inulinivorans: importance of inducible enzymes in the utilization of inulin and starch. *Proceedings of the National Academy of Sciences (Proceedings of the National Academy of Sciences of the United States of America)*. **2011**;108 Suppl 1(Suppl 1):4672-4679.
50. Difilippo E., Pan F., Logtenberg M., Willems R.H., Braber S., Fink-Gremmels J., Schols H.A., Gruppen H. In Vitro Fermentation of Porcine Milk Oligosaccharides and Galacto-oligosaccharides Using Piglet Fecal Inoculum. *Journal of Agricultural & Food Chemistry*. **2016**;64(10):2127-2133.
51. Logtenberg M.J., Akkerman R., Hobe R.G., Donners K.M.H., Van Leeuwen S.S., Hermes G.D.A., de Haan B.J., Faas M.M., Buwalda P.L., Zoetendal E.G., de Vos P., Schols H.A. Structure-specific fermentation of galacto-oligosaccharides, isomalto-oligosaccharides and isomalto/malto-polysaccharides by Infant fecal microbiota and impact on dendritic cell cytokine responses. *Molecular Nutrition & Food Research*. **2021**;65(16):e2001077.
52. Shulman R.J. Starch malabsorption in infants. *Journal of Pediatric Gastroenterology and Nutrition*. **2018**;66 Suppl 3:S65-S67.
53. Westrom B.R., Ohlsson B., Karlsson B.W. Development of porcine pancreatic hydrolases and their isoenzymes from the fetal period to adulthood. *Pancreas*. **1987**;2(5):589-596.
54. Hill C.J., Lynch D.B., Murphy K., Ulaszewska M., Jeffery I.B., O'Shea C.A., Watkins C., Dempsey E., Mattivi F., Tuohy K., Ross R.P., Ryan C.A., PW O.T., Stanton C. Evolution of gut microbiota composition from birth to 24 weeks in the INFANTMET Cohort. *Microbiome*. **2017**;5(1):4.
55. Jonathan M.C., Borne J.J., van Wiechen P., da Silva C.S., Schols H.A., Gruppen H. In vitro fermentation of 12 dietary fibres by faecal inoculum from pigs and humans. *Food Chemistry*. **2012**;133(3):889-897.
56. Leijdekkers A.G., Aguirre M., Venema K., Bosch G., Gruppen H., Schols H.A. In vitro fermentability of sugar beet pulp derived oligosaccharides using human and pig fecal inocula. *Journal of Agricultural and Food Chemistry*. **2014**;62(5):1079-1087.
57. Feng G., Mikkelsen D., Hoedt E.C., Williams B.A., Flanagan B.M., Morrison M., Gidley M.J. In vitro fermentation outcomes of arabinoxylan and galactoxylglucan depend on fecal inoculum more than substrate chemistry. *Food & Function*. **2020**;11(9):7892-7904.
58. Sanchez B., Noriega L., Ruas-Madiedo P., de los Reyes-Gavilan C.G., Margolles A. Acquired resistance to bile increases fructose-6-phosphate phosphoketolase activity in Bifidobacterium. *FEMS Microbiology Letters*. **2004**;235(1):35-41.
59. Jacobasch G., Dongowski G., Schmiedl D., Muller-Schmehl K. Hydrothermal treatment of Novelose 330 results in high yield of resistant starch type 3 with beneficial prebiotic properties and decreased secondary bile acid formation in rats. *British Journal of Nutrition*. **2006**;95(6):1063-1074.
60. Fassler C., Arrigoni E., Venema K., Hafner V., Brouns F., Amado R. Digestibility of resistant starch containing preparations using two in vitro models. *European Journal of Nutrition*. **2006**;45(8):445-453.
61. Tuncil Y.E., Thakkar R.D., Arioglu-Tuncil S., Hamaker B.R., Lindemann S.R. Fecal microbiota responses to bran particles are specific to cereal type and in vitro digestion methods that mimic upper gastrointestinal tract passage. *Journal of Agricultural and Food Chemistry*. **2018**;66(47):12580-12593.
62. Bernabé A.M., Srikaeo K., Schlüter M. Resistant starch content, starch digestibility and the fermentation of some tropical starches in vitro. *Food Digestion*. **2011**;2:37-42.

63. Wang Y., Mortimer E.K., Katundu K.G.H., Kalanga N., Leong L.E.X., Gopalsamy G.L., Christophersen C.T., Richard A.C., Shivasami A., Abell G.C.J., Young G.P., Rogers G.B. The capacity of the fecal microbiota from Malawian infants to ferment resistant starch. *Frontiers in Microbiology*. **2019**;10:1459.
64. Zhou Z., Cao X., Zhou J.Y.H. Effect of resistant starch structure on short-chain fatty acids production by human gut microbiota fermentation in vitro. *Starch-Starke*. **2013**;65(5-6):509-516.
65. Zhou D., Ma Z., Hu X. Isolated pea resistant starch substrates with different structural features modulate the production of short-chain fatty acids and metabolism of microbiota in anaerobic fermentation in vitro. *Journal of Agricultural and Food Chemistry*. **2021**;69(18):5392-5404.
66. Lin A.H., Lee B.H., Chang W.J. Small intestine mucosal α -glucosidase: A missing feature of in vitro starch digestibility. *Food Hydrocolloids*. **2016**;53(163-171).
67. Dhital S., Lin A.H., Hamaker B.R., Gidley M.J., Muniandy A. Mammalian mucosal alpha-glucosidases coordinate with alpha-amylase in the initial starch hydrolysis stage to have a role in starch digestion beyond glucogenesis. *PLoS One*. **2013**;8(4):e62546.
68. Brodkorb A., Egger L., Alming M., Alvito P., Assuncao R., Ballance S., Bohn T., Bourlieu-Lacanal C., Boutrou R., Carriere F., Clemente A., Corredig M., Dupont D., Dufour C., Edwards C., Golding M., Karakaya S., Kirkhus B., Le Feunteun S., Lesmes U., Macierzanka A., Mackie A.R., Martins C., Marze S., McClements D.J., Menard O., Minekus M., Portmann R., Santos C.N., Souchon I., Singh R.P., Vegarud G.E., Wickham M.S.J., Weitschies W., Recio I. INFOGEST static in vitro simulation of gastrointestinal food digestion. *Nature Protocols*. **2019**;14(4):991-1014.
69. Edwards C.H., Warren F.J. Starchy foods: human nutrition and public health. In: Gouseti O., Bornhorst G., Bakalis S., Mackie A., editors. *Interdisciplinary approaches to food digestion*: Springer, Cham; 2019.
70. Ao Z., Quezada-Calvillo R., Sim L., Nichols B.L., Rose D.R., Sterchi E.E., Hamaker B.R. Evidence of native starch degradation with human small intestinal maltase-glucoamylase (recombinant). *FEBS Letters*. **2007**;581(13):2381-2388.
71. Shin H., Seo D.H., Seo J., Lamothe L.M., Yoo S.H., Lee B.H. Optimization of in vitro carbohydrate digestion by mammalian mucosal α -glucosidases and its applications to hydrolyze the various sources of starches. *Food Hydrocolloids*. **2019**;87:470-476.
72. Lee B.H., Hamaker B.R. Maltase has most versatile α -hydrolytic activity among the mucosal α -glucosidases of the small intestine. *Journal of Pediatric Gastroenterology and Nutrition*. **2018**;66:S7-S10.
73. Warren F.J., Zhang B., Waltzer G., Gidley M.J., Dhital S. The interplay of alpha-amylase and amyloglucosidase activities on the digestion of starch in in vitro enzymic systems. *Carbohydrate Polymers*. **2015**;117:192-200.
74. Janecek S., Marecek F., MacGregor E.A., Svensson B. Starch-binding domains as CBM families-history, occurrence, structure, function and evolution. *Biotechnology Advances*. **2019**;37(8):107451.
75. Cockburn D., Nielsen M.M., Christiansen C., Andersen J.M., Rannes J.B., Blennow A., Svensson B. Surface binding sites in amylase have distinct roles in recognition of starch structure motifs and degradation. *International Journal of Biological Macromolecules*. **2015**;75:338-345.
76. Svensson B., Svendsen T.G., Svendsen I.B., Sakai T., Ottesen M. Characterization of two forms of glucoamylase from *aspergillus niger*. *Carlsberg Research Communications*. **1982**;47:55-69.
77. Patel H., Royall P.G., Gaisford S., Williams G.R., Edwards C.H., Warren F.J., Flanagan B.M., Ellis P.R., Butterworth P.J. Structural and enzyme kinetic studies of retrograded starch: Inhibition of alpha-amylase and consequences for intestinal digestion of starch. *Carbohydrate Polymers*. **2017**;164:154-161.

78. Chang D., Ma Z., Li X., Hu X. Structural modification and dynamic in vitro fermentation profiles of precooked pea starch as affected by different drying methods. *Food & Function*. **2021**;12(24):12706-12723.
79. Lebet V., Arrigoni E., Amado R. Digestion procedure using mammalian enzymes to obtain substrates for in vitro fermentation studies. *LWT - Food Science and Technology*. **1998**;31(6):509-515.
80. Liu H., Wang J., He T., Becker S., Zhang G., Li D., Ma X. Butyrate: a double-edged sword for health? *Advances in Nutrition*. **2018**;9(1):21-29.
81. McOrist A.L., Miller R.B., Bird A.R., Keogh J.B., Noakes M., Topping D.L., Conlon M.A. Fecal butyrate levels vary widely among individuals but are usually increased by a diet high in resistant starch. *Journal of Nutrition*. **2011**;141(5):883-889.

NI6-A
R. bromii
24 h



3 μ m

A scanning electron micrograph (SEM) showing a highly textured, three-dimensional surface. The surface is composed of numerous rounded, bulbous protrusions of varying sizes, some of which are interconnected by thin, irregular ridges and valleys. The overall appearance is reminiscent of a rough, crystalline material or a biological structure like a sponge or coral. The lighting is directional, coming from the upper left, which creates strong highlights on the raised surfaces and deep shadows in the recessed areas, emphasizing the topographical complexity.

Summary

The aim of this research was to investigate how to improve the resistant starch content of resistant starch type 3 (RS-3) preparations and how highly resistant RS-3 substrates are fermented by various faecal inocula. These results will contribute to find new food ingredients that could reach the distal colon and enhance butyrate production over there.

The first chapter contains a state of the art literature overview describing research already performed on improving the RS content of RS-3 preparations. Previous research primarily used α -1,4 glucans of polydisperse mixtures to prepare RS-3 preparations, whereas narrow disperse α -1,4 glucans tend to crystallize better and could thus potentially improve the resistance to upper gastro-intestinal tract (GIT) digestion. Although highly resistant RS-3 preparations (> 85 % RS) were prepared in the past decade, knowledge on the fermentability of such highly resistant RS-3 by gut microbiota is still lacking and needed to understand the prebiotic potential of such ingredients. Only few microbes are known that are efficiently degrading and/or fermenting highly resistant starch in the gut.

We investigated which physico-chemical characteristics are of importance to increase the RS content of RS-3 preparations (**Chapter 2**). For this, α -1,4 glucans varying in chain length (DPn 14 – DPn 76) and Mw distribution were prepared. Polydisperse α -1,4 glucans were obtained by debranching amylopectins of various (modified) sources, whereas narrow disperse α -1,4 glucans of similar average chain length were prepared by enzymatic synthesis. Subsequently, the obtained α -1,4 glucans were crystallized at 4 or 50 °C into B- and A-type polymorphs, respectively, resulting in twelve RS-3 preparations varying in chain length, Mw distribution and crystal type. The twelve RS-3 preparations were tested for their digestibility using pancreatin and amyloglucosidase. Crystal type had the largest influence on resistance to digestion (A >>> B), followed by chain length (high DP >> low DP) and Mw distribution (narrow disperse > polydisperse). Overall, six RS-3 preparations were obtained that were highly resistant to digestion (\geq 80 % RS), whereas six others contained a varying RS content (0 – 70 % RS).

The six highly resistant RS-3 substrates (intrinsic RS) and two RS enriched fractions obtained after pre-digestion of RS-rich RS-3 preparations were fermented *in vitro* using a pooled inoculum of four healthy adult faecal samples (**Chapter 3**). All substrates were yielding relatively high butyrate levels after fermentation, whereas propionate production was limited. Furthermore, we observed increases in relative abundance of primarily three genera. Especially *Ruminococcus* increased in relative abundance when a pooled adult faecal

inoculum was used to ferment RS-3 substrates prepared from narrow disperse α -1,4 glucans, whereas *Lachnospiraceae* and *Bifidobacterium* increased in relative abundance after fermentation of all substrates using the same inoculum.

The six RS-3 preparations with varying RS content (0 - 70 % RS) were fermented *in vitro* without a pre-digestion treatment, using a pooled healthy adult faecal inoculum (**Chapter 4**). The results showed that, depending on the digestible starch fraction present, the microbiota composition after fermentation was fully dominated by *Bifidobacterium*, resulting in acetate and lactate accumulation. No cross-feeding was observed and, when the digestible starch was fully fermented, the further fermentation of the RS fraction was inhibited. This study thus showed the importance of pre-digestion prior to *in vitro* fermentation when researching the prebiotic potential of RS, since the presence of digestible starch may hugely impact the fermentation of resistant starch. Furthermore, the results showed that digestible starch was fermentable by many different microbial populations, whereas this was not the case for intrinsic RS-3, clearly distinguishing these two starch categories.

The prebiotic potential of RS-3 preparations was also investigated for strongly developing microbiota, by *in vitro* fermentation of selected RS-3 preparations using pooled faecal inocula obtained from pre- and post-weaning piglets (**Chapter 5**). The results showed that RS-3 preparations containing a digestible starch fraction cannot be considered a prebiotic for pre- and post-weaning piglets, since such substrates were not stimulating specific microbes. In contrast, intrinsic RS-3 might have prebiotic potential for post-weaning piglets, since it stimulated specific phylotypes (ASVs) within *Prevotella* and *Roseburia*. The slow degradation rate using post-weaning piglet faecal microbiota and the limited degradation by pre-weaning piglet faecal microbiota of intrinsic RS-3 illustrated the difficult-to-degrade nature of this fibre.

To investigate if highly resistant RS-3 preparations were degradable by well-known RS-degrading species *Ruminococcus bromii* and *Bifidobacterium adolescentis*, a selection of intrinsic RS-3 substrates was inoculated with these species, whereas native potato and regular maize starch were taken along as controls (**Chapter 6**). The results showed that *R. bromii* degraded all substrates to primarily glucose and maltose, without further fermentation. *B. adolescentis* fermented raw starch granules efficiently, fermented A-type RS-3 substrates minorly and did not at all ferment B-type intrinsic RS-3. This suggests that intrinsic RS-3 might be a more specific dietary fibre than e.g. raw potato starch. Scanning electron microscopy was used to evaluate the changes in starch morphology due to degradation by these gut microbes, which showed us how

distinctly different the intrinsic RS-3 of varying physico-chemical characteristics were, and that the way of degradation by the two gut microbes differed enormously.

Chapter 7 provides a general discussion, in which we compare the results obtained in this project and reflect on the main findings and implications. The relatively large number of RS-3 substrates studied in this research allowed us to have a better understanding on the effect of RS-3 physico-chemical characteristics on *in vitro* digestion and fermentation and taught us how to design highly resistant RS-3 with preferred digestion and fermentation characteristics. Such highly resistant RS-3 could potentially be used to stimulate butyrate production in the distal colon.

NI6-A
R. bromii
72 h

10 μm



Acknowledgements



The PhD journey has finished... I feel extremely happy that it has come to an end and at the same time I feel sad that this marks the end of an era. When I started this project, I was very happy and grateful to have been given the opportunity to explore the world of resistant starch. This, together with my great supervisor team of Dutchies Piet, Henk and Harry; and in my mind I was smiling because of this stereotypic list of names, also including Paul. And there we were, Luis and me, not really fitting within this list of names... =D.

I am immensely grateful to **Piet**, who believed in my abilities and appointed me as a PhD candidate in this position. Unfortunately, it was not even a year that you were my main supervisor, but this time is full of nice memories. I liked your philosophic way of thinking and your ability to use music-related metaphors to explain science, even using orchestra examples. Also, I admired your enthusiasm and incredible starch knowledge and I will always remember your whistling through our corridors. I learned a lot from you, but wish to have had you around much longer... With your passing, a great scientist, inspirator, supervisor and a kind person was lost.

I couldn't be more grateful to **Henk**, who took over the main supervision from Piet. I remember being scared of you, when I was still doing my MSc, but I cannot imagine that anymore! Thanks a lot for all the help, motivational talks, bears looking the other way, tissues and an occasional self-grown tomato or cucumber. I am very happy to have had you as my supervisor and you truly made me the scientist I am right now. It is definitely thanks to you that I really like to work on carbohydrates! Let's enjoy a Belgium beer together soon! Box! (With two tiny hands and one enormous fist, hihi).

Harry, my topic was a bit odd within BCT, but I am very grateful to you for giving me the opportunity to do my PhD research within BCT and at the same time learn so much from a very different field. I even remember asking my officemate, after 2 months within BCT: "what is the difference between homogeneous and heterogeneous catalysis?". I am also grateful for the possibility of a microbiology lab within such a chemistry group (yes, my own private lab). Your door was always open for small or big issues. I will always remember your vegetable-dislike, although I'm not entirely sure that this dislike is really so extreme as you sometimes tend to state... =).

Paul & Luis, thanks a lot for working together on this project and letting me think in a different way! Although the project changed due to the well-known circumstances, I am grateful for the help and nice papers we have together! Luis,

thanks a lot for our biweekly meetings, your kindness and the nice trip to Gent for collecting the piglet faeces!

Dearest **Martha & Marina**, CarboBiotics buddies from Wageningen! Already during the VLAG PhD week, I imagined how nice it would be to collaborate and here we are! I am very grateful to you both, teaching me basic microbiology, anaerobic cultivation and leading me through microbiota composition analysis. You always answered all my stupid questions with great patience and I also really liked working in the lab with you!

Erwin & Hauke, thanks a lot for helping me with my manuscripts and your active contribution during the CCC CarboBiotics team meetings. **Annemarie**! Jij mag zeker niet ontbreken, met al je hulp om onze *E. coli* enzympjes te laten maken. Liters en liters hebben we geïncubeerd, om uiteindelijk een schamele paar mg opgezuiverd enzym te krijgen. Heerlijk om met jou het eerste jaar het lab te delen! Over *E. coli* gesproken, **Hans**, jij ook ontzettend bedankt, natuurlijk voor de *E. coli*'s, maar ook voor al je hulp tijdens dit project, je motiverende woorden en het zó snel geven van feedback of goedkeuring voor de manuscripten. Ik zou nog veel van je willen leren! **Lizette, Arjen, Geert** and all other CCC-CarboBiotics members, thanks a lot for the great input during our (online) meetings. In enjoyed working in the consortium a lot and thank you for making that possible! **Bianca**, dankjewel voor je motiverende woorden, hulp en scherpe oog met betrekking tot het biggetjes-manuscript.

Lieve **Susan**, bedankt voor alle hulp met de HPLCs, van het bijvullen van eluent zodat mijn run eeuwig kon duren, tot het weer schoonmaken van de kolom. Heel erg bedankt ook voor je gezelligheid en je knuffels als ik die nodig had, ik mis je nu al! **Danielle, Jolanda & Nadine**, bedankt voor de adviezen en het beantwoorden van al mijn vragen. **Edwin** en **René**, bedankt voor het bestellen van de gasflessen en de goede zorgen voor de anaerobe kast! Datie nu maar braaf anoxisch mag blijven. Ook **Margaret, Mark, Peter** en **Ineke** bedankt! **Marcel & Jelmer**, bedankt voor alle hulp met de SEM!

Dankjewel **Hilda**, voor de leuke tijd die we hebben gehad bij de α -amylase conferenties! Thanks also to students **Rong, Evert, Jet, Mignon, Ailing, David & Cynte**, for contributing to my research project and giving me the ability to work together in my own small team! Dankjewel Evert, voor alle gezelligheid en de wandelingen door de mooie Nederlandse natuur.

Lieve **Marlene**, ik ben je zo ontzettend dankbaar voor alles wat je voor me hebt betekend en gedaan in de afgelopen 4.5 jaar. Je nam altijd de tijd om naar me te luisteren, me te knuffelen, me te troosten en vooral om heel veel te kletsen.

Lachen, wandelen, koffietjes bij Impulse, samen eten, schrijfweken, biertjes drinken, naar het Heerenstraattheater, weekendjes weg, muziek maken en je kreeg me zelfs zover om te gaan zwemmen! Je bent een prachtig mens en ik ben je voor altijd dankbaar dat je zo'n goede vriendin bent geworden en vandaag mijn paranymf wilt zijn! Op naar nog meer avontuur samen :).

Katha! Niederländisch? Oder Deutsch? Wie reden wir heute?? That definitely marks our friendship and it is just weird to talk English to you! Dankjewel voor wie je bent, je filosofische manier van denken, je luisterend oor, je adviezen, het altijd langs mogen komen, voor de wandelingetjes op de dijk, voor de Troelstraweg-bioscoop, het varen op de Weissensee en voor je inspirerende jou! Dankzij jou heb ik R2D2 leren kennen en zal hij voor altijd een luide plek in mijn hart hebben xD. Dankjewel dat je in jouw drukste periode toch mijn paranymf wilt zijn. Dankjewel ook voor je humor, voor de gezellige etentjes, ook met Luki en Bas! Voor nu: Tschüssi, baba, pfiati, bussi, tschau und bis bald!

Dear FCH-colleagues, thank you for adopting me during the PhD trip to the North of the Netherlands, it was great fun! And thanks a lot for all the great input during the ~~Carbohydrate~~ α -ox-meetings. Dear **Krishna**, **Dimitris**, **Carolina** and **Dazhi**, thank you for the amazing time at EPNOE in Nantes! Thanks Dazhi, for teaching me how to peel eggs in a very convenient way, I'm honoustly still using your trick on a weekly basis. Thanks Krishna for the nice discussions, hugs and letting me taste your amazing food! Thanks Dimitris for all the help and the nice conversations. **Silvia!** You were my FCH-buddy during the coffee research project and I'm immensely grateful to have got to know you and will always remember our nice conversions and laughter. Thank you **Melliana**, for teaching me all kind of things in the lab, your ability to see the spring with a different eye and the motivational talks. Thank you dearest **Natalia**, for your incredible kindness, support and listening. Dear **Eva** & **Madelon**, thanks a lot for the nice chats and advice! Thanks Madelon, for teaching me how to handle the anaerobic chamber. I also would like to mention **Sylvia**, **Peicheng**, **Romy**, **Pim**, **Weiwei** and all others, thanks for making FCH such a nice and warm environment to work in!

Dear BCT-colleagues, thanks a lot for the help, fun and sometimes awkward coffee breaks! Dear **Umay**, my roomy! Thanks a lot for all the listening to my frustrations, the hugs and your picture above my desk, so that I would not miss you too much during your holidays! **Tim**, my starch-buddy! Thanks a lot for being you, making BCT-lunches and borrels extra fun and that you came right to my place after we heard the news about Piet. Dear **Nazila**, thanks for your help, your smartness and kindness, and your patience; you made BCT a true

warm place. Dear **Eleni, Simha** and **Laura**, thanks for the nice times we had, together with Marlene; drinking beers at the Spot or at the Zaaier, occasionally having dinner together. **Matthijs, Ivo, Torin, Freek, Zhaoxiang, Maggie, Raghavendra, Dmitry** and **Lorenz**, thanks a lot for the nice times and good luck with finalizing your own PhDs!

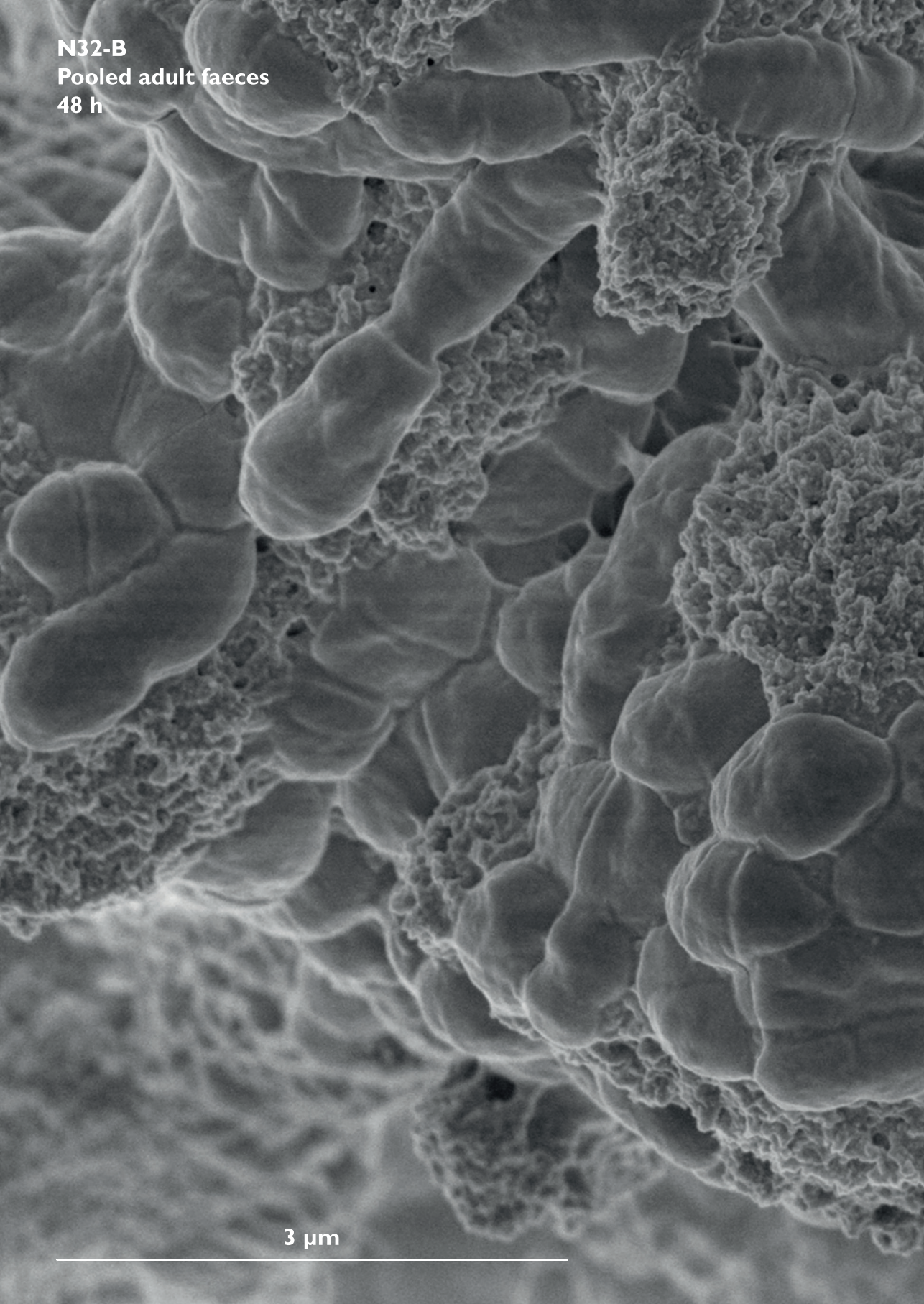
Dear **Sanne, Lukas, Rebecca** and **Pascal**, thanks for participating in the Krimidiner and the nice times, games, walks and beers after work! Liefste **Roula** en **Rogier**! Jullie hebben immens bijgedragen aan mijn welzijn. Bedankt voor onze gezamenlijke twee-wekelijkse etentjes en jullie vertrouwen dat het echt echt echt goedkomt. Gauw weer Dvořák spelen? Lieve **Jorieke** en **Daan** en natuurlijk ook **Thijmen**, bedankt voor jullie steun, de wandelingetjes, de lekkere etentjes, de weekendjes weg en de knuffels! Lieve **Nina, Evie** en **Lydie**, dankjulliewel voor jullie steun en de nodige afleiding in de afgelopen jaren! Natuurlijk ook de rest van J.C. G.E.K., bedankt! **Anne, Merle** en **Evelien**, ook jullie bedankt! Onze jaarlijkse weekendjes weg zijn altijd om weer naar uit te kijken.

Daphiee! Als ik aan jou denk, dan lach ik meteen! En hoewel we elkaar niet zo vaak zien, ben je een zeer waardevolle vriendin en niet in de laatste plaats om de heerlijke chocolade die je altijd meebrengt, hihi. Ik kom gauw jullie niet-meer-zo-nieuwe stekje in Brussel bewonderen. Lieve **Anna Sophie**, bedankt voor je luisterend oor en onze al-zo-lange vriendschap, de mooie gesprekken en je ongelooflijk inspirerende vioolspel! Lief **Nederlands Strijkersgilde**, elk jaar kijk ik er weer zo naar uit! Een waar lichtpuntje om even helemaal weg te zijn uit het dagelijkse leven. Samen muziek maken is het allerfijnste wat er is. Lieve **Jelmer**, bedankt voor je altijd oprechte interesse en steun! Lieve **Simone**, jij ook bedankt voor je vriendschap, je bijzondere en inspirerende kijk op de wereld!

Lieve **Jean, Jeanette, Luuk** en **Yante**, dankjulliewel voor alle steun! Lieve **Thomas, Corinna, Ismene, Marco** en **Kasper**, jullie ook bedankt voor alle steun! Dank ook aan **papa** en **Frederiek**. Lieve **mama**, dankjewel dat je er altijd voor me bent, voor je knuffels, voor je onvoorwaardelijke liefde, voor je grappige gedachten en je vaardigheid om overal iets positiefs in te zien!

Lieve **Bas**, wie had dat gedacht, blijkbaar lukt het toch! Bedankt voor je steun, je eeuwige geduld om naar al mijn presentaties te luisteren, je troost, voor je lieve woorden, voor je gekheid, voor onze gezamenlijke kwaal om in alles een melodietje of ritmetje te horen. Voor je creatieve hoofd, voor het zingen van lieve liedjes (behalve "My Funny Valentine..."), voor je energie, je ontbijtjes op bed en voor je armen om me heen! Ik ben blij dat het-zusje-van en de-vriend-van nog altijd samen zijn!

N32-B
Pooled adult faeces
48 h



3 μm

A scanning electron micrograph (SEM) showing a highly textured surface. The foreground features a cluster of rounded, bulbous structures, possibly cells or microorganisms, with a granular, porous appearance. The background consists of a more uniform, wavy, and undulating surface. The overall image is in grayscale, emphasizing the intricate details and topography of the material.

About the author



Curriculum vitae

Cynthia E. Klostermann was born in November 1992 in Laag-Zuthem, the Netherlands. After graduating her secondary school (Gymnasium Celeanum, Zwolle) in 2011, she started her bachelor Food Technology at Wageningen University & Research. Her bachelor study was completed with a thesis on the effect of different drying methods on the quality of tropical fruits at the chair of Food Quality & Design. In 2015, Cynthia started her master Food Technology at Wageningen University & Research with a specialization in Ingredient Functionality. During this master study, she visited the Universität für Bodenkultur in Vienna, Austria, for one semester as an Erasmus exchange student. Her master thesis focussed on enzymatic fingerprinting of isomalto/malto-polysaccharides and was performed at the Laboratory of Food Chemistry and Biobased Chemistry & Technology. She completed her master with an internship on adduct formation of aroma and coffee compounds and its possible reversibility at Jacobs Douwe Egberts in Utrecht. After finishing her master in 2017, she worked for one year as Junior Researcher on coffee galactomannans at the Laboratory of Food Chemistry. In 2018, she started as a PhD candidate at Biobased Chemistry & Technology under supervision of Dr. Piet L. Buwalda, Prof. Dr. Johannes H. Bitter and Prof. Dr. Henk A. Schols (Laboratory of Food Chemistry). This research was performed within the public-private partnership CarboBiotics coordinated by the Carbohydrate Competence Center. The project, entitled “Towards versatile, antibiotic-specific carbohydrate-formulations for decreasing antibiotics-use and side-effects”, was in close collaboration with Dr. Luis Silva Lagos and Prof. Dr. Paul de Vos from University Medical Center Groningen. The most important results of her PhD research are presented in this dissertation.



Contact: cynthiaklostermann@live.nl

List of publications

C.E. Klostermann, M. Fassarella, E.G. Zoetendal & H.A. Schols. Degradation of intrinsic resistant starch type 3 crystals by gut microbes *Bifidobacterium adolescentis* & *Ruminococcus bromii*. *To be submitted for publication*.

C.E. Klostermann, T.M.C. Quadens, L. Silva Lagos, P.L. Buwalda, G. Bruggeman, P. de Vos, J.H. Bitter, H. Smidt, B.M.J. Martens & H.A. Schols. The prebiotic potential of RS-3 preparations for pre- and post-weaning piglets. *Submitted for publication*.

C.E. Klostermann, M.F. Endika, P.L. Buwalda, P. de Vos, E.G. Zoetendal, J.H. Bitter & H.A. Schols. Presence of digestible starch impacts *in vitro* fermentation of resistant starch. *Submitted for publication*.

C.E. Klostermann, M.F. Endika, E. ten Cate, P.L. Buwalda, P. de Vos, J.H. Bitter, E.G. Zoetendal & H.A. Schols. Type of intrinsic resistant starch type 3 determines *in vitro* fermentation by pooled adult faecal inoculum. *Accepted for publication in Carbohydrate Polymers*.

L. Silva Lagos, **C.E. Klostermann**, G. López-Velázquez, C. Fernández-Lainez, H. Leemhuis, A.A.C.M. Oudhuis, P.L. Buwalda, H.A. Schols & P. de Vos. Crystal type, chain length and polydispersity impact the resistant starch type 3 immunomodulatory capacity via Toll-like receptors. *Submitted for publication*.

M.F. Endika, D.J. Barnett, **C.E. Klostermann**, H.A. Schols, I.C. Arts, J. Penders, A. Nauta, H. Smidt & K. Venema. Microbiota-dependent influence on prebiotics on the resilience of infant gut microbiota to amoxicillin/clavulanate perturbation in an *in vitro* colon model. *Frontiers in Microbiology*, 2023, 14.

D.J.M. Barnett, M.F. Endika, **C.E. Klostermann**, F. Gu, C. Thijs, A. Nauta, H.A. Schols, H. Smidt, I.C.W. Arts & J. Penders. Human milk oligosaccharides, antimicrobial drugs, and the gut microbiota of term neonates: observations from the KOALA birth cohort study. *Gut Microbes*, 2023, 15(1), 2164152.

C.E. Klostermann, P.L. Buwalda, H. Leemhuis, P. de Vos, H.A. Schols & J.H. Bitter. Digestibility of resistant starch type 3 is affected by crystal type, molecular weight and molecular weight distribution. *Carbohydrate Polymers*, 2021, 265, 118069.

C. Kong, R. Akkerman, **C.E. Klostermann**, M. Beukema, M.M. Oerlemans, H.A. Schols & P. de Vos. Distinct fermentation of human milk oligosaccharides 3-FL and LNT2 and GOS/inulin by infant gut microbiota and impact on adhesion of *Lactobacillus plantarum* WCFS1 to gut epithelial cells. *Food & Function*, 2021, 12(24), 12513-12525.

S.A. Verkhnyskaya*, C. Kong*, **C.E. Klostermann***, H.A. Schols, P. de Vos & M.T. Walvoort. Digestion, fermentation, and pathogen anti-adhesive properties of the hMO-mimic di-fucosyl- β -cyclodextrin. *Food & Function*, 2021, 12(11), 5018-5026.

*These authors contributed equally to this work

C.E. Klostermann, P.H. Van der Zaal, H.A. Schols, P.L. Buwalda & J.H. Bitter. The influence of α -1,4-glucan substrates on 4,6- α -D-glucanotransferase reaction dynamics during isomalto/malto-polysaccharide synthesis. *International Journal of Biological Macromolecules*, 2021, 181, 762-768.

P.H. Van der Zaal, **C.E. Klostermann**, H.A. Schols, J.H. Bitter & P.L. Buwalda. Enzymatic fingerprinting of isomalto/malto-polysaccharides. *Carbohydrate Polymers*, 2019, 205, 279-286.

Overview of completed training activities

Discipline specific activities

Courses

| | |
|---|------------------------------|
| Summer course Glycosciences ¹ | VLAG, Wageningen, 2018 |
| Advanced Food Analysis ¹ | VLAG, Wageningen, 2019 |
| Applied biocatalysis | ENTEG/VLAG, Wageningen, 2019 |
| Intestinal microbiome of humans and animals | VLAG, Wageningen, 2019 |
| Basic Scanning Electron Microscopy (SEM) | WEMC, Wageningen, 2019 |

Conferences and meetings

| | |
|---|--------------------------------|
| The 7 th Symposium on the α -amylase family ¹¹ | IMB, Smolenice, Slovakia, 2019 |
| Mini-symposium – <i>in vitro</i> studies of the human intestinal microbiota | WUR-MIB, Wageningen, 2020 |
| Starch Convention (online) ² | AGF, Detmold, Germany, 2021 |
| The 7 th European Polysaccharide Network of Excellence (EPNOE) Conference ^{1,2} | EPNOE, Nantes, France, 2021 |
| The 8 th International Dietary Fibre Conference ^{1,2} | ICC, Leuven, Belgium, 2022 |
| The 8 th Symposium on the α -amylase family ^{1,21} | IMB, Smolenice, Slovakia, 2022 |
| CCC Symposium ^{11,2} | CCC, Groningen, 2019-2022 |

General courses

| | |
|--|------------------------|
| VLAG PhD introduction week | VLAG, Baarlo, 2019 |
| Philosophy and ethics in Food Science and Technology | WGS, Wageningen, 2019 |
| Scientific Writing | WGS, Wageningen, 2019 |
| Presenting with impact | WGS, Wageningen, 2021 |
| Introduction to R | VLAG, Wageningen, 2020 |
| Applied Statistics | VLAG, Wageningen, 2020 |
| Chemometrics | VLAG, Wageningen, 2020 |
| Career perspectives | WGS, Wageningen, 2021 |
| Scientific Artwork, Data visualisation and Infographics with Adobe Illustrator | WGS, Wageningen, 2021 |

Optional courses and activities

| | |
|-------------------------------------|-----------------------------------|
| Preparation of research proposal | BCT, Wageningen, 2019 |
| PhD study trip FCH | FCH, Netherlands, 2021 |
| PhD study trip BCT ³ | BCT, Lyon and Paris, France, 2022 |
| BSc/MSc thesis students supervision | BCT/FCH, Wageningen, 2019-2022 |
| BCT seminars and colloquia | BCT, Wageningen, 2018-2022 |
| FCH Carbohydrate meetings | FCH, Wageningen, 2018-2022 |
| Project meetings CarboBiotics | CCC Consortium, 2018-2022 |

¹Poster presentation, ²Oral presentation, ¹Award winning, ³Organizing committee

Abbreviations: VLAG, Graduate School for Advanced Studies in Food Technology, Agrobiotechnology, Nutrition and Health Science; ENTÉG, Engineering and Technology institute Groningen; WEMC, Wageningen Electron Microscopy Centre; IMB, Institute of Molecular Biology – Slovak Academy of Sciences; WUR-MIB, Laboratory of Microbiology, Wageningen University & Research; ICC, International Association for Cereal Science and Technology; CCC, Carbohydrate Competence Center; WGS, Wageningen Graduate School; FCH, Laboratory of Food Chemistry; BCT, Biobased Chemistry & Technology

The research presented in this thesis was performed within the public-private partnership “CarboBiotics” coordinated by the Carbohydrate Competence Center (CCC, www.cccresearch.nl). CarboBiotics is financed by participating industrial partners Cooperative Royal Avebe U.A., Nutrition Sciences N.V. and Royal FrieslandCampina N.V., and allowances of The Dutch Research Council (NWO).

Financial support from Wageningen University for printing this thesis is gratefully acknowledged.

Cover artwork and design by Doortje Beemster (www.doortjeviooltje.nl)

Printed by Proefschrift-AIO, the Netherlands, on recycled paper
Edition: 170 copies

Cynthia E. Klostermann, 2023